

Physical and chemical properties of Wolf-Rayet planetary nebulae

A. Danehkar ¹

¹ Department of Astronomy, University of Michigan, 1085 S. University Ave, Ann Arbor, MI 48109, USA

Received 2021 June 16; accepted 2021 August 25

Abstract

Wolf-Rayet ([WR]) and weak emission-line (*wels*) central stars of planetary nebulae (PNe) have hydrogen-deficient atmospheres, whose origins are not well understood. In the present study, we have conducted plasma diagnostics and abundance analyses of 18 Galactic PNe surrounding [WR] and *wels* nuclei, using collisionally excited lines (CELs) and optical recombination lines (ORLs) measured with the Wide Field Spectrograph on the ANU 2.3-m telescope at the Siding Spring Observatory complemented with optical archival data. Our plasma diagnostics imply that the electron densities and temperatures derived from CELs are correlated with the intrinsic nebular H β surface brightness and excitation class, respectively. Self-consistent plasma diagnostics of heavy element ORLs of N²⁺ and O²⁺ suggest that a small fraction of cool ($\lesssim 7000$ K), dense ($\sim 10^4$ – 10^5 cm⁻³) materials may be present in some objects, though with large uncertainties. Our abundance analyses indicate that the abundance discrepancy factors (ADF \equiv ORLs/CELs) of O²⁺ are correlated with the dichotomies between forbidden-line and He I temperatures. Our results likely point to the presence of a tiny fraction of cool, oxygen-rich dense clumps within the diffuse warm ionized nebulae. Moreover, our elemental abundances derived from CELs are mostly consistent with AGB models in the range of initial masses from 1.5 to 5M $_{\odot}$. Further studies are necessary to understand better the origins of abundance discrepancies in PNe around [WR] and *wels* stars.

Unified Astronomy Thesaurus concepts: [Planetary nebulae \(1249\)](#); [Interstellar medium \(847\)](#); [Chemical abundances \(224\)](#); [Wolf-Rayet stars\(1806\)](#)

Supporting material: figure sets, machine-readable tables

1. Introduction

Planetary nebulae (PNe) are important astrophysical objects because they can be used as tracers of the composition of the interstellar medium (ISM) in galaxies, as well as to probe the uncertain physics of asymptotic giant branch (AGB) stars. Observations of PNe are employed to determine the elemental abundances of the ISM present in our own and other galaxies (e.g. Aller & Czyzak 1983; Kingsburgh & Barlow 1994; Stasińska et al. 1998; García-Rojas et al. 2012). Mixing processes during the progenitor’s life (e.g., first and second dredge up prior to the AGB, and third dredge up and hot bottom burning during the AGB) will change the envelope composition of He, C, N and possibly O and Ne (Péquignot et al. 2000; Karakas & Lattanzio 2003; Karakas et al. 2009). Other elements such as S, Ar, and Cl are left untouched by the evolution and nucleosynthesis in low- to intermediate-mass (1–8M $_{\odot}$) stars. For this reason, PN elemental abundances not only reflect the composition of the ISM at the time, when the progenitor was born, but also can be used to constrain the nucleosynthesis and mixing in AGB stars (e.g. Straniero et al. 1997; Werner & Herwig 2006; Karakas et al. 2009; Stasińska et al. 2013).

Historically, strong and easy to measure collisionally excited lines (CELs) provided reliable chemical tracers, and they have been extensively used to derive the abundances of heavy

elements such as N, O, Ne, Ar and S relative to H (see e.g. Kingsburgh & Barlow 1994; Kwitter & Henry 2001; Tsamis et al. 2003a; Henry et al. 2004; Liu et al. 2004). CEL emissivities depend exponentially on the electron temperature, so temperature variations introduce uncertainties into their results (e.g. Garnett 1992; Stasińska 2005). On the other hand, optical recombination lines (ORLs) have a much weaker dependence on the electron temperature and density, thus in principle resulting in more reliable abundance analyses. ORLs from heavy element ions are extremely weak relative to H β , but are observable in deep spectra of nearby PNe. Numerous studies indicated that the abundances derived from ORLs are systematically higher than those obtained from CELs in PNe (Liu et al. 2000, 2001; Luo et al. 2001; Wesson et al. 2003; Tsamis et al. 2004; Wesson & Liu 2004; Wesson et al. 2005; Tsamis et al. 2008; García-Rojas et al. 2009). The causes of the CEL/ORL abundance discrepancies are not fully understood and remain the open problem in nebular astrophysics. This abundance discrepancy problem was already found in gaseous nebulae about eighty years ago (Wyse 1942; Aller & Menzel 1945).

The dichotomy between electron temperatures measured from CELs and those from ORLs is another long-standing problem in the study of PNe, which may be closely linked to the abundance discrepancy problem. Nearly five decades ago, Peimbert (1967, 1971) found that the difference between [O III] and H I Balmer jump (BJ) temperatures, $T_e([\text{O III}]) > T_e(\text{BJ})$, in H II regions and PNe, and suggested the presence of temperature fluctuations. These temperature fluctuations could lead to overestimating the electron temperature deduced from

Table 1. Journal of the ANU observations, including the stellar characteristics.

PN	PN G (A92)	R.A. Dec./J2000	CSPN (A03)	T_{eff} (kK)	Aperture (arcsec ²)	Exp. (sec)	Obs. Date
PB 6	278.8+04.9	10 ^h 13 ^m 15 ^s 9 – 50° 19′ 59″.1	[WO 1]	103(K91)	14 × 14	1200	2010 Apr 20
M 3-30	017.9–04.8	18 ^h 41 ^m 14 ^s 9 – 15° 33′ 43″.6	[WO 1]	49(A03)	14 × 15	1200	2010 Apr 21
Hb 4 (shell)	003.1+02.9	17 ^h 41 ^m 52 ^s 7 – 24° 42′ 08″.0	[WO 3]	85(A03)	10 × 10	300, 1200	2010 Apr 21
Hb 4 (N-knot)	003.1+02.9	17 ^h 41 ^m 52 ^s 7 – 24° 42′ 08″.0	[WO 3]	85(A03)	6 × 5	300, 1200	2010 Apr 21
Hb 4 (S-knot)	003.1+02.9	17 ^h 41 ^m 52 ^s 7 – 24° 42′ 08″.0	[WO 3]	85(A03)	6 × 4	300, 1200	2010 Apr 21
IC 1297	358.3–21.6	19 ^h 17 ^m 23 ^s 5 – 39° 36′ 46″.4	[WO 3]	91(A03)	12 × 13	60, 1200	2010 Apr 21
Th 2-A	306.4–00.6	13 ^h 22 ^m 33 ^s 8 – 63° 21′ 01″.3	[WO3] _{pec} (W08)	157(P89)	19 × 16	1200	2010 Apr 20
Pe 1-1	285.4+01.5	10 ^h 38 ^m 27 ^s 6 – 56° 47′ 06″.5	[WO 4]	85(A02)	9 × 7	60, 1200	2010 Apr 21
M 1-32	011.9+04.2	17 ^h 56 ^m 20 ^s 1 – 16° 29′ 04″.6	[WO 4] _{pec}	56 ^a	15 × 12	1200	2010 Apr 20
M 3-15	006.8+04.1	17 ^h 45 ^m 31 ^s 7 – 20° 58′ 01″.6	[WC 4]	55(A03)	6 × 8	60, 1200	2010 Apr 20
M 1-25	004.9+04.9	17 ^h 38 ^m 30 ^s 3 – 22° 08′ 38″.8	[WC 5-6]	56(A03)	6 × 8	60, 1200	2010 Apr 20
Hen 2-142	327.1–02.2	15 ^h 59 ^m 57 ^s 6 – 55° 55′ 32″.9	[WC 9]	35(A03)	7 × 7	60, 1200	2010 Apr 20
Hen 3-1333	332.9–09.9	17 ^h 09 ^m 00 ^s 9 – 56° 54′ 48″.1	[WC 10]	30(D98)	7 × 7	1200	2010 Apr 20
Hen 2-113	321.0+03.9	14 ^h 59 ^m 53 ^s 5 – 54° 18′ 07″.5	[WC 10]	30(D98)	9 × 9	60, 1200	2010 Apr 20
K 2-16	352.9+11.4	16 ^h 44 ^m 49 ^s 1 – 28° 04′ 04″.7	[WC 11]	19(A03)	19 × 21	1200	2010 Apr 20
NGC 6578	010.8–01.8	18 ^h 16 ^m 16 ^s 5 – 20° 27′ 02″.7	<i>wels</i> (T93)	63(S89)	10 × 10	60, 1200	2010 Apr 22
M 2-42	008.2–04.8	18 ^h 22 ^m 32 ^s 0 – 24° 09′ 28″.4	<i>wels</i> (D11)	75(P89)	6 × 7	1200	2010 Apr 22
NGC 6567	011.7–00.6	18 ^h 13 ^m 45 ^s 2 – 19° 04′ 34″.2	<i>wels</i> (T93)	47(G97)	10 × 10	60, 1200	2010 Apr 22
NGC 6629	009.4–05.0	18 ^h 25 ^m 42 ^s 5 – 23° 12′ 10″.2	<i>wels</i> (T93)	35(G97)	10 × 10	60, 1200	2010 Apr 22
Sa 3-107	358.0–04.6	17 ^h 59 ^m 55 ^s 0 – 32° 59′ 11″.8	<i>wels</i> (D11)	46 ^a	7 × 7	1200	2010 Apr 22

^a Calculated from the nebular excitation class (EC) and the EC– T_{eff} correlation given by Dopita & Meatheringham (1990, 1991).

Note. References are as follows: A92 – Acker et al. (1992); A02 – Acker et al. (2002); A03 – Acker & Neiner (2003); D98 – De Marco & Crowther (1998); D11 – Depew et al. (2011); G97 – Gorny et al. (1997); K91 – Kaler et al. (1991); P89 – Preite-Martinez et al. (1989); S89 – Shaw & Kaler (1989); T93 – Tylenda et al. (1993); W08 – Weidmann et al. (2008).

CELs, resulting in underestimated ionic abundances (Peimbert 1967). However, the detailed analysis of NGC 6543 by Wesson & Liu (2004) for example showed that the temperature fluctuations are too small to explain the abundance discrepancy problem. Moreover, Wesson et al. (2005) found that the derived temperatures mostly follow the relation $T_e(\text{[O III]}) > T_e(\text{[B J]}) > T_e(\text{He I}) > T_e(\text{O II})$. This relation was predicted by the two-phase models (Liu 2003; Liu et al. 2004), containing some cold ($T_e \sim 10^3$ K) hydrogen-deficient small-scale structures, highly enriched in helium and heavy elements, embedded in the diffuse warm ($T_e \sim 10^4$ K) nebular gas of normal abundances. The study of Abell 30 by Wesson et al. (2003) pointed to the presence of cold ionized material in its hydrogen-deficient knots.

Although most central stars of PNe (CSPNe) have ‘hydrogen-rich’ surface abundances, a considerable fraction ($\lesssim 25\%$) of them show ‘hydrogen-deficient’ fast expanding atmospheres characterized by a large mass-loss rate (Tylenda et al. 1993; Leuenhagen et al. 1996; Leuenhagen & Hamann 1998; Acker & Neiner 2003). Their surface abundances exhibit helium, carbon, oxygen and neon, products of the helium-burning phase and a post-helium flash (Werner & Herwig 2006). Most of these CSPNe were classified as the carbon sequence of Wolf-Rayet (or [WR]) stars, resembling those of massive Wolf-Rayet (WR) stars (van der Hucht et al. 1981; van der Hucht 2001), where the square bracket distinguishes them from massive counterparts. About half of them show very high

effective temperature, ranging from 80 000 K to 150 000 K, and are identified as the early-type ([WCE]), including spectral class [WO1]–[WC5] (Koesterke & Hamann 1997; Peña et al. 1998). Others having surface temperature between 20–80 kK are called the late-type ([WCL]), containing spectral class [WC6–11] (Leuenhagen et al. 1996; Leuenhagen & Hamann 1998). A few central stars of PNe show narrower and weaker emission lines (C IV $\lambda 5805$ and C III $\lambda 5695$), which are not identical to those of [WR] classes. They were named weak emission-line stars (*wels*) by Tylenda et al. (1993). It has been suggested that [WR] stars are produced by a born-again scenario, i.e., a (very-) late thermal pulse (see e.g. Blöcker 2001; Herwig 2001; Koesterke 2001; Werner & Herwig 2006). Therefore, one might expect a link between the hydrogen-deficient inclusions within the nebulae and their central stars.

In this paper, we perform detailed plasma diagnostics and abundance analyses using CELs and ORLs for 18 Galactic PNe around hydrogen-rich [WR] stars and *wels*, which might provide clues about the origin of their hydrogen-rich central stars. In Section 2, we describe briefly our observations. In Section 3, we present physical conditions derived from CELs and ORLs. In Section 4, we present ionic and elemental abundances, followed by a discussion of the ORL/CEL abundance discrepancy and CEL–ORL temperature dichotomy in Section 5. In Section 6, we discuss the implication of our observations for AGB stellar models. Finally, our conclusions and discussions are presented in Section 7.

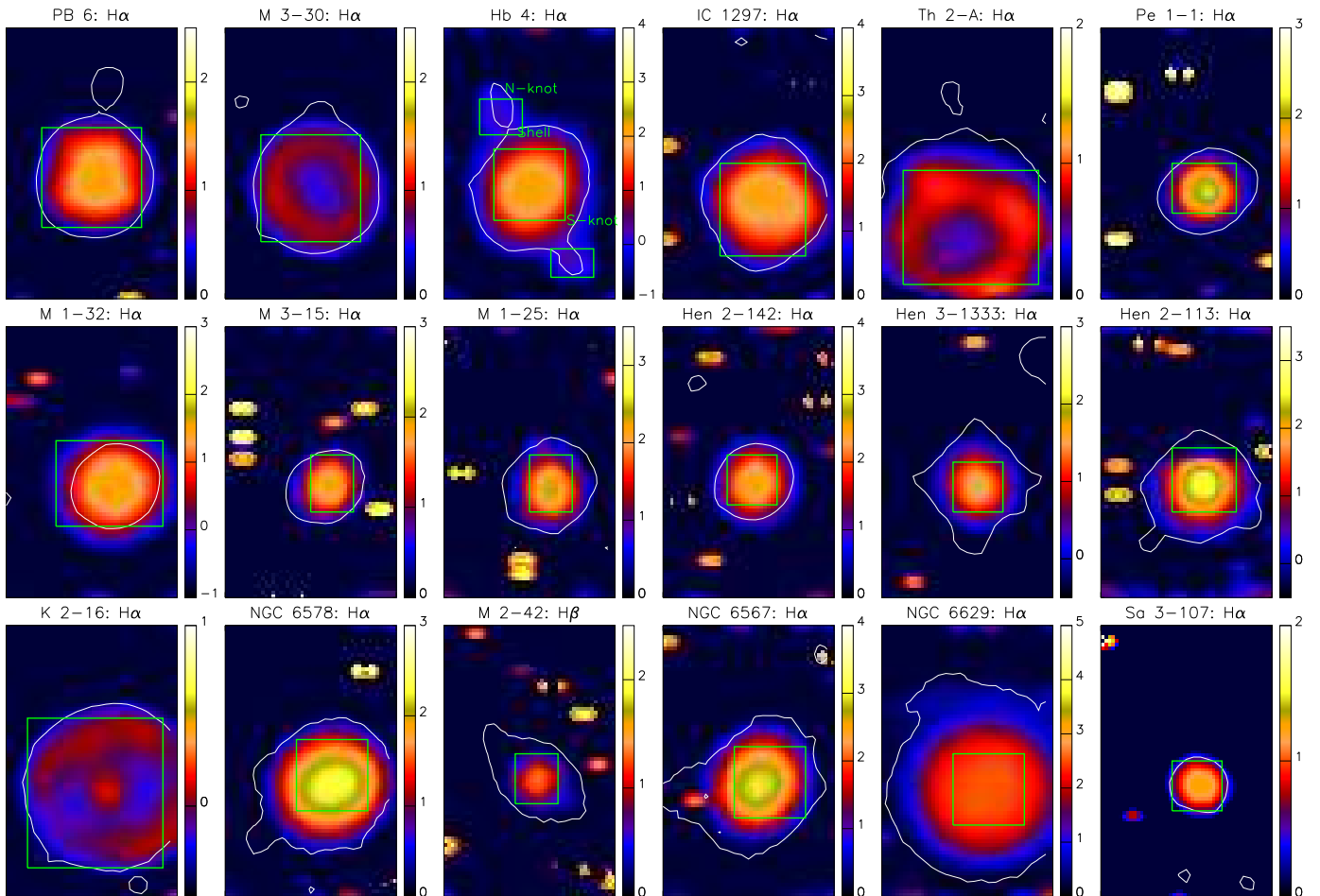


Figure 1. From left to right, and top to bottom, flux maps of the $H\alpha$ emission in the WiFeS FOV (24×38 arcsec²) for PB 6, M 3-30, Hb 4, IC 1297, Th 2-A, Pe 1-1, M 1-32, M 3-15, M 1-25, Hen 2-142, Hen 3-1333, Hen 2-113, K 2-16, NGC 6578, M 2-42 ($H\beta$ emission), NGC 6567, NGC 6629, and Sa 3-107 on logarithmic scales of 10^{-15} erg cm⁻² s⁻¹ spaxel⁻¹. The green rectangles show apertures with the sizes listed in Table 1 used to extract the integrated spectra. The white contours show ~ 10 percent of the nebular average surface brightness in the $H\alpha$ emission from the SuperCOSMOS $H\alpha$ Sky Survey (SHS; Parker et al. 2005), or in the r -band from the SuperCOSMOS Sky Surveys (SSS; Hambly et al. 2001). North is up and east is toward the left-hand side.

2. Observations

The optical integral field unit (IFU) spectra of PNe for this work were obtained at Siding Spring Observatory, Australia, using the Wide Field Spectrograph (WiFeS; Dopita et al. 2007, 2010) mounted on the 2.3-m Australian National University (ANU) telescope in April 2010 under program number 1100147 (PI: Q. A. Parker). WiFeS is an image-slicing IFU developed and built for the ANU 2.3-m telescope, feeding a double-beam spectrograph. WiFeS samples 0.5 arcsec along each of twenty five 38 arcsec \times 1 arcsec slitlets that provides a field-of-view (FOV) of 25 arcsec \times 38 arcsec and a spatial resolution element of 1.0 arcsec \times 0.5 arcsec. The spectrograph uses volume phase holographic gratings to provide a spectral resolution of $R \sim 3000$ and $R \sim 7000$. WiFeS has recently been used for a number of southern Galactic PNe (e.g. Ali et al. 2015, 2016; Basurah et al. 2016; Dopita et al. 2017).

Our observations were carried out with the spectral resolution of $R \sim 7000$, covering $\lambda\lambda 4415\text{--}5589$ Å in the blue channel and $\lambda\lambda 5222\text{--}7070$ Å in the red channel. Exposure times ranged from 60–1200 sec depending on the nebular $H\beta$ surface brightness. Spectroscopic standard stars were observed for the flux calibration purposes, notably EG 274 and LTT

3864. We also acquired series of bias, dome flat-field frames, twilight sky flats, arc lamp exposures, and wire frames for data reduction, flat-fielding, wavelength calibration and spatial calibration.

Table 1 presents a journal of the ANU observations that includes spectral classes of the central stars (Column 4), the stellar effective temperature (Column 5), the observing aperture (Column 6, see Figure 1), the exposure time (Column 7) used for each PN, and the observing date (Column 8). The rectangle aperture used to extract the integrated spectrum of each object is shown on the WiFeS FOV in Figure 1. The same aperture and FOV were employed for different gratings and exposure times in each target. The spectral classes of the [WR]-type stars are based on the classification schemes by Crowther et al. (1998) and Acker & Neiner (2003), and those of the *wels* according to Tylenda et al. (1993) and Depew et al. (2011). Although the CSPN M 2-42 was identified as *wels* (Depew et al. 2011), N III lines and He II identified in its stellar spectrum might associate it with [WN 8] stars (Danekhar et al. 2016). The CSPN M 1-32 was classified under the *peculiar* [WO 4]_{pec} subclass according to the width of C IV-5801/12 doublet (Acker & Neiner 2003). Similarly, the Th 2-A contain a [WO 3]_{pec} star (Weidmann et al. 2008), with collimated bipolar outflows discovered recently (Danekhar 2015). Bipolar

Table 2. Comparison of the observed fluxes of the diagnostic emission lines He II, [O III], and [N II] measured by the WiFeS observations with those from the adopted archival data, on a scale relative to H β , where H β = 100.

PN	PN G	He II λ 4686		[O III] λ 5007		[N II] λ 6584		Lit. Ref.	Lit. Observing Log		
		D21	Lit.	D21	Lit.	D21	Lit.		Slit (arcsec ²)	Exp. (sec)	Obs. Date
PB 6	278.8+04.9	130.2	147.0	1243.4	1010.0	341.3	306.0	K91	4×370, 45°	1200	1986 Mar 16
M 3-30	017.9–04.8	77.3	78.5	598.3	604.5	71.0	53.9	P01	4×13	2×900	1996 Jun 17
M 3-30	017.9–04.8	77.3	76.3	598.3	428.0	71.0	76.7	G07	2.1×270	2400,300	1994 Mar/Jul 1995 Jul
Hb 4 (shell)	003.1+02.9	11.9	10.3	1381.8	1481.4	419.9	620.0	P01	4×13	2×900,3×600	1996 Jul 14
Hb 4 (shell)	003.1+02.9	11.9	13.8	1381.8	1321.0	419.9	345.0	G07	2.1×270	2400,300	1994 Mar/Jul 1995 Jul
IC 1297	358.3–21.6	37.0	34.4	1342.3	1367.0	53.9	56.3	M02	5×320, 45°	210 (R/B)	1997 Mar/Apr
Th 2-A	306.4–00.6	49.5	46.8	1672.9	1719.0	296.9	260.0	M02	5×320, 45°	1800(B),1200(R)	1997 Mar/Apr
Pe 1-1	285.4+01.5	0.0	0.0	1186.2	1140.1	494.1	375.1	G12	1×5	60,900,2×1200	2010 Jun 5
M 1-32	011.9+04.2	0.0	0.4	533.5	475.6	1455.5	1230.6	G12	1×5	60,3×1500	2010 Jun 6
M 3-15	006.8+04.1	0.0	0.0	1188.9	1122.5	274.3	249.1	P01	4×13	3×900	1996 Jun 17
M 1-25	004.9+04.9	0.0	0.0	548.0	530.0	714.4	625.0	G07	2.1×270	2400,300	1994 Mar/Jul 1995 Jul
Hen 2-142	327.1–02.2	0.0	0.0	6.0	6.3	896.2	1195.0	G07	2.1×270	2400,300	1994 Mar/Jul 1995 Jul
Hen 3-1333	332.9–09.9	0.0	0.0	0.0	0.0	207.6 ^a	131.3 ^a	D97	1.5×330	3×600,2×1200	1993 Mar 14/15
Hen 2-113	321.0+03.9	0.0	0.0	0.0	0.0	121.2 ^a	117.6 ^a	D97	1.5×330	500,4×600,2×1200	1993 Mar 14/15
K 2-16	352.9+11.4	0.0	0.0	139.0	120.9	446.1	277.4	P01	4×13	3×900 2×900	1996 Jun 14 1997 Aug 3
NGC 6578	010.8–01.8	0.5	1.4	864.3	944.0	40.5	50.7	K03	5×320, 45°	1180(B),300(R)	1997 Mar
M 2-42	008.2–04.8	0.3	0.3	707.2	879.2	80.1	90.8	W07	2.1×270	60,300	1996 Jul
NGC 6567	011.7–00.6	0.6	1.4	1011.9	1016.0	26.1	26.2	K03	5×320, 45°	390(B),330 (R)	1997 Mar
NGC 6629	009.4–05.0	0.0	0.0	712.8	723.0	17.6	21.1	M02	5×320, 45°	420(B),360(R)	1997 Mar/Apr

^a For Hen 3-1333 and Hen 2-113, [N II] λ 6548 emission fluxes are listed.

Note. References for line fluxes from the literature are as follows: D21, This work; D97, De Marco et al. (1997); G07, Girard et al. (2007); G12, García-Rojas et al. (2012); K91, Kaler et al. (1991); K03, Kwitter et al. (2003); M02, Milingo et al. (2002); P01, Peña et al. (2001) and Peña et al. (1998); W07, Wang & Liu (2007). Archival spectra associated with nebular regions were extracted from long-slits passing through the central stars, oriented with the position angles (given in degrees ° on the right-hand side of the slit dimensions) if specified, and some of them were taken using different exposures for blue (B) and red (R) arms.

collimated outflows were also present in the other PNe of our sample: M 1-32, M 3-15 (Akras & López 2012), M 2-42 (Danehkar et al. 2016), and Hb 4 (Derlopa et al. 2019; Danehkar 2021).

The spectra were reduced using the IRAF pipeline *wifes* (version 2.14; see Dopita et al. 2010). The reduction involves flat-fielding, wavelength calibration, spatial calibration, sky subtraction and flux calibration (described in detail by Danehkar et al. 2013, 2014; Danehkar 2014).

To extract flux intensities and uncertainties based on the root-mean-squared (RMS) deviation, we applied the IDL library MGFIT to the spectrum of each object, which matches multiple Gaussian functions to a list of emission lines using a random walk method optimized based on a genetic algorithm (Wesson 2016). We also verified the automatically identified lines and manually removed any misidentified lines from the final list. The RMS deviation of the continuum near each line is quantified in order to estimate uncertainties of each fitted line according to the signal-dependent noise models (Landman et al. 1982; Lenz & Ayres 1992).

We explored the literature to include those optical lines outside the wavelength coverage of the ANU/WiFeS observations that are necessary for our comprehensive plasma diagnostics and abundance analyses. As ionization structures of PNe are typically inhomogeneous (see e.g. Danehkar et al. 2018; Akas & Gonçalves 2016; Akas et al. 2020), different

observations of a nebula can be combined if they are roughly associated with the same region having the same excitation conditions. Thus, we adopted those archival data, which have similar ionization properties based on observed fluxes of the diagnostic emission lines He II λ 4686, [O III] λ 5007, and [N II] λ 6584 (or λ 6548). These observations mostly employed the slits placed over the entire nebulae passing through the central stars, which are similar to the apertures covering the nebulae used to extract our WiFeS spectra (see Figure 1). Table 2 compares the observed fluxes of the diagnostic lines He II, [O III], and [N II] measured by the WiFeS with those from the selected archival data. It can be seen that there are generally reasonable agreements between the WiFeS and archival data included in our study. Table 2 also presents the observing logs of the archival data, including the observing long-slit dimensions (Column 10; also the position angle if it is specified), exposure time (Column 11), and observing date (Column 12).

Basic data for the nebulae are presented in Table 3, including the absolute total flux of H β (Column 3), the radio flux densities at 1.4 and 5 GHz (Columns 4 and 5) and the nebular angular-dimensions measured in the optical and in radio observations (Columns 6 and 7), and the interstellar extinctions (Columns 8–10; described in § 2.1). The nebular angular-dimensions are mostly based on Tylenda et al. (2003),

Table 3. Basic data for the nebulae, including the absolute total $H\beta$ flux, the 1.4 and 5 GHz radio flux densities, the optical and radio angular-dimensions, and the interstellar extinctions $c(H\beta)$ from the Balmer flux ratio $H\alpha/H\beta$, the radio- $H\beta$ method, and the literature.

Name	PNG	$\log F(H\beta)(C92)$ ($\text{erg cm}^{-2} \text{s}^{-1}$)	$F(1.4 \text{ GHz})$ (C98)(mJy)	$F(5 \text{ GHz})$ (S10)(mJy)	Angular diameter (arcsec)		$c(H\beta)$		
					(optical)	(radio)	(Balmer)	(radio)	(literature)
PB 6	278.8+04.9	-11.87	-	30.0	11.0(A92)	-	$0.543^{+0.036}_{-0.031}$	0.738	0.52(A03)
M 3-30	017.9-04.8	-12.29	8.6	7.3	$19.2 \times 18.5(\text{T03})$	22.0(A92)	$1.005^{+0.013}_{-0.013}$	0.602	1.30(A03)
Hb 4 (shell)	003.1+02.9	-11.96	158.0	166.0	$11.4 \times 7.4(\text{T03})$	7.5(A92)	$1.851^{+0.008}_{-0.009}$	1.689	1.99(A03)
Hb 4 (N-knot)	003.1+02.9	-	-	-	-	-	$2.089^{+0.029}_{-0.033}$	-	-
Hb 4 (S-knot)	003.1+02.9	-	-	-	-	-	$1.908^{+0.045}_{-0.057}$	-	-
IC 1297	358.3-21.6	-10.95	59.9	69.0	$10.9 \times 9.9(\text{T03})$	-	$0.221^{+0.015}_{-0.013}$	0.284	0.19(A03)
Th 2-A	306.4-00.6	-12.80(A92)	-	60.0	$27.7 \times 25.2(\text{T03})$	-	$1.079^{+0.022}_{-0.021}$	2.059	0.93(M02)
Pe 1-1	285.4+01.5	-12.26	-	125.3	3.0(A92)	-	$1.943^{+0.005}_{-0.007}$	1.886	1.87(A03)
M 1-32	011.9+04.2	-12.20(A92)	70.5	64.0	$9.4 \times 8.3(\text{T03})$	9.0(A92)	$1.347^{+0.024}_{-0.028}$	1.542	1.59(A03)
M 3-15	006.8+04.1	-12.45(A92)	48.4	65.0	4.2(A92)	5.0(A92)	$2.251^{+0.010}_{-0.011}$	1.828	2.10(A03)
M 1-25	004.9+04.9	-11.90	40.3	55.0	4.6(A92)	3.2(A92)	$1.596^{+0.005}_{-0.004}$	1.197	1.46(A03)
Hen 2-142	327.1-02.2	-11.85	-	65.0	$4.4 \times 3.5(\text{T03})$	-	$1.554^{+0.091}_{-0.087}$	1.234	1.73(A03)
Hen 3-1333	332.9-09.9	-12.15	-	26.0(P82)	$3.6 \times 3.4(\text{T03})$	-	$1.064^{+0.020}_{-0.021}$	-	1.00(A03)
Hen 2-113	321.0+03.9	-11.82	-	115.0(P82)	$3.7 \times 4.8(\text{D15})$	-	$1.335^{+0.028}_{-0.025}$	-	1.48(A03)
K 2-16	352.9+11.4	-12.62(F13) ^a	2.5	-	$26.6 \times 24.3(\text{T03})$	-	$0.499^{+0.043}_{-0.040}$	-	0.97(A03)
NGC 6578	010.8-01.8	-11.57	162.4	166.0	$12.1 \times 11.8(\text{T03})$	-	$1.510^{+0.010}_{-0.009}$	1.341	1.39(K03)
M 2-42	008.2-04.8	-12.12	9.8	14.0	$4.0 \times 4.0(\text{S08})$	-	$0.979^{+0.031}_{-0.028}$	0.806	1.03(A91)
NGC 6567	011.7-00.6	-10.95	163.3	161.0	$8.1 \times 6.4(\text{T03})$	-	$0.770^{+0.008}_{-0.006}$	0.672	0.70(K03)
NGC 6629	009.4-05.0	-10.93	264.0	265.8	$16.6 \times 15.5(\text{T03})$	-	$0.975^{+0.008}_{-0.009}$	0.905	0.90(P11)
Sa 3-107	358.0-04.6	-12.95(F13) ^a	5.2(C99)	-	8.0×8.0^b	-	$1.616^{+0.009}_{-0.010}$	-	-

^a Calculated from the observed intensity of $H\alpha$ using the logarithmic extinction formula.

^b Determined at ~ 10 percent of mean surface brightness isophote of $H\alpha$ images obtained from Parker et al. (2005).

Note. References are as follows: A91 – Acker et al. (1991); A92 – Acker et al. (1992); A03 – Acker & Neiner (2003); C92 – Cahn et al. (1992); C98 – Condon & Kaplan (1998); C99 – Condon et al. (1999); D15 – Danehkar & Parker (2015); F13 – Frew et al. (2013); K03 – Kwitter et al. (2003); M02 – Milingo et al. (2002); P11 – Pottasch et al. (2011); P82 – Purton et al. (1982); S08 – Stanghellini et al. (2008); S10 – Stanghellini & Haywood (2010); T03 – Tylenda et al. (2003).

one of them is from ~ 10 percent of mean $H\alpha$ surface brightness (Parker et al. 2005).

2.1. Flux Measurement and Interstellar Extinction

Table 4 presents a full list of observed lines and their measured fluxes (the full table is available in the machine-readable format). The laboratory wavelength, the emission line identification, and the observed wavelength are given in the first 3 columns, followed by the observed fluxes with the RMS errors (in percentage), and the fluxes after correction for interstellar extinction with the associated errors (in percentage) at the 90% confidence levels in the next columns. The multiplet number, the lower and upper terms of the transition, and the statistical weights of the lower and upper levels are presented in the ending columns. All fluxes are given relative to $H\beta$, on a scale where $H\beta = 100$. The line fluxes adopted from the archival data are also listed in Table 4.

The logarithmic extinction $c(H\beta)$ at $H\beta$ was obtained from the observed Balmer emission line $H\alpha/H\beta$ flux ratio and its theoretical line ratio for case B recombination (Storey & Hummer 1995, based on the physical conditions of low-excited CELs derived in § 3). For M 2-42, the $H\alpha$ emission was saturated in some spaxels over the main shell in the WiFeS

observation, so we adopted the $H\alpha$ emission flux measured by Wang & Liu (2007). Each flux intensity was then dereddened using the formula, $I(\lambda) = 10^{c(H\beta)[1+f(\lambda)]} F(\lambda)$, where $F(\lambda)$ and $I(\lambda)$ are the observed and intrinsic line flux, respectively, and $f(\lambda)$ is the standard Galactic extinction law of $R_V = 3.1$ (Seaton 1979; Howarth 1983) normalized such that $f(H\beta) = 0$.

The radio- $H\beta$ extinction was also determined from the observed radio free-free continuum radiation at 5 GHz and the measured $H\beta$ flux using the formula given by Milne & Aller (1975):

$$c(H\beta) = \log \left(\frac{3.28 \times 10^{-9} t^{-0.4} [S_{5\text{GHz}}/F(H\beta)]}{\ln(9900t^{3/2})[1 + (1 - x'')y + 3.7x''y]} \right) \quad (1)$$

where $S_{5\text{GHz}}$ in Jy is the observed 5 GHz flux density (Column 5 in Table 3), $F(H\beta)$ the observed $H\beta$ flux in $\text{erg cm}^{-2} \text{s}^{-1}$ (Column 4 in Table 3), $t \equiv T_e(X^+)/10^4$ is the electron temperature of singly-ionized forbidden lines in 10^4 K (derived in § 3.1), $y = N(\text{He})/N(\text{H})$ the number abundance of helium, and $x'' = N(\text{He}^{++})/N(\text{He})$ the fraction of doubly ionized helium atoms (derived in § 4.2). We assume that hydrogen is fully ionized.

Table 4. Observed and dereddened line fluxes on a scale relative to $H\beta$, where $H\beta = 100$. Observed fluxes are denoted by $F(\lambda)$ and dereddened fluxes by $I(\lambda)$. The symbol ‘*’ in the observed and dereddened fluxes indicates that the listed line is blended with the above listed line.

λ_{lab}	Ion	λ_{obs}	$F(\lambda)$	$\varepsilon_{F(\lambda)}(\%)$	$I(\lambda)$	$\varepsilon_{I(\lambda)}(\%)$	Mult	Lower term	Upper term	g1	g2
PB 6 (PNG278.8+04.9)											
3726.03	[O II] ^a	3726.03	50.700	±0.0	69.898	±2.6	F1	2p3 4S*	2p3 2D*	4	4
3728.82	[O II] ^a	3728.82	*		*		F1	2p3 4S*	2p3 2D*	4	6
3868.75	[Ne III] ^a	3868.75	84.000	±0.0	112.065	±2.3	F1	2p4 3P	2p4 1D	5	5
3889.05	H 8 ^a	3889.05	11.500	±0.0	15.266	+2.3 -1.9	H8	2p+ 2P*	8d+ 2D	8	*
3967.46	[Ne III] ^a	3967.46	30.800	±0.0	40.079	+2.1 -1.8	F1	2p4 3P	2p4 1D	3	5
4101.74	H 6 ^a	4101.74	22.500	±0.0	28.240	±1.8	H6	2p+ 2P*	6d+ 2D	8	72
4340.47	H 5 ^a	4340.47	44.200	±0.0	51.795	±1.3	H5	2p+ 2P*	5d+ 2D	8	50
4363.21	[O III] ^a	4363.21	17.100	±0.0	19.904	+1.3 -1.0	F2	2p2 1D	2p2 1S	5	1
4452.37	O II	4453.76	0.053	±16.7	0.060	+20.9 -22.8	V5	3s 2P	3p 2D*	4	4
4471.50	He I	4472.51	2.061	±1.5	2.322	±2.2	V14	2p 3P*	4d 3D	9	15
4491.23	O II	4493.19	0.019	±23.1	0.021	+28.7 -31.2	V86a	3d 2P	4f D3*	4	6
4510.91	N III	4511.90	0.207	±4.5	0.230	±5.8	V3	3s' 4P*	3p' 4D	2	4
4514.86	N III	4516.17	0.066	±19.8	0.073	+24.4 -26.7	V3	3s' 4P*	3p' 4D	6	8
4541.59	He II	4542.59	4.340	±0.6	4.787	+1.1 -1.0	4.9	4f+ 2F*	9g+ 2G	32	*
4562.60	Mg I]	4563.59	0.112	±7.1	0.123	+8.8 -9.3		3s2 1S	3s3p 3P*	1	5
4571.10	Mg I]	4572.04	0.174	±5.4	0.190	±6.7		3s2 1S	3s3p 3P*	1	3
4607.03	[Fe III]	4607.70	0.233	±5.3	0.252	+6.5 -7.1	F3	3d6 5D	3d6 3F2	9	7
...											

^a Fluxes adopted from the literature: PB 6 (K91), M 3-30 (P01,G07), Hb 4 shell (P01,G07), Hb 4 N-knot (H97), Hb 4 S-knot (H97), IC 1297 (M02), Th 2-A (M02), Pe 1-1 (G12), M 1-32 (G12), M 3-15 (P01), M 1-25 (G07), Hen 2-142 (G07), Hen 3-1333 (D97), Hen 2-113 (D97), K 2-16 (P01), NGC 6578 (K03), M 2-42 (W07), NGC 6567 (K03), NGC 6629 (M02). References for line fluxes from the literature are as follows: D97, De Marco et al. (1997); G07, Girard et al. (2007); G12, García-Rojas et al. (2012); H97, Hajian et al. (1997); K91, Kaler et al. (1991); K03, Kwitter et al. (2003); M02, Milingo et al. (2002); P01, Peña et al. (2001) and Peña et al. (1998); W07, Wang & Liu (2007).

Note: Table 4 is published in its entirety in the machine-readable format. A portion is shown here for guidance regarding its form and content.

Table 3 compares $c(H\beta)$ derived from the Balmer flux ratio $H\alpha/H\beta$ (Column 8) with those from the radio- $H\beta$ method (Column 9) and the literature (Column 10). We see that there are generally good agreements between them. However, there are some discrepancies in a small number, which could be due to the uncertainties in the measured values of $F(H\beta)$, derived electron temperatures, helium ionic abundances and observed 5-GHz continuum fluxes.

3. Plasma Diagnostics

3.1. CEL Plasma Diagnostics

Nebular electron temperatures T_e and densities N_e were obtained from the intrinsic intensities of CELs by solving level populations for an n -level (≥ 5) atomic model using the IDL library proEQUIB (Danehkar 2018b). To propagate uncertainties in fluxes, we utilized an IDL implementation of the affine-invariant Markov chain Monte Carlo (MCMC) ensemble sampler proposed by Goodman & Weare (2010). For the MCMC computations, we adopted a confidence level of 90% and a uniform distribution on the range covered by the errors of each observed line flux to propagate flux uncertainties into the extinction, dereddened line fluxes, physical conditions and chemical abundances.

The atomic data references are listed in Table 5. For the abundance analyses, we carefully adopted the atomic data

sets from the CHIANTI database version 7.0 (Landi et al. 2012) and 9.0 (Dere et al. 2019), assembled into the AtomNeb library (Danehkar 2019), including the energy levels (E_j), collision strengths (Ω_{ij}), and transition probabilities (A_{ij}) for CELs, and effective recombination coefficients (α_{eff}) and branching ratios (Br) for ORLs. The diagnostic procedure was done in an iterative way to provide self-consistent results for $N_e([S II])$ and $T_e([N II])$, i.e., a representative initial $T_e([N II])$ was assumed to calculate N_e ; then T_e was derived in conjunction with the derived $N_e([S II])$, and the procedure iterated to provide self-consistent results. We used the temperature $T_e([N II])$ for deriving $N_e([O II])$, whereas the temperature $T_e([O III])$ from high-excitation CELs was adopted for $N_e([Ar IV])$ and $N_e([Cl III])$ where adequate lines were available. The density from high-excitation CELs, either $[Ar IV]$ or $[Cl III]$, was also used to calculate $T_e([O III])$.

The derived electron temperatures and densities for our sample of PNe are presented in Table 6. The diagnostic type (T_e or N_e), ion, diagnostic lines are given in Columns 1–3, respectively. The derived values of T_e are N_e with the corresponding uncertainties are given for each PN in the last column. Figure 2 shows the N_e – T_e diagnostic diagram of PB 6 (the corresponding diagrams for all the other objects can be found in the online version of the journal).

Table 5. References for atomic data.

Ion	Transition probabilities	Collision strengths
N ⁰	Tachiev & Froese Fischer (2002)	Tayal (2006)
N ⁺	Tachiev & Froese Fischer (2001)	Tayal (2011)
O ⁰	Froese Fischer & Tachiev (2004)	Zatsarinny & Tayal (2003), Bell et al. (1998)
O ⁺	Zeippen (1982)	Kisielius et al. (2009)
O ²⁺	Storey & Zeippen (2000), Tachiev & Froese Fischer (2001)	Lennon & Burke (1994), Bhatia & Kastner (1993)
Ne ²⁺	Daw et al. (2000), Landi & Bhatia (2005)	McLaughlin & Bell (2000)
Ne ³⁺	Merkelis et al. (1999)	Ramsbottom et al. (1998)
S ⁺	Nahar (unpublished, 2001)	Ramsbottom et al. (1996)
S ²⁺	Froese Fischer et al. (2006), Tayal (1997)	Hudson et al. (2012)
Cl ²⁺	Mendoza & Zeippen (1982)	Ramsbottom et al. (2001)
Ar ²⁺	Biémont & Hansen (1986)	Galavis et al. (1995)
Ar ³⁺	Dere et al. (2019)	Ramsbottom et al. (1997), Ramsbottom & Bell (1997)
Ar ⁴⁺	Biemont & Bromage (1983)	Galavis et al. (1995)
Fe ²⁺	Ercolano et al. (2008)	Ercolano et al. (2008)
Ion	Effective recombination coefficients	Case
H ⁺	Storey & Hummer (1995)	B
He ⁺	Porter et al. (2013)	B
He ²⁺	Storey & Hummer (1995)	B
C ²⁺	Davey et al. (2000)	A, B
C ³⁺	Péquignot et al. (1991)	A
N ²⁺	Fang et al. (2011, 2013)	B
N ³⁺	Péquignot et al. (1991)	A
O ²⁺	Storey et al. (2017)	B

3.1.1. Electron Densities

The electron densities deduced from various CEL diagnostic ratios, [S II], [O II], [Ar IV] and [Cl III], are presented in Table 6. The ionization potential of S⁺ and O⁺, 10.4 and 13.6 eV, are below those of Cl²⁺ and Ar³⁺, 23.8 and 40.7 eV, respectively, so these density-diagnostic lines are emitted from dissimilar ionization zones. For PB 6, the electron density derived from [Ar IV] is lower than those from [Cl III], while these lines arise from high excitation regions. For the shell of Hb 4, the density derived from [O II] doublet is lower by a factor of 2 than that from [S II] and [Cl III]. IC 1297 does not seem to have a large density variation, since densities from different ions are roughly close. The discrepancy between densities from low- and high-excited CELs in some objects could be related to inhomogeneous condensations. We notice that the [Ar IV] $\lambda\lambda 4711, 4740$ doublet lines have the highest critical densities among all the density-diagnostic lines.¹ With the relatively low densities prevailing in PB 6, M 3-30, and IC 1297, the $\lambda 4711/\lambda 4740$ flux ratios are less sensitive to density, so small errors in the measurement of those lines give rise to very high uncertainties in the derived densities. The [S II] and [O II] doublets yield roughly the similar density in Pe 1-1. However, for M 3-30, Hb 4, M 1-32 and M 3-15, the

¹ Critical densities N_{cr} with $T_e = 10\,000$ K and the atomic data from Table 5: [S II] $\lambda\lambda 6717, 6731$, $N_{\text{cr}} = 1730, 5010 \text{ cm}^{-3}$; [O II] $\lambda\lambda 3726, 3729$, $N_{\text{cr}} = 4090, 1210 \text{ cm}^{-3}$; [Ar IV] $\lambda\lambda 4711, 4740$, $N_{\text{cr}} = 12\,510, 96\,920 \text{ cm}^{-3}$; [Cl III] $\lambda\lambda 5518, 5538$, $N_{\text{cr}} = 5200, 24\,950 \text{ cm}^{-3}$, respectively.

densities derived from the [S II] and [O II] are very different, while they are emitted from similar ionization zone. This might be due to the poor quality of the [O II] $\lambda\lambda 3726, 3729$ emission lines measured from the blue end of the spectrum (see e.g. Rodríguez 2020). Alternatively, it may be explained by the atomic data (see Kisielius et al. 2009). For PB 6, the density derived from the [Cl III] diagnostic line ratios is slightly higher than that from the [S II] doublet. The [Cl III] diagnostic lines with higher critical densities could preferentially be emitted from a higher density medium. This behavior suggests the presence of density inhomogeneities in this object.

Fig. 3 (top panel) shows the electron density N_e from singly-ionized CELs ([S II]; apart from [O II] in K 2-16) plotted against the intrinsic nebular H β surface brightness. The dashed line represents a linear fit to the logarithmic values for the 18 PNe, which has a Pearson correlation coefficient of $r = 0.77$ and a null-hypothesis testing p -value of 0.0002:

$$\log N_e = (4.582 \pm 0.219) + (0.508 \pm 0.105) \log S(\text{H}\beta) \quad (2)$$

where the dereddened nebular H β surface brightness is defined as the integrated H β flux divided by the nebular area, $S(\text{H}\beta) = I(\text{H}\beta)/(\pi r^2)$, in unit of $\text{erg cm}^{-2} \text{ s}^{-1} \text{ sr}^{-1}$, the intrinsic H β flux $I(\text{H}\beta) = 10^{c(\text{H}\beta)} F(\text{H}\beta)$, and r is the nebular optical angular radius (see Table 1). It is in agreement with the theoretical relation approximated by O'Dell (1962), $S(\text{H}\beta) \propto \varepsilon r N_e^2 \propto \varepsilon^{2/3} M^{1/3} N_e^{5/3}$, where M is the total mass of the nebula and ε is the filling factor. The nebular H β surface brightness was found to decline with radii as the nebula expands and the density drops (Stanghellini et al. 2002, 2003,

Table 6. Plasma diagnostics based on CELs.

Type	Ion	Diagnostic	Value
PB 6 (PNG278.8+04.9)			
T_e	[N II]	6548.10+6583.50 /5754.60	11300^{+200}_{-260}
$T_{e\text{rc}}$	[N II]	6548.10+6583.50 /5754.60	10270^{+220}_{-220}
T_e	[O III]	4958.91+5006.84 /4363.21	14220^{+110}_{-90}
$T_{e\text{rc}}$	[O III]	4958.91+5006.84 /4363.21	14040^{+90}_{-130}
N_e	[S II]	6730.82 /6716.44	1800^{+400}_{-320}
N_e	[Ar IV]	4740.17 /4711.37	1370^{+70}_{-100}
N_e	[Cl III]	5537.60 /5517.66	2190^{+390}_{-270}
...			

Note: Table 6 is published in its entirety in the machine-readable format. A portion is shown here for guidance regarding its form and content. The label “rc” indicates that the auroral lines, [N II] $\lambda 5755$ and [O III] $\lambda 4363$, are corrected for recombination contribution.

2008; Frew et al. 2016), so it can represent an evolutionary indicator of the nebula.

3.1.2. Electron Temperatures

The electron temperatures deduced from the ratios of the nebular lines to auroral lines are presented in Table 6. We also derived $T_e(\text{[N II]})$ and $T_e(\text{[O III]})$ after removing recombination contributions from the auroral lines where adequate recombination lines were available (labeled by “rc”).

Recombination excitation can make a significant contribution to the [N II] $\lambda 5755$ auroral line, the [O II] $\lambda\lambda 3726, 3729$ nebular lines, and the [O II] $\lambda\lambda 7320, 7330$ auroral lines; but only a small contribution to the [O III] $\lambda 4363$ auroral line. Most nitrogen is in the form of N^{2+} , so the recombination contribution to the [N II] auroral line is significant. As most oxygen is in the form of O^{2+} , the recombination contribution from O^{3+} to the [O III] auroral line is insignificant. The recombination contribution can lead to apparently high temperatures deduced from the [N II] $(\lambda 6548 + \lambda 6584) / \lambda 5755$ ratio. Furthermore, this could also lead to over-estimated temperatures in nebulae containing inhomogeneous condensations, whose density is higher than the critical densities of the nebular lines (Viegas & Clegg 1994). Owing to the relatively low critical densities of the [N II] nebular lines,² the presence of density inhomogeneities may lead to apparently high electron temperatures. Because of the fairly low critical densities of the [O II] $\lambda\lambda 3726, 3729$ nebular lines, their recombination emissivities depend also on electron density, in addition to electron temperature and abundance, which make these lines difficult to interpret when

² Critical densities N_{cr} with $T_e = 10\,000\text{ K}$ and the atomic data from Table 5: [N II] $\lambda\lambda 5755, 6584$, $N_{\text{cr}} = 1.646 \times 10^7, 8.88 \times 10^4\text{ cm}^{-3}$; [O III] $\lambda\lambda 4363, 5007$, $N_{\text{cr}} = 2.554 \times 10^7, 6.874 \times 10^5\text{ cm}^{-3}$, respectively.

the nebula contains inhomogeneous condensations and/or chemical inhomogeneities.

The recombination contribution to the [N II] $\lambda 5755$ auroral line can be estimated using the formula given by Liu et al. (2000):

$$\frac{I_{\text{R}}(\lambda 5755)}{I(\text{H}\beta)} = 3.19 t^{0.30} \left(\frac{\text{N}^{2+}}{\text{H}^+} \right)_{\text{ORLs}}, \quad (3)$$

where $t \equiv T_e(\text{ORL})/10^4$ is the electron temperature adopted for the ORL abundance analysis in 10^4 K (§ 4.2), and N^{2+}/H^+ is derived from the N II ORLs (described in § 4.2).

We estimate the recombination contribution to the [O III] $\lambda 4363$ auroral line using the following formula by Liu et al. (2000):

$$\frac{I_{\text{R}}(\lambda 4363)}{I(\text{H}\beta)} = 12.4 t^{0.79} \left(\frac{\text{O}^{3+}}{\text{H}^+} \right)_{\text{ORLs}}, \quad (4)$$

where the O^{3+}/H^+ ratio is computed using $\text{O}^{3+}/\text{H}^+ = [(\text{He}/\text{H}^+)^{2/3} - 1] \times (\text{O}^+/\text{H}^+ + \text{O}^{2+}/\text{H}^+)$. The O^{2+}/H^+ ratio is obtained from the O II ORLs (described in § 4.2), while the O^+/H^+ ratio is excluded.

For example in PB 6, which has $T_e(\text{[N II]}) = 11300\text{ K}$, the observed flux of N II lines yields $\text{N}^{2+}/\text{H}^+ = 3.455 \times 10^{-3}$ for $T_e(\text{He I}) = 5580\text{ K}$ and $N_e = 1800\text{ cm}^{-3}$. Inserting them into equation (3), we estimate $I_{\text{R}}(\lambda 5754) = 0.925$ (where $\text{H}\beta = 100$), or 20 per cent of the observed intensity of the $\lambda 5755$ line. After subtracting the recombination contribution from the observed intensity, the [N II] line ratio yields $T_e(\text{[N II]}) = 10270\text{ K}$. We summarize our findings for all objects in Table 6.

Fig. 3 (middle panel) plots $T_e(\text{[O III]})/T_e(\text{[N II]})$ versus the excitation class (EC), where a trend with increasing the EC is seen. We employ the EC defined by Dopita & Meatheringham (1990) as $\text{EC} = 0.45 \times F(\text{[O III] } \lambda 5007) / F(\text{H}\beta)$ if $F(\text{He II } \lambda 4685) / F(\text{H}\beta) \leq 0.12$, otherwise $\text{EC} = 5.54 \times [F(\text{He II } \lambda 4685) / F(\text{H}\beta) + 0.78]$. A linear fit (dashed line) to the 13 PNe in the figure yields

$$\frac{T_e(\text{[O III]})}{T_e(\text{[N II]})} = (0.908 \pm 0.055) + (0.0292 \pm 0.0092) \text{EC}, \quad (5)$$

with a Pearson r -value of 0.69 and a null-hypothesis p -value of 0.009. However, if we instead use the electron temperatures corrected for recombination contribution where available, we obtain a weaker correlation $T_e(\text{[O III]})/T_e(\text{[N II]}) = (0.949 \pm 0.071) + (0.0277 \pm 0.0119) \text{EC}$ with $r = 0.57$ ($p = 0.041$). We caution that the recombination-corrected [N II] temperature is not always reliable due to the N^{2+}/H^+ overestimated from the N II ORLs contaminated by fluorescence (Escalante & Morisset 2005; Escalante et al. 2012).

Eq. (5) is similar to the correlations between $T_e(\text{[O III]})/T_e(\text{[N II]})$ and $I(\lambda 4686)$ obtained by Kingsburgh & Barlow (1994) and Wang & Liu (2007). This thermal trend with the EC can be explained by radiation fields from the central stars. For the same 13 PNe in Fig. 3 (bottom panel), $T_e(\text{[O III]})$ is plotted against $T_e(\text{[N II]})$ having the following linear correlation (dashed line):

$$T_e(\text{[O III]}) = -(1064 \pm 2703) + (1.181 \pm 0.285) T_e(\text{[N II]}) \quad (6)$$

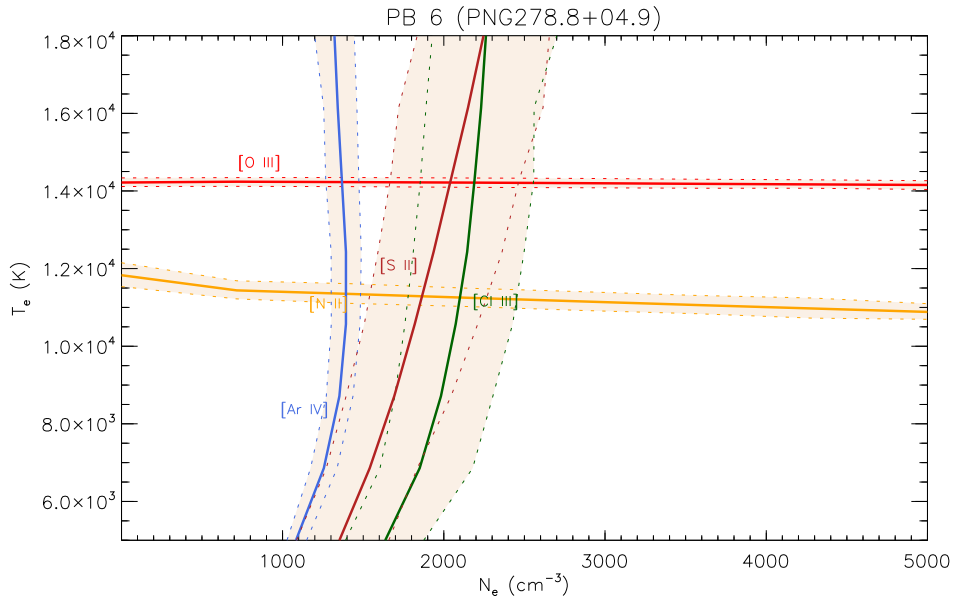


Figure 2. N_e - T_e diagnostic diagram of PB 6 based on CELs. The upper and lower limits at the 90% confidence level are plotted by the dotted lines. The complete figure set (19 images) is available in the online journal.

Fig. Set 2. N_e - T_e diagnostic diagram based on CELs. The upper and lower limits at the 90% confidence level are plotted by the dotted lines.

with $r = 0.78$ and $p = 0.002$. If we instead employ the recombination-corrected temperatures where applicable, we derive a weaker correlation $T_e([\text{O III}]) = -(40 \pm 3433) + (1.125 \pm 0.381) T_e([\text{N II}])$ with $r = 0.67$ ($p = 0.013$).

Eq. (6) confirms that the electron temperatures derived from the $[\text{N II}]$ and $[\text{O III}]$ lines could be associated with the excitation class. However, the recombination-corrected $[\text{N II}]$ temperatures may not correctly describe the ionization structure due to the N II lines created by resonance fluorescence in low-excited PNe.

3.2. ORL Plasma Diagnostics

3.2.1. He I Electron Temperatures

Table 7 presents helium temperatures derived from the flux ratios $\text{He I } \lambda\lambda 5876/4472$, $\lambda\lambda 6678/4472$, $\lambda\lambda 7281/4472$, $\lambda\lambda 7281/5876$ and $\lambda\lambda 7281/6678$. To obtain the electron temperature from the helium line ratios, we used the analytic formula given for the emissivities of He I lines by Benjamin et al. (1999) and fitting parameters calculated by Zhang et al. (2005). The method by Benjamin et al. (1999) is valid for temperatures from 5000–20,000 K. However, Zhang et al. (2005) combined the He I recombination model of Smits (1996) and the collisional excitation rates for the $2s^3\text{S}$ and $2s^1\text{S}$ meta-stable levels by Sawey & Berrington (1993), and provided a new electron temperature diagnostic based on the method developed by Benjamin et al. (1999), but also applicable in the case of $T_e < 5000$ K. Similarly, we employ the MCMC-based approach to propagate the flux errors of the He I lines into our calculations of the helium temperatures. It can be seen that our derived He I temperatures are lower than the forbidden-line temperatures in 8 PNe (see Table 9). However, the helium temperatures is roughly in the range of the temperatures derived from CELs in Pe 1-1, M 3-15, M 1-25, and NGC 6629, and higher than the CEL temperatures in M 2-42.

3.2.2. Physical Conditions from Heavy Element ORLs

Using the fact that emissivities of heavy element ORLs have a relatively weak, power-law dependence on the electron temperature, the relative intensities of ORLs can be used to determine electron temperatures (see e.g. McNabb et al. 2013; Storey & Sochi 2013). Although the plasma diagnostics based on the flux intensity ratio of two different ORLs are the most common way, least squares minimization, relying on a number of lines, can be used as an alternative method. This method is based on minimizing the difference between the normalized intrinsic line flux intensities and the normalized values calculated by the theoretical model. In the least squares minimization method, a single fitting parameter is used, i.e. the electron temperature. We can also use this method to determine the electron density from ORLs. The electron temperatures derived from ORLs were adopted to calculate the ORL ionic abundances in some PNe where applicable (see Table 10).

To determine the physical conditions from heavy element ORLs, we employed a self-consistent method based on a least-squares minimization (see Fig. 4), which is similar to the ORL plasma diagnostics used in McNabb et al. (2013) and Storey & Sochi (2013). For the ORL plasma diagnostics and abundance analyses, we utilized the effective recombination coefficients α_{eff} of the ions C^{2+} , N^{2+} (case B), and O^{2+} (case B) listed in Table 5. Note that N^{2+} and O^{2+} are the only ions whose density-dependent recombination coefficients have recently been calculated in the density range from 10^2 to 10^5 cm^{-3} , as well as in the temperature range from 125 to 20,000 K for the N^{2+} ion, and from 100 to 25,000 K for the O^{2+} ion.

The effective recombination coefficients α_{eff} are used to calculate the theoretical flux intensity of each emission line at the wavelength λ in the full ranges of the physical conditions N_e and T_e for the N^{2+} and O^{2+} ions (using N_e -dependent

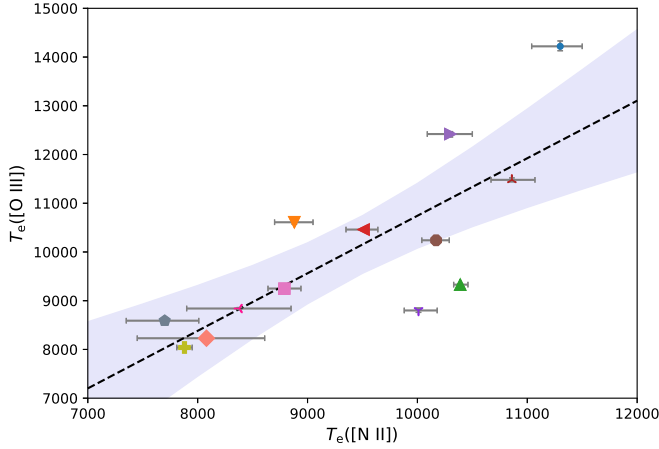
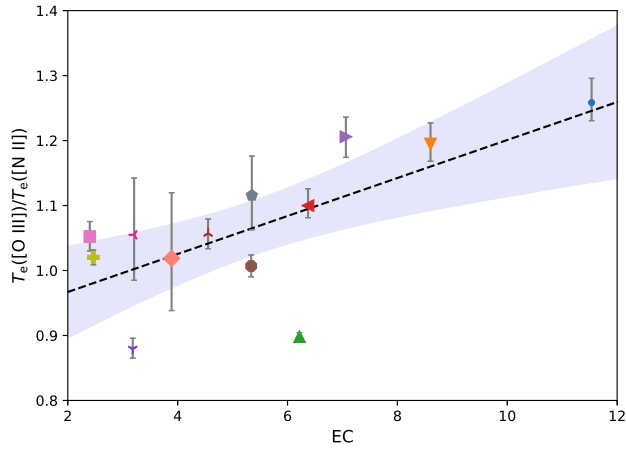
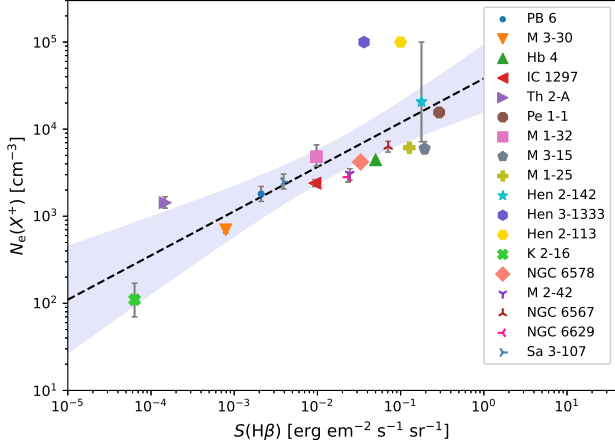


Figure 3. *Top Panel:* The electron density $N_e(X^+)$ (cm^{-3}) from the singly-ionized forbidden lines ([S II], except for [O II] in K2-16) plotted against the intrinsic nebular H β surface brightness $S(\text{H}\beta)$ ($\text{erg cm}^{-2} \text{s}^{-1} \text{sr}^{-1}$). The dashed line is a linear fit to $\log N_e(X^+)$ as a function of $\log S(\text{H}\beta)$ for the 18 PNe, discussed in the text. *Middle Panel:* Variation of $T_e([\text{O III}])/T_e([\text{N II}])$ with excitation class (EC). The dashed line is a linear fit to the 13 points in the figure, discussed in the text. *Bottom Panel:* The electron temperature $T_e([\text{O III}])$ plotted against $T_e([\text{N II}])$, along with a linear fit shown by a dashed line. The gray shaded area in each panel corresponds to the 90% confidence interval of the linear fit.

Table 7. Plasma diagnostics based on He I lines.

Type	Ion	Diagnostic	Value
PB 6 (PNG278.8+04.9)			
T_e	He I	5875.66 / 4471.50	4160^{+540}_{-620}
T_e	He I	6678.16 / 4471.50	6990^{+1690}_{-1190}
T_e	He I	Mean	5580^{+1110}_{-1020}
...			

Note: Table 7 is published in its entirety in the machine-readable format. A portion is shown here for guidance regarding its form and content.

Table 8. Plasma diagnostics based on heavy element ORLs.

Type	Ion	Diagnostic	Value
PB 6 (PNG278.8+04.9)			
T_e	N II	4613.87, 4788.13, 5676.02, 5931.78	6300^{+9700}_{-3100}
N_e	N II	4613.87, 4788.13, 5676.02, 5931.78	80600^{+0}_{-79900}
...			

Note: Table 8 is published in its entirety in the machine-readable format. A portion is shown here for guidance regarding its form and content.

α_{eff}), and in the full ranges of T_e for C^{2+} :

$$I_{\text{theo}}(\lambda_j) = \frac{\alpha_{\text{eff}}(\lambda_j)}{\alpha_{\text{eff}}(\text{H}\beta)} \frac{4861.33}{\lambda_j(\text{\AA})} \frac{N(X^{i+})}{N(\text{H}^+)} \times 100, \quad (7)$$

where $N(X^{i+})/N(\text{H}^+)$ is the ionic abundance of ion X^{i+} derived from ORLs, whose initial value in the first iteration is calculated using the temperature and density from the CELs.

The physical conditions (N_e and T_e for N^{2+} and O^{2+} , and T_e for C^{2+}) are identified at the minimum value of the following weighted least-squares for ion X^{i+} :

$$\chi^2 = \frac{1}{w_{\text{sum}}} \sum_{j=1}^N w_j (I_{\text{obs}}(\lambda_j) - I_{\text{theo}}(\lambda_j))^2, \quad (8)$$

where χ^2 is the sum of the weighted least-squares over N ORLs used for ion X^{i+} , I_{theo} is the theoretical flux intensity of the emission line λ_j predicted by Eq. (7), I_{obs} is the dereddened flux intensity of the emission line λ_j measured from the observation, the weight is given by $w_j = 1/\sigma_{I_{\text{obs}}(\lambda_j)}^2$, $\sigma_{I_{\text{obs}}(\lambda_j)}$ is the absolute error of the dereddened flux intensity $I_{\text{obs}}(\lambda_j)$ of the observed line λ_j , and $w_{\text{sum}} = \sum_{j=1}^N w_j$ is the total of weights.

The physical conditions (T_e and if possible N_e) derived from the weighted least-squares minimization method are used to calculate the ionic abundance $N(X^{i+})/N(\text{H}^+)$. The new

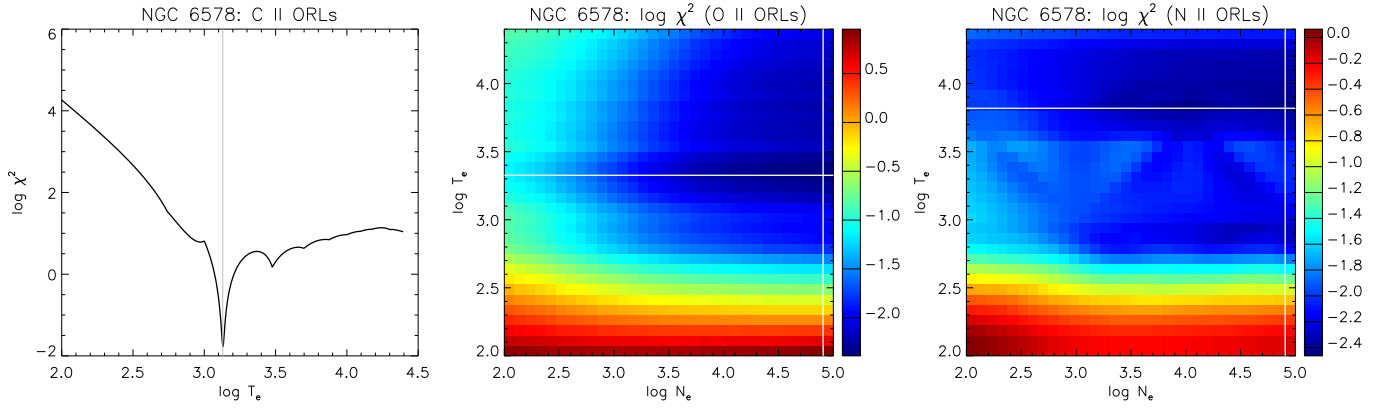


Figure 4. T_e diagnostic diagrams of NGC 6578 based on C II ORLs, N_e – T_e diagnostic diagrams based on O II and N II ORLs. The best-fitting physical conditions at χ^2_{\min} are shown by the solid lines. The complete figure set (21 images) is available in the online journal.

Fig. Set 4. T_e diagnostic diagrams based on C II ORLs, and N_e – T_e diagnostic diagrams based on O II and N II ORLs. The best-fitting physical conditions at χ^2_{\min} are shown by the solid lines.

Table 9. Summary of electron temperatures (T_e) and densities (N_e) obtained from CELs and ORLs.

Name	PNG	$T_e/T_{e\text{rc}}[\text{N II}]$ (CEL)	$T_e/T_{e\text{rc}}[\text{O III}]$ (CEL)	$N_e[\text{S II}]$ (CEL)	$N_e[\text{Cl III}]$ (CEL)	$N_e[\text{Ar IV}]$ (CEL)	T_e He I (ORL)	T_e N II (ORL)	T_e O II (ORL)	T_e C II (ORL)	N_e N II (ORL)	N_e O II (ORL)
PB 6	278.8+04.9	11300 / 10270	14220 / 14040	1800	2190	1370	5580	6300			$10^{4.9}$	
M 3-30	017.9–04.8	8880	10610 / 9170	700		540	2640	6700			$10^{4.9}$	
Hb 4	003.1+02.9	10390 / 9410	9330 / 9180	4440	4130	5590	2790	6300	2100		$10^{4.9}$	$10^{4.9}$
IC 1297	358.3–21.6	9510 / 9160	10460 / 10400	2400	1960	1780	6560	6700	700	7500	100	$10^{4.9}$
Th 2-A	306.4–00.6	10300 / 9060	12420 / 11740	1430				6700			100	
Pe 1-1	285.4+01.5	10170 / 9190	10240	15580			9390	6600		8800	$10^{4.9}$	
M 1-32	011.9+04.2	8790 / 8480	9250	4840	3930		1320	700		6300	27400	
M 3-15	006.8+04.1	7700	8590	6010		5540	8600	6600			$10^{4.9}$	
M 1-25	004.9+04.9	7880 / 6950	8040	6120	4090		7560					
Hen 2-142	327.1–02.2	8810		20630	21160							
Hen 3-1333	332.9–09.9	7290		10^5								
Hen 2-113	321.0+03.9	8220		10^5								
K 2-16	352.9+11.4	9420		110^a								
NGC 6578	010.8–01.8	8080	8230 / 8220	4200	3390	3250	4710	6600	2100	1300	$10^{4.9}$	$10^{4.9}$
M 2-42	008.2–04.8	10010	8800	3050	2420	3430	11750	800	2100	1600	34000	$10^{4.9}$
NGC 6567	011.7–00.6	10860	11480 / 11470	6340	5340	2440	2590			1900		
NGC 6629	009.4–05.0	8380	8840	2810	2100		7540					
Sa 3-107	358.0–04.6	10840		2480	1400		2160			5500		

^a Electron density derived from the [O II] lines.

Note. The label “rc” indicates that the auroral lines [N II] and [O III] are corrected for recombination contribution. Uncertainties are presented in Tables 6–8.

ionic abundance is then substituted into Eq. (7) to calculate the theoretical intensities of the emission lines in the full ranges of the physical conditions. Again, new physical conditions are determined from the minimization value of the weighted least-squares, χ^2_{\min} , expressed by Eq. (8). This iterative procedure was performed in a self-consistent manner until there are no variation in the physical conditions, which constrains the temperature (and density for O^{2+} and N^{2+}).

Figure 4 shows the least-square distributions ($\log \chi^2$) calculated for O II and N II ORLs in the T_e – N_e space with the minimum value of least-squares χ^2_{\min} at the crossing point of the two solid lines, and the least-square diagram ($\log \chi^2$) for C II ORLs in the T_e range with χ^2_{\min} located at the solid line. Following Storey & Sochi (2013), the uncertainties are

determined at the lower and upper limits $\chi^2_{\min} + 1$ of the least-squares normalized by χ^2_{\min} .

Table 8 presents the electron temperatures (T_e) and densities (N_e) derived from heavy element ORLs for those PNe where adequate recombination lines were available. It can be seen that the ORLs are emitted from ionized regions having temperatures lower than the regions from which CELs originate in several PNe. Seven PNe have detection of the multiplet V17.04 ($\lambda 6461.95$; 6g–4f) and V16.04 ($\lambda 6151.43$; 6f–4d). The $\lambda 6462$ line is the strongest C II recombination line which was detected in these PNe. We used the Case A effective recombination for $\lambda 6462$, and the Case B for $\lambda 6151$ from the atomic data of Davey et al. (2000) covering 500 to 20 000 K. The Case A effective recombination for $\lambda 6151$ differs from its Case B value by only 2 per cent, indicating that this transition

is case insensitive. The contribution from the blended N II $\lambda 6150.75$ (4p–3d) line is typically negligible.

Table 8 lists the physical condition derived from N II ORLs for 10 PNe. The effective recombination coefficients of N II calculated by Fang et al. (2011, 2013) are in the range from 125 to 20,000 K, which allow us to identify any cold ionized regions. The well-detected $\lambda 5931.78$ line in 5 PNe (PB 6, Hb 4, IC 1297, Th 2-A, and Pe 1-1) are likely to provide the most reliable diagnostic line as this line can mostly be produced by recombination from the $3p^3P-3d^3D^\circ$ level of N^{2+} and the V28 multiplet in high-excited nebulae. Using all lines from the same multiplet might reduce the effect of any errors caused by atomic data, which were not available in all the objects. The lines $\lambda 5666.63$ and $\lambda 5679.56$ can be produced by recombination from the $3p^3D-3s^3P^\circ$ level of N^{2+} and the V3 multiplet, but these lines can be largely contaminated by fluorescence (Escalante & Morisset 2005; Escalante et al. 2012), especially in low-excited PNe. The line $\lambda 5679.56$ in M 3-30, M 1-32, M 3-15, NGC 6578, and NGC 6567 with the $T_{\text{eff}} \sim 50-60$ kK could be produced by fluorescence, so they were not employed in our analysis of these objects. Similarly, the line $\lambda 5666.63$ detected in M 1-32, M 1-25, and NGC 6567 was excluded. For M 2-42, we did not use the strong lines $\lambda 5666.63$ and $\lambda 5679.56$, which could be largely excited by resonance fluorescence. The lines $\lambda 5679.56$, 5666.63 , 5931.78 and 5710.77 , which are possibly produced by fluorescence, were also excluded in Sa 3-107. However, we kept these lines in other objects with $T_{\text{eff}} \gtrsim 75$ kK where they could be excited by recombination process. The $\lambda 5676.02$ line from the V3 multiplet ($3p^3D-3s^3P^\circ$) is the strongest N II recombination line with low uncertainty detected in Hb 4, whereas $\lambda 4442.02$ (V55a) has a higher uncertainty, and $\lambda 4621.39$ (V92) and $\lambda 5931.78$ (V28) are relatively very weak. For Th 2-A with $T_{\text{eff}} \sim 157$ kK, the $\lambda 5679.56$ line is produced by recombination from the $3p^3D-3s^3P^\circ$ level of N^{2+} and the V3 multiplet, and $\lambda 5931.78$ line from the V28 multiplet. The $\lambda 5676.02$ ORL from the V3 multiplet is stronger than those from $\lambda 5931.78$ from the V28 multiplet in the spectra of Hb 4.

Table 8 also lists the physical conditions obtained from O II ORLs for 4 PNe. The recombination lines from the V1 multiplet ($3p^4D^\circ-3s^4P$), here $\lambda 4641.81$, $\lambda 4661.63$ and $\lambda 4676.24$, are likely to provide the most reliable temperature diagnostics (see e.g. Wesson et al. 2005; McNabb et al. 2013). Using several ORLs from the same multiplet might reduce any effects of deviation from local thermodynamic equilibrium (LTE) at low densities. Tsamis et al. (2003b) found that the relative intensities of O II V1 multiplet components deviate from LTE predictions for those PNe having electron densities lower than 1000 cm^{-3} (e.g. NGC 3132 with $N_e = 600 \text{ cm}^{-3}$). This effect may be reduced by using all the lines from the V1 multiplet (e.g. Wesson et al. 2005).

4. Abundance Analyses

4.1. Ionic Abundances from CELs

We determined abundances for ionic species of N, O, Ne, S, Cl, Ar and Fe from CELs. To derive ionic abundances, we solve the statistical equilibrium equations for each ion using the IDL library proEQUIB, giving level population and line emissivities for specified T_e and N_e . In Table 9,

we summarize physical conditions obtained from CELs and ORLs. Table 10 also lists the T_e and N_e adopted for our CEL abundance analysis. The electron temperatures derived from [N II] and [O III] in § 3.1.2 were employed for low- and high-excited lines, respectively, where they are available and reliable. We were careful to use the recombination-corrected temperatures due to potentially overestimated N^{2+} as discussed in § 3.1.2. Similarly, the electron densities obtained in § 3.1.1 were utilized for low and high-excited CELs where they are available and applicable. The CELs used to determine ionic abundances are listed in Table 11 (the full table is available in the machine-readable format). The uncertainties in ionic abundances are determined using the MCMC ensemble sampler from the flux errors without accounting for the uncertainties estimated for T_e and N_e . As the CEL emissivity calculation has an exponential dependence on T_e , including the uncertainties of the physical conditions leads to large uncertainties in abundances. The accurate determination of abundances depends on the adopted physical conditions. Once the level population are solved, the ionic abundances X^{i+}/H^+ are calculated from the intrinsic intensities of CELs as follows:

$$\frac{N(X^{i+})}{N(H^+)} = \frac{I(\lambda_{ij})}{I(H\beta)} \frac{\lambda_{ij}(\text{\AA})}{4861.33} \frac{\alpha_{\text{eff}}(H\beta)}{A_{ij}} \frac{N_e}{n_i}, \quad (9)$$

where $I(\lambda_{ij})$ is the dereddened flux of the emission line λ_{ij} emitted by ion X^{i+} following the transition from the upper level i to the lower level j , $I(H\beta)$ the dereddened flux of $H\beta$, $\alpha_{\text{eff}}(H\beta)$ the effective recombination coefficient of $H\beta$, $n_i(T_e, N_e, A_{ij}, \Omega_{ij})$ the fractional population of the upper level i , A_{ij} the Einstein spontaneous transition probability, and Ω_{ij} the collision strength of the transition.

The weighted-average ionic abundances of N lines (see Table 13 and § 4.3) are calculated as follows:

$$\left(\frac{N(X^{i+})}{N(H^+)} \right)_{\text{mean}} = \frac{1}{W_{\text{tot}}} \sum_{j=1}^N \frac{N(X^{i+})}{N(H^+)}, \quad (10)$$

where $W_{\text{tot}} = \sum_{j=1}^N W_j$ is the sum of the weights, and W_j are the weights given in Table 11 calculated based on the predicted intrinsic fluxes at the given physical conditions and normalized by the minimum value of W_j .

For the CEL abundance analysis of each object, we adopted the density and temperature based on the results from our CEL plasma diagnostics in Section 3, as listed in Table 9. Following Kingsburgh & Barlow (1994), we mostly adopted $T_e(\text{[N II]})$ for singly ionized species and $T_e(\text{[O III]})$ for ions of higher excitation ions in the CEL abundance calculations where applicable (see Table 10).

The forbidden lines of [O III] $\lambda\lambda 4959, 5007$ were used to derive O^{2+}/H^+ ionic ratios. For O^+/H^+ ionic abundances, we adopted the observed fluxes of the [O II] $\lambda 3727$ doublet and [O II] $\lambda\lambda 7320, 7330$ lines from the literature. We should note that the O^+/H^+ abundance ratios derived from the [O II] $\lambda 3727$ doublet may be more reliable than those derived from the [O II] $\lambda\lambda 7320, 7330$ lines, which may contain recombination contributions and/or being biased towards higher density regions ($N_{\text{cr}} = 3.3-4.9 \times 10^6 \text{ cm}^{-3}$). Moreover, Rodríguez (2020) found that the O^+/H^+ ionic abundances derived from [O II] $\lambda 3727$ and $\lambda 7325$ are largely different due to

Table 10. Electron density and temperatures adopted for our CEL and ORL abundance analyses.

Nebula	PNG	T_e	N_e	T_e	N_e	T_e	N_e
		CEL (Low)	CE (Low)	CEL (High)	CEL (High)	ORL	ORL
PB 6	278.8+04.9	[N II] _{rc}	[S II]	[O III] _{rc}	[Cl III]	He I	[S II]
M 3-30	017.9–04.8	[N II]	[S II]	[O III] _{rc}	[Ar IV]	N II	[S II]
Hb 4 (shell)	003.1+02.9	[N II] _{rc}	[S II]	[O III] _{rc}	[Cl III]	N II	[S II]
Hb 4 (N-knot)	003.1+02.9	[N II]	[S II]	[N II]	[S II]	[N II]	[S II]
Hb 4 (S-knot)	003.1+02.9	[N II]	[S II]	[N II]	[S II]	[N II]	[S II]
IC 1297	358.3–21.6	[N II] _{rc}	[S II]	[O III] _{rc}	[Cl III]	C II	[S II]
Th 2-A	306.4–00.6	[N II] _{rc}	[S II]	[O III] _{rc}	[S II]	N II	[S II]
Pe 1-1	285.4+01.5	[N II] _{rc}	[S II]	[O III]	[S II]	He I	[S II]
M 1-32	011.9+04.2	[N II] _{rc}	[S II]	[O III]	[S II]	C II	[S II]
M 3-15	006.8+04.1	[N II]	[S II]	[O III]	[S II]	He I	[S II]
M 1-25	004.9+04.9	[N II]	[S II]	[O III]	[S II]	He I	[S II]
Hen 2-142	327.1–02.2	[N II]	[Cl III]	[N II]	[Cl III]	[N II]	[Cl III]
Hen 3-1333	332.9–09.9	[N II]	[S II]	[N II]	[S II]	[N II]	[S II]
Hen 2-113	321.0+03.9	[N II]	[S II]	[N II]	[S II]	[N II]	[S II]
K 2-16	352.9+11.4	[N II]	[O II]	[N II]	[O II]	[N II]	[O II]
NGC 6578	010.8–01.8	[N II]	[S II]	[O III] _{rc}	[S II]	He I	[S II]
M 2-42	008.2–04.8	[N II]	[S II]	[O III]	[Ar IV]	[N II]	[S II]
NGC 6567	011.7–00.6	[N II]	[S II]	[O III]	[Cl III]	[N II]	[S II]
NGC 6629	009.4–05.0	[N II]	[S II]	[O III]	[S II]	He I	[S II]
Sa 3-107	358.0–04.6	[N II]	[S II]	[N II]	[S II]	C II	[S II]

Note: The label “rc” indicates that the auroral lines are corrected for recombination contribution. The flux uncertainties are directly propagated into our abundance analysis without considering the uncertainties in the physical conditions. The electron temperature T_e derived for the N-knot is assumed for the S-knot in Hb 4.

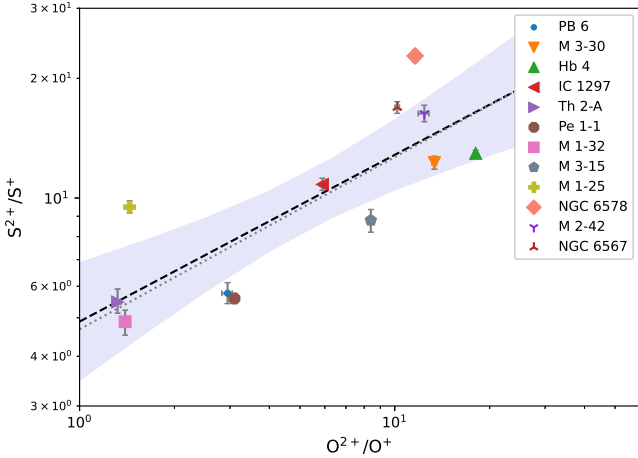


Figure 5. S^{2+}/S^+ versus O^{2+}/O^+ . The dashed line is a least-squares fit that yields $S^{2+}/S^+ = 4.892 (O^{2+}/O^+)^{0.419}$ with the 90% confidence level shown by the lightly shaded area. The dotted gray line shows $S^{2+}/S^+ = 4.677 (O^{2+}/O^+)^{0.433}$ from Kingsburgh & Barlow (1994).

observational uncertainties. The N^+/H^+ abundance ratio was derived from the [N II] $\lambda 6548$ and $\lambda 6584$ lines. We did not use the weak auroral line [N II] $\lambda 5755$ due to its high uncertainty and the recombination contribution from N^{2+} . For most PNe, we determined the S^+/H^+ abundance ratio from the [S II] $\lambda \lambda 6716, 6731$ doublets, and S^{2+}/H^+ from the [S III] $\lambda 6312$. We should note that the [S II] $\lambda \lambda 4068, 4076$ lines are usually weak and affected by recombination processes and density effects. For most PNe, we were able to determine the Ar^{2+}/H^+ abundance ratio from the [Ar III] $\lambda 7136$ and $\lambda 7751$ lines and the Ar^{3+}/H^+ abundance ratio from the [Ar IV] $\lambda \lambda 4711, 4740$ doublet. For some PNe with [WO] central stars, we also derived the Ar^{4+}/H^+ abundance ratio from the [Ar V] $\lambda 4625$ and $\lambda 7005$ lines.

For Sa 3-107, where O^{2+} but not O^+ is observed, the O^+/H^+ ionic ratio was estimated by using a correlation between $\log(O^{2+}/O^+)$ and $\log(S^{2+}/S^+)$. A least-squares fit to the 12 PNe (around stars with $T_{\text{eff}} > 35$ kK) plotted in Fig. 5 yields $S^{2+}/S^+ = 4.892^{+1.009}_{-0.837} (O^{2+}/O^+)^{0.419 \pm 0.099}$ with $r = 0.8$ ($p = 0.0017$) that can be used to estimate O^+ from S^{2+}/S^+ when only O^{2+} is available. Previously, Kingsburgh & Barlow (1994) obtained $S^{2+}/S^+ = 4.677 (O^{2+}/O^+)^{0.433}$ using a least-squares fit to the 22 PNe, which was then used to estimate S^{2+} when only S^+ was observed, and vice versa.

4.2. Ionic Abundances from ORLs

We determined abundances for ionic species of He, C, N and O from ORLs for our sample where adequate observed lines were available. In our calculation, we adopted the electron temperature and density listed in Table 9 (selected T_e and N_e listed in Table 10). The temperatures derived from either CELs or ORLs were delicately chosen for our ORL abundance analysis where they are reliable and applicable. As the densities derived from heavy element ORLs are highly uncertain, we carefully adopted the densities obtained from CELs. The atomic data sets used for the effective recombination coefficients of ORLs are listed in Table 5. Using these effective recombination coefficients, we determine ionic abundances from the measured intensities of ORLs as follows:

$$\frac{N(X^{i+})}{N(H^+)} = \frac{I(\lambda)}{I(H\beta)} \frac{\lambda(\text{\AA})}{4861.33} \frac{\alpha_{\text{eff}}(H\beta)}{\alpha_{\text{eff}}(\lambda)}, \quad (11)$$

where $I(\lambda)$ is the intrinsic line flux of the emission line λ emitted by ion X^{i+} , $I(H\beta)$ is the intrinsic line flux of $H\beta$, $\alpha_{\text{eff}}(H\beta)$ the effective recombination coefficient of $H\beta$, and $\alpha_{\text{eff}}(\lambda)$ the effective recombination coefficient for the emission line λ .

The ionic abundances derived from the ORLs are given in Table 12. To obtain the weighted-average He^+/H^+ ionic

Table 11. Ionic abundances derived from CELs.

Ion	Line	Weight	Abund.
PB 6 (PNG278.8+04.9)			
N ⁺	[N II] λ 6548.10	1	$4.225^{+0.142}_{-0.164} \times 10^{-5}$
N ⁺	[N II] λ 6583.50	3	$4.426^{+0.185}_{-0.188} \times 10^{-5}$
O ⁰	[O I] λ 6300.34	3	$6.456^{+0.203}_{-0.240} \times 10^{-6}$
O ⁰	[O I] λ 6363.78	1	$6.947^{+0.255}_{-0.273} \times 10^{-6}$
O ⁺	[O II] λ 3726.03	1	$4.928^{+0.164}_{-0.142} \times 10^{-5}$
O ²⁺	[O III] λ 4958.91	1	$1.378^{+0.008}_{-0.010} \times 10^{-4}$
O ²⁺	[O III] λ 5006.84	3	$1.477^{+0.018}_{-0.021} \times 10^{-4}$
Ne ²⁺	[Ne III] λ 3868.75	3	$3.645^{+0.105}_{-0.090} \times 10^{-5}$
Ne ²⁺	[Ne III] λ 3967.46	1	$4.327^{+0.110}_{-0.092} \times 10^{-5}$
Ne ³⁺	[Ne IV] λ 4724.15	1	$2.825^{+0.134}_{-0.148} \times 10^{-4}$
S ⁺	[S II] λ 6716.44	1	$3.867^{+0.156}_{-0.162} \times 10^{-7}$
S ⁺	[S II] λ 6730.82	1	$3.869^{+0.139}_{-0.158} \times 10^{-7}$
S ²⁺	[S III] λ 6312.10	1	$2.229^{+0.072}_{-0.082} \times 10^{-6}$
Cl ²⁺	[Cl III] λ 5517.66	1	$2.935^{+0.105}_{-0.120} \times 10^{-8}$
Cl ²⁺	[Cl III] λ 5537.60	1	$2.935^{+0.077}_{-0.092} \times 10^{-8}$
Ar ²⁺	[Ar III] λ 7135.80	1	$5.410^{+0.232}_{-0.258} \times 10^{-7}$
Ar ³⁺	[Ar IV] λ 4711.37	1	$7.817^{+0.061}_{-0.058} \times 10^{-7}$
Ar ³⁺	[Ar IV] λ 4740.17	1	$7.205^{+0.051}_{-0.045} \times 10^{-7}$
Ar ⁴⁺	[Ar V] λ 4625.53	1	$4.082^{+1.177}_{-1.224} \times 10^{-7}$
Ar ⁴⁺	[Ar V] λ 7005.67	72	$3.711^{+0.165}_{-0.175} \times 10^{-7}$
Fe ²⁺	[Fe III] λ 4607.03	1	$5.833^{+0.457}_{-0.483} \times 10^{-7}$
Fe ²⁺	[Fe III] λ 4881.11	2	$5.353^{+1.437}_{-1.484} \times 10^{-8}$
Fe ²⁺	[Fe III] λ 5270.40	2	$6.421^{+1.082}_{-1.044} \times 10^{-8}$
...			

Note: Table 11 is published in its entirety in the machine-readable format. A portion is shown here for guidance regarding its form and content.

abundance, the ionic abundances derived from the He I ORLs were averaged with weights according to the predicted intrinsic intensity ratios of the available lines. The He²⁺/H⁺ ionic abundance was derived from the He II λ 4686 line. The C²⁺/H⁺ ratios were derived from some high-excitation C II ORLs (4f–6g λ 6461.95 and 4d–6f λ 6151.43).

We have detected a number of N II multiplets in most PNe. They were used to calculate ORL N²⁺/H⁺ ionic ratios, as presented in Table 12. The multiplet V3 lines are more reliable as they are less sensitive to optical depth effects, and they have been detected in several objects. Other multiplets are extremely case-sensitive, and also quite weak, with large flux uncertainties, so they are less reliable. We detected the extremely case-sensitive multiplet V28 in many PNe, which sometimes has a departure from the case B approximation for the triplets, so its calculated N²⁺/H⁺ ionic ratio is usually unreliable. However, the N II lines can be largely contaminated by fluorescence in low-excited PNe (Escalante et al. 2012), so their ionic ratios could be unreliable in those with cool central stars ($T_{\text{eff}} \lesssim 60$ kK). In the case of the detected λ 4640.64

Table 12. Ionic abundances derived from ORLs.

Ion	Line	Weight	Abund.
PB 6 (PNG278.8+04.9)			
He ⁺	He I λ 4471.50	1	$4.508^{+0.065}_{-0.078} \times 10^{-2}$
He ⁺	He I λ 5875.66	3	$4.670^{+0.057}_{-0.064} \times 10^{-2}$
He ⁺	He I λ 6678.16	1	$4.338^{+0.096}_{-0.123} \times 10^{-2}$
He ²⁺	He II λ 4685.68	1	$1.028^{+0.003}_{-0.004} \times 10^{-1}$
C ²⁺	C II λ 6461.95	1	$3.546^{+0.221}_{-0.197} \times 10^{-4}$
N ²⁺	N II λ 4613.87	1	$7.217^{+1.653}_{-1.962} \times 10^{-4}$
N ²⁺	N II λ 4788.13	2	$5.221^{+0.242}_{-0.283} \times 10^{-3}$
N ²⁺	N II λ 5676.02	3	$4.043^{+0.094}_{-0.115} \times 10^{-3}$
N ²⁺	N II λ 5931.78	2	$2.171^{+0.094}_{-0.115} \times 10^{-3}$
N ³⁺	N III λ 4640.64	1	$3.310^{+0.192}_{-0.200} \times 10^{-4}$
O ²⁺	O II λ 4491.23	1	$6.238^{+1.245}_{-1.566} \times 10^{-4}$
...			

Note: Table 12 is published in its entirety in the machine-readable format. A portion is shown here for guidance regarding its form and content.

(V2) N III recombination line, N³⁺ abundance is also available in 6 PNe. However, the λ 4640.64 N III recombination line is usually affected by continuum fluorescence (Ferland 1992). Therefore, the ionic ratio derived from this line is unreliable.

Table 12 lists the ORL O²⁺/H⁺ ionic ratios calculated from the O II lines of mostly multiplet V1 and some multiplet V28. The abundances from the quartet-quartet transition of multiplet V1 are less case-sensitive, and it has only 4 per cent difference between case A and B. However, multiplet V28 is extremely case-sensitive, and the case B effective recombination coefficient is 20 times the case A value. The ORL O²⁺/H⁺ ionic ratio derived from the case-sensitive multiplet V28 is higher than those from multiplet V1, indicating a departure from Case B conditions. The faint O II lines of multiplet V28 with high flux uncertainties make the derived ionic abundances quite uncertain.

4.3. Total Elemental Abundances

Table 13 presents the mean ionic abundances, the ionization correction factors (*icf*), and the total elemental abundances of the PNe in our sample, with their corresponding uncertainties (the full table is available in the machine readable format). Total elemental abundances were calculated from the mean ionic abundances using the conventional *icf* schemes of Kingsburgh & Barlow (1994), except for *icf*(CEL Cl) from Liu et al. (2000), *icf*(CEL Fe) from Izotov et al. (1994), *icf*(ORLs) from Wang & Liu (2007), and *icf*(ORL O) from Wesson et al. (2005) (see Appendix A). For comparison, we also derived total elemental abundances using the *icf* formulas given by Delgado-Inglada et al. (2014). In Table 14, we summarize the elemental abundances by number in logarithmic units relative to hydrogen where $\log N(\text{H}) = 12$. We see that the total abundances derived from the methods by Delgado-Inglada et al. (2014) are mostly in agreement with those made with the conventional *icf* schemes.

Table 13. Mean ionic and total elemental abundances relative to hydrogen derived from ORLs and CELs.

Ion	Typ.	Ref.	Abund.	Ion	Typ.	Ref.	Abund.
PB 6 (PNG278.8+04.9)							
He ⁺ /H	ORL		$4.571^{+0.051}_{-0.057} \times 10^{-2}$	Ne/H	CEL	KB94	$1.121^{+0.064}_{-0.041} \times 10^{-4}$
He ²⁺ /H	ORL		$1.028^{+0.003}_{-0.004} \times 10^{-1}$	<i>icf</i> (Ne)	CEL	DMS14	$3.457^{+1.789}_{-1.765}$
He/H	ORL		$1.486^{+0.008}_{-0.008} \times 10^{-1}$	Ne/H	CEL	DMS14	$1.319^{+0.822}_{-0.804} \times 10^{-4}$
C ²⁺ /H	ORL		$3.546^{+0.221}_{-0.197} \times 10^{-4}$	S ⁺ /H	CEL		$3.868^{+0.136}_{-0.134} \times 10^{-7}$
<i>icf</i> (C)	ORL	WL07	$2.938^{+0.103}_{-0.081}$	S ²⁺ /H	CEL		$2.229^{+0.072}_{-0.082} \times 10^{-6}$
C/H	ORL	WL07	$1.042^{+0.103}_{-0.071} \times 10^{-3}$	<i>icf</i> (S)	CEL	KB94	$1.481^{+0.022}_{-0.019}$
<i>icf</i> (C)	ORL	DMS14	$3.728^{+1.793}_{-1.978}$	S/H	CEL	KB94	$3.873^{+0.182}_{-0.175} \times 10^{-6}$
C/H	ORL	DMS14	$1.322^{+0.735}_{-0.899} \times 10^{-3}$	<i>icf</i> (S)	CEL	DMS14	$2.626^{+1.365}_{-1.441}$
N ²⁺ /H	ORL		$3.455^{+0.098}_{-0.113} \times 10^{-3}$	S/H	CEL	DMS14	$6.869^{+4.523}_{-4.240} \times 10^{-6}$
N ³⁺ /H	ORL		$3.310^{+0.192}_{-0.200} \times 10^{-4}$	Cl ²⁺ /H	CEL		$2.935^{+0.083}_{-0.091} \times 10^{-8}$
<i>icf</i> (N)	ORL	WL07	$1.131^{+0.007}_{-0.007}$	<i>icf</i> (Cl)	CEL	L00	$1.738^{+0.138}_{-0.104}$
N/H	ORL	WL07	$4.280^{+0.176}_{-0.166} \times 10^{-3}$	Cl/H	CEL	L00	$5.101^{+0.479}_{-0.413} \times 10^{-8}$
O ²⁺ /H	ORL		$6.238^{+1.245}_{-1.566} \times 10^{-4}$	<i>icf</i> (Cl)	CEL	DMS14	$3.931^{+2.162}_{-2.433}$
<i>icf</i> (O)	ORL	WL07	$2.938^{+0.051}_{-0.038}$	Cl/H	CEL	DMS14	$1.154^{+0.780}_{-0.840} \times 10^{-7}$
O/H	ORL	WL07	$1.833^{+0.496}_{-0.503} \times 10^{-3}$	Ar ²⁺ /H	CEL		$5.410^{+0.232}_{-0.258} \times 10^{-7}$
N ⁺ /H	CEL		$4.376^{+0.172}_{-0.162} \times 10^{-5}$	Ar ³⁺ /H	CEL		$7.511^{+0.050}_{-0.042} \times 10^{-7}$
<i>icf</i> (N)	CEL	KB94	$8.661^{+0.408}_{-0.337}$	Ar ⁴⁺ /H	CEL		$3.716^{+0.199}_{-0.201} \times 10^{-7}$
N/H	CEL	KB94	$3.790^{+0.332}_{-0.215} \times 10^{-4}$	<i>icf</i> (Ar)	CEL	KB94	$1.131^{+0.013}_{-0.016}$
<i>icf</i> (N)	CEL	DMS14	$7.525^{+5.819}_{-4.423}$	Ar/H	CEL	KB94	$1.881^{+0.060}_{-0.060} \times 10^{-6}$
N/H	CEL	DMS14	$3.293^{+3.016}_{-2.089} \times 10^{-4}$	<i>icf</i> (Ar)	CEL	DMS14	$2.870^{+2.944}_{-2.870}$
O ⁰ /H	CEL		$6.579^{+0.219}_{-0.229} \times 10^{-6}$	Ar/H	CEL	DMS14	$1.552^{+1.966}_{-1.552} \times 10^{-6}$
O ⁺ /H	CEL		$4.928^{+0.164}_{-0.142} \times 10^{-5}$	Fe ²⁺ /H	CEL		$1.638^{+0.141}_{-0.138} \times 10^{-7}$
O ²⁺ /H	CEL		$1.453^{+0.017}_{-0.018} \times 10^{-4}$	<i>icf</i> (Fe)	CEL	ITL94	$10.826^{+0.566}_{-0.497}$
<i>icf</i> (O)	CEL	KB94	$2.194^{+0.023}_{-0.020}$	Fe/H	CEL	ITL94	$1.773^{+0.212}_{-0.182} \times 10^{-6}$
O/H	CEL	KB94	$4.268^{+0.107}_{-0.085} \times 10^{-4}$	<i>adf</i> (N ²⁺)	ORL/CEL		$26.782^{+2.406}_{-2.402}$
<i>icf</i> (O)	CEL	DMS14	$2.402^{+0.673}_{-0.673}$	<i>adf</i> (N)	ORL/CEL	KB94	$11.292^{+1.123}_{-1.345}$
O/H	CEL	DMS14	$4.672^{+1.562}_{-1.452} \times 10^{-4}$	<i>adf</i> (N)	ORL/CEL	DMS14	$12.997^{+48.697}_{-12.997}$
Ne ²⁺ /H	CEL		$3.816^{+0.111}_{-0.083} \times 10^{-5}$	<i>adf</i> (O ²⁺)	ORL/CEL		$4.295^{+1.097}_{-1.245}$
Ne ³⁺ /H	CEL		$2.825^{+0.134}_{-0.148} \times 10^{-4}$	<i>adf</i> (O)	ORL/CEL	KB94	$4.295^{+1.452}_{-1.470}$
<i>icf</i> (Ne)	CEL	KB94	$2.938^{+0.103}_{-0.067}$	<i>adf</i> (O)	ORL/CEL	DMS14	$3.923^{+3.117}_{-2.141}$
				...			

Note: Table 13 is published in its entirety in the machine-readable format. A portion is shown here for guidance regarding its form and content. References for *icf* formulas are as follows: DMS14 – Delgado-Inglada et al. (2014); ITL94 – Izotov et al. (1994); KB94 – Kingsburgh & Barlow (1994); L00 – Liu et al. (2000); WL07 – Wang & Liu (2007). For Sa 3-107, the CEL O⁺ ionic abundance estimated by using the correlation $S^{2+}/S^{+} = 4.892 (O^{2+}/O^{+})^{0.419}$ derived in Section 4.1 (see Fig. 5).

5. ORL/CEL Discrepancy and Temperature Dichotomy

In this section, we explore possible correlations among various parameters. The ORL/CEL abundance discrepancies have been found to be correlated with various nebular physical quantities such as surface brightness, diameter, metallicity, density and excitation class (Liu et al. 2001; Tsamis et al. 2004; Liu et al. 2004; Zhang et al. 2004; Wesson et al. 2005; Wang & Liu 2007; Tsamis et al. 2008; García-Rojas et al. 2013). We define the abundance discrepancy factors as $ADF(X^{2+}) \equiv (X^{2+}/H^{+})_{\text{ORL}}/(X^{2+}/H^{+})_{\text{CEL}}$, and the

temperature dichotomies as differences between the forbidden-line and recombination-line temperatures $T_e(\text{CEL}) - T_e(\text{ORL})$. We estimate the CEL N²⁺ ionic abundances from N⁺ by assuming $N^{2+}/N^{+} = O^{2+}/O^{+}$ based on their ionization potentials.

Table 14. Summary of elemental abundances obtained from ORLs and CELs, on a logarithmic scale where H = 12.

Name	PN G	X <i>icf</i> (X)	He/H (ORL)	C/H (ORL)	N/H (ORL)	O/H (ORL)	N/H (CEL)	O/H (CEL)	Ne/H (CEL)	S/H (CEL)	Cl/H (CEL)	Ar/H (CEL)	Fe/H (CEL)
PB 6	278.8+04.9	KB94	11.17	9.02	9.63	9.26	8.58	8.63	8.05	6.59	4.71	6.27	6.25
		DMS14	11.17	9.12			8.52	8.67	8.12	6.84	5.06	6.19	
M 3-30	017.9–04.8	KB94	11.18	9.42	9.65	9.79	8.30	8.61	8.17	7.03	5.10	6.34	7.76
		DMS14	11.18	9.61			8.20	8.61	8.20	7.13	5.97	6.52	
Hb 4	003.1+02.9	KB94	11.06	8.92	9.23	9.79	8.73	8.80	7.97	7.28	5.30	6.53	6.73
		DMS14	11.06	8.86			8.73	8.80	8.00	7.28	6.45	6.61	
IC 1297	358.3–21.6	KB94	11.05	9.07	8.92	9.09	8.01	8.76	8.27	6.89	4.93	6.25	6.17
		DMS14	11.05	9.15			7.94	8.75	8.30	6.93	5.65	6.28	
Th 2-A	306.4–00.6	KB94	11.05	10.01	9.52	10.27	8.05	8.88	8.49	6.56	5.07	6.41	6.70
		DMS14	11.05	9.95			7.99	8.88	8.49	6.62	5.35	6.32	
Pe 1-1	285.4+01.5	KB94	11.01	9.45	9.39	9.43	8.16	8.64	8.05	6.71	4.51	7.43	6.75
		DMS14	11.01	9.43			8.64	8.64	8.31	6.67	4.97	6.29	
M 1-32	011.9+04.2	KB94	11.11	9.51	9.59	10.02	8.64	8.57	7.49	7.12	5.15	6.77	7.38
		DMS14	11.11	9.47			9.01	8.57	7.81	7.07	5.42	6.55	
M 3-15	006.8+04.1	KB94	11.04	9.81	9.45		8.35	8.83	7.93	6.99		5.58	6.73
		DMS14	11.04	9.34			8.92	8.83	8.12	6.98			
M 1-25	004.9+04.9	KB94	11.07	9.33	9.58	9.85	8.36	8.81	7.56	7.15	4.85	6.81	6.59
		DMS14	11.07	9.10			8.74	8.81	7.87	7.11	5.17	6.58	
Hen 2-142	327.1–02.2	KB94	10.34				8.02	8.65		6.55	5.09		
		DMS14	10.34				8.02	8.65		6.53	4.97		
Hen 3-1333	332.9–09.9	KB94					8.54	9.50		7.67			
		DMS14					8.54	9.50		7.64			
Hen 2-113	321.0+03.9	KB94					8.07	8.62		6.84			
		DMS14					8.07	8.62		6.82			
K 2-16	352.9+11.4	KB94					7.98	8.30		7.08			
		DMS14					8.16	8.30		6.46			
NGC 6578	010.8–01.8	KB94	11.07	9.36	8.94	9.57	7.81	8.78	8.38	6.94	5.06	6.50	7.50
		DMS14	11.07	9.20			8.03	8.78	9.63	6.93	5.93	6.55	
M 2-42	008.2–04.8	KB94	10.99	9.60	9.45	9.15	8.03	8.59	7.97	6.98	5.18	6.23	6.79
		DMS14	10.99	8.88			8.26	8.59	9.39	6.98	6.05	6.26	
NGC 6567	011.7–00.6	KB94	10.96	9.50	9.25	9.81	7.46	8.36	7.69	6.27	4.48	5.71	6.13
		DMS14	10.96	9.22			7.64	8.36	8.28	6.27	5.30	5.73	
NGC 6629	009.4–05.0	KB94	11.00	8.69		8.99	7.24	8.63	8.11	6.42	4.85	6.29	6.50
		DMS14	11.00	8.81			7.77	8.63	8.34	6.39	5.48	6.29	
Sa 3-107	358.0–04.6	KB94	11.08	9.17	8.99		7.52	7.94		6.01	4.48	5.76	6.83
		DMS14	11.08	9.13			7.67	7.94		6.00	5.43	5.87	

Note. Total abundances in the first row for each object calculated using the ionization correction factors (*icf*) from Kingsburgh & Barlow (1994, KB94), except for Cl (Liu et al. 2000), Fe (Izotov et al. 1994), ORLs (Wang & Liu 2007), and O ORLs (Wesson et al. 2005), described in Appendix A, and in the second row calculated with the *icf* formulas from Delgado-Inglada et al. (2014, DMS14).

The dichotomy $T_e(\text{CEL}) - T_e(\text{He I})$ and $\text{ADF}(\text{O}^{2+})$ for the objects plotted in Fig. 6 (top panels) are fitted by,

$$\log \text{ADF}(\text{O}^{2+}) = (0.589 \pm 0.144) + (7.401 \pm 2.860) \times 10^{-5} \times [T_e([\text{N II}]) - T_e(\text{He I})], \quad (12)$$

$$\log \text{ADF}(\text{O}^{2+}) = (0.636 \pm 0.155) + (5.477 \pm 2.694) \times 10^{-5} \times [T_e([\text{O III}]) - T_e(\text{He I})], \quad (13)$$

with $r = 0.65$ ($p = 0.03$) and $r = 0.56$ ($p = 0.07$), respectively.

Previously, Liu et al. (2001) found that $\text{ADF}(\text{O}^{2+})$ is directly correlated with the difference between the [O III] forbidden-line and H I Balmer jump electron temperatures. Tsamis et al. (2004) also derived a similar correlation for a sample of 16 PNe. As seen in Fig. 6 (top-left), the ADFs of O^{2+} are correlated with the dichotomy between the nebular to auroral

forbidden-line [N II] temperature and the He I temperature. We see that higher values of ADFs are associated with higher CEL-ORL temperature dichotomies. These correlations likely corroborate the previous findings that there could be an intimate connection between the nebular thermal structure and the ORL/CEL abundance discrepancy. However, we did not find any robust associations between the ADFs of N^{2+} and $T_e(\text{CEL}) - T_e(\text{He I})$.

Previously, an anti-correlation between $T_e([\text{O III}]) - T_e(\text{BJ})$ and $\log S(\text{H}\beta)$ of the 25 PNe was also found by Tsamis et al. (2004). This suggests that the temperature dichotomies could be increased by decreasing nebular surface brightness. In Fig. 6 (bottom panels), we also plot the CEL-He I temperature dichotomy as a function of the intrinsic nebular $\text{H}\beta$ surface

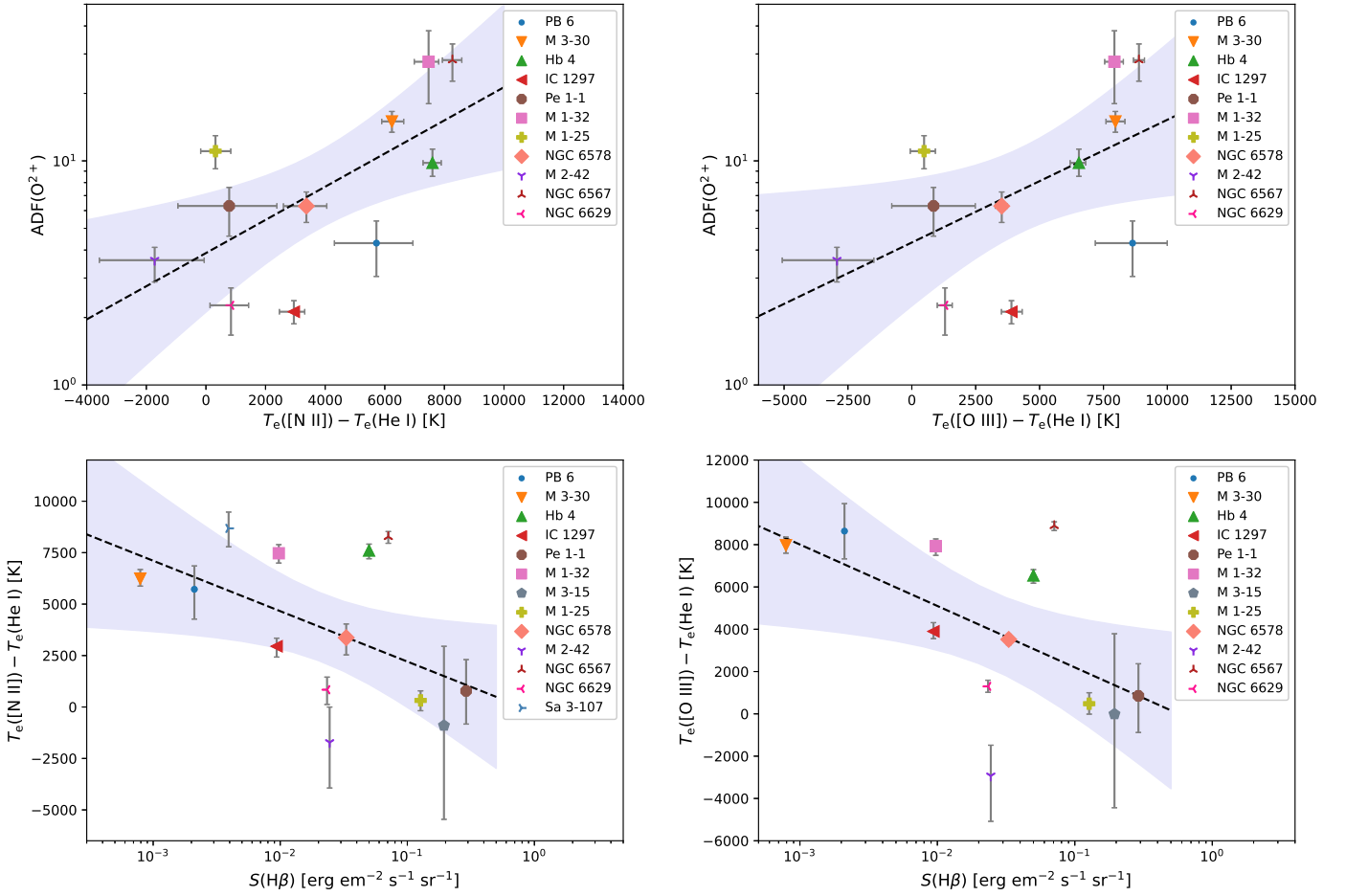


Figure 6. *Top Panels:* The ADF for O^{2+} plotted against the dichotomy between the [N II] and He I temperatures (left), and between the [O III] and He I temperatures (right). The dashed lines show linear fits to $\log ADF(O^{2+})$ as a function of the CEL–He I temperature dichotomy, discussed in the text. *Bottom Panels:* The dichotomy between the [N II] and He I temperatures (left), and between the [O III] and He I temperatures (right) plotted against the intrinsic nebular $H\beta$ surface brightness $S(H\beta)$ ($\text{erg cm}^{-2} \text{s}^{-1} \text{sr}^{-1}$). The dashed lines show linear fits to the temperature dichotomy as a function of $\log S(H\beta)$, discussed in the text. The lightly shaded area in each panel shows the 90% confidence level of the linear fit.

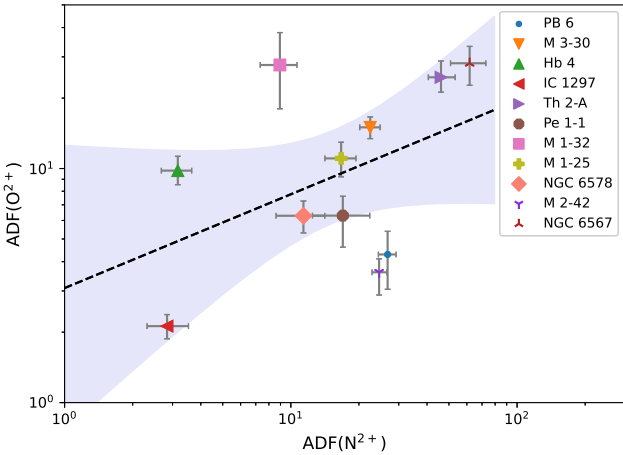


Figure 7. $ADF(O^{2+})$ versus $ADF(N^{2+})$. The dashed line is a least-squares fit, discussed in the text, with the 90% confidence level shown by the gray area.

brightness $S(H\beta)$, and the following anti-correlations exist:

$$[T_e([N II]) - T_e(\text{He I})] = (-243 \mp 2270) - (2450 \pm 1251) \times \log S(H\beta), \quad (14)$$

$$[T_e([O III]) - T_e(\text{He I})] = (-710 \mp 2410) - (2905 \pm 1373) \times \log S(H\beta), \quad (15)$$

with $r = -0.51$ ($p = 0.08$) and $r = -0.56$ ($p = 0.06$), respectively. The nebular surface brightness is an indicator of the nebular evolution, since it decreases due to the expansion of the nebula as the density drops. Although the ADFs of some PNe were also found to be anti-correlated with their surface brightness (Liu et al. 2004; Tsamis et al. 2004; Wang & Liu 2007), we did not obtain any statistically significant correlations between ADFs and surface brightness.

In Fig. 7, the $ADF(O^{2+})$ and $ADF(N^{2+})$ for 11 PNe are fitted by

$$ADF(O^{2+}) = 3.086_{-1.651}^{+3.551} [ADF(N^{2+})]^{0.401 \pm 0.266}, \quad (16)$$

with a Pearson r -value of 0.449 and a null-hypothesis p -value of 0.166.

The correlations (12)–(13) likely confirm previous suggestions that a fraction of cool, oxygen-rich dense clumps

may be present in diffuse warm ionized gases. The correlation (16) also depicts a weak dependence of $\text{ADF}(\text{N}^{2+})$ on $\text{ADF}(\text{O}^{2+})$, while N II ORLs could be contaminated by resonance fluorescence in some objects. Moreover, the anti-correlations (14)–(15) possibly suggest that the temperature dichotomy is weakly related to the nebular evolution, though we did not find any remarkable correlations between the ADF and $S(\text{H}\beta)$.

6. Comparison with AGB Models

The elemental abundances of PNe are associated with the products of the nucleosynthesis and mixing processes that happened in previous evolutionary phases. The richest nucleosynthesis occurs during the AGB, where the third dredge up (TDU) mixes carbon and other helium burning products to the surface. Hot bottom burning (HBB) also occurs in intermediate-mass AGB stars with masses $\gtrsim 4.5M_{\odot}$. Although we have a good qualitative picture of the evolution of low and intermediate-mass stars, the details of the mixing and nucleosynthesis during the AGB are uncertain (e.g. Busso et al. 1999; Herwig 2005; Karakas & Lattanzio 2014). Elemental abundances derived from PNe can be used as a tool to trace these uncertain mixing processes, and to gain insight into non-standard physics such as rotation (e.g. Charbonnel & Lagarde 2010).

For comparison in Figure 8, we plot the logarithmic N/O abundance ratio from CELs against $12 + \log(\text{N}/\text{H})_{\text{CEL}s}$ (top) and $12 + \log(\text{He}/\text{H})_{\text{ORL}s}$ (middle), and the logarithmic C/O abundance ratio from ORLs against $12 + \log(\text{C}/\text{H})_{\text{ORL}s}$ (bottom) for our PNe and the integrated yields for AGB models with progenitor masses between $1.5\text{--}6M_{\odot}$ at solar metallicity $Z = 0.014$ (red triangles) and $2.5\text{--}6M_{\odot}$ at $Z = 0.007$ (blue squares) from Karakas & Lugaro (2016). We consider the elemental abundances calculated using the conventional *icf* formulas (KB94). The composition of the AGB model yields were weighted toward the tip of the AGB, which is when most of the mass is lost, so they are suitable for comparison to PNe. The initial composition of the $Z = 0.014$ models assumed the proto-solar composition from Asplund et al. (2009). The initial composition in the $Z = 0.007$ models are the scaled-solar abundances from Anders & Grevesse (1989). The models with masses below $6M_{\odot}$ were included, as more massive AGB models likely evolve too quickly to form PNe. Likewise, models below $1.5M_{\odot}$ likely evolve too slowly during their post-AGB evolution (Blöcker 1995). Models with HBB, which produces Type I PNe ($\text{N}/\text{O} > 0.8$; Kingsburgh & Barlow 1994), include masses $\geq 4.5M_{\odot}$.

We compare the predictions for the models with $Z = 0.014$ and 0.007 to our elemental abundances (see KB94 in Table 14). The oxygen abundance is used as a metallicity indicator. According to the O/H elemental abundance derived from CELs, 9 objects have around solar metallicity (PB 6, M 3-30, IC 1297, Pe 1-1, M 1-32, Hen 2-142, Hen 2-113, M 2-42, and NGC 6629), 4 objects with slightly over solar metallicity (Hb 4, M 3-15, M 1-25, and NGC 6578), two PNe with super-solar metallicity (Th 2-A, and Hen 3-1333) and the remaining 3 PNe having half-solar to LMC metallicities (K 2-16, NGC 6567, and Sa 3-107).

Comparing N/H, N/O and He/H with those derived from AGB models plotted in Figure 8, M 1-25, Hen 2-142, Hen 2-

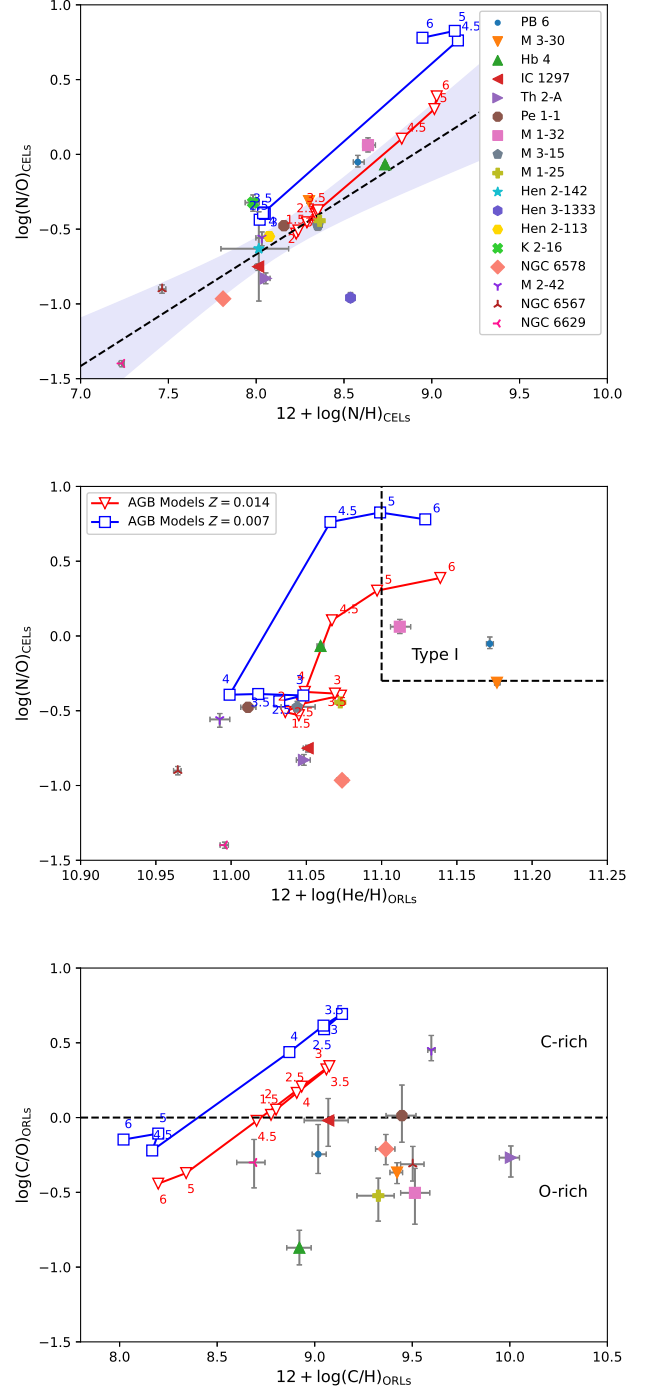


Figure 8. *Top Panel:* $\log(\text{N}/\text{O})_{\text{CEL}s}$ plotted against $12 + \log(\text{N}/\text{H})_{\text{CEL}s}$ derived from the PNe in our sample and elemental yields predicted by the AGB models with initial masses $1.5\text{--}6M_{\odot}$ at the solar metallicity ($Z = 0.014$; red triangles) and $2.5\text{--}6M_{\odot}$ at the sub-solar metallicity ($Z = 0.007$; blue squares) from Karakas & Lugaro (2016). The dashed line is a least-squares fit to our data, discussed in the text, with the 90% confidence level shown by the shaded area. *Middle Panel:* $\log(\text{N}/\text{O})_{\text{CEL}s}$ versus $12 + \log(\text{He}/\text{H})_{\text{ORL}s}$ for our sample PN and the AGB model yields with $Z = 0.014$ and 0.007 . The top-right dashed-line box shows the boundaries of Type I PNe as defined by Peimbert & Torres-Peimbert (1983). *Bottom Panel:* $\log(\text{C}/\text{O})_{\text{ORL}s}$ versus $12 + \log(\text{C}/\text{H})_{\text{ORL}s}$ for our PNe and the AGB model predictions ($Z = 0.014$ and 0.007). The horizontal dashed line distinguishes between the PNe with C-rich and O-rich abundances derived from ORLs.

113, Pe 1-1, and M 2-42 probably evolved from AGB stars with $Z = 0.014$ and initial masses between 1 and $2 M_{\odot}$, whereas M 3-30 and M 3-15 from progenitor stars with $Z = 0.014$ and initial mass between 2 and $3.5 M_{\odot}$. Similarly, an AGB model with $Z = 0.007$ and a progenitor mass of $2.5\text{--}4 M_{\odot}$ could likely produce the abundance patterns of K 2-16. Fig. 8 (middle panel) shows the regions of Type I PNe ($\text{He}/\text{H} \geq 0.125$ and $\log \text{N}/\text{O} \geq -0.3$) as classified by Peimbert & Torres-Peimbert (1983). The abundance patterns of PB 6 and M 1-32 (also possibly M 3-30) suggest that they could be Type I PNe and likely evolved from AGB stars with initial masses of about $4\text{--}5 M_{\odot}$ in order to undergo the HBB phase (see Karakas 2014). Moreover, the abundance ratio $\text{N}/\text{O} > 0.5$ in H β 4 could also correspond to HBB in an AGB star with a progenitor mass of $\sim 4.5 M_{\odot}$. Similarly, the nebulae M 3-15, M 1-25, and Pe 1-1 with $\text{N}/\text{O} > 0.5$ (DMS14) may be produced by AGB stars with $Z = 0.014$ and initial masses of $\sim 4.5 M_{\odot}$ if we consider the elemental abundances calculated by *icf* formulas from Delgado-Inglada et al. (2014) (see DMS14 in Table 14). IC 1297, Th 2-A, and NGC 6578 are likely associated with progenitor mass $\lesssim 1.5 M_{\odot}$ and metallicity $Z \gtrsim 0.014$. Note that we do not have any calculated models for super-solar metallicity (Hen 3-1333) and very poor metallicity (Sa 3-107).

Figure 8 (bottom panel) also shows the C/O abundance ratio as a function of the C/H abundance derived from ORLs. We see that C/O predicted by ORLs have $\text{C}/\text{O} < 1$, except for Pe 1-1 and M 2-42, implying that ORLs are mostly emitted from O-rich environments. However, the C/H abundances derived from ORLs in our PN sample are higher than the yields predicted by AGB stellar models, whereas their abundances from CELs are mostly consistent with AGB models with progenitor masses $1.5\text{--}5 M_{\odot}$. From our results in § 5 and the C/H in Figure 8, the ORLs could originate from cool, oxygen-rich clumpy structures having the chemical composition that cannot directly be associated with heavy elements produced by AGB stars.

For our PN sample, a linear fit to the N/O abundance ratio and the N/H abundance of the 17 PNe plotted in Figure 8 (top panel) yields $\log(\text{N}/\text{O}) = (0.75 \pm 0.15) \times [12 + \log(\text{N}/\text{H})] - (6.64 \pm 1.24)$ with $r = 0.79$ and $p = 0.0002$, in agreement with $\log(\text{N}/\text{O}) = 0.73 \times [12 + \log(\text{N}/\text{H})] - 6.50$ found by García-Rojas et al. (2013). It can be seen that the most of PNe with solar metallicity are close to this linear correlation (dashed in Figure 8, top). However, NGC 6567 and NGC 6629 around *wels* are not consistent with the AGB predictions, while they still follow the N/O vs. N/H correlation.

AGB modeling parameters such as mass loss and convection are highly uncertain, and variations in either would alter the predicted elemental yields. For example, higher mass loss rates will lead to a shorter AGB lifetime and less TDU episodes, so a smaller C/O ratio is produced from a model with $\sim 3 M_{\odot}$ (Marigo 2002; Stancliffe & Jeffery 2007; Karakas 2010). More efficient convection would lead to hotter temperatures during HBB and a larger N/O ratio (e.g. Ventura & D’Antona 2005; Ventura et al. 2013). The neon abundance can be enhanced in lower mass AGB models (2.5 and $3 M_{\odot}$) via the partial mixing of protons and third dredge-up (Karakas & Lattanzio 2003; Karakas et al. 2009), and mildly (by ~ 0.3 dex) through HBB and dredge-up in the metal-poor AGB star models ($Z = 0.007$) with initial masses of 5 and $6 M_{\odot}$. Neutron captures mildly increase chlorine abundance in the metal-poor massive

($\gtrsim 3 M_{\odot}$) AGB models (Karakas et al. 2009). The sulfur abundance can be reduced via the depletion into dust (Pottasch & Bernard-Salas 2006; Henry et al. 2012).

7. Conclusions and Discussions

We have carried out detailed plasma diagnostics and abundance analyses for a sample of 18 Galactic PNe surrounding [WR]-type and *wels* stars, using both CELs and ORLs. The electron density derived from CELs are closely correlated with the intrinsic nebular H β surface brightness, which agrees with the theoretical prediction of $S(\text{H}\beta) \propto \varepsilon r N_e^2$ (O’Dell 1962). The nebular H β surface brightness is associated with the nebular evolution, and it drops as the nebula is expanding. Moreover, the electron temperature ratio $T_e([\text{O III}])/T_e([\text{N II}])$ derived from CELs is correlated with the excitation class (EC), which agrees with the previous results (Kingsburgh & Barlow 1994; Wang & Liu 2007). Self-consistent plasma diagnostics of ORLs using atomic data of N^{2+} (Fang et al. 2013) and O^{2+} (Storey et al. 2017) also suggest the presence of cool ($\lesssim 7000$ K), dense ($\sim 10^4\text{--}10^5 \text{ cm}^{-3}$) small-scale structures in some PNe (see Table 9). However, we caution that some N II ORLs in low-excited PNe could be potentially contaminated by fluorescence (see e.g. Escalante et al. 2012).

Our abundance analyses indicate that there could be a dependence of the ORL/CEL ADFs of O^{2+} upon the difference between temperatures derived from forbidden lines and those from He I recombination lines (see Fig. 6 top panels). Previously, the ADFs were found to be closely correlated with the difference between $T_e([\text{O III}])$ and $T_e(\text{BJ})$ (Liu et al. 2001, 2004; Tsamis et al. 2004; Wesson et al. 2005; Wang & Liu 2007). We also found a weak correlation between the ADFs of O^{2+} and N^{2+} (Fig. 7). The weak anti-correlations between the CEL–He I temperature dichotomies and nebular surface brightness found here (see Fig. 6 bottom panels) are also consistent with Tsamis et al. (2004). However, we did not obtain any statistically significant correlations between the ADFs and surface brightness, which were found in the previous studies (Liu et al. 2004; Tsamis et al. 2004; Wang & Liu 2007). The correlations between ADF(O^{2+}) and CEL–He I temperature dichotomies possibly imply that the observed O II ORLs could originate from cool ionized gases located in some oxygen-rich clumpy structures of high density within the diffuse warm nebula.

The correlations between ADF and temperature dichotomy has been predicted by the bi-abundance model proposed by Liu et al. (2000) that includes a fraction of cool metal-rich knots within the diffuse warm nebula. The feasibility of this model has been demonstrated using several photoionization models (Ercolano et al. 2003; Tsamis & Péquignot 2005; Yuan et al. 2011; Danehkar 2018a; Gómez-Llanos & Morisset 2020). Nevertheless, the presence and origin of metal-rich inclusion are not well understood. The born-again scenario (Iben & Renzini 1983; Iben et al. 1983) is one possibility, whereby H-deficient material would have been ejected from the stellar surface during the (very-) late thermal pulse, such as hydrogen-poor ejecta in Abell 30, Abell 58 (V605 Aql), and Abell 78 (e.g. Hazard et al. 1980; Jacoby & Ford 1983; Pollacco et al. 1992; Borkowski et al. 1993; Guerrero & Machado 1996; Fang et al. 2014). The detailed abundance analyses of the

‘born-again’ PNe Abell 30 (Wesson et al. 2003) and Abell 58 (Wesson et al. 2008) supported the idea that they contain some very cold hydrogen-deficient knots. In the both cases, the knots were found to be oxygen-rich and also neon-rich in contrast to the expectations of a very late thermal pulse. However, the infrared spectroscopic and imaging studies of the born-again PNe Abell 30 and Abell 78 by Toalá et al. (2021) indicate that the C/O mass ratios of their hydrogen-poor ejecta are larger than 1 in agreement with the very late thermal pulse model, and they also contain hot carbon-rich dust grains spatially coincident with the hydrogen-poor ejecta. Alternatively, Liu (2003) suggested that H-deficient material could be introduced by the evaporation and destruction of planets by stars. However, Henney & Stasińska (2010) argued that the destruction of solid bodies during the PN phase cannot produce enough gas-phase metallicity to explain the observed abundance discrepancies in PNe, though the sublimation of solid bodies during the final stages of the AGB phase might generate enough metal-rich material. The implications of these scenarios need more observations and detailed abundance analysis of a large sample of PNe.

Nicholls et al. (2012, 2013) also proposed that a κ -distribution of electron energies could explain the abundance discrepancy and temperature dichotomy. In this scenario, the electrons in the gas have a non-thermal equilibrium energy distribution whose departure from the Maxwell-Boltzmann distribution is characterized by a κ index. Dopita et al. (2013) concluded that κ -distributions with $\kappa \sim 20$, or somewhat larger, are able to predict the abundance discrepancy and temperature dichotomy in H II Regions. However, Storey & Sochi (2013) found that Maxwell-Boltzmann distributions fit their data best but without statistically ruling out κ -distributions. Moreover, Mendoza & Bautista (2014) found that in some cases κ -distributed electrons can reconcile observations with theory but that this is in a minority of cases, and Maxwell-Boltzmann distributions are not firmly ruled out even then. Furthermore, Zhang et al. (2014) found that both the scenarios, bi-abundance models and κ -distributed electrons, are adequately consistent with observations of four PNe with very large ADFs, and concluded the spectra are emitted from cold and low- κ plasmas rather than a single Maxwell-Boltzmann electron energy distribution. Nevertheless, Zhang et al. (2016) did not find any conclusive results for supporting κ -distributed electrons in PNs. Recently, κ -distributed recombination coefficients for hydrogen (Storey & Sochi 2015b), and collision strengths for [O III] (Storey & Sochi 2015a) became available. Upcoming κ -distributed recombination coefficients for O II ORLs shall allow us to assess whether κ -distributed electrons have a key role in the ADF of O^{2+} ion. It is unclear whether the metal-rich inclusion could introduce non-Maxwell-Boltzmann equilibrium electrons to the nebula. The relations between both the scenarios should be evaluated further.

Moreover, abundance discrepancy factors could be related to binarity (e.g. Lau et al. 2011; Corradi et al. 2015; Bautista & Ahmed 2018; Wesson et al. 2018). Lau et al. (2011) envisaged that H-deficient material in V605 Aql might be ejected by either merger of a main-sequence star and a massive white dwarf, or a classical nova. Moreover, Bautista & Ahmed (2018) proposed that resonant temperature

fluctuations produced in the nebula photoionized by short-period binary stars are responsible for temperature and abundance discrepancies. Deep spectroscopic studies of 3 PNe with post common-envelope binary stars showed very large abundance discrepancies: ADFs ~ 120 in Abell 46 and $\gtrsim 300$ in its inner part, ADF ~ 50 in Ou 5, and ADF ~ 10 in Abell 63 (Corradi et al. 2015). A statistical analysis of PNe by Wesson et al. (2018) also demonstrated that extreme abundance discrepancies could be linked to binary central stars and possible implications of a nova-like eruption shortly after the common-envelope phase. Jones et al. (2016) obtained $ADF(O^{2+}) \approx 18$ in the PN NGC 6778 around a short-period binary. Moreover, the direct imaging of NGC 6778 by García-Rojas et al. (2016) also revealed that weak O II $\lambda\lambda 4649+50$ recombination emission originates from the central region of this PN where it is not spatially associated with strong [O III] $\lambda 5007$ emission. Recently, Jacoby et al. (2020) suggested the presence of a binary central star in the born-again PN Abell 30 based on its light curves.

In conclusion, our detailed analyses of PNe around [WR]-type and *wels* stars have allowed us to determine physical conditions and chemical abundances from forbidden and recombination lines. The correlations between the $ADF(O^{2+})$ and CEL–He I temperature dichotomy, as well as the physical properties derived from plasma diagnostics of heavy element ORLs, likely suggest that some dense metal-rich clumpy structures may be present in ionized gaseous nebulae. The nebular evolution does not seem to play a central role in the abundance discrepancy problem. Therefore, the ORL/CEL problem could be due to a hitherto unknown component or mechanism within PNe or/and complicated evolutionary history of CSPNe.

This article is partially based on the dissertation by the author (Danehkar 2014), supported by a Macquarie University Research Excellence Scholarship (MQRES) and a Sigma Xi Grants-in-Aid of Research (GIAR). The author would like to thank the referee for helpful comments and suggestions that greatly improved the paper, Quentin Parker for supporting the 2010 ANU observations, Amanda Karakas for valuable comments on AGB models, Roger Wesson for helpful discussions, David Frew for helping with the observing proposal, the staff at the Siding Spring Observatory and Kyle DePew for undertaking the WiFeS observations in 2010, Bruce Balick for sharing the long-slit data of Hb 4 taken with the Palomar 5.1-m telescope in July 1993.

Software: IDL Astronomy User’s Library (Landsman 1993), IDL Coyote Library (Fanning 2011), NumPy (Harris et al. 2020), SciPy (Virtanen et al. 2020), Matplotlib (Hunter 2007).

Facility: ATT (WiFeS).

Appendix

A. Ionization Correction Factors

The total elemental He abundance relative to H is often obtained by simply taking the sum of He^+/H^+ and He^{2+}/H^+ ionic abundances.

Following Kingsburgh & Barlow (1994) and Wang & Liu (2007), the ORL carbon is derived, correcting for the unseen

stages of ionization for the case if only C^{2+} is measured using:

$$\left(\frac{C}{H}\right)_{\text{ORLs}} = \left(\frac{C^{2+}}{H^+}\right) \left(\frac{O}{O^{2+}}\right)_{\text{CELs}}, \quad (\text{A1})$$

and if C^{2+} and C^{3+} are observed:

$$\left(\frac{C}{H}\right)_{\text{ORLs}} = \left(\frac{C^{2+}}{H^+} + \frac{C^{3+}}{H^+}\right) \left(\frac{O^+ + O^{2+}}{O^{2+}}\right)_{\text{CELs}}. \quad (\text{A2})$$

However, carbon ionic ratios derived from ORLs are generally not equal to those derived from CELs (Tsamis et al. 2003a, 2004), and oxygen ionic abundances derived from CELs may not be suitable choices for the ionization correction factor of the ORL carbon.

For ORL nitrogen, when only N^{2+} was measurable, the unobserved ionization stages are corrected for by assuming $N/N^{2+} = O/O^{2+}$, so

$$\left(\frac{N}{H}\right)_{\text{ORLs}} = \left(\frac{N^{2+}}{H^+}\right) \left(\frac{O}{O^{2+}}\right)_{\text{CELs}}, \quad (\text{A3})$$

while when both N^{2+} and N^{3+} were measured, the elemental abundance is derived assuming $N/N^+ = O/O^+$, with N/H then given by

$$\left(\frac{N}{H}\right)_{\text{ORLs}} = \left(\frac{N^{2+}}{H^+} + \frac{N^{3+}}{H^+}\right) \left[1 - \left(\frac{O^+}{O}\right)_{\text{CELs}}\right]^{-1}. \quad (\text{A4})$$

The ionization correction factor for O is $(\text{He}/\text{He}^+)^{2/3}$ (Kingsburgh & Barlow 1994). However, only O^{2+} is measured from ORLs. Following Wesson et al. (2005) and Wang & Liu (2007), we assume that O^+/O^{2+} derived from CELs is applicable to ORLs, so instead the elemental abundance is derived using

$$\left(\frac{O}{H}\right)_{\text{ORLs}} = \left(\frac{O^{2+}}{H^+}\right) \left(\frac{\text{He}}{\text{He}^+}\right)^{2/3} \left[1 + \left(\frac{O^+}{O^{2+}}\right)_{\text{CELs}}\right]. \quad (\text{A5})$$

The CEL oxygen abundance is calculated from the O^+/H^+ and O^{2+}/H^+ ratios, correcting for the unseen O^{3+}/H^+ using,

$$\left(\frac{O}{H}\right)_{\text{CELs}} = \left(\frac{O^+}{H^+} + \frac{O^{2+}}{H^+}\right) \left(\frac{\text{He}}{\text{He}^+}\right)_{\text{ORLs}}^{2/3}, \quad (\text{A6})$$

where the He^+ and He abundances are derived from ORLs.

The CEL nitrogen is calculated from the N^+/H^+ ratio, correcting for the unseen N^{2+}/H^+ and N^{3+}/H^+ using,

$$\left(\frac{N}{H}\right)_{\text{CELs}} = \left(\frac{N^+}{H^+}\right) \left(\frac{O}{O^+}\right). \quad (\text{A7})$$

To estimate the CEL/ORL neon, the unseen Ne^+/H^+ is corrected for, using

$$\frac{\text{Ne}}{H} = \left(\frac{\text{Ne}^{2+}}{H^+}\right) \left(\frac{O}{O^{2+}}\right). \quad (\text{A8})$$

For the case where both S^+ and S^{2+} observed, the elemental S abundance is derived using

$$\left(\frac{S}{H}\right)_{\text{CELs}} = \left(\frac{S^+}{H^+} + \frac{S^{2+}}{H^+}\right) \left[1 - \left(1 - \frac{O^+}{O}\right)^3\right]^{-1/3}. \quad (\text{A9})$$

For the case where only S^+ observed, the elemental S abundance is derived as follows (Kingsburgh & Barlow 1994):

$$\left(\frac{S}{H}\right)_{\text{CELs}} = \left(\frac{S^+}{H^+}\right) \left[1 + 4.677 \left(\frac{O^{2+}}{O^+}\right)^{0.433}\right] \times \left[1 - \left(1 - \frac{O^+}{O}\right)^3\right]^{-1/3}. \quad (\text{A10})$$

For the case where both Ar^{2+} and Ar^{3+} observed, the elemental Ar abundance is derived using the following equation, assuming $\text{Ar}^+/\text{Ar} = \text{N}^+/\text{N}$:

$$\left(\frac{\text{Ar}}{H}\right)_{\text{CELs}} = \left(\frac{\text{Ar}^{2+}}{H^+} + \frac{\text{Ar}^{3+}}{H^+} + \frac{\text{Ar}^{4+}}{H^+}\right) \left(1 - \frac{\text{N}^+}{\text{N}}\right)^{-1}. \quad (\text{A11})$$

For the case where only Ar^{2+} observed, the elemental Ar abundance is derived as follows:

$$\left(\frac{\text{Ar}}{H}\right)_{\text{CELs}} = 1.87 \left(\frac{\text{Ar}^{2+}}{H^+}\right). \quad (\text{A12})$$

For elemental Cl abundance, we use the following equation given by Liu et al. (2000) according to the ionization potential of Cl and S ion stages:

$$\left(\frac{\text{Cl}}{H}\right)_{\text{CELs}} = \left(\frac{\text{Cl}^{2+}}{H^+}\right) \left(\frac{S}{S^{2+}}\right). \quad (\text{A13})$$

Following Izotov et al. (1994), the elemental Fe abundance is estimated when only Fe^{2+} is observed as follows:

$$\left(\frac{\text{Fe}}{H}\right)_{\text{CELs}} = \left(\frac{\text{Fe}^{2+}}{H^+}\right) \left[1.25 \left(\frac{O}{O^+}\right)\right], \quad (\text{A14})$$

which is based on photoionization H II models (Stasińska 1990).

B. Supplementary Data

The following tables and figure sets are available for the electronic edition of this article:

Table 4. Observed and dereddened line fluxes on a scale relative to $H\beta$, where $H\beta = 100$.

Table 6. Plasma diagnostics based on CELs.

Table 7. Plasma diagnostics based on He I lines.

Table 8. Plasma diagnostics based on heavy element ORLs.

Table 11. Ionic abundances derived from CELs.

Table 12. Ionic abundances derived from ORLs.

Table 13. Mean ionic and total elemental abundances derived from ORLs and CELs.

Fig. Set 2. N_e - T_e diagnostic diagrams based on CELs.

Fig. Set 4. T_e diagnostic diagrams based on C II ORLs, and N_e - T_e diagnostic diagrams based on O II and N II ORLs.

Tables 4, 6–8, and 11–13 are published in the machine-readable format.

ORCID iDs

A. Danehkar  <https://orcid.org/0000-0003-4552-5997>

References

- Acker, A., Gesicki, K., Grosdidier, Y., & Durand, S. 2002, *A&A*, **384**, 620
- Acker, A., Marcout, J., Ochsenbein, F., et al. 1992, The Strasbourg-ESO Catalogue of Galactic Planetary Nebulae. Parts I, II.
- Acker, A. & Neiner, C. 2003, *A&A*, **403**, 659
- Acker, A., Raytchev, B., Koepfen, J., & Stenholm, B. 1991, *A&AS*, **89**, 237
- Akras, S. & Gonçalves, D. R. 2016, *MNRAS*, **455**, 930
- Akras, S. & López, J. A. 2012, *MNRAS*, **425**, 2197
- Akras, S., Monteiro, H., Aleman, I., et al. 2020, *MNRAS*, **493**, 2238
- Ali, A., Amer, M. A., Dopita, M. A., Vogt, F. P. A., & Basurah, H. M. 2015, *A&A*, **583**, A83
- Ali, A., Dopita, M. A., Basurah, H. M., et al. 2016, *MNRAS*, **462**, 1393
- Aller, L. H. & Czyzak, S. J. 1983, *ApJS*, **51**, 211
- Aller, L. H. & Menzel, D. H. 1945, *ApJ*, **102**, 239
- Anders, E. & Grevesse, N. 1989, *Geochim. Cosmochim. Acta*, **53**, 197
- Asplund, M., Grevesse, N., Sauval, A. J., & Scott, P. 2009, *ARA&A*, **47**, 481
- Basurah, H. M., Ali, A., Dopita, M. A., et al. 2016, *MNRAS*, **458**, 2694
- Bautista, M. A. & Ahmed, E. E. 2018, *ApJ*, **866**, 43
- Bell, K. L., Berrington, K. A., & Thomas, M. R. J. 1998, *MNRAS*, **293**, L83
- Benjamin, R. A., Skillman, E. D., & Smits, D. P. 1999, *ApJ*, **514**, 307
- Bhatia, A. K. & Kastner, S. O. 1993, *Atom. Data Nucl. Data Tabl.*, **54**, 133
- Biemont, E. & Bromage, G. E. 1983, *MNRAS*, **205**, 1085
- Biémont, E. & Hansen, J. E. 1986, *Phys. Scr.*, **34**, 116
- Blöcker, T. 1995, *A&A*, **299**, 755
- Blöcker, T. 2001, *Ap&SS*, **275**, 1
- Borkowski, K. J., Harrington, J. P., Tsvetanov, Z., & Clegg, R. E. S. 1993, *ApJ*, **415**, L47
- Busso, M., Gallino, R., & Wasserburg, G. J. 1999, *ARA&A*, **37**, 239
- Cahn, J. H., Kaler, J. B., & Stanghellini, L. 1992, *A&AS*, **94**, 399
- Charbonnel, C. & Lagarde, N. 2010, *A&A*, **522**, A10
- Condon, J. J. & Kaplan, D. L. 1998, *ApJS*, **117**, 361
- Condon, J. J., Kaplan, D. L., & Terzian, Y. 1999, *ApJS*, **123**, 219
- Corradi, R. L. M., García-Rojas, J., Jones, D., & Rodríguez-Gil, P. 2015, *ApJ*, **803**, 99
- Crowther, P. A., De Marco, O., & Barlow, M. J. 1998, *MNRAS*, **296**, 367
- Danehkar, A. 2014, *Evolution of Planetary Nebulae with WR-type Central Stars*, PhD thesis, Macquarie University
- Danehkar, A. 2015, *ApJ*, **815**, 35
- Danehkar, A. 2018a, *Publ. Astron. Soc. Australia*, **35**, e005
- Danehkar, A. 2018b, *J. Open Source Softw.*, **3**, 899
- Danehkar, A. 2019, *J. Open Source Softw.*, **4**, 898
- Danehkar, A. 2021, *arXiv e-prints*, [arXiv:2107.03994](https://arxiv.org/abs/2107.03994), *ApJS*, submitted
- Danehkar, A., Karovska, M., Maksym, W. P., & Montez, Rodolfo, J. 2018, *ApJ*, **852**, 87
- Danehkar, A. & Parker, Q. A. 2015, *MNRAS*, **449**, L56
- Danehkar, A., Parker, Q. A., & Ercolano, B. 2013, *MNRAS*, **434**, 1513
- Danehkar, A., Parker, Q. A., & Steffen, W. 2016, *AJ*, **151**, 38
- Danehkar, A., Todt, H., Ercolano, B., & Kniazev, A. Y. 2014, *MNRAS*, **439**, 3605
- Davey, A. R., Storey, P. J., & Kisielius, R. 2000, *A&AS*, **142**, 85
- Daw, A., Parkinson, W. H., Smith, P. L., & Calamai, A. G. 2000, *ApJ*, **533**, L179
- De Marco, O., Barlow, M. J., & Storey, P. J. 1997, *MNRAS*, **292**, 86
- De Marco, O. & Crowther, P. A. 1998, *MNRAS*, **296**, 419
- Delgado-Inglada, G., Morisset, C., & Stasińska, G. 2014, *MNRAS*, **440**, 536
- Depew, K., Parker, Q. A., Miszalski, B., et al. 2011, *MNRAS*, **414**, 2812
- Dere, K. P., Del Zanna, G., Young, P. R., Landi, E., & Sutherland, R. S. 2019, *ApJS*, **241**, 22
- Derlopa, S., Akras, S., Boumis, P., & Steffen, W. 2019, *MNRAS*, **484**, 3746
- Dopita, M., Hart, J., McGregor, P., et al. 2007, *Ap&SS*, **310**, 255
- Dopita, M., Rhee, J., Farage, C., et al. 2010, *Ap&SS*, **327**, 245
- Dopita, M. A., Ali, A., Sutherland, R. S., Nicholls, D. C., & Amer, M. A. 2017, *MNRAS*, **470**, 839
- Dopita, M. A. & Meatheringham, S. J. 1990, *ApJ*, **357**, 140
- Dopita, M. A. & Meatheringham, S. J. 1991, *ApJ*, **377**, 480
- Dopita, M. A., Sutherland, R. S., Nicholls, D. C., Kewley, L. J., & Vogt, F. P. A. 2013, *ApJS*, **208**, 10
- Ercolano, B., Barlow, M. J., Storey, P. J., et al. 2003, *MNRAS*, **344**, 1145
- Ercolano, B., Young, P. R., Drake, J. J., & Raymond, J. C. 2008, *ApJS*, **175**, 534
- Escalante, V. & Morisset, C. 2005, *MNRAS*, **361**, 813
- Escalante, V., Morisset, C., & Georgiev, L. 2012, *MNRAS*, **426**, 2318
- Fang, X., Guerrero, M. A., Marquez-Lugo, R. A., et al. 2014, *ApJ*, **797**, 100
- Fang, X., Storey, P. J., & Liu, X.-W. 2011, *A&A*, **530**, A18
- Fang, X., Storey, P. J., & Liu, X.-W. 2013, *A&A*, **550**, C2
- Fanning, D. W. 2011, *Coyote's Guide to Traditional IDL Graphics* (Coyote Book Publishing)
- Ferland, G. J. 1992, *ApJ*, **389**, L63
- Frew, D. J., Bojičić, I. S., & Parker, Q. A. 2013, *MNRAS*, **431**, 2
- Frew, D. J., Parker, Q. A., & Bojičić, I. S. 2016, *MNRAS*, **455**, 1459
- Froese Fischer, C. & Tachiev, G. 2004, *Atom. Data Nucl. Data Tabl.*, **87**, 1
- Froese Fischer, C., Tachiev, G., & Irimia, A. 2006, *Atom. Data Nucl. Data Tabl.*, **92**, 607
- Galaviz, M. E., Mendoza, C., & Zeppen, C. J. 1995, *A&AS*, **111**, 347
- García-Rojas, J., Corradi, R. L. M., Monteiro, H., et al. 2016, *ApJ*, **824**, L27
- García-Rojas, J., Peña, M., Morisset, C., et al. 2013, *A&A*, **558**, A122
- García-Rojas, J., Peña, M., Morisset, C., Mesa-Delgado, A., & Ruiz, M. T. 2012, *A&A*, **538**, A54
- García-Rojas, J., Peña, M., & Peimbert, A. 2009, *A&A*, **496**, 139
- Garnett, D. R. 1992, *AJ*, **103**, 1330
- Girard, P., Köppen, J., & Acker, A. 2007, *A&A*, **463**, 265
- Gómez-Llanos, V. & Morisset, C. 2020, *MNRAS*, **497**, 3363
- Goodman, J. & Weare, J. 2010, *Comm. App. Math. & Comp. Sci.*, **5**, 5
- Gorny, S. K., Stasińska, G., & Tylanda, R. 1997, *A&A*, **318**, 256
- Guerrero, M. A. & Manchado, A. 1996, *ApJ*, **472**, 711
- Hajian, A. R., Balick, B., Terzian, Y., & Perinotto, M. 1997, *ApJ*, **487**, 304
- Hambly, N. C., MacGillivray, H. T., Read, M. A., et al. 2001, *MNRAS*, **326**, 1279
- Harris, C. R., Millman, K. J., van der Walt, S. J., et al. 2020, *Nature*, **585**, 357
- Hazard, C., Terlevich, R., Morton, D. C., Sargent, W. L. W., & Ferland, G. 1980, *Nature*, **285**, 463
- Henney, W. J. & Stasińska, G. 2010, *ApJ*, **711**, 881
- Henry, R. B. C., Kwitter, K. B., & Balick, B. 2004, *AJ*, **127**, 2284
- Henry, R. B. C., Speck, A., Karakas, A. I., Ferland, G. J., & Maguire, M. 2012, *ApJ*, **749**, 61
- Herwig, F. 2001, *Ap&SS*, **275**, 15
- Herwig, F. 2005, *ARA&A*, **43**, 435
- Howarth, I. D. 1983, *MNRAS*, **203**, 301
- Hudson, C. E., Ramsbottom, C. A., & Scott, M. P. 2012, *ApJ*, **750**, 65
- Hunter, J. D. 2007, *Comput. Sci. Eng.*, **9**, 90
- Iben, Jr., I., Kaler, J. B., Truran, J. W., & Renzini, A. 1983, *ApJ*, **264**, 605
- Iben, Jr., I., & Renzini, A. 1983, *ARA&A*, **21**, 271
- Izotov, Y. I., Thuan, T. X., & Lipovetsky, V. A. 1994, *ApJ*, **435**, 647
- Jacoby, G. H. & Ford, H. C. 1983, *ApJ*, **266**, 298
- Jacoby, G. H., Hillwig, T. C., & Jones, D. 2020, *MNRAS*, **498**, L114
- Jones, D., Wesson, R., García-Rojas, J., Corradi, R. L. M., & Boffin, H. M. J. 2016, *MNRAS*, **455**, 3263
- Kaler, J. B., Shaw, R. A., Feibelman, W. A., & Imhoff, C. L. 1991, *PASP*, **103**, 67
- Karakas, A. I. 2010, *MNRAS*, **403**, 1413
- Karakas, A. I. 2014, *MNRAS*, **445**, 347
- Karakas, A. I. & Lattanzio, J. C. 2003, *Publ. Astron. Soc. Australia*, **20**, 393
- Karakas, A. I. & Lattanzio, J. C. 2014, *Publ. Astron. Soc. Australia*, **31**, 30
- Karakas, A. I. & Lugaro, M. 2016, *ApJ*, **825**, 26
- Karakas, A. I., van Raai, M. A., Lugaro, M., Sterling, N. C., & Dinerstein, H. L. 2009, *ApJ*, **690**, 1130
- Kingsburgh, R. L. & Barlow, M. J. 1994, *MNRAS*, **271**, 257
- Kisielius, R., Storey, P. J., Ferland, G. J., & Keenan, F. P. 2009, *MNRAS*, **397**, 903
- Koesterke, L. 2001, *Ap&SS*, **275**, 41
- Koesterke, L. & Hamann, W.-R. 1997, *A&A*, **320**, 91
- Kwitter, K. B. & Henry, R. B. C. 2001, *ApJ*, **562**, 804
- Kwitter, K. B., Henry, R. B. C., & Milingo, J. B. 2003, *PASP*, **115**, 80
- Landi, E. & Bhatia, A. K. 2005, *Atom. Data Nucl. Data Tabl.*, **89**, 195
- Landi, E., Del Zanna, G., Young, P. R., Dere, K. P., & Mason, H. E. 2012, *ApJ*, **744**, 99
- Landman, D. A., Roussel-Dupre, R., & Tanigawa, G. 1982, *ApJ*, **261**, 732
- Landsman, W. B. 1993, in *ASP Conf. Ser.*, Vol. 52, *Astronomical Data Analysis Software and Systems II*, ed. R. J. Hanisch, R. J. V. Brissenden, & J. Barnes (San Francisco, CA: ASP), **246**
- Lau, H. H. B., De Marco, O., & Liu, X. W. 2011, *MNRAS*, **410**, 1870
- Lennon, D. J. & Burke, V. M. 1994, *A&AS*, **103**, 273
- Lenz, D. D. & Ayres, T. R. 1992, *PASP*, **104**, 1104
- Leuening, U. & Hamann, W.-R. 1998, *A&A*, **330**, 265
- Leuening, U., Hamann, W.-R., & Jeffery, C. S. 1996, *A&A*, **312**, 167
- Liu, X.-W. 2003, in *IAU Symposium*, Vol. 209, *Planetary Nebulae: Their Evolution and Role in the Universe*, ed. S. Kwok, M. Dopita, & R. Sutherland, **339**
- Liu, X.-W., Luo, S.-G., Barlow, M. J., Danziger, I. J., & Storey, P. J. 2001, *MNRAS*, **327**, 141
- Liu, X.-W., Storey, P. J., Barlow, M. J., et al. 2000, *MNRAS*, **312**, 585
- Liu, Y., Liu, X.-W., Barlow, M. J., & Luo, S.-G. 2004, *MNRAS*, **353**, 1251
- Luo, S.-G., Liu, X.-W., & Barlow, M. J. 2001, *MNRAS*, **326**, 1049
- Marigo, P. 2002, *A&A*, **387**, 507
- McLaughlin, B. M. & Bell, K. L. 2000, *J. Phys. B*, **33**, 597
- McNabb, I. A., Fang, X., Liu, X.-W., Bastin, R. J., & Storey, P. J. 2013, *MNRAS*, **428**, 3443
- Mendoza, C. & Bautista, M. A. 2014, *ApJ*, **785**, 91
- Mendoza, C. & Zeppen, C. J. 1982, *MNRAS*, **198**, 127
- Merkelis, G., Martinson, I., Kisielius, R., & Vilkas, M. J. 1999, *Phys. Scr.*, **59**, 122
- Milingo, J. B., Kwitter, K. B., Henry, R. B. C., & Cohen, R. E. 2002, *ApJS*, **138**, 279
- Milne, D. K. & Aller, L. H. 1975, *A&A*, **38**, 183
- Nicholls, D. C., Dopita, M. A., & Sutherland, R. S. 2012, *ApJ*, **752**, 148
- Nicholls, D. C., Dopita, M. A., Sutherland, R. S., Kewley, L. J., & Palay, E. 2013, *ApJS*, **207**, 21
- O'Dell, C. R. 1962, *ApJ*, **135**, 371
- Parker, Q. A., Phillipps, S., Pierce, M., & et al. 2005, *MNRAS*, **362**, 689
- Peña, M., Stasińska, G., Esteban, C., et al. 1998, *A&A*, **337**, 866
- Peña, M., Stasińska, G., & Medina, S. 2001, *A&A*, **367**, 983
- Peimbert, M. 1967, *ApJ*, **150**, 825

- Peimbert, M. 1971, *Boletín de los Observatorios Tonantzintla y Tacubaya*, **6**, 29
- Peimbert, M. & Torres-Peimbert, S. 1983, in *IAU Symposium*, Vol. 103, *Planetary Nebulae*, ed. D. R. Flower, 233–241
- Péquignot, D., Petitjean, P., & Boisson, C. 1991, *A&A*, **251**, 680
- Péquignot, D., Walsh, J. R., Zijlstra, A. A., & Dudziak, G. 2000, *A&A*, **361**, L1
- Pollacco, D. L., Lawson, W. A., Clegg, R. E. S., & Hill, P. W. 1992, *MNRAS*, **257**, 33P
- Porter, R. L., Ferland, G. J., Storey, P. J., & Detisch, M. J. 2013, *MNRAS*, **433**, L89
- Pottasch, S. R. & Bernard-Salas, J. 2006, *A&A*, **457**, 189
- Pottasch, S. R., Surendiranath, R., & Bernard-Salas, J. 2011, *A&A*, **531**, A23
- Preite-Martínez, A., Acker, A., Koeppen, J., & Stenholm, B. 1989, *A&AS*, **81**, 309
- Purton, C. R., Feldman, P. A., Marsh, K. A., Allen, D. A., & Wright, A. E. 1982, *MNRAS*, **198**, 321
- Ramsbottom, C. A. & Bell, K. L. 1997, *Atom. Data Nucl. Data Tabl.*, **66**, 65
- Ramsbottom, C. A., Bell, K. L., & Keenan, F. P. 1997, *MNRAS*, **284**, 754
- Ramsbottom, C. A., Bell, K. L., & Keenan, F. P. 1998, *MNRAS*, **293**, 233
- Ramsbottom, C. A., Bell, K. L., & Keenan, F. P. 2001, *Atom. Data Nucl. Data Tabl.*, **77**, 57
- Ramsbottom, C. A., Bell, K. L., & Stafford, R. P. 1996, *Atom. Data Nucl. Data Tabl.*, **63**, 57
- Rodríguez, M. 2020, *MNRAS*, **495**, 1016
- Sawey, P. M. J. & Berrington, K. A. 1993, *Atom. Data Nucl. Data Tabl.*, **55**, 81
- Seaton, M. J. 1979, *MNRAS*, **187**, 785
- Shaw, R. A. & Kaler, J. B. 1989, *ApJS*, **69**, 495
- Smits, D. P. 1996, *MNRAS*, **278**, 683
- Stancliffe, R. J. & Jeffery, C. S. 2007, *MNRAS*, **375**, 1280
- Stanghellini, L. & Haywood, M. 2010, *ApJ*, **714**, 1096
- Stanghellini, L., Shaw, R. A., Balick, B., et al. 2003, *ApJ*, **596**, 997
- Stanghellini, L., Shaw, R. A., Mutchler, M., et al. 2002, *ApJ*, **575**, 178
- Stanghellini, L., Shaw, R. A., & Villaver, E. 2008, *ApJ*, **689**, 194
- Stasińska, G. 1990, *A&AS*, **83**, 501
- Stasińska, G. 2005, *A&A*, **434**, 507
- Stasińska, G., Peña, M., Bresolin, F., & Tsamis, Y. G. 2013, *A&A*, **552**, A12
- Stasińska, G., Richer, M. G., & McCall, M. L. 1998, *A&A*, **336**, 667
- Storey, P. J. & Hummer, D. G. 1995, *MNRAS*, **272**, 41
- Storey, P. J. & Sochi, T. 2013, *MNRAS*, **430**, 599
- Storey, P. J. & Sochi, T. 2015a, *MNRAS*, **449**, 2974
- Storey, P. J. & Sochi, T. 2015b, *MNRAS*, **446**, 1864
- Storey, P. J., Sochi, T., & Bastin, R. 2017, *MNRAS*, **470**, 379
- Storey, P. J. & Zeippen, C. J. 2000, *MNRAS*, **312**, 813
- Straniero, O., Chieffi, A., Limongi, M., et al. 1997, *ApJ*, **478**, 332
- Tachiev, G. & Froese Fischer, C. 2001, *Can. J. Phys.*, **79**, 955
- Tachiev, G. I. & Froese Fischer, C. 2002, *A&A*, **385**, 716
- Tayal, S. S. 1997, *Atom. Data Nucl. Data Tabl.*, **67**, 331
- Tayal, S. S. 2006, *ApJS*, **163**, 207
- Tayal, S. S. 2011, *ApJS*, **195**, 12
- Toalá, J. A., Jiménez-Hernández, P., Rodríguez-González, J. B., et al. 2021, *MNRAS*, **503**, 1543
- Tsamis, Y. G., Barlow, M. J., Liu, X.-W., Danziger, I. J., & Storey, P. J. 2003a, *MNRAS*, **345**, 186
- Tsamis, Y. G., Barlow, M. J., Liu, X.-W., Danziger, I. J., & Storey, P. J. 2003b, *MNRAS*, **338**, 687
- Tsamis, Y. G., Barlow, M. J., Liu, X.-W., Storey, P. J., & Danziger, I. J. 2004, *MNRAS*, **353**, 953
- Tsamis, Y. G. & Péquignot, D. 2005, *MNRAS*, **364**, 687
- Tsamis, Y. G., Walsh, J. R., Péquignot, D., et al. 2008, *MNRAS*, **386**, 22
- Tylenda, R., Acker, A., & Stenholm, B. 1993, *A&AS*, **102**, 595
- Tylenda, R., Siódmiak, N., Górny, S. K., Corradi, R. L. M., & Schwarz, H. E. 2003, *A&A*, **405**, 627
- van der Hucht, K. A. 2001, *New Astro. Rev.*, **45**, 135
- van der Hucht, K. A., Conti, P. S., Lundstrom, I., & Stenholm, B. 1981, *Space Sci. Rev.*, **28**, 227
- Ventura, P. & D'Antona, F. 2005, *A&A*, **431**, 279
- Ventura, P., Di Criscienzo, M., Carini, R., & D'Antona, F. 2013, *MNRAS*, **431**, 3642
- Viegas, S. M. & Clegg, R. E. S. 1994, *MNRAS*, **271**, 993
- Virtanen, P., Gommers, R., Oliphant, T. E., et al. 2020, *Nature Methods*, **17**, 261
- Wang, W. & Liu, X.-W. 2007, *MNRAS*, **381**, 669
- Weidmann, W. A., Gamen, R., Díaz, R. J., & Niemela, V. S. 2008, *A&A*, **488**, 245
- Werner, K. & Herwig, F. 2006, *PASP*, **118**, 183
- Wesson, R. 2016, *MNRAS*, **456**, 3774
- Wesson, R., Barlow, M. J., Liu, X.-W., et al. 2008, *MNRAS*, **383**, 1639
- Wesson, R., Jones, D., García-Rojas, J., Boffin, H. M. J., & Corradi, R. L. M. 2018, *MNRAS*, **480**, 4589
- Wesson, R. & Liu, X.-W. 2004, *MNRAS*, **351**, 1026
- Wesson, R., Liu, X.-W., & Barlow, M. J. 2003, *MNRAS*, **340**, 253
- Wesson, R., Liu, X.-W., & Barlow, M. J. 2005, *MNRAS*, **362**, 424
- Wyse, A. B. 1942, *ApJ*, **95**, 356
- Yuan, H.-B., Liu, X.-W., Péquignot, D., et al. 2011, *MNRAS*, **411**, 1035
- Zatsarinny, O. & Tayal, S. S. 2003, *ApJS*, **148**, 575
- Zeippen, C. J. 1982, *MNRAS*, **198**, 111
- Zhang, Y., Liu, X.-W., Liu, Y., & Rubin, R. H. 2005, *MNRAS*, **358**, 457
- Zhang, Y., Liu, X.-W., Wesson, R., et al. 2004, *MNRAS*, **351**, 935
- Zhang, Y., Liu, X.-W., & Zhang, B. 2014, *ApJ*, **780**, 93
- Zhang, Y., Zhang, B., & Liu, X.-W. 2016, *ApJ*, **817**, 68

Appendix

B. Supplementary Data

The following tables and figure sets are available for the electronic edition of this article:

Table 4. Observed and dereddened line fluxes on a scale relative to $H\beta$, where $H\beta = 100$.

Table 6. Plasma diagnostics based on CELs.

Table 7. Plasma diagnostics based on He I lines.

Table 8. Plasma diagnostics based on heavy element ORLs.

Table 11. Ionic abundances derived from CELs.

Table 12. Ionic abundances derived from ORLs.

Table 13. Mean ionic and total elemental abundances derived from ORLs and CELs.

Fig. Set 2. N_e-T_e diagnostic diagrams based on CELs.

Fig. Set 4. T_e diagnostic diagrams based on C II ORLs, and N_e-T_e diagnostic diagrams based on O II and N II ORLs.

Tables 4, 6–8, and 11–13 are published in the machine-readable format.

Table 4. Observed and dereddened line fluxes on a scale relative to $H\beta$, where $H\beta = 100$. Observed fluxes are denoted by $F(\lambda)$ and dereddened fluxes by $I(\lambda)$. The symbol ‘*’ in the observed and dereddened fluxes indicates that the listed line is blended with the above listed line.

λ_{lab}	Ion	λ_{obs}	$F(\lambda)$	$\varepsilon_{F(\lambda)}(\%)$	$I(\lambda)$	$\varepsilon_{I(\lambda)}(\%)$	Mult	Lower term	Upper term	g1	g2
PB 6 (PNG278.8+04.9)											
3726.03	[O II] ^a	3726.03	50.700	±0.0	69.898	±2.6	F1	2p3 4S*	2p3 2D*	4	4
3728.82	[O II] ^a	3728.82	*		*		F1	2p3 4S*	2p3 2D*	4	6
3868.75	[Ne III] ^a	3868.75	84.000	±0.0	112.065	±2.3	F1	2p4 3P	2p4 1D	5	5
3889.05	H 8 ^a	3889.05	11.500	±0.0	15.266	+2.3 -1.9	H8	2p+ 2P*	8d+ 2D	8	*
3967.46	[Ne III] ^a	3967.46	30.800	±0.0	40.079	+2.1 -1.8	F1	2p4 3P	2p4 1D	3	5
4101.74	H 6 ^a	4101.74	22.500	±0.0	28.240	±1.8	H6	2p+ 2P*	6d+ 2D	8	72
4340.47	H 5 ^a	4340.47	44.200	±0.0	51.795	±1.3	H5	2p+ 2P*	5d+ 2D	8	50
4363.21	[O III] ^a	4363.21	17.100	±0.0	19.904	+1.3 -1.0	F2	2p2 1D	2p2 1S	5	1
4452.37	O II	4453.76	0.053	±16.7	0.060	+20.9 -22.8	V5	3s 2P	3p 2D*	4	4
4471.50	He I	4472.51	2.061	±1.5	2.322	±2.2	V14	2p 3P*	4d 3D	9	15
4491.23	O II	4493.19	0.019	±23.1	0.021	+28.7 -31.2	V86a	3d 2P	4f D3*	4	6
4510.91	N III	4511.90	0.207	±4.5	0.230	±5.8	V3	3s' 4P*	3p' 4D	2	4
4514.86	N III	4516.17	0.066	±19.8	0.073	+24.4 -26.7	V3	3s' 4P*	3p' 4D	6	8
4541.59	He II	4542.59	4.340	±0.6	4.787	+1.1 -1.0	4.9	4f+ 2F*	9g+ 2G	32	*
4562.60	Mg I	4563.59	0.112	±7.1	0.123	+8.8 -9.3		3s2 1S	3s3p 3P*	1	5
4571.10	Mg I	4572.04	0.174	±5.4	0.190	±6.7		3s2 1S	3s3p 3P*	1	3
4607.03	[Fe III]	4607.70	0.233	±5.3	0.252	+6.5 -7.1	F3	3d6 5D	3d6 3F2	9	7
4613.87	N II	4620.82	0.020	±26.1	0.022	+31.8 -35.3	V5	3s 3P*	3p 3P	3	3
4625.53	[Ar V]	4626.73	0.058	±18.9	0.062	+23.0 -25.2		3p2 1D	3p2 1S	5	1
4634.14	N III	4635.14	0.455	±14.9	0.488	+17.9 -20.2	V2	3p 2P*	3d 2D	2	4
4640.64	N III	4641.93	1.187	±5.5	1.270	+6.7 -7.5	V2	3p 2P*	3d 2D	4	6
4685.68	He II	4686.81	130.215	±0.1	137.443	±0.4	3.4	3d+ 2D	4f+ 2F*	18	32
4711.37	[Ar IV]	4712.47	9.700	±0.4	10.158	±0.6	F1	3p3 4S*	3p3 2D*	4	6
4724.15	[Ne IV]	4725.86	3.499	±3.2	3.650	+3.9 -4.3	F1	2p3 2D*	2p3 2P*	4	4
4740.17	[Ar IV]	4741.36	8.546	±0.4	8.871	±0.6	F1	3p3 4S*	3p3 2D*	4	4
4788.13	N II	4783.09	0.259	±5.4	0.265	±6.3	V20	3p 3D	3d 3D*	5	5
4861.33	H 4	4862.58	100.000	±1.0	100.002	±1.2	H4	2p+ 2P*	4d+ 2D	8	32
4881.11	[Fe III]	4882.37	0.040	±18.5	0.040	+21.5 -23.2	F2	3d6 5D	3d6 3H	9	9
4958.91	[O III]	4960.39	383.101	±0.4	371.794	±0.5	F1	2p2 3P	2p2 1D	3	5
5006.84	[O III]	5008.38	1243.383	±0.8	1189.087	+1.0 -1.2	F1	2p2 3P	2p2 1D	5	5
5270.40	[Fe III]	5272.14	0.069	±10.6	0.061	±13.1	F1	3d6 5D	3d6 3P2	7	5
5411.52	He II	5413.34	12.983	±0.6	10.987	±1.3	4.7	4f+ 2F*	7g+ 2G	32	98
5517.66	[Cl III]	5519.65	0.867	±2.0	0.715	+2.7 -3.3	F1	2p3 4S*	2p3 2D*	4	6
5537.60	[Cl III]	5539.71	0.942	±1.4	0.774	±2.1	F1	2p3 4S*	2p3 2D*	4	4
5676.02	N II	5678.39	0.452	±2.7	0.360	+3.5 -4.3	V3	3s 3P*	3p 3D	1	3
5695.92	C III	5703.43	0.041	±12.1	0.033	+13.9 -15.6	V2	3p 1P*	3d 1D	3	5
5754.60	[N II]	5755.96	5.958	±0.3	4.672	+1.7 -2.1	F3	2p2 1D	2p2 1S	5	1
5801.51	C IV	5802.60	0.623	±2.7	0.484	+3.6 -4.2	V1	3s 2S	3p 2P*	2	4
5812.14	C IV	5813.39	0.319	±4.7	0.247	+5.8 -6.6	V1	3s 2S	3p 2P*	2	2
5875.66	He I	5877.04	9.246	±0.4	7.070	+1.9 -2.3	V11	2p 3P*	3d 3D	9	15
5931.78	N II	5933.38	0.198	±4.9	0.150	+6.0 -6.9	V28	3p 3P	3d 3D*	3	5
5978.97	S III	5978.55	0.234	±2.1	0.175	±3.3	V4				
6036.70	He II	6038.22	0.290	±1.2	0.215	+2.5 -3.1	5.21	5g+ 2G	21h+ 2H*	50	*
6074.10	He II	6075.61	0.273	±2.5	0.201	+3.8 -4.2	5.20	5g+ 2G	20h+ 2H*	50	*
6101.83	[K IV]	6103.09	0.522	±2.4	0.381	+3.8 -4.2	F1	3p4 3P	3d4 1D	5	5
6118.20	He II	6119.79	0.382	±5.2	0.278	+6.7 -7.4	5.19	5g+ 2G	19h+ 2H*	50	*

Danehkar

6233.80	He II	6235.24	0.593	±1.0	0.422	+2.6 -3.1	5.17	5g+ 2G	17h+ 2H*	50	*
6300.34	[O I]	6301.80	5.600	±0.9	3.937	+2.6 -3.1	F1	2p4 3P	2p4 1D	5	5
6312.10	[S III]	6313.39	4.703	±0.8	3.299	+2.5 -3.1	F3	2p2 1D	2p2 1S	5	1
6363.78	[O I]	6365.26	1.950	±1.4	1.355	+3.0 -3.4	F1	2p4 3P	2p4 1D	3	5
6393.60	[Mn V]	6395.31	0.079	±9.1	0.055	+11.1 -12.2		3d3 4F	3d3 4P	10	6
6406.30	He II	6407.88	0.987	±1.3	0.680	+2.9 -3.4	5.15	5g+ 2G	15h+ 2H*	50	*
6461.95	C II	6462.94	0.062	±5.8	0.042	+7.6 -8.1		4f 2F*	6g 2G	14	18
6527.11	He II	6528.60	1.101	±0.8	0.742	+2.8 -3.4	5.14	5g+ 2G	14h+ 2H*	50	*
6548.10	[N II]	6549.57	109.808	±0.3	73.770	+2.7 -3.4	F1	2p2 3P	2p2 1D	3	5
6562.77	H 3	6564.34	424.997	±1.7	284.771	±3.3	H3	2p+ 2P*	3d+ 2D	8	18
6583.50	[N II]	6584.93	341.264	±0.9	227.825	±3.1	F1	2p2 3P	2p2 1D	5	5
6678.16	He I	6679.70	2.860	±0.8	1.878	±3.1	V46	2p 1P*	3d 1D	3	5
6683.20	He II	6684.74	1.360	±1.5	0.892	±3.5	5.13	5g+ 2G	13h+ 2H*	50	*
6716.44	[S II]	6718.02	9.572	±0.8	6.244	±3.1	F2	2p3 4S*	2p3 2D*	4	6
6730.82	[S II]	6732.40	12.788	±0.7	8.321	+2.9 -3.5	F2	2p3 4S*	2p3 2D*	4	4
6795.00	[K IV]	6796.50	0.142	±3.7	0.091	±5.6	F1	3p4 3P	3p4 1D	3	5
6890.88	He I	6892.48	1.530	±1.0	0.969	±3.4	5.12	5g+ 2G	12h+ 2H	50	*
7005.67	[Ar V]	7007.39	6.484	±0.4	4.032	±3.3	F1	3s2 3P	3s2 1D	5	5
7065.25	He I	7066.76	2.553	±4.2	1.572	±6.6	V10	2p 3P*	3s 3S	9	3
7135.80	[Ar III] ^a	7135.80	19.700	±0.0	12.001	+3.4 -4.1	F1	3p4 3P	3p4 1D	5	5

M 3-30 (PNG017.9–04.8)

3726.03	[O II] ^a	3726.03	8.670	±0.0	15.700	+1.0 -1.0	F1	2p3 4S*	2p3 2D*	4	4
3728.82	[O II] ^a	3728.82	6.600	±0.0	11.939	+1.0 -1.0	F1	2p3 4S*	2p3 2D*	4	6
3868.75	[Ne III] ^a	3868.75	34.470	±0.0	58.743	±0.9	F1	2p4 3P	2p4 1D	5	5
4363.21	[O III] ^a	4363.21	3.200	±0.0	4.237	±0.4	F2	2p2 1D	2p2 1S	5	1
4471.50	He I	4471.99	3.059	±1.8	3.814	±2.3	V14	2p 3P*	4d 3D	9	15
4510.91	N III	4511.36	0.149	±7.0	0.182	±8.7	V3	3s' 4P*	3p' 4D	2	4
4541.59	He II	4542.07	2.150	±1.2	2.578	±1.5	4.9	4f+ 2F*	9g+ 2G	32	*
4601.48	N II	4603.27	0.185	±9.5	0.214	±11.6	V5	3s 3P*	3p 3P	3	5
4607.03	[Fe III]	4610.14	0.199	±12.0	0.230	+13.9 -14.2	F3	3d6 5D	3d6 3F2	9	7
4613.14	O II	4613.76	0.043	±33.8	0.050	+40.0 -40.4	V92b	3d 2D	4f F3*	6	6
4613.87	N II	4616.45	0.040	±42.9	0.046	+50.3 -49.7	V5	3s 3P*	3p 3P	3	3
4641.84	N III	4641.12	3.197	±4.2	3.622	+5.0 -5.0	V2	3p 2P*	3d 2D	4	4
4650.84	O II	4649.67	1.042	±7.4	1.174	±8.6	V1	3s 4P	3p 4D*	2	2
4661.63	O II	4662.25	0.446	±24.8	0.500	+29.4 -28.5	V1	3s 4P	3p 4D*	4	4
4676.24	O II	4676.82	0.207	±18.0	0.230	±21.3	V1	3s 4P	3p 4D*	6	6
4685.68	He II	4686.28	77.280	±0.2	85.400	±0.3	3.4	3d+ 2D	4f+ 2F*	18	32
4711.37	[Ar IV]	4711.92	1.860	±1.8	2.026	±2.1	F1	3p3 4S*	3p3 2D*	4	6
4740.17	[Ar IV]	4740.77	1.479	±2.0	1.585	±2.4	F1	3p3 4S*	3p3 2D*	4	4
4861.33	H 4	4861.96	100.000	±0.5	100.004	±0.6	H4	2p+ 2P*	4d+ 2D	8	32
4923.93	[Fe II]	4922.44	0.845	±2.9	0.815	±3.4		4s2 4P	4p 6P*	6	4
4958.91	[O III]	4959.64	193.313	±0.4	182.894	±0.5	F1	2p2 3P	2p2 1D	3	5
5006.84	[O III]	5007.61	598.266	±0.6	550.852	±0.8	F1	2p2 3P	2p2 1D	5	5
5411.52	He II	5412.56	8.574	±1.0	6.297	±1.4	4.7	4f+ 2F*	7g+ 2G	32	98
5517.66	[Cl III]	5518.59	0.850	±3.4	0.595	±4.2	F1	2p3 4S*	2p3 2D*	4	6
5537.60	[Cl III]	5538.87	0.617	±4.8	0.429	±5.9	F1	2p3 4S*	2p3 2D*	4	4
5679.56	N II	5680.43	0.412	±7.2	0.271	±8.7	V3	3s 3P*	3p 3D	5	7
5754.60	[N II]	5755.41	0.568	±3.3	0.362	±4.2	F3	2p2 1D	2p2 1S	5	1
5812.14	C IV	5813.05	0.068	±25.6	0.042	+31.6 -32.4	V1	3s 2S	3p 2P*	2	2
5875.66	He I	5876.43	20.781	±0.4	12.651	±1.0	V11	2p 3P*	3d 3D	9	15
5927.81	N II	5932.14	0.130	±6.2	0.078	±7.6	V28	3p 3P	3d 3D*	1	3

Physical and chemical properties of WR planetary nebulae

6233.80	He II	6234.39	0.588	±4.3	0.314	±5.3	5.17	5g+ 2G	17h+ 2H*	50	*
6312.10	[S III]	6312.67	2.630	±1.5	1.365	$^{+2.2}_{-1.9}$	F3	2p2 1D	2p2 1S	5	1
6406.30	He II	6407.29	0.408	±5.2	0.205	±6.3	5.15	5g+ 2G	15h+ 2H*	50	*
6461.95	C II	6462.82	0.387	±6.6	0.191	±8.1		4f 2F*	6g 2G	14	18
6527.11	He II	6527.90	0.710	±3.4	0.343	±4.3	5.14	5g+ 2G	14h+ 2H*	50	*
6548.10	[N II]	6549.12	21.820	±1.0	10.456	±1.8	F1	2p2 3P	2p2 1D	3	5
6562.77	H 3	6563.60	604.726	±0.7	288.395	±1.6	H3	2p+ 2P*	3d+ 2D	8	18
6583.50	[N II]	6584.25	71.033	±0.4	33.646	±1.4	F1	2p2 3P	2p2 1D	5	5
6678.16	He I	6678.99	7.653	±0.6	3.515	±1.6	V46	2p 1P*	3d 1D	3	5
6716.44	[S II]	6717.31	13.180	±0.4	5.981	±1.5	F2	2p3 4S*	2p3 2D*	4	6
6730.82	[S II]	6731.69	13.568	±0.4	6.129	±1.5	F2	2p3 4S*	2p3 2D*	4	4
6890.88	He I	6891.63	1.062	±2.4	0.457	±3.4	5.12	5g+ 2G	12h+ 2H	50	*
7065.25	He I	7065.96	4.525	±7.6	1.847	±9.6	V10	2p 3P*	3s 3S	9	3
7135.80	[Ar III] ^a	7135.80	33.600	±0.0	13.436	±1.5	F1	3p4 3P	3p4 1D	5	5

Hb 4 (shell) (PNG003.1+02.9)

3726.03	[O II] ^a	3726.03	7.700	±0.0	22.995	±0.6	F1	2p3 4S*	2p3 2D*	4	4
3728.82	[O II] ^a	3728.82	4.870	±0.0	14.514	±0.6	F1	2p3 4S*	2p3 2D*	4	6
3868.75	[Ne III] ^a	3868.75	19.480	±0.0	52.015	±0.5	F1	2p4 3P	2p4 1D	5	5
4363.21	[O III] ^a	4363.21	3.630	±0.0	6.089	±0.3	F2	2p2 1D	2p2 1S	5	1
4442.02	N II	4437.05	0.085	±23.7	0.132	$^{+28.3}_{-27.4}$	V55a	3d 3P*	4f 2[3]	3	5
4459.94	N II	4459.34	0.073	±13.5	0.111	$^{+16.4}_{-15.7}$	V21	3p 3D	3d 3P*	3	1
4471.50	He I	4470.11	3.339	±1.1	5.014	±1.4	V14	2p 3P*	4d 3D	9	15
4510.91	N III	4509.35	0.100	±7.5	0.144	±8.8	V3	3s' 4P*	3p' 4D	2	4
4514.86	N III	4511.94	0.090	±10.6	0.129	$^{+12.9}_{-12.0}$	V3	3s' 4P*	3p' 4D	6	8
4530.86	N III	4529.54	0.014	±36.1	0.020	$^{+42.7}_{-40.4}$	V3	3s' 4P*	3p' 4D	4	2
4534.58	N III	4536.01	0.040	±39.3	0.056	$^{+47.4}_{-43.6}$	V3	3s' 4P*	3p' 4D	6	6
4541.59	He II	4540.17	0.226	±3.7	0.316	±4.5	4.9	4f+ 2F*	9g+ 2G	32	*
4562.60	Mg I]	4560.87	0.055	±12.5	0.075	$^{+14.6}_{-13.3}$		3s2 1S	3s3p 3P*	1	5
4571.10	Mg I]	4569.30	0.105	±8.2	0.142	$^{+9.6}_{-9.0}$		3s2 1S	3s3p 3P*	1	3
4595.96	O II	4594.50	0.026	±30.4	0.034	$^{+35.9}_{-34.3}$	V15	3s' 2D	3p' 2F*	6	6
4610.20	O II	4606.37	0.059	±20.1	0.077	$^{+23.3}_{-22.1}$	V92c	3d 2D	4f F2*	4	6
4621.25	O II	4620.09	0.032	±20.3	0.041	$^{+23.7}_{-22.4}$	V92	3d 2D	4f 2[2]*	6	6
4621.39	N II	4616.85	0.010	±45.5	0.013	$^{+53.9}_{-51.6}$	V5	3s 3P*	3p 3P	3	1
4634.14	N III	4632.95	0.549	±7.9	0.696	$^{+9.2}_{-8.7}$	V2	3p 2P*	3d 2D	2	4
4641.81	O II	4639.24	1.588	±12.2	1.998	$^{+14.3}_{-13.6}$	V1	3s 4P	3p 4D*	4	6
4647.42	C III	4648.21	0.159	±19.0	0.199	$^{+22.5}_{-21.3}$	V1	3s 3S	3p 3P*	3	5
4661.63	O II	4660.01	0.097	±25.3	0.120	±29.0	V1	3s 4P	3p 4D*	4	4
4669.27	O II	4668.52	0.046	±22.4	0.056	$^{+25.7}_{-22.9}$	V89b	3d 2D	4f D2*	4	6
4685.68	He II	4684.31	11.928	±0.3	14.339	±0.4	3.4	3d+ 2D	4f+ 2F*	18	32
4711.37	[Ar IV]	4709.91	1.727	±2.3	2.021	±2.6	F1	3p3 4S*	3p3 2D*	4	6
4733.91	[Fe III]	4732.13	0.020	±23.5	0.023	$^{+25.3}_{-24.4}$	F3	3d6 5D	3d6 3F2	5	5
4740.17	[Ar IV]	4738.81	2.316	±0.9	2.630	$^{+1.0}_{-0.9}$	F1	3p3 4S*	3p3 2D*	4	4
4861.33	H 4	4860.04	100.000	±0.3	100.007	±0.3	H4	2p+ 2P*	4d+ 2D	8	32
4958.91	[O III]	4957.72	440.284	±0.3	397.561	±0.3	F1	2p2 3P	2p2 1D	3	5
5006.84	[O III]	5005.68	1381.826	±0.3	1186.822	±0.3	F1	2p2 3P	2p2 1D	5	5
5270.40	[Fe III]	5269.11	0.063	±15.6	0.041	$^{+16.9}_{-17.3}$	F1	3d6 5D	3d6 3P2	7	5
5411.52	He II	5410.43	1.870	±1.0	1.059	±1.2	4.7	4f+ 2F*	7g+ 2G	32	98
5517.66	[Cl III]	5516.60	1.159	±2.8	0.601	±3.1	F1	2p3 4S*	2p3 2D*	4	6
5537.60	[Cl III]	5536.75	1.656	±2.1	0.846	±2.4	F1	2p3 4S*	2p3 2D*	4	4
5577.34	[O I]	5576.72	0.858	±2.6	0.426	±2.8	F3	2p4 1D	2p4 1S	5	1
5676.02	N II	5678.13	0.080	±15.3	0.037	±17.0	V3	3s 3P*	3p 3D	1	3
5754.60	[N II]	5753.10	4.395	±0.6	1.919	±0.8	F3	2p2 1D	2p2 1S	5	1
5801.51	C IV	5799.76	0.196	±14.5	0.083	$^{+15.8}_{-17.5}$	V1	3s 2S	3p 2P*	2	4

Danehkar

5812.14	C IV	5809.09	0.071	±35.7	0.030	+39.3 -43.4	V1	3s 2S	3p 2P*	2	2
5875.66	He I	5874.06	40.153	±0.3	16.092	±0.6	V11	2p 3P*	3d 3D	9	15
5931.78	N II	5930.72	0.028	±17.0	0.011	+18.9 -20.7	V28	3p 3P	3d 3D*	3	5
6036.70	He II	6035.28	0.063	±7.8	0.023	+8.4 -9.5	5.21	5g+ 2G	21h+ 2H*	50	*
6101.83	[K IV]	6100.08	0.404	±2.7	0.139	±3.1	F1	3p4 3P	3d4 1D	5	5
6118.20	He II	6115.35	0.140	±11.5	0.048	+13.0 -14.8	5.19	5g+ 2G	19h+ 2H*	50	*
6151.43	C II	6149.16	0.065	±9.8	0.022	+11.6 -12.4	V16.04	4d 2D	6f 2F*	10	14
6300.34	[O I]	6298.66	16.971	±0.4	5.111	±0.8	F1	2p4 3P	2p4 1D	5	5
6312.10	[S III]	6310.35	8.242	±0.3	2.463	±0.7	F3	2p2 1D	2p2 1S	5	1
6347.10	Si II	6345.27	0.221	±29.1	0.065	+34.5 -36.3	V2	4s 2S	4p 2P*	2	4
6363.78	[O I]	6362.11	5.974	±0.7	1.728	±1.1	F1	2p4 3P	2p4 1D	3	5
6371.38	S III	6369.70	0.540	±3.1	0.155	±3.8	V2	4s 2S	4p 2P*	2	2
6393.60	[Mn V]	6391.93	0.191	±5.3	0.054	±6.6		3d3 4F	3d3 4P	10	6
6406.30	He II	6404.40	0.294	±4.7	0.083	+5.7 -6.0	5.15	5g+ 2G	15h+ 2H*	50	*
6461.95	C II	6460.34	0.157	±7.8	0.043	±9.3		4f 2F*	6g 2G	14	18
6527.11	He II	6525.37	0.296	±4.7	0.077	+5.7 -6.1	5.14	5g+ 2G	14h+ 2H*	50	*
6548.10	[N II]	6546.33	132.274	±0.2	34.110	±0.7	F1	2p2 3P	2p2 1D	3	5
6562.77	H 3	6560.97	1120.869	±0.4	286.479	±0.9	H3	2p+ 2P*	3d+ 2D	8	18
6583.50	[N II]	6581.70	419.944	±0.3	105.994	±0.8	F1	2p2 3P	2p2 1D	5	5
6678.16	He I	6676.42	14.921	±0.5	3.559	±1.0	V46	2p 1P*	3d 1D	3	5
6716.44	[S II]	6714.69	26.000	±0.2	6.064	±0.8	F2	2p3 4S*	2p3 2D*	4	6
6730.82	[S II]	6729.07	45.983	±0.2	10.635	±0.8	F2	2p3 4S*	2p3 2D*	4	4
6795.00	[K IV]	6793.31	0.122	±9.8	0.027	+11.7 -12.4	F1	3p4 3P	3p4 1D	3	5
6890.88	He I	6889.00	0.355	±2.1	0.075	±2.7	5.12	5g+ 2G	12h+ 2H	50	*
7005.67	[Ar V]	7003.82	0.210	±7.7	0.042	±9.1	F1	3s2 3P	3s2 1D	5	5
7065.25	He I	7063.41	33.585	±1.2	6.443	±1.7	V10	2p 3P*	3s 3S	9	3
7135.80	[Ar III] ^a	7135.80	118.000	±0.0	21.802	±0.9	F1	3p4 3P	3p4 1D	5	5

Hb 4 (N-knot) (PNG003.1+02.9)

3726.03	[O II] ^a	3726.03	58.040	±0.0	199.476	±2.3	F1	2p3 4S*	2p3 2D*	4	4
3728.82	[O II] ^a	3728.82	*		*		F1	2p3 4S*	2p3 2D*	4	6
3868.75	[Ne III] ^a	3868.75	45.170	±0.0	136.829	±2.1	F1	2p4 3P	2p4 1D	5	5
4861.33	H 4	4860.94	100.000	±1.7	100.008	+2.2 -1.9	H4	2p+ 2P*	4d+ 2D	8	32
4958.91	[O III]	4958.27	363.612	±1.2	324.053	±1.6	F1	2p2 3P	2p2 1D	3	5
5006.84	[O III]	5006.19	1222.438	±0.9	1029.611	±1.3	F1	2p2 3P	2p2 1D	5	5
5754.60	[N II]	5754.48	8.794	±10.4	3.452	+13.3 -11.9	F3	2p2 1D	2p2 1S	5	1
5875.66	He I	5875.55	34.191	±2.4	12.184	+4.1 -3.2	V11	2p 3P*	3d 3D	9	15
6300.34	[O I]	6299.82	29.111	±6.7	7.515	+9.3 -7.6	F1	2p4 3P	2p4 1D	5	5
6363.78	[O I]	6363.35	5.856	±9.1	1.444	+12.2 -10.2	F1	2p4 3P	2p4 1D	3	5
6548.10	[N II]	6548.13	340.142	±1.0	73.700	+3.7 -2.9	F1	2p2 3P	2p2 1D	3	5
6562.77	H 3	6562.52	1333.281	±0.6	285.998	+3.5 -2.8	H3	2p+ 2P*	3d+ 2D	8	18
6583.50	[N II]	6583.52	1127.143	±1.0	238.382	+3.8 -2.9	F1	2p2 3P	2p2 1D	5	5
6678.16	He I	6677.95	14.728	±13.7	2.922	+18.3 -16.1	V46	2p 1P*	3d 1D	3	5
6716.44	[S II]	6716.49	97.428	±3.0	18.848	+5.8 -4.5	F2	2p3 4S*	2p3 2D*	4	6
6730.82	[S II]	6730.91	117.556	±2.4	22.528	+5.2 -4.1	F2	2p3 4S*	2p3 2D*	4	4
7065.25	He I	7064.77	89.439	±5.6	13.878	+9.0 -7.3	V10	2p 3P*	3s 3S	9	3
7135.80	[Ar III] ^a	7135.80	125.610	±0.0	18.683	+4.3 -3.5	F1	3p4 3P	3p4 1D	5	5
7319.99	[O II] ^a	7319.99	58.150	±0.0	7.772	+4.6 -3.7	F2	2p3 2D*	2p3 2P*	6	4
7330.73	[O II] ^a	7330.73	*		*		F2	2p3 2D*	2p3 2P*	4	4

Hb 4 (S-knot) (PNG003.1+02.9)

Physical and chemical properties of WR planetary nebulae

3726.03	[O II] ^a	3726.03	74.860	±0.0	231.195	+3.3 -4.3	F1	2p3 4S*	2p3 2D*	4	4
3728.82	[O II] ^a	3728.82	*		*		F1	2p3 4S*	2p3 2D*	4	6
3868.75	[Ne III] ^a	3868.75	31.230	±0.0	85.944	+2.9 -3.9	F1	2p4 3P	2p4 1D	5	5
4861.33	H 4	4859.38	100.000	±2.7	100.007	±3.5	H4	2p+ 2P*	4d+ 2D	8	32
4958.91	[O III]	4957.27	270.460	±0.9	243.452	±1.3	F1	2p2 3P	2p2 1D	3	5
5006.84	[O III]	5005.28	935.680	±0.8	799.890	+1.3 -1.0	F1	2p2 3P	2p2 1D	5	5
5875.66	He I	5872.74	25.520	±3.7	9.944	+7.0 -4.8	V11	2p 3P*	3d 3D	9	15
6300.34	[O I]	6296.81	44.710	±3.8	12.977	+8.0 -5.6	F1	2p4 3P	2p4 1D	5	5
6363.78	[O I]	6360.21	16.780	±17.3	4.671	+25.0 -21.7	F1	2p4 3P	2p4 1D	3	5
6548.10	[N II]	6544.68	274.170	±1.5	67.819	+6.5 -4.0	F1	2p2 3P	2p2 1D	3	5
6562.77	H 3	6559.63	1167.540	±1.4	286.164	+6.3 -3.9	H3	2p+ 2P*	3d+ 2D	8	18
6583.50	[N II]	6580.01	962.340	±0.7	232.840	+5.9 -3.9	F1	2p2 3P	2p2 1D	5	5
6716.44	[S II]	6712.99	83.800	±2.2	18.690	+7.3 -4.8	F2	2p3 4S*	2p3 2D*	4	6
6730.82	[S II]	6727.38	91.440	±1.8	20.219	+6.9 -4.5	F2	2p3 4S*	2p3 2D*	4	4
7135.80	[Ar III] ^a	7135.80	106.950	±0.0	18.762	+7.0 -4.5	F1	3p4 3P	3p4 1D	5	5
7319.99	[O II] ^a	7319.99	43.200	±0.0	6.873	+7.3 -4.6	F2	2p3 2D*	2p3 2P*	6	4
7330.73	[O II] ^a	7330.73	*		*		F2	2p3 2D*	2p3 2P*	4	4

IC 1297 (PNG358.3-21.6)

3726.03	[O II] ^a	3726.03	49.100	±0.0	55.949	+1.1 -1.0	F1	2p3 4S*	2p3 2D*	4	4
3728.82	[O II] ^a	3728.82	*		*		F1	2p3 4S*	2p3 2D*	4	6
3868.75	[Ne III] ^a	3868.75	109.000	±0.0	122.557	+1.0 -0.9	F1	2p4 3P	2p4 1D	5	5
3889.05	H 8 ^a	3889.05	19.200	±0.0	21.544	+1.0 -0.9	H8	2p+ 2P*	8d+ 2D	8	*
3967.46	[Ne III] ^a	3967.46	50.700	±0.0	56.431	±0.9	F1	2p4 3P	2p4 1D	3	5
4026.21	He I ^a	4026.21	2.100	±0.0	2.323	±0.8	V18	2p 3P*	5d 3D	9	15
4101.74	H 6 ^a	4101.74	26.000	±0.0	28.517	±0.8	H6	2p+ 2P*	6d+ 2D	8	72
4340.47	H 5 ^a	4340.47	45.700	±0.0	48.744	±0.5	H5	2p+ 2P*	5d+ 2D	8	50
4363.21	[O III] ^a	4363.21	9.300	±0.0	9.892	±0.5	F2	2p2 1D	2p2 1S	5	1
4448.19	O II	4448.51	0.103	±14.1	0.108	+20.7 -18.3	V35	3p' 2F*	3d' 2F	8	8
4471.50	He I	4471.16	4.253	±1.3	4.465	±1.9	V14	2p 3P*	4d 3D	9	15
4510.91	N III	4510.26	0.116	±12.2	0.121	+17.7 -16.5	V3	3s' 4P*	3p' 4D	2	4
4541.59	He II	4541.15	1.060	±1.6	1.103	±2.4	4.9	4f+ 2F*	9g+ 2G	32	*
4552.53	N II	4552.38	0.018	±41.7	0.019	+60.6 -55.4	V58a	3d 1F*	4f 2[4]	7	9
4571.10	Mg I]	4570.81	0.149	±8.1	0.154	+12.1 -10.8		3s2 1S	3s3p 3P*	1	3
4607.16	N II	4607.14	0.012	±34.5	0.012	+51.1 -47.0	V5	3s 3P*	3p 3P	1	3
4610.20	O II	4604.61	0.066	±9.2	0.068	+13.5 -12.4	V92c	3d 2D	4f F2*	4	6
4634.14	N III	4633.53	0.777	±3.7	0.799	±5.6	V2	3p 2P*	3d 2D	2	4
4640.64	N III	4640.22	2.000	±1.7	2.056	±2.5	V2	3p 2P*	3d 2D	4	6
4647.42	C III	4648.61	0.146	±39.2	0.150	+57.4 -52.2	V1	3s 3S	3p 3P*	3	5
4658.64	C IV	4657.62	0.227	±11.6	0.233	+17.1 -15.5	V8	5f 2F*	6g 2G	14	18
4661.63	O II	4661.21	0.107	±12.9	0.110	+18.5 -17.3	V1	3s 4P	3p 4D*	4	4
4676.24	O II	4676.12	0.047	±19.2	0.048	+27.5 -25.4	V1	3s 4P	3p 4D*	6	6
4678.14	N II	4676.13	0.059	±13.4	0.060	+18.8 -17.7	V61b	3d 1P*	4f 2[2]	3	5
4685.68	He II	4685.40	37.038	±0.2	37.861	±0.3	3.4	3d+ 2D	4f+ 2F*	18	32
4711.37	[Ar IV]	4711.03	2.003	±2.0	2.041	±2.9	F1	3p3 4S*	3p3 2D*	4	6
4740.17	[Ar IV]	4739.93	1.836	±1.2	1.864	±1.7	F1	3p3 4S*	3p3 2D*	4	4
4769.40	[Fe III]	4766.78	0.037	±17.4	0.037	+24.7 -23.2	F3				
4788.13	N II	4783.65	0.022	±22.3	0.022	+31.9 -29.4	V20	3p 3D	3d 3D*	5	5
4803.29	N II	4802.19	0.016	±21.8	0.016	+31.5 -28.6	V20	3p 3D	3d 3D*	7	7
4814.53	[Fe II]	4816.17	0.032	±31.4	0.032	+46.1 -41.9	F20				
4861.33	H 4	4861.19	100.000	±0.5	100.001	±0.7	H4	2p+ 2P*	4d+ 2D	8	32
4881.11	[Fe III]	4881.50	0.058	±13.6	0.058	+19.4 -17.7	F2	3d6 5D	3d6 3H	9	9

Danehkar

4958.91	[O III]	4958.92	462.910	±0.4	457.304	±0.6	F1	2p2 3P	2p2 1D	3	5
5006.84	[O III]	5006.88	1342.273	±0.2	1318.120	±0.3	F1	2p2 3P	2p2 1D	5	5
5199.84	[N I]	5198.58	0.151	±15.0	0.145	+21.0 -19.5	F1	2p3 4S*	2p3 2D*	4	4
5270.40	[Fe III]	5270.81	0.039	±17.1	0.037	+23.8 -21.5	F1	3d6 5D	3d6 3P2	7	5
5411.52	He II	5411.88	3.098	±0.8	2.895	±1.2	4.7	4f+ 2F*	7g+ 2G	32	98
5517.66	[Cl III]	5517.88	0.659	±2.2	0.609	+3.1 -2.9	F1	2p3 4S*	2p3 2D*	4	6
5537.60	[Cl III]	5537.97	0.702	±2.8	0.648	±3.8	F1	2p3 4S*	2p3 2D*	4	4
5666.63	N II	5665.47	0.036	±23.7	0.033	+33.2 -29.4	V3	3s 3P*	3p 3D	3	5
5679.56	N II	5679.33	0.021	±45.9	0.019	+63.6 -55.4	V3	3s 3P*	3p 3D	5	7
5686.21	N II	5688.71	0.021	±25.7	0.019	+35.5 -31.0	V3	3s 3P*	3p 3D	3	3
5695.92	C III	5693.00	0.013	±36.7	0.012	+51.0 -42.7	V2	3p 1P*	3d 1D	3	5
5754.60	[N II]	5754.22	0.692	±2.1	0.627	±2.9	F3	2p2 1D	2p2 1S	5	1
5801.51	C IV	5801.02	0.094	±13.5	0.085	+18.1 -14.9	V1	3s 2S	3p 2P*	2	4
5875.66	He I	5875.25	14.660	±0.3	13.144	+0.9 -1.1	V11	2p 3P*	3d 3D	9	15
5931.78	N II	5931.76	0.025	±29.5	0.022	+40.0 -34.2	V28	3p 3P	3d 3D*	3	5
6036.70	He II	6036.31	0.077	±7.3	0.068	+9.4 -8.6	5.21	5g+ 2G	21h+ 2H*	50	*
6074.10	He II	6073.71	0.047	±13.4	0.041	+17.4 -15.5	5.20	5g+ 2G	20h+ 2H*	50	*
6101.83	[K IV]	6101.40	0.104	±7.4	0.092	+9.8 -8.8	F1	3p4 3P	3d4 1D	5	5
6118.20	He II	6117.88	0.074	±10.2	0.065	+13.1 -11.7	5.19	5g+ 2G	19h+ 2H*	50	*
6151.43	C II	6150.61	0.041	±18.7	0.036	+24.8 -21.6	V16.04	4d 2D	6f 2F*	10	14
6233.80	He II	6233.44	0.136	±3.9	0.118	+5.1 -4.7	5.17	5g+ 2G	17h+ 2H*	50	*
6300.34	[O I]	6300.00	1.859	±1.0	1.611	±1.5	F1	2p4 3P	2p4 1D	5	5
6312.10	[S III]	6311.54	2.670	±1.0	2.312	±1.6	F3	2p2 1D	2p2 1S	5	1
6363.78	[O I]	6363.46	0.607	±1.9	0.523	±2.5	F1	2p4 3P	2p4 1D	3	5
6371.38	S III	6371.05	0.091	±9.6	0.078	+12.2 -11.3	V2	4s 2S	4p 2P*	2	2
6406.30	He II	6405.60	0.283	±4.8	0.243	±5.8	5.15	5g+ 2G	15h+ 2H*	50	*
6461.95	C II	6461.72	0.095	±19.2	0.081	+24.1 -22.8		4f 2F*	6g 2G	14	18
6527.11	He II	6526.53	0.270	±5.5	0.230	±6.7	5.14	5g+ 2G	14h+ 2H*	50	*
6548.10	[N II]	6547.64	17.283	±0.6	14.702	±1.2	F1	2p2 3P	2p2 1D	3	5
6562.77	H 3	6562.30	338.174	±0.6	287.358	±1.2	H3	2p+ 2P*	3d+ 2D	8	18
6583.50	[N II]	6583.02	53.908	±0.9	45.739	±1.4	F1	2p2 3P	2p2 1D	5	5
6678.16	He I	6677.65	2.891	±1.8	2.436	±2.2	V46	2p 1P*	3d 1D	3	5
6716.44	[S II]	6716.02	5.679	±0.6	4.773	±1.2	F2	2p3 4S*	2p3 2D*	4	6
6730.82	[S II]	6730.40	8.392	±0.7	7.046	±1.2	F2	2p3 4S*	2p3 2D*	4	4
6890.88	He I	6890.58	0.289	±4.0	0.240	+4.5 -5.3	5.12	5g+ 2G	12h+ 2H	50	*
7065.25	He I	7064.92	3.095	±2.0	2.541	+2.1 -3.2	V10	2p 3P*	3s 3S	9	3
7135.80	[Ar III] ^a	7135.80	18.000	±0.0	14.714	±1.5	F1	3p4 3P	3p4 1D	5	5
7281.35	He I ^a	7281.35	0.600	±0.0	0.486	±1.6	V45	2p 1P*	3s 1S	3	1
7751.43	[Ar III] ^a	7751.43	3.800	±0.0	2.997	+1.8 -2.1	F1	3p4 3P	3p4 1D	3	5

Th 2-A (PNG306.4--00.6)

3728.82	[O II] ^a	3728.82	72.900	±0.0	137.788	±1.6	F1	2p3 4S*	2p3 2D*	4	6
3868.75	[Ne III] ^a	3868.75	111.000	±0.0	196.786	±1.4	F1	2p4 3P	2p4 1D	5	5
3889.05	H 8 ^a	3889.05	7.200	±0.0	12.638	±1.3	H8	2p+ 2P*	8d+ 2D	8	*
3967.46	[Ne III] ^a	3967.46	48.000	±0.0	80.986	±1.3	F1	2p4 3P	2p4 1D	3	5
4101.74	H 6 ^a	4101.74	26.600	±0.0	41.772	+1.1 -1.0	H6	2p+ 2P*	6d+ 2D	8	72
4340.47	H 5 ^a	4340.47	37.800	±0.0	51.794	±0.8	H5	2p+ 2P*	5d+ 2D	8	50
4363.21	[O III] ^a	4363.21	13.800	±0.0	18.657	±0.7	F2	2p2 1D	2p2 1S	5	1
4432.74	N II	4438.16	0.515	±9.4	0.668	+11.6 -12.6	V55a	3d 3P*	4f 2[3]	5	7
4448.19	O II	4447.11	0.668	±7.7	0.859	+9.5 -10.3	V35	3p' 2F*	3d' 2F	8	8
4471.50	He I	4470.75	2.193	±2.7	2.780	±3.4	V14	2p 3P*	4d 3D	9	15
4510.91	N III	4510.53	0.266	±9.3	0.329	±11.3	V3	3s' 4P*	3p' 4D	2	4
4523.58	N III	4523.71	0.216	±15.4	0.265	+18.8 -19.7	V3	3s' 4P*	3p' 4D	4	4
4541.59	He II	4540.84	1.532	±4.3	1.862	±5.3	4.9	4f+ 2F*	9g+ 2G	32	*

Physical and chemical properties of WR planetary nebulae

4658.64	C IV	4657.49	1.524	±4.9	1.725	±6.0	V8	5f 2F*	6g 2G	14	18
4562.60	Mg I]	4561.25	0.670	±9.0	0.804	±11.2		3s2 1S	3s3p 3P*	1	5
4571.10	Mg I]	4569.08	0.392	±15.6	0.468	+19.0 -20.4		3s2 1S	3s3p 3P*	1	3
4640.64	N III	4640.34	0.343	±14.4	0.392	+17.4 -18.1	V2	3p 2P*	3d 2D	4	6
4658.64	C IV	4657.49	1.524	±4.9	1.725	±6.1	V8	5f 2F*	6g 2G	14	18
4678.14	N II	4675.89	0.088	±56.1	0.098	+69.3 -72.8	V61b	3d 1P*	4f 2[2]	3	5
4685.68	He II	4684.94	49.477	±0.6	55.082	±0.8	3.4	3d+ 2D	4f+ 2F*	18	32
4711.37	[Ar IV]	4710.62	2.467	±2.3	2.704	±2.9	F1	3p3 4S*	3p3 2D*	4	6
4740.17	[Ar IV]	4739.40	1.809	±3.5	1.948	±4.5	F1	3p3 4S*	3p3 2D*	4	4
4754.70	[Fe III]	4753.99	0.101	±12.1	0.108	+14.9 -15.9	F3				
4788.13	N II	4787.83	0.083	±22.8	0.087	+28.6 -29.8	V20	3p 3D	3d 3D*	5	5
4803.29	N II	4801.95	0.191	±18.6	0.198	+23.6 -24.2	V20	3p 3D	3d 3D*	7	7
4861.33	H 4	4860.62	100.000	±0.8	100.004	+1.0 -1.0	H4	2p+ 2P*	4d+ 2D	8	32
4881.11	[Fe III]	4880.47	0.737	±6.2	0.728	±7.8	F2	3d6 5D	3d6 3H	9	9
4924.53	O II	4921.35	0.551	±11.0	0.530	+13.8 -14.3	V28	3p 4S*	3d 4P	4	6
4958.91	[O III]	4958.29	549.839	±0.5	518.074	±0.6	F1	2p2 3P	2p2 1D	3	5
5006.84	[O III]	5006.26	1672.895	±0.5	1530.917	±0.6	F1	2p2 3P	2p2 1D	5	5
5270.40	[Fe III]	5269.35	0.618	±13.3	0.482	+16.6 -17.4	F1	3d6 5D	3d6 3P2	7	5
5411.52	He II	5411.10	5.528	±1.2	3.968	±1.5	4.7	4f+ 2F*	7g+ 2G	32	98
5517.66	[Cl III]	5517.48	2.183	±2.3	1.489	+2.8 -3.1	F1	2p3 4S*	2p3 2D*	4	6
5676.02	N II	5674.28	0.229	±27.4	0.146	+34.4 -35.1	V3	3s 3P*	3p 3D	1	3
5679.56	N II	5678.97	0.379	±10.6	0.241	±13.4	V3	3s 3P*	3p 3D	5	7
5695.92	C III	5695.67	0.232	±26.8	0.147	+35.9 -34.9	V2	3p 1P*	3d 1D	3	5
5710.77	N II	5714.90	0.444	±12.5	0.279	±16.3	V3	3s 3P*	3p 3D	5	5
5754.60	[N II]	5753.64	3.488	±1.9	2.152	±2.7	F3	2p2 1D	2p2 1S	5	1
5801.51	C IV	5800.33	0.660	±7.4	0.399	±9.7	V1	3s 2S	3p 2P*	2	4
5812.14	C IV	5811.12	0.088	±35.2	0.053	+44.8 -46.2	V1	3s 2S	3p 2P*	2	2
5875.66	He I	5874.64	19.454	±0.9	11.415	±1.7	V11	2p 3P*	3d 3D	9	15
5931.78	N II	5931.09	0.213	±17.5	0.122	±22.8	V28	3p 3P	3d 3D*	3	5
6118.20	He II	6117.76	0.455	±14.3	0.242	+19.0 -18.1	5.19	5g+ 2G	19h+ 2H*	50	*
6151.43	C II	6144.81	0.837	±10.8	0.440	±13.6	V16.04	4d 2D	6f 2F*	10	14
6233.80	He II	6233.52	0.369	±11.1	0.188	±14.5	5.17	5g+ 2G	17h+ 2H*	50	*
6300.34	[O I]	6299.19	10.807	±2.7	5.368	±3.8	F1	2p4 3P	2p4 1D	5	5
6312.10	[S III]	6310.95	4.332	±0.8	2.142	+2.0 -2.1	F3	2p2 1D	2p2 1S	5	1
6363.78	[O I]	6362.61	3.596	±3.2	1.745	±4.4	F1	2p4 3P	2p4 1D	3	5
6393.60	[Mn V]	6390.57	0.203	±17.1	0.097	±22.0		3d3 4F	3d3 4P	10	6
6461.95	C II	6459.76	0.538	±11.3	0.252	±14.5		4f 2F*	6g 2G	14	18
6548.10	[N II]	6546.86	89.676	±1.4	40.694	±2.5	F1	2p2 3P	2p2 1D	3	5
6562.77	H 3	6561.56	637.340	±1.0	287.720	±2.3	H3	2p+ 2P*	3d+ 2D	8	18
6583.50	[N II]	6582.24	296.859	±0.6	133.037	±2.0	F1	2p2 3P	2p2 1D	5	5
6678.16	He I	6676.75	4.564	±2.4	1.979	±3.6	V46	2p 1P*	3d 1D	3	5
6716.44	[S II]	6715.18	14.421	±1.1	6.172	±2.5	F2	2p3 4S*	2p3 2D*	4	6
6730.82	[S II]	6729.61	18.246	±1.7	7.771	+2.9 -3.0	F2	2p3 4S*	2p3 2D*	4	4
7065.25	He I	7063.76	7.031	±6.4	2.685	+7.9 -8.4	V10	2p 3P*	3s 3S	9	3
7135.80	[Ar III] ^a	7135.80	64.000	±0.0	23.913	±2.4	F1	3p4 3P	3p4 1D	5	5
7751.43	[Ar III] ^a	7751.43	14.900	±0.0	4.674	+2.9 -3.0	F1	3p4 3P	3p4 1D	3	5
9068.60	[S III] ^a	9068.60	98.900	±0.0	23.140	±3.6		3p2 3P	3p2 1D	3	5

Pe 1-1 (PNG285.4+01.5)

3726.03	[O II] ^a	3726.03	13.150	±0.0	41.457	±0.3	F1	2p3 4S*	2p3 2D*	4	4
3728.82	[O II] ^a	3728.82	5.210	±0.0	16.390	±0.3	F1	2p3 4S*	2p3 2D*	4	6
3868.75	[Ne III] ^a	3868.75	31.050	±0.0	87.043	±0.3	F1	2p4 3P	2p4 1D	5	5
3889.05	H 8 ^a	3889.05	7.500	±0.0	20.653	±0.3	H8	2p+ 2P*	8d+ 2D	8	*
3967.46	[Ne III] ^a	3967.46	9.520	±0.0	24.412	±0.3	F1	2p4 3P	2p4 1D	3	5
4101.74	H 6 ^a	4101.74	12.150	±0.0	27.380	±0.3	H6	2p+ 2P*	6d+ 2D	8	72

4340.47	H 5 ^a	4340.47	29.130	±0.0	51.356	±0.2	H5	2p+ 2P*	5d+ 2D	8	50
4363.21	[O III] ^a	4363.21	4.310	±0.0	7.417	±0.2	F2	2p2 1D	2p2 1S	5	1
4432.74	N II	4433.26	0.143	±32.4	0.228	±40.6	V55a	3d 3P*	4f 2[3]	5	7
4432.75	N II	4432.27	0.176	±26.9	0.281	±33.4	V55b	3d 3P*	4f 2[3]	5	7
4437.55	He I	4439.32	0.522	±13.2	0.830	+16.9 -17.1	V50	2p 1P*	5s 1S	3	1
4452.37	O II	4450.22	0.450	±16.9	0.704	±21.7	V5	3s 2P	3p 2D*	4	4
4471.50	He I	4471.97	3.911	±4.2	5.993	±5.2	V14	2p 3P*	4d 3D	9	15
4488.75	[Fe II]	4489.51	0.187	±29.3	0.281	+36.9 -37.7	F6	4s 6D	4s 4F	6	6
4510.91	N III	4508.75	0.499	±15.4	0.733	±19.4	V3	3s' 4P*	3p' 4D	2	4
4514.86	N III	4521.09	0.302	±49.3	0.442	+60.4 -62.8	V3	3s' 4P*	3p' 4D	6	8
4571.10	Mg I	4571.40	0.253	±10.1	0.348	±12.2		3s2 1S	3s3p 3P*	1	3
4596.18	O II	4596.85	0.222	±18.8	0.297	±23.4	V15	3s' 2D	3p' 2F*	4	6
4625.53	[Ar V]	4625.93	0.464	±10.3	0.601	±12.5		3p2 1D	3p2 1S	5	1
4634.14	N III	4633.07	0.761	±12.5	0.977	+15.0 -15.6	V2	3p 2P*	3d 2D	2	4
4647.42	C III	4649.71	0.175	±29.9	0.221	+34.9 -37.8	V1	3s 3S	3p 3P*	3	5
4661.63	O II	4661.64	0.202	±20.0	0.252	+23.8 -24.7	V1	3s 4P	3p 4D*	4	4
4678.14	N II	4677.74	0.046	±56.5	0.056	+70.0 -70.6	V61b	3d 1P*	4f 2[2]	3	5
4711.37	[Ar IV]	4713.51	0.342	±18.3	0.403	+22.6 -23.4	F1	3p3 4S*	3p3 2D*	4	6
4733.91	[Fe III]	4735.15	0.098	±41.7	0.113	+51.7 -50.2	F3	3d6 5D	3d6 3F2	5	5
4769.40	[Fe III]	4766.90	0.189	±29.5	0.209	±35.2	F3				
4788.13	N II	4785.44	0.144	±25.1	0.156	+29.4 -30.2	V20	3p 3D	3d 3D*	5	5
4814.53	[Fe II]	4816.23	0.254	±14.8	0.267	+17.1 -18.1	F20				
4815.55	S II	4821.04	0.370	±9.8	0.389	±11.6	V9	4s 4P	4p 4S*	6	4
4861.33	H 4	4862.03	100.000	±0.2	100.007	±0.2	H4	2p+ 2P*	4d+ 2D	8	32
4881.11	[Fe III]	4880.60	0.652	±11.7	0.638	±13.9	F2	3d6 5D	3d6 3H	9	9
4923.93	[Fe II]	4922.64	0.312	±10.8	0.291	±12.6		4s2 4P	4p 6P*	6	4
4931.80	[O III]	4932.32	0.173	±20.6	0.160	+24.0 -24.8	F1	2p2 3P	2p2 1D	1	5
4958.91	[O III]	4959.81	372.914	±0.2	335.030	±0.2	F1	2p2 3P	2p2 1D	3	5
5006.84	[O III]	5007.82	1186.224	±0.2	1011.173	±0.3	F1	2p2 3P	2p2 1D	5	5
5270.40	[Fe III]	5270.17	0.219	±21.6	0.140	+25.4 -27.2	F1	3d6 5D	3d6 3P2	7	5
5453.83	S II	5452.00	0.323	±25.1	0.170	+29.7 -30.8	V6	4s 4P	4p 4D*	6	8
5537.60	[Cl III]	5539.38	0.530	±16.7	0.262	+19.5 -20.7	F1	2p3 4S*	2p3 2D*	4	4
5754.60	[N II]	5755.00	6.141	±1.7	2.573	±2.1	F3	2p2 1D	2p2 1S	5	1
5801.51	C IV	5798.50	0.355	±15.7	0.144	+18.3 -19.7	V1	3s 2S	3p 2P*	2	4
5875.66	He I	5876.08	42.592	±0.4	16.313	±0.7	V11	2p 3P*	3d 3D	9	15
5931.78	N II	5931.80	0.150	±13.0	0.055	±15.0	V28	3p 3P	3d 3D*	3	5
5941.65	N II	5942.94	0.200	±17.1	0.073	+19.5 -21.1	V28	3p 3P	3d 3D*	5	7
6151.43	C II	6150.58	0.240	±2.4	0.075	±2.9	V16.04	4d 2D	6f 2F*	10	14
6300.34	[O I]	6300.76	33.516	±0.3	9.511	±0.7	F1	2p4 3P	2p4 1D	5	5
6312.10	[S III]	6312.54	5.705	±2.4	1.606	±2.9	F3	2p2 1D	2p2 1S	5	1
6347.10	Si II	6347.76	0.209	±14.3	0.057	+17.1 -18.2	V2	4s 2S	4p 2P*	2	4
6363.78	[O I]	6364.24	10.488	±1.0	2.852	±1.4	F1	2p4 3P	2p4 1D	3	5
6393.60	[Mn V]	6392.94	0.178	±25.7	0.047	+30.2 -32.6		3d3 4F	3d3 4P	10	6
6461.95	C II	6462.19	0.735	±8.2	0.187	+9.8 -10.3		4f 2F*	6g 2G	14	18
6548.10	[N II]	6548.53	151.172	±0.3	36.452	±0.8	F1	2p2 3P	2p2 1D	3	5
6562.77	H 3	6563.26	1198.148	±0.3	286.217	±0.8	H3	2p+ 2P*	3d+ 2D	8	18
6583.50	[N II]	6583.91	494.105	±0.3	116.490	±0.8	F1	2p2 3P	2p2 1D	5	5
6678.16	He I	6678.52	15.511	±1.2	3.446	±1.7	V46	2p 1P*	3d 1D	3	5
6716.44	[S II]	6716.93	10.792	±0.8	2.342	±1.2	F2	2p3 4S*	2p3 2D*	4	6
6730.82	[S II]	6731.34	24.211	±0.4	5.208	±0.9	F2	2p3 4S*	2p3 2D*	4	4
7065.25	He I	7065.79	21.555	±2.6	3.810	±3.2	V10	2p 3P*	3s 3S	9	3
7135.80	[Ar III] ^a	7135.80	113.030	±0.0	19.208	±0.8	F1	3p4 3P	3p4 1D	5	5
7281.35	He I ^a	7281.35	5.350	±0.0	0.840	±0.9	V45	2p 1P*	3s 1S	3	1
7751.43	[Ar III] ^a	7751.43	35.470	±0.0	4.399	±1.0	F1	3p4 3P	3p4 1D	3	5
9068.60	[S III] ^a	9068.60	337.700	±0.0	24.710	+1.2 -1.0		3p2 3P	3p2 1D	3	5

M 1-32 (PNG011.9+04.2)											
3726.03	[O II] ^a	3726.03	34.294	±0.0	76.039	+1.5 -2.0	F1	2p3 4S*	2p3 2D*	4	4
3728.82	[O II] ^a	3728.82	15.476	±0.0	34.263	+1.5 -2.0	F1	2p3 4S*	2p3 2D*	4	6
3868.75	[Ne III] ^a	3868.75	5.766	±0.0	11.785	±1.4	F1	2p4 3P	2p4 1D	5	5
4101.74	H 6 ^a	4101.74	13.481	±0.0	23.682	±1.1	H6	2p+ 2P*	6d+ 2D	8	72
4340.47	H 5 ^a	4340.47	31.152	±0.0	46.159	±0.8	H5	2p+ 2P*	5d+ 2D	8	50
4363.21	[O III] ^a	4363.21	1.638	±0.0	2.387	+0.7 -1.0	F2	2p2 1D	2p2 1S	5	1
4452.37	O II	4450.82	0.142	±16.8	0.194	+21.3 -20.4	V5	3s 2P	3p 2D*	4	4
4471.50	He I	4469.68	3.962	±1.7	5.327	±2.4	V14	2p 3P*	4d 3D	9	15
4552.53	N II	4551.16	0.099	±20.2	0.125	±25.8	V58a	3d 1F*	4f 2[4]	7	9
4562.60	Mg I	4560.30	0.115	±20.5	0.144	±26.9		3s2 1S	3s3p 3P*	1	5
4571.10	Mg I	4569.33	0.358	±8.0	0.447	±10.2		3s2 1S	3s3p 3P*	1	3
4595.96	O II	4594.47	0.103	±22.4	0.126	+27.7 -28.2	V15	3s' 2D	3p' 2F*	6	6
4601.48	N II	4599.77	0.103	±14.8	0.126	±19.1	V5	3s 3P*	3p 3P	3	5
4658.10	[Fe III]	4655.55	0.472	±6.8	0.551	±8.6	F3	3d6 5D	3d6 3F2	9	9
4658.64	C IV	4656.47	3.471	±1.2	4.051	±1.5	V8	5f 2F*	6g 2G	14	18
4701.62	[Fe III]	4700.29	0.400	±9.4	0.452	±11.5	F3	3d6 5D	3d6 3F2	7	7
4711.37	[Ar IV]	4711.17	0.319	±6.4	0.358	+7.9 -8.2	F1	3p3 4S*	3p3 2D*	4	6
4754.70	[Fe III]	4753.25	0.444	±5.9	0.482	±7.2	F3				
4788.13	N II	4788.03	0.117	±24.1	0.124	+29.5 -30.5	V20	3p 3D	3d 3D*	5	5
4861.33	H 4	4859.67	100.000	±0.8	100.005	±1.0	H4	2p+ 2P*	4d+ 2D	8	32
4881.11	[Fe III]	4879.12	1.515	±2.4	1.492	±3.0	F2	3d6 5D	3d6 3H	9	9
4890.86	O II	4888.50	0.070	±24.7	0.068	±31.9	V28	3p 4S*	3d 4P	4	2
4958.91	[O III]	4957.37	173.557	±0.9	161.131	±1.2	F1	2p2 3P	2p2 1D	3	5
5006.84	[O III]	5005.36	533.485	±0.9	477.569	±1.2	F1	2p2 3P	2p2 1D	5	5
5199.84	[N I]	5196.25	2.046	±1.5	1.583	±2.0	F1	2p3 4S*	2p3 2D*	4	4
5200.26	[N I]	5199.42	1.306	±2.1	1.010	±2.7	F1	2p3 4S*	2p3 2D*	4	6
5270.40	[Fe III]	5269.28	2.953	±1.0	2.167	±1.4	F1	3d6 5D	3d6 3P2	7	5
5517.66	[Cl III]	5516.24	1.121	±3.4	0.695	±4.4	F1	2p3 4S*	2p3 2D*	4	6
5537.60	[Cl III]	5536.50	1.563	±3.3	0.959	+4.3 -4.0	F1	2p3 4S*	2p3 2D*	4	4
5666.63	N II	5663.94	0.254	±7.3	0.146	±9.5	V3	3s 3P*	3p 3D	3	5
5679.56	N II	5677.06	0.588	±8.0	0.335	+10.3 -9.9	V3	3s 3P*	3p 3D	5	7
5686.21	N II	5683.46	0.051	±19.7	0.029	+25.7 -24.2	V3	3s 3P*	3p 3D	3	3
5695.92	C III	5694.57	0.069	±17.8	0.039	+23.4 -22.7	V2	3p 1P*	3d 1D	3	5
5710.77	N II	5708.67	0.175	±12.4	0.098	+16.7 -16.0	V3	3s 3P*	3p 3D	5	5
5754.60	[N II]	5752.45	11.481	±1.1	6.281	+2.0 -1.7	F3	2p2 1D	2p2 1S	5	1
5875.66	He I	5873.46	38.698	±1.0	19.891	+2.2 -1.8	V11	2p 3P*	3d 3D	9	15
6151.43	C II	6148.60	0.182	±13.3	0.082	+17.6 -16.8	V16.04	4d 2D	6f 2F*	10	14
6300.34	[O I]	6297.95	22.821	±1.0	9.528	±2.6	F1	2p4 3P	2p4 1D	5	5
6312.10	[S III]	6309.81	6.773	±1.9	2.812	+3.4 -2.9	F3	2p2 1D	2p2 1S	5	1
6347.10	Si II	6344.62	0.409	±12.4	0.167	+16.3 -15.9	V2	4s 2S	4p 2P*	2	4
6363.78	[O I]	6361.40	7.522	±1.2	3.049	±2.9	F1	2p4 3P	2p4 1D	3	5
6371.38	S III	6368.93	0.220	±10.8	0.089	+14.6 -14.0	V2	4s 2S	4p 2P*	2	2
6461.95	C II	6459.64	0.561	±10.1	0.217	+13.4 -12.9		4f 2F*	6g 2G	14	18
6527.11	He II	6524.97	0.254	±7.7	0.096	+10.5 -9.8	5.14	5g+ 2G	14h+ 2H*	50	*
6548.10	[N II]	6545.58	446.066	±1.7	166.344	±3.5	F1	2p2 3P	2p2 1D	3	5
6562.77	H 3	6560.29	778.908	±1.7	288.587	±3.5	H3	2p+ 2P*	3d+ 2D	8	18
6583.50	[N II]	6580.95	1455.491	±1.5	534.363	+3.4 -2.9	F1	2p2 3P	2p2 1D	5	5
6678.16	He I	6675.64	15.474	±1.9	5.452	±3.8	V46	2p 1P*	3d 1D	3	5
6716.44	[S II]	6713.93	36.143	±1.9	12.528	±3.9	F2	2p3 4S*	2p3 2D*	4	6
6730.82	[S II]	6728.30	65.801	±2.1	22.670	±4.0	F2	2p3 4S*	2p3 2D*	4	4
7065.25	He I	7062.57	12.274	±5.5	3.690	±7.7	V10	2p 3P*	3s 3S	9	3
7135.80	[Ar III] ^a	7135.80	103.457	±0.0	30.268	+3.3 -2.6	F1	3p4 3P	3p4 1D	5	5

M 3-15 (PNG006.8+04.1)											
3726.03	[O II] ^a	3726.03	5.190	±0.0	19.639	±0.7	F1	2p3 4S*	2p3 2D*	4	4
3728.82	[O II] ^a	3728.82	2.080	±0.0	7.851	±0.7	F1	2p3 4S*	2p3 2D*	4	6
3868.75	[Ne III] ^a	3868.75	10.740	±0.0	35.469	±0.7	F1	2p4 3P	2p4 1D	5	5
4363.21	[O III] ^a	4363.21	2.000	±0.0	3.752	±0.3	F2	2p2 1D	2p2 1S	5	1
4448.19	O II	4450.14	0.435	±14.7	0.734	^{+19.7} _{-17.9}	V35	3p' 2F*	3d' 2F	8	8
4471.50	He I	4472.59	3.710	±5.7	6.084	^{+7.7} _{-7.2}	V14	2p 3P*	4d 3D	9	15
4518.15	N III	4521.50	0.305	±30.4	0.472	^{+41.3} _{-37.9}	V3	3s' 4P*	3p' 4D	2	2
4523.58	N III	4523.61	0.415	±27.0	0.637	^{+36.8} _{-34.5}	V3	3s' 4P*	3p' 4D	4	4
4590.97	O II	4589.97	0.470	±20.9	0.663	^{+27.4} _{-25.7}	V15	3s' 2D	3p' 2F*	6	8
4620.26	C II	4624.75	0.379	±23.6	0.515	^{+30.6} _{-29.5}					
4643.08	N II	4643.50	0.185	±31.1	0.244	^{+40.9} _{-38.9}	V5	3s 3P*	3p 3P	5	3
4651.47	C III	4652.14	0.385	±30.9	0.503	^{+39.7} _{-37.4}	V1	3s 3S	3p 3P*	3	1
4711.37	[Ar IV]	4713.46	0.589	±17.2	0.713	^{+22.6} _{-20.4}	F1	3p3 4S*	3p3 2D*	4	6
4740.17	[Ar IV]	4741.87	0.800	±12.3	0.934	^{+15.3} _{-14.4}	F1	3p3 4S*	3p3 2D*	4	4
4754.70	[Fe III]	4750.22	0.329	±11.3	0.377	±13.9	F3				
4769.40	[Fe III]	4770.85	0.061	±79.5	0.069	^{+99.6} _{-93.2}	F3				
4802.23	C II	4801.39	0.430	±7.8	0.464	±9.7		4f 2F*	8g 2G	14	18
4803.29	N II	4801.71	0.133	±14.6	0.143	^{+18.5} _{-17.3}	V20	3p 3D	3d 3D*	7	7
4861.33	H 4	4862.73	100.000	±0.3	100.008	±0.4	H4	2p+ 2P*	4d+ 2D	8	32
4958.91	[O III]	4960.51	365.804	±0.3	323.093	±0.4	F1	2p2 3P	2p2 1D	3	5
5006.84	[O III]	5008.52	1188.922	±0.2	988.072	±0.3	F1	2p2 3P	2p2 1D	5	5
5679.56	N II	5681.96	0.275	±35.4	0.107	^{+44.0} _{-42.8}	V3	3s 3P*	3p 3D	5	7
5695.92	C III	5693.36	0.758	±14.2	0.291	±17.6	V2	3p 1P*	3d 1D	3	5
5710.77	N II	5715.76	0.369	±21.6	0.140	^{+27.5} _{-26.1}	V3	3s 3P*	3p 3D	5	5
5754.60	[N II]	5756.07	1.154	±7.8	0.421	^{+10.1} _{-9.8}	F3	2p2 1D	2p2 1S	5	1
5875.66	He I	5877.11	50.755	±0.5	16.689	±1.0	V11	2p 3P*	3d 3D	9	15
6151.43	C II	6153.48	0.227	±21.6	0.059	^{+27.3} _{-27.0}	V16.04	4d 2D	6f 2F*	10	14
6300.34	[O I]	6301.91	10.848	±1.6	2.520	±2.2	F1	2p4 3P	2p4 1D	5	5
6312.10	[S III]	6313.72	4.885	±3.3	1.124	±4.3	F3	2p2 1D	2p2 1S	5	1
6363.78	[O I]	6365.31	3.086	±5.2	0.682	±6.6	F1	2p4 3P	2p4 1D	3	5
6393.60	[Mn V]	6395.89	0.782	±20.6	0.169	±26.3		3d3 4F	3d3 4P	10	6
6548.10	[N II]	6549.65	87.038	±0.8	16.740	±1.5	F1	2p2 3P	2p2 1D	3	5
6562.77	H 3	6564.38	1526.000	±0.5	290.326	±1.2	H3	2p+ 2P*	3d+ 2D	8	18
6583.50	[N II]	6585.04	274.349	±0.6	51.405	±1.3	F1	2p2 3P	2p2 1D	5	5
6678.16	He I	6679.78	21.718	±1.3	3.799	^{+2.0} _{-1.9}	V46	2p 1P*	3d 1D	3	5
6716.44	[S II]	6718.08	15.754	±1.0	2.681	±1.8	F2	2p3 4S*	2p3 2D*	4	6
6730.82	[S II]	6732.50	30.480	±1.1	5.135	±1.9	F2	2p3 4S*	2p3 2D*	4	4
7065.25	He I	7067.02	18.490	±4.0	2.481	±5.3	V10	2p 3P*	3s 3S	9	3

M 1-25 (PNG004.9+04.9)

3726.03	[O II] ^a	3726.03	30.400	±0.0	78.074	±0.3	F1	2p3 4S*	2p3 2D*	4	4
3728.82	[O II] ^a	3728.82	*		*		F1	2p3 4S*	2p3 2D*	4	6
3868.75	[Ne III] ^a	3868.75	3.100	±0.0	7.229	±0.3	F1	2p4 3P	2p4 1D	5	5
4101.74	H 6 ^a	4101.74	13.100	±0.0	25.534	±0.2	H6	2p+ 2P*	6d+ 2D	8	72
4340.47	H 5 ^a	4340.47	31.700	±0.0	50.506	±0.2	H5	2p+ 2P*	5d+ 2D	8	50
4363.21	[O III] ^a	4363.21	0.900	±0.0	1.406	±0.2	F2	2p2 1D	2p2 1S	5	1
4448.19	O II	4445.21	0.208	±21.0	0.301	±25.2	V35	3p' 2F*	3d' 2F	8	8
4452.37	O II	4450.55	0.175	±23.8	0.253	±29.0	V5	3s 2P	3p 2D*	4	4
4457.05	Ne II	4457.60	0.264	±14.8	0.380	±17.6	V61d	3d 2D	4f 2[2]*	4	6
4471.50	He I	4471.20	3.697	±1.7	5.249	±2.1	V14	2p 3P*	4d 3D	9	15
4510.91	N III	4508.80	0.118	±30.2	0.162	^{+35.5} _{-36.8}	V3	3s' 4P*	3p' 4D	2	4
4518.15	N III	4514.99	0.152	±24.4	0.207	±29.4	V3	3s' 4P*	3p' 4D	2	2

Physical and chemical properties of WR planetary nebulae

4562.60	Mg I]	4560.92	0.094	±27.1	0.123	+32.8 -31.9		3s2 1S	3s3p 3P*	1	5
4590.97	O II	4588.13	0.159	±24.7	0.203	+30.8 -29.7	V15	3s' 2D	3p' 2F*	6	8
4630.54	N II	4629.81	0.322	±16.7	0.397	±20.6	V5	3s 3P*	3p 3P	5	5
4634.14	N III	4635.85	0.371	±22.3	0.455	+27.8 -26.7	V2	3p 2P*	3d 2D	2	4
4638.86	O II	4640.19	0.409	±17.6	0.500	±21.4	V1	3s 4P	3p 4D*	2	4
4647.42	C III	4649.38	0.207	±35.1	0.251	±43.2	V1	3s 3S	3p 3P*	3	5
4658.10	[Fe III]	4657.84	0.400	±9.8	0.481	+12.1 -11.9	F3	3d6 5D	3d6 3F2	9	9
4711.37	[Ar IV]	4712.98	0.308	±8.2	0.353	+10.3 -9.9	F1	3p3 4S*	3p3 2D*	4	6
4861.33	H 4	4861.35	100.000	±0.2	100.006	±0.2	H4	2p+ 2P*	4d+ 2D	8	32
4881.11	[Fe III]	4881.44	0.103	±10.1	0.101	±12.2	F2	3d6 5D	3d6 3H	9	9
4958.91	[O III]	4959.11	173.703	±0.2	159.071	±0.2	F1	2p2 3P	2p2 1D	3	5
5006.84	[O III]	5007.11	547.976	±0.2	480.621	±0.2	F1	2p2 3P	2p2 1D	5	5
5191.82	[Ar III]	5189.47	0.100	±28.0	0.074	+35.1 -33.6	F3	2p4 1D	2p4 1S	5	1
5199.84	[N I]	5197.30	0.186	±10.1	0.137	±12.8	F1	2p3 4S*	2p3 2D*	4	4
5270.40	[Fe III]	5270.89	0.328	±12.7	0.227	+16.2 -15.8	F1	3d6 5D	3d6 3P2	7	5
5517.66	[Cl III]	5518.40	0.400	±9.8	0.227	±12.9	F1	2p3 4S*	2p3 2D*	4	6
5537.60	[Cl III]	5538.81	0.576	±11.6	0.323	+15.3 -14.6	F1	2p3 4S*	2p3 2D*	4	4
5666.63	N II	5665.76	0.160	±15.6	0.083	±20.5	V3	3s 3P*	3p 3D	3	5
5710.77	N II	5708.47	0.371	±13.3	0.187	±17.3	V3	3s 3P*	3p 3D	5	5
5754.60	[N II]	5754.34	3.925	±1.6	1.921	±2.1	F3	2p2 1D	2p2 1S	5	1
5875.66	He I	5875.45	44.084	±0.3	20.041	±0.4	V11	2p 3P*	3d 3D	9	15
6101.83	[K IV]	6101.35	0.112	±25.4	0.045	+34.3 -32.9	F1	3p4 3P	3d4 1D	5	5
6300.34	[O I]	6300.05	6.119	±1.8	2.174	±2.4	F1	2p4 3P	2p4 1D	5	5
6312.10	[S III]	6311.82	4.675	±1.6	1.650	±2.1	F3	2p2 1D	2p2 1S	5	1
6363.78	[O I]	6363.51	1.545	±3.5	0.530	±4.6	F1	2p4 3P	2p4 1D	3	5
6371.38	S III	6370.63	0.431	±15.0	0.147	+20.1 -19.0	V2	4s 2S	4p 2P*	2	2
6393.60	[Mn V]	6400.48	0.077	±25.9	0.026	+34.5 -32.8		3d3 4F	3d3 4P	10	6
6461.95	C II	6462.94	0.281	±13.6	0.091	+17.8 -16.9		4f 2F*	6g 2G	14	18
6548.10	[N II]	6547.81	225.181	±0.2	69.998	±0.4	F1	2p2 3P	2p2 1D	3	5
6562.77	H 3	6562.53	939.711	±0.2	289.877	±0.4	H3	2p+ 2P*	3d+ 2D	8	18
6583.50	[N II]	6583.18	714.364	±0.2	217.993	±0.4	F1	2p2 3P	2p2 1D	5	5
6678.16	He I	6678.19	12.508	±1.2	3.635	±1.6	V46	2p 1P*	3d 1D	3	5
6716.44	[S II]	6716.20	18.991	±0.5	5.414	±0.7	F2	2p3 4S*	2p3 2D*	4	6
6730.82	[S II]	6730.60	36.721	±0.4	10.393	±0.6	F2	2p3 4S*	2p3 2D*	4	4
7065.25	He I	7065.19	17.168	±2.5	4.135	±3.2	V10	2p 3P*	3s 3S	9	3
7135.80	[Ar III] ^a	7135.80	95.000	±0.0	22.154	±0.4	F1	3p4 3P	3p4 1D	5	5
7281.35	He I ^a	7281.35	3.430	±0.0	0.750	±0.4	V45	2p 1P*	3s 1S	3	1

Hen 2-142 (PNG327.1-02.2)

3726.03	[O II] ^a	3726.03	45.500	±0.0	113.997	±6.9	F1	2p3 4S*	2p3 2D*	4	4
3728.82	[O II] ^a	3728.82	*		*		F1	2p3 4S*	2p3 2D*	4	6
4101.74	H 6 ^a	4101.74	20.100	±0.0	38.499	±4.9	H6	2p+ 2P*	6d+ 2D	8	72
4340.47	H 5 ^a	4340.47	46.800	±0.0	73.658	±3.3	H5	2p+ 2P*	5d+ 2D	8	50
4471.50	He I	4476.58	0.740	±14.0	1.041	+19.1 -18.4	V14	2p 3P*	4d 3D	9	15
4861.33	H 4	4860.29	100.000	±5.3	100.006	±6.8	H4	2p+ 2P*	4d+ 2D	8	32
4958.91	[O III]	4957.32	1.540	±1.2	1.414	±1.6	F1	2p2 3P	2p2 1D	3	5
5006.84	[O III]	5005.36	6.050	±0.8	5.325	±1.3	F1	2p2 3P	2p2 1D	5	5
5517.66	[Cl III]	5516.90	0.400	±7.9	0.231	+10.4 -11.8	F1	2p3 4S*	2p3 2D*	4	6
5537.60	[Cl III]	5536.23	1.100	±6.0	0.626	+8.1 -9.4	F1	2p3 4S*	2p3 2D*	4	4
5754.60	[N II]	5752.53	9.720	±0.4	4.848	+4.7 -5.1	F3	2p2 1D	2p2 1S	5	1
6233.80	He II	6231.19	0.200	±14.2	0.076	+18.2 -20.7	5.17	5g+ 2G	17h+ 2H*	50	*
6300.34	[O I]	6298.01	10.220	±0.5	3.732	+6.8 -7.2	F1	2p4 3P	2p4 1D	5	5
6312.10	[S III]	6309.66	1.690	±3.9	0.613	+8.2 -9.4	F3	2p2 1D	2p2 1S	5	1
6363.78	[O I]	6361.43	3.260	±1.6	1.150	+6.9 -7.8	F1	2p4 3P	2p4 1D	3	5

Danehkar											
6548.10	[N II]	6545.68	286.080	±0.3	91.697	+7.3 -8.2	F1	2p2 3P	2p2 1D	3	5
6562.77	H 3	6560.39	901.900	±0.2	286.932	+7.7 -8.0	H3	2p+ 2P*	3d+ 2D	8	18
6583.50	[N II]	6581.04	896.230	±0.4	282.141	+7.4 -8.1	F1	2p2 3P	2p2 1D	5	5
6678.16	He I	6675.66	3.370	±3.2	1.012	+8.8 -9.7	V46	2p 1P*	3d 1D	3	5
6716.44	[S II]	6714.02	7.580	±0.4	2.233	±8.1	F2	2p3 4S*	2p3 2D*	4	6
6730.82	[S II]	6728.38	17.500	±0.5	5.120	±8.3	F2	2p3 4S*	2p3 2D*	4	4
Hen 3-1333 (PNG332.9-09.9)											
3726.03	[O II] ^a	3726.03	45.600	±0.0	85.525	±1.4	F1	2p3 4S*	2p3 2D*	4	4
3728.82	[O II] ^a	3728.82	*		*		F1	2p3 4S*	2p3 2D*	4	6
4861.33	H 4	4860.06	100.000	±1.0	100.004	±1.1	H4	2p+ 2P*	4d+ 2D	8	32
5754.60	[N II]	5752.99	11.108	±2.8	6.898	±3.5	F3	2p2 1D	2p2 1S	5	1
6300.34	[O I]	6298.57	90.714	±1.0	45.505	+2.2 -1.8	F1	2p4 3P	2p4 1D	5	5
6363.78	[O I]	6361.93	33.041	±3.2	16.192	±4.1	F1	2p4 3P	2p4 1D	3	5
6548.10	[N II]	6546.21	207.557	±0.9	95.233	+2.2 -1.8	F1	2p2 3P	2p2 1D	3	5
6562.77	H 3	6560.96	630.049	±0.7	287.607	+2.2 -1.7	H3	2p+ 2P*	3d+ 2D	8	18
6716.44	[S II]	6715.01	23.223	±20.7	10.058	+23.6 -26.0	F2	2p3 4S*	2p3 2D*	4	6
6730.82	[S II]	6728.79	117.269	±4.9	50.543	±6.1	F2	2p3 4S*	2p3 2D*	4	4
7319.99	[O II] ^a	7319.99	71.650	±0.0	25.702	±2.7	F2	2p3 2D*	2p3 2P*	6	4
7330.73	[O II] ^a	7330.73	36.180	±0.0	12.938	±2.6	F2	2p3 2D*	2p3 2P*	4	4
9068.60	[S III] ^a	9068.60	8.700	±0.0	2.077	±3.7		3p2 3P	3p2 1D	3	5
Hen 2-113 (PNG321.0+03.9)											
3726.03	[O II] ^a	3726.03	6.410	±0.0	14.112	+2.2 -1.8	F1	2p3 4S*	2p3 2D*	4	4
3728.82	[O II] ^a	3728.82	6.290	±0.0	13.828	+2.2 -1.8	F1	2p3 4S*	2p3 2D*	4	6
4861.33	H 4	4860.42	100.000	±1.1	100.005	±1.4	H4	2p+ 2P*	4d+ 2D	8	32
5754.60	[N II]	5753.34	9.387	±1.2	5.163	+2.0 -2.3	F3	2p2 1D	2p2 1S	5	1
6300.34	[O I]	6298.92	11.726	±1.9	4.934	+3.0 -3.5	F1	2p4 3P	2p4 1D	5	5
6312.10	[S III]	6310.61	1.522	±4.7	0.637	±6.1	F3	2p2 1D	2p2 1S	5	1
6363.78	[O I]	6362.24	4.967	±2.8	2.030	+3.9 -4.2	F1	2p4 3P	2p4 1D	3	5
6548.10	[N II]	6546.55	121.161	±0.4	45.580	±2.2	F1	2p2 3P	2p2 1D	3	5
6562.77	H 3	6561.29	767.207	±1.0	286.770	±2.4	H3	2p+ 2P*	3d+ 2D	8	18
6583.50	[N II]	6581.91	403.152	±1.7	149.335	+3.0 -3.4	F1	2p2 3P	2p2 1D	5	5
6716.44	[S II]	6714.65	5.941	±8.8	2.079	+10.9 -11.4	F2	2p3 4S*	2p3 2D*	4	6
6730.82	[S II]	6729.40	20.512	±4.2	7.134	±5.5	F2	2p3 4S*	2p3 2D*	4	4
9068.60	[S III] ^a	9068.60	47.190	±0.0	7.822	±4.4		3p2 3P	3p2 1D	3	5
K 2-16 (PNG352.9+11.4)											
3726.03	[O II] ^a	3726.03	96.330	±0.0	129.391	±2.8	F1	2p3 4S*	2p3 2D*	4	4
3728.82	[O II] ^a	3728.82	128.710	±0.0	172.789	+2.8 -3.0	F1	2p3 4S*	2p3 2D*	4	6
4861.33	H 4	4861.35	100.000	±2.4	100.002	±2.6	H4	2p+ 2P*	4d+ 2D	8	32
4958.91	[O III]	4959.00	42.123	±3.1	40.979	±3.2	F1	2p2 3P	2p2 1D	3	5
5006.84	[O III]	5006.84	139.000	±1.7	133.413	+1.9 -2.1	F1	2p2 3P	2p2 1D	5	5
5754.60	[N II]	5754.92	4.490	±10.8	3.591	+11.8 -13.0	F3	2p2 1D	2p2 1S	5	1
6548.10	[N II]	6547.98	97.027	±5.1	67.321	+7.0 -6.8	F1	2p2 3P	2p2 1D	3	5
6562.77	H 3	6562.63	415.634	±1.0	287.691	±3.9	H3	2p+ 2P*	3d+ 2D	8	18
6583.50	[N II]	6583.22	446.144	±0.7	307.766	±3.8	F1	2p2 3P	2p2 1D	5	5
6716.44	[S II]	6716.29	100.061	±1.1	67.571	+4.2 -3.9	F2	2p3 4S*	2p3 2D*	4	6
6730.82	[S II]	6730.70	66.064	±6.1	44.512	±8.5	F2	2p3 4S*	2p3 2D*	4	4
NGC 6578 (PNG010.8-01.8)											

3726.03	[O II] ^a	3726.03	7.500	±0.0	18.309	±0.7	F1	2p3 4S*	2p3 2D*	4	4
3728.82	[O II] ^a	3728.82	*		*		F1	2p3 4S*	2p3 2D*	4	6
3868.75	[Ne III] ^a	3868.75	30.400	±0.0	67.740	±0.7	F1	2p4 3P	2p4 1D	5	5
3889.05	H 8 ^a	3889.05	10.000	±0.0	21.976	±0.6	H8	2p+ 2P*	8d+ 2D	8	*
3967.46	[Ne III] ^a	3967.46	18.800	±0.0	39.088	±0.6	F1	2p4 3P	2p4 1D	3	5
4068.60	[S II] ^a	4068.60	0.900	±0.0	1.736	±0.5	F1	2p3 4S*	2p3 2P*	4	4
4101.74	H 6 ^a	4101.74	15.300	±0.0	28.772	±0.5	H6	2p+ 2P*	6d+ 2D	8	72
4340.47	H 5 ^a	4340.47	32.900	±0.0	51.122	±0.4	H5	2p+ 2P*	5d+ 2D	8	50
4363.21	[O III] ^a	4363.21	1.600	±0.0	2.440	±0.3	F2	2p2 1D	2p2 1S	5	1
4432.74	N II	4432.74	0.075	±35.3	0.108	+48.6 -44.6	V55a	3d 3P*	4f 2[3]	5	7
4452.37	O II	4452.37	0.088	±44.7	0.125	+60.1 -55.8	V5	3s 2P	3p 2D*	4	4
4457.05	Ne II	4459.11	0.363	±18.5	0.512	+25.3 -23.9	V61d	3d 2D	4f 2[2]*	4	6
4471.50	He I	4471.22	3.995	±1.7	5.567	±2.3	V14	2p 3P*	4d 3D	9	15
4477.90	O II	4480.49	0.096	±24.5	0.133	+33.9 -32.0	V88	3d 2P	4f G3*	4	6
4481.21	Mg II	4480.85	0.193	±18.0	0.267	+24.7 -23.1	V4	3d 2D	4f 2F*	10	14
4485.45	S II	4486.12	0.267	±17.3	0.368	+23.4 -22.6	V43	3d 2D	4f 2[3]	4	6
4487.72	O II	4485.95	0.104	±70.4	0.143	+97.7 -89.9	V104	3d' 2P	4f' D2*	2	4
4491.07	C II	4491.19	0.079	±50.1	0.108	+69.0 -64.5		4f 2F*	9g 2G	14	18
4491.23	O II	4491.19	0.077	±50.7	0.106	+71.3 -64.8	V86a	3d 2P	4f D3*	4	6
4514.86	N III	4513.64	0.130	±15.7	0.175	+21.7 -20.2	V3	3s' 4P*	3p' 4D	6	8
4518.15	N III	4520.70	0.134	±25.2	0.180	+34.9 -31.9	V3	3s' 4P*	3p' 4D	2	2
4534.58	N III	4535.42	0.189	±18.6	0.250	+25.6 -23.6	V3	3s' 4P*	3p' 4D	6	6
4541.59	He II	4537.58	0.053	±45.4	0.070	+62.8 -58.2	4.9	4f+ 2F*	9g+ 2G	32	*
4571.10	Mg I]	4569.85	0.159	±16.0	0.204	+22.0 -20.2		3s2 1S	3s3p 3P*	1	3
4590.97	O II	4588.45	0.140	±16.8	0.176	+22.8 -20.8	V15	3s' 2D	3p' 2F*	6	8
4596.18	O II	4595.92	0.135	±10.6	0.169	+14.5 -13.2	V15	3s' 2D	3p' 2F*	4	6
4602.13	O II	4598.31	0.031	±54.2	0.039	+75.0 -67.4	V92b	3d 2D	4f F3*	4	6
4634.14	N III	4634.03	0.132	±20.8	0.160	+28.1 -25.4	V2	3p 2P*	3d 2D	2	4
4640.64	N III	4640.27	0.406	±16.8	0.490	+23.5 -20.6	V2	3p 2P*	3d 2D	4	6
4647.42	C III	4649.45	0.479	±8.8	0.575	+12.0 -10.9	V1	3s 3S	3p 3P*	3	5
4661.63	O II	4661.13	0.321	±8.1	0.381	+11.0 -10.0	V1	3s 4P	3p 4D*	4	4
4685.68	He II	4685.53	0.449	±4.8	0.522	+6.5 -5.9	3.4	3d+ 2D	4f+ 2F*	18	32
4701.62	[Fe III]	4699.88	0.038	±47.1	0.044	+65.5 -60.3	F3	3d6 5D	3d6 3F2	7	7
4711.37	[Ar IV]	4711.97	0.900	±6.1	1.023	+8.1 -7.7	F1	3p3 4S*	3p3 2D*	4	6
4733.91	[Fe III]	4735.96	0.065	±18.1	0.072	+24.7 -23.1	F3	3d6 5D	3d6 3F2	5	5
4740.17	[Ar IV]	4740.05	1.000	±3.7	1.109	±5.0	F1	3p3 4S*	3p3 2D*	4	4
4788.13	N II	4785.52	0.052	±33.2	0.055	+44.5 -43.8	V20	3p 3D	3d 3D*	5	5
4814.53	[Fe II]	4816.92	0.045	±51.4	0.047	+70.6 -69.6	F20				
4861.33	H 4	4861.27	100.000	±0.4	100.005	±0.5	H4	2p+ 2P*	4d+ 2D	8	32
4881.11	[Fe III]	4880.24	0.223	±12.6	0.219	±17.4	F2	3d6 5D	3d6 3H	9	9
4890.86	O II	4891.05	0.111	±17.3	0.108	+23.4 -24.0	V28	3p 4S*	3d 4P	4	2
4931.80	[O III]	4932.07	0.026	±34.1	0.024	+46.2 -47.2	F1	2p2 3P	2p2 1D	1	5
4958.91	[O III]	4959.01	277.365	±0.4	255.205	±0.5	F1	2p2 3P	2p2 1D	3	5
5006.84	[O III]	5007.01	864.308	±0.5	763.433	±0.7	F1	2p2 3P	2p2 1D	5	5
5411.52	He II	5411.69	0.226	±17.1	0.142	±23.3	4.7	4f+ 2F*	7g+ 2G	32	98
5517.66	[Cl III]	5517.93	0.506	±8.5	0.296	±11.7	F1	2p3 4S*	2p3 2D*	4	6
5537.60	[Cl III]	5538.04	0.674	±6.9	0.390	±9.2	F1	2p3 4S*	2p3 2D*	4	4
5577.34	[O I]	5576.93	0.321	±11.3	0.181	±15.2	F3	2p4 1D	2p4 1S	5	1
5676.02	N II	5675.09	0.076	±24.7	0.040	+33.6 -34.1	V3	3s 3P*	3p 3D	1	3
5679.56	N II	5678.93	0.131	±14.7	0.070	±19.6	V3	3s 3P*	3p 3D	5	7
5686.21	N II	5688.83	0.111	±17.2	0.059	+23.0 -23.1	V3	3s 3P*	3p 3D	3	3
5695.92	C III	5698.02	0.076	±34.1	0.040	±45.2	V2	3p 1P*	3d 1D	3	5

5754.60	[N II]	5753.98	0.232	±11.9	0.118	+15.9 -16.2	F3	2p2 1D	2p2 1S	5	1
5801.51	C IV	5801.12	0.310	±6.9	0.153	±9.2	V1	3s 2S	3p 2P*	2	4
5812.14	C IV	5811.08	0.200	±8.7	0.098	±11.3	V1	3s 2S	3p 2P*	2	2
5875.66	He I	5875.28	37.026	±0.3	17.561	±0.7	V11	2p 3P*	3d 3D	9	15
5927.81	N II	5930.77	0.056	±31.4	0.026	+40.6 -42.0	V28	3p 3P	3d 3D*	1	3
5941.65	N II	5941.41	0.052	±14.0	0.024	+17.5 -18.6	V28	3p 3P	3d 3D*	5	7
6151.43	C II	6151.26	0.074	±31.4	0.030	+39.3 -41.8	V16.04	4d 2D	6f 2F*	10	14
6300.34	[O I]	6300.34	0.256	±21.5	0.096	+27.5 -29.3	F1	2p4 3P	2p4 1D	5	5
6312.10	[S III]	6311.63	2.118	±1.3	0.791	±1.8	F3	2p2 1D	2p2 1S	5	1
6363.78	[O I]	6364.61	0.101	±15.9	0.037	+20.5 -21.3	F1	2p4 3P	2p4 1D	3	5
6371.38	S III	6370.76	0.331	±13.1	0.120	+16.9 -17.6	V2	4s 2S	4p 2P*	2	2
6461.95	C II	6461.44	0.368	±5.9	0.127	±7.6		4f 2F*	6g 2G	14	18
6548.10	[N II]	6547.74	12.343	±0.7	4.086	±1.3	F1	2p2 3P	2p2 1D	3	5
6562.77	H 3	6562.33	881.620	±0.3	289.705	+0.9 -1.0	H3	2p+ 2P*	3d+ 2D	8	18
6583.50	[N II]	6583.10	40.482	±0.4	13.167	+1.0 -1.1	F1	2p2 3P	2p2 1D	5	5
6678.16	He I	6677.71	15.939	±1.0	4.951	±1.6	V46	2p 1P*	3d 1D	3	5
6716.44	[S II]	6716.16	2.579	±0.9	0.787	±1.6	F2	2p3 4S*	2p3 2D*	4	6
6730.82	[S II]	6730.52	4.555	±1.1	1.380	±1.8	F2	2p3 4S*	2p3 2D*	4	4
7065.25	He I	7064.86	12.096	±1.6	3.145	±2.4	V10	2p 3P*	3s 3S	9	3
7135.80	[Ar III] ^a	7135.80	63.600	±0.0	16.039	±1.1	F1	3p4 3P	3p4 1D	5	5
7281.35	He I ^a	7281.35	2.900	±0.0	0.688	±1.1	V45	2p 1P*	3s 1S	3	1
7751.43	[Ar III] ^a	7751.43	17.700	±0.0	3.494	±1.3	F1	3p4 3P	3p4 1D	3	5
9068.60	[S III] ^a	9068.60	158.000	±0.0	20.698	±1.5		3p2 3P	3p2 1D	3	5

M 2-42 (PNG008.2-04.8)

3726.03	[O II] ^a	3726.03	19.370	±0.0	34.551	±2.4	F1	2p3 4S*	2p3 2D*	4	4
3728.82	[O II] ^a	3728.82	*		*		F1	2p3 4S*	2p3 2D*	4	6
3868.75	[Ne III] ^a	3868.75	29.090	±0.0	48.907	+2.1 -1.8	F1	2p4 3P	2p4 1D	5	5
3889.05	H 8 ^a	3889.05	9.740	±0.0	16.229	+2.2 -1.8	H8	2p+ 2P*	8d+ 2D	8	*
3967.46	[Ne III] ^a	3967.46	5.690	±0.0	9.146	±2.0	F1	2p4 3P	2p4 1D	3	5
3970.07	H 7 ^a	3970.07	7.040	±0.0	11.302	+2.0 -1.7	H7	2p+ 2P*	7d+ 2D	8	98
4068.60	[S II] ^a	4068.60	1.300	±0.0	1.990	±1.9	F1	2p3 4S*	2p3 2P*	4	4
4101.74	H 6 ^a	4101.74	15.300	±0.0	23.043	±1.8	H6	2p+ 2P*	6d+ 2D	8	72
4340.47	H 5 ^a	4340.47	34.770	±0.0	46.272	±1.2	H5	2p+ 2P*	5d+ 2D	8	50
4363.21	[O III] ^a	4363.21	2.050	±0.0	2.695	±1.2	F2	2p2 1D	2p2 1S	5	1
4437.55	He I	4438.63	0.019	±26.0	0.024	+25.3 -30.7	V50	2p 1P*	5s 1S	3	1
4471.50	He I	4472.59	4.607	±0.7	5.713	±1.2	V14	2p 3P*	4d 3D	9	15
4477.90	O II	4482.82	0.025	±38.7	0.031	+39.3 -47.3	V88	3d 2P	4f G3*	4	6
4491.07	C II	4491.99	0.045	±55.7	0.055	+57.8 -67.4		4f 2F*	9g 2G	14	18
4491.23	O II	4491.99	0.050	±51.6	0.061	+52.9 -61.8	V86a	3d 2P	4f D3*	4	6
4510.91	N III	4512.25	0.043	±19.9	0.052	+21.3 -24.1	V3	3s' 4P*	3p' 4D	2	4
4518.15	N III	4518.33	0.011	±30.7	0.013	+32.7 -37.7	V3	3s' 4P*	3p' 4D	2	2
4530.86	N III	4532.34	0.012	±17.5	0.014	+18.7 -20.7	V3	3s' 4P*	3p' 4D	4	2
4562.60	Mg I	4563.59	0.021	±25.4	0.025	+26.6 -31.0		3s2 1S	3s3p 3P*	1	5
4571.10	Mg I	4572.28	0.048	±13.8	0.056	+14.4 -16.0		3s2 1S	3s3p 3P*	1	3
4590.97	O II	4592.18	0.031	±10.7	0.036	+11.0 -12.9	V15	3s' 2D	3p' 2F*	6	8
4596.18	O II	4597.19	0.027	±26.6	0.031	+29.0 -32.1	V15	3s' 2D	3p' 2F*	4	6
4602.13	O II	4602.49	0.011	±51.0	0.013	+53.5 -61.2	V92b	3d 2D	4f F3*	4	6
4607.16	N II	4607.98	0.033	±16.6	0.038	+18.4 -20.0	V5	3s 3P*	3p 3P	1	3
4609.44	O II	4610.80	0.057	±8.9	0.066	±10.0	V92a	3d 2D	4f F4*	6	8
4640.64	N III	4642.21	0.587	±4.6	0.663	±5.3	V2	3p 2P*	3d 2D	4	6
4651.47	C III	4650.38	0.347	±4.5	0.390	±5.2	V1	3s 3S	3p 3P*	3	1
4658.10	[Fe III]	4659.54	0.034	±24.5	0.038	+27.7 -29.5	F3	3d6 5D	3d6 3F2	9	9
4661.63	O II	4662.50	0.081	±11.7	0.090	±13.0	V1	3s 4P	3p 4D*	4	4

Physical and chemical properties of WR planetary nebulae

4673.73	O II	4677.36	0.077	±14.7	0.085	+16.7 -17.5	V1	3s 4P	3p 4D*	4	2
4685.68	He II	4687.27	0.300	±2.5	0.331	±2.9	3.4	3d+ 2D	4f+ 2F*	18	32
4701.62	[Fe III]	4702.63	0.011	±42.7	0.012	+47.5 -49.4	F3	3d6 5D	3d6 3F2	7	7
4711.37	[Ar IV]	4713.74	0.900	±3.4	0.978	±3.8	F1	3p3 4S*	3p3 2D*	4	6
4733.91	[Fe III]	4735.31	0.014	±30.9	0.015	±34.7	F3	3d6 5D	3d6 3F2	5	5
4740.17	[Ar IV]	4741.49	1.000	±1.9	1.070	±2.2	F1	3p3 4S*	3p3 2D*	4	4
4754.70	[Fe III]	4755.95	0.032	±13.9	0.034	±15.5	F3				
4769.40	[Fe III]	4770.88	0.091	±6.6	0.096	±7.4	F3				
4788.13	N II	4782.68	0.305	±3.9	0.318	±4.3	V20	3p 3D	3d 3D*	5	5
4861.33	H 4	4862.79	100.000	±0.3	100.004	±0.3	H4	2p+ 2P*	4d+ 2D	8	32
4881.11	[Fe III]	4882.46	0.042	±8.3	0.042	±9.1	F2	3d6 5D	3d6 3H	9	9
4921.93	He I	4924.05	0.176	±8.5	0.170	±9.3	V48	2p 1P*	4d 1D	3	5
4958.91	[O III]	4960.52	228.183	±0.5	216.189	±0.6	F1	2p2 3P	2p2 1D	3	5
5006.84	[O III]	5008.54	707.172	±1.4	652.495	±1.6	F1	2p2 3P	2p2 1D	5	5
5191.82	[Ar III]	5193.27	0.050	±14.0	0.042	±16.1	F3	2p4 1D	2p4 1S	5	1
5199.84	[N I]	5201.61	0.154	±6.2	0.128	+6.9 -7.1	F1	2p3 4S*	2p3 2D*	4	4
5200.26	[N I]	5202.03	0.113	±8.3	0.094	±9.4	F1	2p3 4S*	2p3 2D*	4	6
5270.40	[Fe III]	5272.49	0.072	±5.4	0.058	±6.2	F1	3d6 5D	3d6 3P2	7	5
5411.52	He II	5413.87	0.043	±6.4	0.032	±7.3	4.7	4f+ 2F*	7g+ 2G	32	98
5453.83	S II	5455.64	0.021	±19.5	0.015	+21.9 -22.0	V6	4s 4P	4p 4D*	6	8
5517.66	[Cl III]	5519.89	0.730	±2.0	0.516	±2.4	F1	2p3 4S*	2p3 2D*	4	6
5537.60	[Cl III]	5540.01	0.850	±1.0	0.596	±1.6	F1	2p3 4S*	2p3 2D*	4	4
5577.34	[O I]	5576.74	0.869	±3.9	0.600	±4.6	F3	2p4 1D	2p4 1S	5	1
5666.63	N II	5668.24	0.049	±12.4	0.033	±13.9	V3	3s 3P*	3p 3D	3	5
5679.56	N II	5681.41	0.065	±8.9	0.043	+10.1 -9.2	V3	3s 3P*	3p 3D	5	7
5710.77	N II	5715.84	0.013	±27.8	0.009	+32.4 -30.9	V3	3s 3P*	3p 3D	5	5
5754.60	[N II]	5756.14	0.959	±0.9	0.619	±1.8	F3	2p2 1D	2p2 1S	5	1
5801.51	C IV	5805.39	0.025	±22.8	0.016	+26.4 -24.9	V1	3s 2S	3p 2P*	2	4
5812.14	C IV	5811.94	0.093	±14.6	0.059	+17.2 -16.7	V1	3s 2S	3p 2P*	2	2
5875.66	He I	5877.23	24.319	±0.4	14.993	±1.8	V11	2p 3P*	3d 3D	9	15
5978.97	S III	5980.58	0.029	±15.2	0.017	±17.5	V4				
6074.10	He II	6068.63	0.021	±23.1	0.012	±27.0	5.20	5g+ 2G	20h+ 2H*	50	*
6101.83	[K IV]	6103.36	0.052	±10.0	0.030	+12.0 -11.3	F1	3p4 3P	3d4 1D	5	5
6151.43	C II	6153.31	0.025	±9.5	0.014	+11.8 -10.8	V16.04	4d 2D	6f 2F*	10	14
6300.34	[O I]	6301.93	4.464	±1.2	2.366	±2.7	F1	2p4 3P	2p4 1D	5	5
6312.10	[S III]	6313.72	2.203	±0.4	1.163	±2.3	F3	2p2 1D	2p2 1S	5	1
6347.10	Si II	6348.83	0.094	±7.4	0.049	±9.6	V2	4s 2S	4p 2P*	2	4
6363.78	[O I]	6365.42	1.543	±2.1	0.800	±3.6	F1	2p4 3P	2p4 1D	3	5
6371.38	S III	6373.15	0.057	±8.6	0.029	+11.0 -10.1	V2	4s 2S	4p 2P*	2	2
6461.95	C II	6463.48	0.114	±4.3	0.057	±5.8		4f 2F*	6g 2G	14	18
6548.10	[N II]	6549.75	26.004	±0.3	12.697	±2.4	F1	2p2 3P	2p2 1D	3	5
6562.77	H 3 ^a	6564.62	593.000	±1.7	288.322	±3.3	H3	2p+ 2P*	3d+ 2D	8	18
6583.50	[N II]	6585.14	80.103	±0.2	38.670	±2.5	F1	2p2 3P	2p2 1D	5	5
6683.20	He II	6679.95	8.148	±1.0	3.812	+2.9 -3.0	5.13	5g+ 2G	13h+ 2H*	50	*
6716.44	[S II]	6718.21	8.122	±0.3	3.760	±2.7	F2	2p3 4S*	2p3 2D*	4	6
6730.82	[S II]	6732.59	12.817	±0.3	5.908	±2.6	F2	2p3 4S*	2p3 2D*	4	4
6795.00	[K IV]	6797.09	0.019	±22.6	0.009	+27.4 -26.8	F1	3p4 3P	3p4 1D	3	5
7065.25	He I	7067.22	6.528	±1.9	2.726	+3.4 -4.0	V10	2p 3P*	3s 3S	9	3
7135.80	[Ar III] ^a	7135.80	23.470	±0.0	9.607	+2.8 -3.3	F1	3p4 3P	3p4 1D	5	5

NGC 6567 (PNG011.7-00.6)

3726.03	[O II] ^a	3726.03	15.600	±0.0	24.587	±0.6	F1	2p3 4S*	2p3 2D*	4	4
3728.82	[O II] ^a	3728.82	*		*		F1	2p3 4S*	2p3 2D*	4	6
3868.75	[Ne III] ^a	3868.75	43.500	±0.0	65.443	±0.5	F1	2p4 3P	2p4 1D	5	5
3889.05	H 8 ^a	3889.05	10.200	±0.0	15.237	±0.5	H8	2p+ 2P*	8d+ 2D	8	*
3967.46	[Ne III] ^a	3967.46	17.100	±0.0	24.833	±0.5	F1	2p4 3P	2p4 1D	3	5

Danehkar

4101.74	H 6 ^a	4101.74	15.300	±0.0	21.110	±0.4	H6	2p+ 2P*	6d+ 2D	8	72
4340.47	H 5 ^a	4340.47	36.600	±0.0	45.819	±0.3	H5	2p+ 2P*	5d+ 2D	8	50
4363.21	[O III] ^a	4363.21	7.600	±0.0	9.424	±0.3	F2	2p2 1D	2p2 1S	5	1
4452.37	O II	4454.71	0.097	±10.8	0.116	±15.0	V5	3s 2P	3p 2D*	4	4
4471.50	He I	4472.84	4.059	±0.8	4.807	±1.2	V14	2p 3P*	4d 3D	9	15
4488.20	O II	4492.85	0.016	±47.6	0.019	^{+65.9} _{-66.8}	V104	3d' 2P	4f' D2*	4	6
4518.15	N III	4520.70	0.018	±22.9	0.021	±32.7	V3	3s' 4P*	3p' 4D	2	2
4571.10	Mg I	4572.35	0.176	±3.8	0.200	±5.5		3s2 1S	3s3p 3P*	1	3
4590.97	O II	4592.52	0.026	±25.3	0.029	±36.2	V15	3s' 2D	3p' 2F*	6	8
4620.26	C II	4621.17	0.096	±16.9	0.107	^{+24.4} _{-23.7}					
4641.84	N III	4642.16	0.198	±6.2	0.218	^{+9.1} _{-8.9}	V2	3p 2P*	3d 2D	4	4
4651.47	C III	4650.92	0.212	±10.5	0.232	±15.5	V1	3s 3S	3p 3P*	3	1
4685.68	He II	4687.28	0.601	±3.2	0.649	±4.8	3.4	3d+ 2D	4f+ 2F*	18	32
4711.37	[Ar IV]	4714.24	0.650	±10.0	0.694	±14.3	F1	3p3 4S*	3p3 2D*	4	6
4740.17	[Ar IV]	4741.70	0.642	±3.1	0.677	±4.5	F1	3p3 4S*	3p3 2D*	4	4
4754.70	[Fe III]	4758.50	0.052	±13.0	0.054	±18.8	F3				
4788.13	N II	4782.67	0.073	±12.5	0.075	±17.5	V20	3p 3D	3d 3D*	5	5
4802.23	C II	4804.28	0.024	±11.5	0.025	±16.5		4f 2F*	8g 2G	14	18
4861.33	H 4	4863.07	100.000	±0.3	100.003	±0.4	H4	2p+ 2P*	4d+ 2D	8	32
4890.86	O II	4887.90	0.066	±14.7	0.065	^{+21.2} _{-20.7}	V28	3p 4S*	3d 4P	4	2
4958.91	[O III]	4960.83	326.557	±0.3	312.986	±0.4	F1	2p2 3P	2p2 1D	3	5
5006.84	[O III]	5008.84	1011.878	±0.6	949.849	±0.8	F1	2p2 3P	2p2 1D	5	5
5047.74	He I	5049.64	0.185	±3.9	0.171	±5.5	V47	2p 1P*	4s 1S	3	1
5191.82	[Ar III]	5193.44	0.064	±15.4	0.055	±21.1	F3	2p4 1D	2p4 1S	5	1
5199.84	[N I]	5200.07	0.051	±8.8	0.044	±12.3	F1	2p3 4S*	2p3 2D*	4	4
5200.26	[N I]	5202.38	0.035	±15.8	0.030	±21.7	F1	2p3 4S*	2p3 2D*	4	6
5270.40	[Fe III]	5273.84	0.063	±20.2	0.053	±28.0	F1	3d6 5D	3d6 3P2	7	5
5411.52	He II	5413.98	0.062	±8.4	0.049	±11.2	4.7	4f+ 2F*	7g+ 2G	32	98
5517.66	[Cl III]	5520.18	0.260	±4.3	0.198	±5.6	F1	2p3 4S*	2p3 2D*	4	6
5537.60	[Cl III]	5540.28	0.401	±2.3	0.303	^{+2.9} _{-3.1}	F1	2p3 4S*	2p3 2D*	4	4
5577.34	[O I]	5577.22	0.043	±62.1	0.032	^{+81.2} _{-84.0}	F3	2p4 1D	2p4 1S	5	1
5666.63	N II	5668.67	0.044	±7.6	0.032	^{+9.4} _{-10.4}	V3	3s 3P*	3p 3D	3	5
5679.56	N II	5677.88	0.026	±19.5	0.019	^{+24.3} _{-26.3}	V3	3s 3P*	3p 3D	5	7
5754.60	[N II]	5756.53	0.440	±2.2	0.312	^{+2.6} _{-3.1}	F3	2p2 1D	2p2 1S	5	1
5801.51	C IV	5803.02	0.737	±2.9	0.515	±3.6	V1	3s 2S	3p 2P*	2	4
5812.14	C IV	5813.53	0.180	±11.1	0.125	^{+13.9} _{-14.7}	V1	3s 2S	3p 2P*	2	2
5875.66	He I	5877.57	22.772	±0.3	15.569	±0.4	V11	2p 3P*	3d 3D	9	15
5978.97	S III	5982.31	0.013	±24.5	0.009	^{+29.6} _{-32.8}	V4				
6101.83	[K IV]	6103.66	0.066	±6.3	0.042	^{+7.6} _{-8.5}	F1	3p4 3P	3d4 1D	5	5
6151.43	C II	6153.34	0.052	±9.9	0.033	^{+11.8} _{-13.3}	V16.04	4d 2D	6f 2F*	10	14
6300.34	[O I]	6302.43	3.400	±1.0	2.064	±1.2	F1	2p4 3P	2p4 1D	5	5
6312.10	[S III]	6314.10	1.295	±0.9	0.784	±1.2	F3	2p2 1D	2p2 1S	5	1
6363.78	[O I]	6366.02	1.263	±1.4	0.754	^{+1.7} _{-2.1}	F1	2p4 3P	2p4 1D	3	5
6461.95	C II	6464.03	0.204	±2.4	0.119	^{+3.0} _{-3.5}		4f 2F*	6g 2G	14	18
6548.10	[N II]	6550.22	8.570	±1.5	4.878	^{+1.8} _{-2.3}	F1	2p2 3P	2p2 1D	3	5
6562.77	H 3	6564.90	503.226	±0.2	285.362	±0.5	H3	2p+ 2P*	3d+ 2D	8	18
6583.50	[N II]	6585.56	26.055	±1.2	14.698	±1.5	F1	2p2 3P	2p2 1D	5	5
6678.16	He I	6680.32	5.106	±1.1	2.813	±1.4	V46	2p 1P*	3d 1D	3	5
6716.44	[S II]	6718.71	1.212	±1.5	0.662	^{+1.9} _{-2.2}	F2	2p3 4S*	2p3 2D*	4	6
6730.82	[S II]	6733.11	2.299	±1.4	1.251	^{+1.7} _{-2.1}	F2	2p3 4S*	2p3 2D*	4	4
7065.25	He I	7067.65	8.777	±1.8	4.417	±2.0	V10	2p 3P*	3s 3S	9	3
7135.80	[Ar III] ^a	7135.80	11.300	±0.0	5.599	±0.7	F1	3p4 3P	3p4 1D	5	5
7319.99	[O II] ^a	7319.99	10.600	±0.0	5.049	±0.8	F2	2p3 2D*	2p3 2P*	6	4
7330.73	[O II] ^a	7330.73	*		*		F2	2p3 2D*	2p3 2P*	4	4
7751.43	[Ar III] ^a	7751.43	2.800	±0.0	1.225	^{+0.9} _{-1.1}	F1	3p4 3P	3p4 1D	3	5

NGC 6629 (PNG009.4–05.0)											
3726.03	[O II] ^a	3726.03	21.200	±0.0	37.715	±0.6	F1	2p3 4S*	2p3 2D*	4	4
3728.82	[O II] ^a	3728.82	*		*		F1	2p3 4S*	2p3 2D*	4	6
3868.75	[Ne III] ^a	3868.75	25.700	±0.0	43.105	±0.5	F1	2p4 3P	2p4 1D	5	5
3889.05	H 8 ^a	3889.05	12.200	±0.0	20.280	±0.5	H8	2p+ 2P*	8d+ 2D	8	*
3967.46	[Ne III] ^a	3967.46	18.500	±0.0	29.672	±0.5	F1	2p4 3P	2p4 1D	3	5
4101.74	H 6 ^a	4101.74	17.600	±0.0	26.457	±0.4	H6	2p+ 2P*	6d+ 2D	8	72
4340.47	H 5 ^a	4340.47	36.900	±0.0	49.042	±0.3	H5	2p+ 2P*	5d+ 2D	8	50
4363.21	[O III] ^a	4363.21	2.100	±0.0	2.757	±0.3	F2	2p2 1D	2p2 1S	5	1
4448.19	O II	4448.93	0.142	±11.2	0.178	^{+14.7} _{-15.4}	V35	3p' 2F*	3d' 2F	8	8
4471.50	He I	4471.25	3.937	±1.5	4.877	±2.0	V14	2p 3P*	4d 3D	9	15
4562.60	Mg I	4561.48	0.126	±12.1	0.149	^{+15.8} _{-16.6}		3s2 1S	3s3p 3P*	1	5
4571.10	Mg I	4571.13	0.108	±8.7	0.127	±11.2		3s2 1S	3s3p 3P*	1	3
4638.86	O II	4639.11	0.056	±59.2	0.063	^{+75.2} _{-77.9}	V1	3s 4P	3p 4D*	2	4
4650.84	O II	4649.55	0.055	±55.2	0.062	^{+69.8} _{-71.8}	V1	3s 4P	3p 4D*	2	2
4658.10	[Fe III]	4657.52	0.107	±28.9	0.120	^{+35.4} _{-38.4}	F3	3d6 5D	3d6 3F2	9	9
4661.63	O II	4660.86	0.144	±10.5	0.161	±13.0	V1	3s 4P	3p 4D*	4	4
4696.35	O II	4690.29	0.068	±30.9	0.074	^{+38.3} _{-39.8}	V1	3s 4P	3p 4D*	6	4
4711.37	[Ar IV]	4713.02	0.427	±5.2	0.464	±6.5	F1	3p3 4S*	3p3 2D*	4	6
4740.17	[Ar IV]	4740.06	0.334	±8.0	0.357	^{+9.9} _{-10.0}	F1	3p3 4S*	3p3 2D*	4	4
4802.23	C II	4807.75	0.038	±36.3	0.039	±44.6		4f 2F*	8g 2G	14	18
4861.33	H 4	4861.32	100.000	±0.4	100.004	±0.5	H4	2p+ 2P*	4d+ 2D	8	32
4881.11	[Fe III]	4880.97	0.103	±9.9	0.102	±11.9	F2	3d6 5D	3d6 3H	9	9
4958.91	[O III]	4959.05	233.290	±0.5	221.083	±0.6	F1	2p2 3P	2p2 1D	3	5
5006.84	[O III]	5007.05	712.773	±0.5	657.906	±0.6	F1	2p2 3P	2p2 1D	5	5
5200.26	[N I]	5199.37	0.025	±38.2	0.021	^{+47.6} _{-46.2}	F1	2p3 4S*	2p3 2D*	4	6
5270.40	[Fe III]	5271.07	0.088	±9.8	0.070	^{+12.2} _{-11.8}	F1	3d6 5D	3d6 3P2	7	5
5517.66	[Cl III]	5518.36	0.473	±3.8	0.335	±4.6	F1	2p3 4S*	2p3 2D*	4	6
5537.60	[Cl III]	5538.36	0.525	±7.8	0.369	±9.5	F1	2p3 4S*	2p3 2D*	4	4
5577.34	[O I]	5576.70	0.172	±23.7	0.119	^{+28.9} _{-29.6}	F3	2p4 1D	2p4 1S	5	1
5754.60	[N II]	5754.43	0.127	±10.7	0.082	^{+12.7} _{-13.5}	F3	2p2 1D	2p2 1S	5	1
5801.51	C IV	5800.78	0.339	±8.2	0.215	^{+10.0} _{-10.5}	V1	3s 2S	3p 2P*	2	4
5812.14	C IV	5811.52	0.150	±16.3	0.095	^{+20.5} _{-21.3}	V1	3s 2S	3p 2P*	2	2
5875.66	He I	5875.40	23.696	±0.5	14.641	±0.8	V11	2p 3P*	3d 3D	9	15
6151.43	C II	6151.14	0.056	±17.6	0.031	^{+21.9} _{-23.2}	V16.04	4d 2D	6f 2F*	10	14
6312.10	[S III]	6311.72	1.063	±2.1	0.563	±2.8	F3	2p2 1D	2p2 1S	5	1
6371.38	S III	6370.23	0.160	±12.8	0.083	^{+15.9} _{-16.7}	V2	4s 2S	4p 2P*	2	2
6461.95	C II	6461.16	0.069	±17.0	0.035	^{+21.1} _{-22.7}		4f 2F*	6g 2G	14	18
6548.10	[N II]	6547.73	5.384	±0.7	2.637	±1.2	F1	2p2 3P	2p2 1D	3	5
6562.77	H 3	6562.47	593.073	±0.3	289.171	±0.8	H3	2p+ 2P*	3d+ 2D	8	18
6583.50	[N II]	6583.08	17.575	±0.3	8.513	±0.8	F1	2p2 3P	2p2 1D	5	5
6678.16	He I	6677.86	9.058	±0.5	4.259	^{+1.0} _{-1.1}	V46	2p 1P*	3d 1D	3	5
6716.44	[S II]	6716.17	0.916	±2.1	0.426	±2.6	F2	2p3 4S*	2p3 2D*	4	6
6730.82	[S II]	6730.48	1.439	±1.0	0.666	±1.4	F2	2p3 4S*	2p3 2D*	4	4
7065.25	He I	7065.08	6.544	±2.1	2.743	±2.6	V10	2p 3P*	3s 3S	9	3
7135.80	[Ar III] ^a	7135.80	29.100	±0.0	11.960	±0.9	F1	3p4 3P	3p4 1D	5	5
7281.35	He I ^a	7281.35	2.000	±0.0	0.790	±0.9	V45	2p 1P*	3s 1S	3	1
9068.60	[S III] ^a	9068.60	33.600	±0.0	9.049	±1.3		3p2 3P	3p2 1D	3	5

Sa 3-107 (PNG358.0–04.6)

4448.19	O II	4444.76	0.066	±36.6	0.096	±47.0	V35	3p' 2F*	3d' 2F	8	8
4452.37	O II	4450.42	0.081	±11.2	0.118	±14.4	V5	3s 2P	3p 2D*	4	4
4457.24	Ne II	4454.66	0.057	±51.8	0.082	+65.5 -63.4	V61d	3d 2D	4f 2[2]*	4	4
4471.50	He I	4468.85	3.886	±2.9	5.542	±3.6	V14	2p 3P*	4d 3D	9	15
4514.86	N III	4514.68	0.101	±20.4	0.139	+26.6 -25.6	V3	3s' 4P*	3p' 4D	6	8
4590.97	O II	4587.18	0.169	±32.0	0.216	+41.2 -38.9	V15	3s' 2D	3p' 2F*	6	8
4596.18	O II	4591.35	0.082	±36.0	0.104	+45.8 -46.4	V15	3s' 2D	3p' 2F*	4	6
4640.64	N III	4637.99	0.384	±13.6	0.470	±17.8	V2	3p 2P*	3d 2D	4	6
4647.42	C III	4648.33	0.242	±12.4	0.294	±15.8	V1	3s 3S	3p 3P*	3	5
4658.10	[Fe III]	4655.32	0.278	±18.3	0.335	±22.8	F3	3d6 5D	3d6 3F2	9	9
4678.14	N II	4673.41	0.064	±38.2	0.076	+48.4 -46.4	V61b	3d 1P*	4f 2[2]	3	5
4685.68	He II	4683.13	1.382	±4.3	1.623	±5.2	3.4	3d+ 2D	4f+ 2F*	18	32
4711.37	[Ar IV]	4710.48	0.287	±11.5	0.329	+14.3 -13.8	F1	3p3 4S*	3p3 2D*	4	6
4754.70	[Fe III]	4755.93	0.045	±19.3	0.050	±24.0	F3				
4769.40	[Fe III]	4766.34	0.126	±25.1	0.137	+31.2 -29.8	F3				
4803.29	N II	4800.55	0.058	±20.6	0.061	+26.5 -24.4	V20	3p 3D	3d 3D*	7	7
4861.33	H 4	4858.70	100.000	±0.4	100.006	±0.5	H4	2p+ 2P*	4d+ 2D	8	32
4958.91	[O III]	4956.40	112.750	±0.4	103.136	±0.5	F1	2p2 3P	2p2 1D	3	5
5006.84	[O III]	5004.37	353.808	±0.5	309.799	±0.7	F1	2p2 3P	2p2 1D	5	5
5191.82	[Ar III]	5191.16	0.078	±19.0	0.058	+23.6 -21.8	F3	2p4 1D	2p4 1S	5	1
5453.83	S II	5452.20	0.186	±12.1	0.109	+15.0 -13.3	V6	4s 4P	4p 4D*	6	8
5270.40	[Fe III]	5268.60	0.173	±18.2	0.119	+22.7 -20.1	F1	3d6 5D	3d6 3P2	7	5
5517.66	[Cl III]	5515.34	0.364	±8.3	0.205	+11.0 -9.3	F1	2p3 4S*	2p3 2D*	4	6
5537.60	[Cl III]	5535.41	0.355	±14.8	0.198	+19.3 -16.5	F1	2p3 4S*	2p3 2D*	4	4
5577.34	[O I]	5576.25	1.380	±10.3	0.749	+13.5 -11.4	F3	2p4 1D	2p4 1S	5	1
5666.63	N II	5663.09	0.099	±31.1	0.051	+41.0 -35.9	V3	3s 3P*	3p 3D	3	5
5679.56	N II	5676.21	0.403	±6.2	0.205	+8.2 -7.1	V3	3s 3P*	3p 3D	5	7
5695.92	C III	5695.12	0.140	±21.5	0.070	+28.5 -24.3	V2	3p 1P*	3d 1D	3	5
5710.77	N II	5707.08	0.126	±17.5	0.063	+23.6 -20.6	V3	3s 3P*	3p 3D	5	5
5754.60	[N II]	5751.33	0.444	±7.0	0.215	+9.2 -8.5	F3	2p2 1D	2p2 1S	5	1
5801.51	C IV	5798.15	1.709	±3.0	0.805	+4.2 -3.7	V1	3s 2S	3p 2P*	2	4
5812.14	C IV	5808.77	1.051	±5.7	0.492	+7.6 -6.9	V1	3s 2S	3p 2P*	2	2
5875.66	He I	5872.29	41.404	±0.6	18.634	+1.1 -0.9	V11	2p 3P*	3d 3D	9	15
5927.81	N II	5924.77	0.104	±15.0	0.045	+20.1 -18.4	V28	3p 3P	3d 3D*	1	3
5931.78	N II	5928.80	0.231	±9.5	0.100	+12.8 -11.5	V28	3p 3P	3d 3D*	3	5
5941.65	N II	5938.22	0.253	±14.1	0.109	+18.1 -16.8	V28	3p 3P	3d 3D*	5	7
6101.83	[K IV]	6098.35	0.083	±19.0	0.033	+24.4 -23.1	F1	3p4 3P	3d4 1D	5	5
6151.43	C II	6147.83	0.092	±14.8	0.035	+19.0 -17.5	V16.04	4d 2D	6f 2F*	10	14
6312.10	[S III]	6308.48	0.846	±7.6	0.295	±9.6	F3	2p2 1D	2p2 1S	5	1
6363.78	[O I]	6362.83	0.481	±6.9	0.163	±8.9	F1	2p4 3P	2p4 1D	3	5
6461.95	C II	6457.85	0.298	±8.9	0.096	+11.5 -10.7		4f 2F*	6g 2G	14	18
6548.10	[N II]	6544.31	11.404	±0.9	3.492	±1.7	F1	2p2 3P	2p2 1D	3	5
6562.77	H 3	6559.01	933.059	±0.3	283.529	+1.1 -1.0	H3	2p+ 2P*	3d+ 2D	8	18
6583.50	[N II]	6579.64	38.197	±0.6	11.481	±1.4	F1	2p2 3P	2p2 1D	5	5
6678.16	He I	6674.36	18.439	±1.2	5.275	±2.0	V46	2p 1P*	3d 1D	3	5
6716.44	[S II]	6712.65	1.932	±2.9	0.542	±3.9	F2	2p3 4S*	2p3 2D*	4	6
6730.82	[S II]	6726.98	2.847	±2.5	0.793	+3.4 -2.9	F2	2p3 4S*	2p3 2D*	4	4
7005.67	[Ar V]	7007.19	0.307	±13.9	0.075	+17.5 -15.6	F1	3s2 3P	3s2 1D	5	5
7065.25	He I	7061.33	13.687	±3.0	3.237	±3.8	V10	2p 3P*	3s 3S	9	3

^a Fluxes adopted from the literature: PB 6 (K91), M 3-30 (P01,G07), Hb 4 shell (P01,G07), Hb 4 N-knot (H97), Hb 4 S-knot (H97), IC 1297 (M02), Th 2-A (M02), Pe 1-1 (G12), M 1-32 (G12), M 3-15 (P01), M 1-25 (G07), Hen 2-142 (G07), Hen 3-1333 (D97), Hen 2-113 (D97), K 2-16 (P01), NGC 6578 (K03), M 2-42 (W07), NGC 6567 (K03), NGC 6629 (M02). References for line fluxes from the literature are as follows: D97, De Marco et al. (1997); G07, Girard et al. (2007); G12, García-Rojas et al. (2012); H97, Hajian et al. (1997); K91, Kaler et al. (1991); K03, Kwitter et al. (2003); M02, Milingo et al. (2002); P01, Peña et al. (2001) and Peña et al. (1998); W07, Wang & Liu (2007).

Table 6. Plasma diagnostics based on CELs.

Type	Ion	Diagnostic	Value
PB 6 (PNG278.8+04.9)			
T_e	[N II]	6548.10+6583.50 /5754.60	11300^{+200}_{-260}
$T_{e\text{ rc}}$	[N II]	6548.10+6583.50 /5754.60	10270^{+220}_{-220}
T_e	[O III]	4958.91+5006.84 /4363.21	14220^{+110}_{-90}
$T_{e\text{ rc}}$	[O III]	4958.91+5006.84 /4363.21	14040^{+90}_{-130}
N_e	[S II]	6730.82 /6716.44	1800^{+400}_{-320}
N_e	[Ar IV]	4740.17 /4711.37	1370^{+70}_{-100}
N_e	[Cl III]	5537.60 /5517.66	2190^{+390}_{-270}
M 3-30 (PNG017.9-04.8)			
T_e	[N II]	6548.10+6583.50 /5754.60	8880^{+170}_{-180}
T_e	[O III]	4958.91+5006.84 /4363.21	10610^{+30}_{-40}
$T_{e\text{ rc}}$	[O III]	4958.91+5006.84 /4363.21	9170^{+30}_{-30}
N_e	[S II]	6730.82 /6716.44	700^{+50}_{-60}
N_e	[O II]	3728.82 /3726.03	1120^{+50}_{-60}
N_e	[Ar IV]	4740.17 /4711.37	540^{+310}_{-300}
Hb 4 (shell) (PNG003.1+02.9)			
T_e	[N II]	6548.10+6583.50 /5754.60	10390^{+70}_{-60}
$T_{e\text{ rc}}$	[N II]	6548.10+6583.50 /5754.60	9410^{+50}_{-40}
T_e	[O III]	4958.91+5006.84 /4363.21	9330^{+10}_{-10}
$T_{e\text{ rc}}$	[O III]	4958.91+5006.84 /4363.21	9180^{+20}_{-10}
N_e	[S II]	6730.82 /6716.44	4440^{+180}_{-230}
N_e	[O II]	3728.82 /3726.03	1960^{+60}_{-70}
N_e	[Ar IV]	4740.17 /4711.37	5590^{+510}_{-460}
N_e	[Cl III]	5537.60 /5517.66	4130^{+380}_{-450}
Hb 4 (N-knot) (PNG003.1+02.9)			
T_e	[N II]	6548.10+6583.50 /5754.60	9860^{+610}_{-670}
N_e	[S II]	6730.82 /6716.44	1250^{+480}_{-340}
Hb 4 (S-knot) (PNG003.1+02.9)			
N_e	[S II]	6730.82 /6716.44	890^{+290}_{-300}
IC 1297 (PNG358.3-21.6)			
T_e	[N II]	6548.10+6583.50 /5754.60	9510^{+130}_{-160}
$T_{e\text{ rc}}$	[N II]	6548.10+6583.50 /5754.60	9160^{+170}_{-160}
T_e	[O III]	4958.91+5006.84 /4363.21	10460^{+30}_{-20}
$T_{e\text{ rc}}$	[O III]	4958.91+5006.84 /4363.21	10400^{+20}_{-30}
N_e	[S II]	6730.82 /6716.44	2400^{+240}_{-210}
N_e	[Ar IV]	4740.17 /4711.37	1780^{+290}_{-340}
N_e	[Cl III]	5537.60 /5517.66	1960^{+430}_{-340}
Th 2-A (PNG306.4-00.6)			
T_e	[N II]	6548.10+6583.50 /5754.60	10300^{+200}_{-210}
$T_{e\text{ rc}}$	[N II]	6548.10+6583.50 /5754.60	9060^{+180}_{-140}
T_e	[O III]	4958.91+5006.84 /4363.21	12420^{+50}_{-60}
$T_{e\text{ rc}}$	[O III]	4958.91+5006.84 /4363.21	11740^{+60}_{-60}
T_e	[S III]	9068.60 /6312.10	11860^{+350}_{-240}
N_e	[S II]	6730.82 /6716.44	1430^{+250}_{-190}

Pe 1-1 (PNG285.4+01.5)			
T_e	[N II]	6548.10+6583.50 /5754.60	10170^{+120}_{-130}
$T_{e\text{ rc}}$	[N II]	6548.10+6583.50 /5754.60	9190^{+120}_{-100}
T_e	[O III]	4958.91+5006.84 /4363.21	10240^{+10}_{-10}
T_e	[S III]	9068.60 /6312.10	10160^{+180}_{-200}
N_e	[S II]	6730.82 /6716.44	15580^{+1750}_{-1910}
N_e	[O II]	3728.82 /3726.03	14280^{+840}_{-860}
M 1-32 (PNG011.9+04.2)			
T_e	[N II]	6548.10+6583.50 /5754.60	8790^{+150}_{-150}
$T_{e\text{ rc}}$	[N II]	6548.10+6583.50 /5754.60	8480^{+140}_{-150}
T_e	[O III]	4958.91+5006.84 /4363.21	9250^{+50}_{-40}
N_e	[S II]	6730.82 /6716.44	4840^{+1780}_{-1080}
N_e	[O II]	3728.82 /3726.03	6200^{+1040}_{-990}
N_e	[Cl III]	5537.60 /5517.66	3930^{+600}_{-710}
M 3-15 (PNG006.8+04.1)			
T_e	[N II]	6548.10+6583.50 /5754.60	7700^{+310}_{-350}
T_e	[O III]	4958.91+5006.84 /4363.21	8590^{+10}_{-10}
N_e	[S II]	6730.82 /6716.44	6010^{+1200}_{-800}
N_e	[O II]	3728.82 /3726.03	12270^{+1490}_{-970}
N_e	[Ar IV]	4740.17 /4711.37	5540^{+6470}_{-3610}
M 1-25 (PNG004.9+04.9)			
T_e	[N II]	6548.10+6583.50 /5754.60	7880^{+70}_{-70}
$T_{e\text{ rc}}$	[N II]	6548.10+6583.50 /5754.60	6950^{+80}_{-90}
T_e	[O III]	4958.91+5006.84 /4363.21	8040^{+10}_{-10}
T_e	[Ar III]	7135.80+7751.43 /5191.82	7710^{+890}_{-1060}
N_e	[S II]	6730.82 /6716.44	6120^{+490}_{-370}
N_e	[Cl III]	5537.60 /5517.66	4090^{+2440}_{-2140}
Hen 2-142 (PNG327.1-02.2)			
T_e	[N II]	6548.10+6583.50 /5754.60	8810^{+420}_{-350}
N_e	[S II]	6730.82 /6716.44	20630^{+79370}_{-13450}
N_e	[Cl III]	5537.60 /5517.66	21160^{+14140}_{-8360}
Hen 3-1333 (PNG332.9-09.9)			
T_e	[N II]	6548.10+6583.50 /5754.60	7290^{+110}_{-120}
N_e	[S II]	6730.82 /6716.44	100000^{+0}_{-0}
Hen 2-113 (PNG321.0+03.9)			
T_e	[N II]	6548.10+6583.50 /5754.60	8220^{+140}_{-110}
N_e	[S II]	6730.82 /6716.44	100000^{+0}_{-410}
K 2-16 (PNG352.9+11.4)			
T_e	[N II]	6548.10+6583.50 /5754.60	9420^{+610}_{-580}
N_e	[O II]	3728.82 /3726.03	110^{+60}_{-40}
NGC 6578 (PNG010.8-01.8)			
T_e	[N II]	6548.10+6583.50 /5754.60	8080^{+530}_{-630}
T_e	[O III]	4958.91+5006.84 /4363.21	8230^{+20}_{-20}
$T_{e\text{ rc}}$	[O III]	4958.91+5006.84 /4363.21	8220^{+20}_{-20}
T_e	[S III]	9068.60 /6312.10	8280^{+90}_{-90}
N_e	[S II]	6730.82 /6716.44	4200^{+640}_{-430}
N_e	[Ar IV]	4740.17 /4711.37	3250^{+1050}_{-1130}
N_e	[Cl III]	5537.60 /5517.66	3390^{+2010}_{-1400}

M 2-42 (PNG008.2–04.8)			
T_e	[N II]	6548.10+6583.50 /5754.60	10010^{+170}_{-130}
T_e	[S II]	6716.44+6730.82 /4068.60+4076.35	17930^{+1630}_{-1610}
T_e	[O III]	4958.91+5006.84 /4363.21	8800^{+50}_{-40}
T_e	[Ar III]	7135.80+7751.43 /5191.82	8340^{+480}_{-600}
N_e	[S II]	6730.82 /6716.44	3050^{+470}_{-460}
N_e	[Ar IV]	4740.17 /4711.37	3430^{+590}_{-550}
N_e	[Cl III]	5537.60 /5517.66	2420^{+330}_{-240}
NGC 6567 (PNG011.7–00.6)			
T_e	[O I]	6300.34+6363.78 /5577.34	11000^{+6750}_{-3750}
T_e	[N II]	6548.10+6583.50 /5754.60	10860^{+210}_{-190}
T_e	[O III]	4958.91+5006.84 /4363.21	11480^{+40}_{-40}
$T_{e\text{ rc}}$	[O III]	4958.91+5006.84 /4363.21	11470^{+40}_{-40}
T_e	[Ar III]	7135.80+7751.43 /5191.82	11110^{+1200}_{-1260}
N_e	[S II]	6730.82 /6716.44	6340^{+910}_{-880}
N_e	[Ar IV]	4740.17 /4711.37	2440^{+2360}_{-1630}
N_e	[Cl III]	5537.60 /5517.66	5340^{+1250}_{-970}
NGC 6629 (PNG009.4–05.0)			
T_e	[N II]	6548.10+6583.50 /5754.60	8380^{+470}_{-480}
T_e	[O III]	4958.91+5006.84 /4363.21	8840^{+20}_{-20}
T_e	[S III]	9068.60 /6312.10	9960^{+160}_{-160}
N_e	[S II]	6730.82 /6716.44	2810^{+390}_{-340}
N_e	[Cl III]	5537.60 /5517.66	2100^{+850}_{-780}
Sa 3-107 (PNG358.0–04.6)			
T_e	[N II]	6548.10+6583.50 /5754.60	10840^{+500}_{-500}
N_e	[S II]	6730.82 /6716.44	2480^{+570}_{-420}
N_e	[Cl III]	5537.60 /5517.66	1400^{+1460}_{-1260}

Note: The label “rc” indicates that the auroral lines, [N II] λ 5755 and [O III] λ 4363, are corrected for recombination contribution.

Table 7. Plasma diagnostics based on H I lines.

Type	Ion	Diagnostic	Value
PB 6 (PNG278.8+04.9)			
T_e	He I	5875.66 /4471.50	4160^{+540}_{-620}
T_e	He I	6678.16 /4471.50	6990^{+1690}_{-1190}
T_e	He I	Mean	5580^{+1110}_{-1020}
M 3-30 (PNG017.9-04.8)			
T_e	He I	5875.66 /4471.50	2310^{+340}_{-330}
T_e	He I	6678.16 /4471.50	2970^{+410}_{-390}
T_e	He I	Mean	2640^{+300}_{-300}
Hb 4 (shell) (PNG003.1+02.9)			
T_e	He I	5875.66 /4471.50	2790^{+280}_{-230}
T_e	He I	Mean	2790^{+280}_{-230}
IC 1297 (PNG358.3-21.6)			
T_e	He I	5875.66 /4471.50	5250^{+600}_{-570}
T_e	He I	7281.35 /4471.50	4050^{+310}_{-300}
T_e	He I	7281.35 /5875.66	4440^{+140}_{-150}
T_e	He I	7281.35 /6678.16	12480^{+640}_{-700}
T_e	He I	Mean	6560^{+310}_{-330}
Pe 1-1 (PNG285.4+01.5)			
T_e	He I	5875.66 /4471.50	9060^{+2870}_{-2530}
T_e	He I	7281.35 /4471.50	9660^{+1660}_{-1270}
T_e	He I	7281.35 /5875.66	9460^{+180}_{-180}
T_e	He I	Mean	9390^{+1370}_{-1230}
M 1-32 (PNG011.9+04.2)			
T_e	He I	6678.16 /4471.50	1320^{+350}_{-280}
T_e	He I	Mean	1320^{+350}_{-280}
M 3-15 (PNG006.8+04.1)			
T_e	He I	5875.66 /4471.50	8600^{+3780}_{-3060}
T_e	He I	Mean	8600^{+3780}_{-3060}
M 1-25 (PNG004.9+04.9)			
T_e	He I	7281.35 /4471.50	10620^{+580}_{-570}
T_e	He I	7281.35 /5875.66	4490^{+60}_{-50}
T_e	He I	Mean	7560^{+410}_{-400}
NGC 6578 (PNG010.8-01.8)			
T_e	He I	5875.66 /4471.50	3170^{+400}_{-370}
T_e	He I	6678.16 /4471.50	3630^{+540}_{-460}
T_e	He I	7281.35 /4471.50	6410^{+450}_{-410}
T_e	He I	7281.35 /5875.66	5060^{+120}_{-100}
T_e	He I	7281.35 /6678.16	5260^{+180}_{-170}
T_e	He I	Mean	4710^{+200}_{-190}
M 2-42 (PNG008.2-04.8)			
T_e	He I	5875.66 /4471.50	11730^{+1720}_{-1230}
T_e	He I	Mean	11730^{+1720}_{-1230}
NGC 6567 (PNG011.7-00.6)			

T_e	He I	5875.66 /4471.50	2590^{+170}_{-150}
T_e	He I	Mean	2590^{+170}_{-150}
NGC 6629 (PNG009.4–05.0)			
T_e	He I	5875.66 /4471.50	4560^{+490}_{-450}
T_e	He I	6678.16 /4471.50	4150^{+460}_{-450}
T_e	He I	7281.35 /5875.66	10980^{+230}_{-210}
T_e	He I	7281.35 /6678.16	10480^{+260}_{-230}
T_e	He I	Mean	7540^{+250}_{-230}
Sa 3-107 (PNG358.0–04.6)			
T_e	He I	5875.66 /4471.50	2010^{+450}_{-390}
T_e	He I	6678.16 /4471.50	2300^{+610}_{-460}
T_e	He I	Mean	2160^{+500}_{-400}

Table 8. Plasma diagnostics based on heavy element ORLs.

Type	Ion	Diagnostic	Value
PB 6 (PNG278.8+04.9)			
T_e	N II	4613.87,4788.13,5676.02,5931.78	6300^{+9700}_{-3100}
N_e	N II	4613.87,4788.13,5676.02,5931.78	80600^{+0}_{-79900}
M 3-30 (PNG017.9-04.8)			
T_e	N II	4601.48,5927.81	6700^{+3100}_{-1300}
N_e	N II	4601.48,5927.81	80600^{+0}_{-53200}
Hb 4 (shell) (PNG003.1+02.9)			
T_e	O II	4610.20,4641.81,4661.63,4669.27	2100^{+22200}_{-1500}
N_e	O II	4610.20,4641.81,4661.63,4669.27	80600^{+0}_{-78900}
T_e	N II	4442.02,4459.93,4621.39,5676.02,5931.78	6300^{+10400}_{-3000}
N_e	N II	4442.02,4459.93,4621.39,5676.02,5931.78	80600^{+0}_{-79700}
IC 1297 (PNG358.3-21.6)			
T_e	C II	6151.43,6461.95	7500^{+5800}_{-2100}
T_e	O II	4610.20,4661.63,4676.23	700^{+24100}_{-300}
N_e	O II	4610.20,4661.63,4676.23	80600^{+0}_{-80000}
T_e	N II	4552.53,4607.16,4788.13,4803.29,5666.63,5679.56,5686.21,5931.78	6700^{+13200}_{-3300}
N_e	N II	4552.53,4607.16,4788.13,4803.29,5666.63,5679.56,5686.21,5931.78	100^{+1000}_0
Th 2-A (PNG306.4-00.6)			
T_e	N II	4432.73,4788.13,4803.29,5676.02,5679.56,5710.77,5931.78	6700^{+15200}_{-3300}
N_e	N II	4432.73,4788.13,4803.29,5676.02,5679.56,5710.77,5931.78	100^{+2400}_0
Pe 1-1 (PNG285.4+01.5)			
T_e	C II	6151.43,6461.95	8800^{+600}_{-500}
T_e	N II	4432.73,4788.13,5931.78,5941.65	6600^{+10600}_{-3000}
N_e	N II	4432.73,4788.13,5931.78,5941.65	80600^{+0}_{-79700}
M 1-32 (PNG011.9+04.2)			
T_e	C II	6151.43,6461.95	6300^{+100}_{-100}
T_e	N II	4552.53,4601.48,4788.13,5686.21,5710.77	700^{+1600}_{-200}
N_e	N II	4552.53,4601.48,4788.13,5686.21,5710.77	27400^{+53200}_{-26300}
M 3-15 (PNG006.8+04.1)			
T_e	N II	4643.09,4803.29,5710.77	6600^{+9700}_{-2600}
N_e	N II	4643.09,4803.29,5710.77	80600^{+0}_{-79500}
NGC 6578 (PNG010.8-01.8)			
T_e	C II	6151.43,6461.95	1300^{+0}_0
T_e	O II	4477.90,4491.23,4602.13,4661.63,4890.86	2100^{+17300}_{-900}
N_e	O II	4477.90,4491.23,4602.13,4661.63,4890.86	80600^{+0}_{-78000}
T_e	N II	4432.73,4788.13,5676.02,5686.21,5927.81,5941.65	6600^{+12800}_{-3200}
N_e	N II	4432.73,4788.13,5676.02,5686.21,5927.81,5941.65	80600^{+0}_{-80100}
M 2-42 (PNG008.2-04.8)			
T_e	C II	6151.43,6461.95	1600^{+100}_{-100}
T_e	O II	4477.90,4491.23,4602.13,4609.44,4661.63,4673.73	2100^{+22700}_{-900}
N_e	O II	4477.90,4491.23,4602.13,4609.44,4661.63,4673.73	80600^{+0}_{-78900}
T_e	N II	4607.16,4788.13,5710.77	800^{+1700}_{-300}
N_e	N II	4607.16,4788.13,5710.77	34000^{+46600}_{-33400}

NGC 6567 (PNG011.7–00.6)			
T_e	C II	6151.43,6461.95	1900_0^{+0}
Sa 3-107 (PNG358.0–04.6)			
T_e	C II	6151.43,6461.95	5500_{-100}^{+100}

Notes: The electron temperatures and densities are determined using least squares minimization on logarithmic T_e - N_e grids.

Table 11. Ionic abundances derived from CELs.

Ion	Line	Weight	Abund.
PB 6 (PNG278.8+04.9)			
N ⁺	[N II] λ 6548.10	1	$4.225^{+0.142}_{-0.164} \times 10^{-5}$
N ⁺	[N II] λ 6583.50	3	$4.426^{+0.185}_{-0.188} \times 10^{-5}$
O ⁰	[O I] λ 6300.34	3	$6.456^{+0.203}_{-0.240} \times 10^{-6}$
O ⁰	[O I] λ 6363.78	1	$6.947^{+0.255}_{-0.273} \times 10^{-6}$
O ⁺	[O II] λ 3726.03	1	$4.928^{+0.164}_{-0.142} \times 10^{-5}$
O ²⁺	[O III] λ 4958.91	1	$1.378^{+0.008}_{-0.010} \times 10^{-4}$
O ²⁺	[O III] λ 5006.84	3	$1.477^{+0.018}_{-0.021} \times 10^{-4}$
Ne ²⁺	[Ne III] λ 3868.75	3	$3.645^{+0.105}_{-0.090} \times 10^{-5}$
Ne ²⁺	[Ne III] λ 3967.46	1	$4.327^{+0.110}_{-0.092} \times 10^{-5}$
Ne ³⁺	[Ne IV] λ 4724.15	1	$2.825^{+0.134}_{-0.148} \times 10^{-4}$
S ⁺	[S II] λ 6716.44	1	$3.867^{+0.156}_{-0.162} \times 10^{-7}$
S ⁺	[S II] λ 6730.82	1	$3.869^{+0.139}_{-0.158} \times 10^{-7}$
S ²⁺	[S III] λ 6312.10	1	$2.229^{+0.072}_{-0.082} \times 10^{-6}$
Cl ²⁺	[Cl III] λ 5517.66	1	$2.935^{+0.105}_{-0.120} \times 10^{-8}$
Cl ²⁺	[Cl III] λ 5537.60	1	$2.935^{+0.077}_{-0.092} \times 10^{-8}$
Ar ²⁺	[Ar III] λ 7135.80	1	$5.410^{+0.232}_{-0.258} \times 10^{-7}$
Ar ³⁺	[Ar IV] λ 4711.37	1	$7.817^{+0.061}_{-0.058} \times 10^{-7}$
Ar ³⁺	[Ar IV] λ 4740.17	1	$7.205^{+0.051}_{-0.045} \times 10^{-7}$
Ar ⁴⁺	[Ar V] λ 4625.53	1	$4.082^{+1.177}_{-1.224} \times 10^{-7}$
Ar ⁴⁺	[Ar V] λ 7005.67	72	$3.711^{+0.165}_{-0.175} \times 10^{-7}$
Fe ²⁺	[Fe III] λ 4607.03	1	$5.833^{+0.457}_{-0.483} \times 10^{-7}$
Fe ²⁺	[Fe III] λ 4881.11	2	$5.353^{+1.437}_{-1.484} \times 10^{-8}$
Fe ²⁺	[Fe III] λ 5270.40	2	$6.421^{+1.082}_{-1.044} \times 10^{-8}$
M 3-30 (PNG017.9-04.8)			
N ⁺	[N II] λ 6548.10	1	$8.908^{+0.185}_{-0.158} \times 10^{-6}$
N ⁺	[N II] λ 6583.50	3	$9.724^{+0.164}_{-0.140} \times 10^{-6}$
O ⁺	[O II] λ 3726.03	1	$2.112^{+0.026}_{-0.025} \times 10^{-5}$
O ⁺	[O II] λ 3728.82	1	$1.798^{+0.021}_{-0.022} \times 10^{-5}$
O ²⁺	[O III] λ 4958.91	1	$2.593^{+0.016}_{-0.017} \times 10^{-4}$
O ²⁺	[O III] λ 5006.84	3	$2.618^{+0.025}_{-0.023} \times 10^{-4}$
Ne ²⁺	[Ne III] λ 3868.75	1	$9.368^{+0.099}_{-0.098} \times 10^{-5}$
S ⁺	[S II] λ 6716.44	1	$4.119^{+0.076}_{-0.064} \times 10^{-7}$
S ⁺	[S II] λ 6730.82	1	$4.121^{+0.074}_{-0.061} \times 10^{-7}$
S ²⁺	[S III] λ 6312.10	1	$5.059^{+0.136}_{-0.116} \times 10^{-6}$
Cl ²⁺	[Cl III] λ 5517.66	1	$6.349^{+0.337}_{-0.326} \times 10^{-8}$
Cl ²⁺	[Cl III] λ 5537.60	1	$5.659^{+0.400}_{-0.380} \times 10^{-8}$
Ar ²⁺	[Ar III] λ 7135.80	1	$1.522^{+0.028}_{-0.026} \times 10^{-6}$
Ar ³⁺	[Ar IV] λ 4711.37	1	$5.486^{+0.143}_{-0.145} \times 10^{-7}$
Ar ³⁺	[Ar IV] λ 4740.17	1	$5.490^{+0.159}_{-0.164} \times 10^{-7}$
Fe ²⁺	[Fe III] λ 4607.03	1	$2.179^{+0.380}_{-0.368} \times 10^{-6}$
Hb 4 (shell) (PNG003.1+02.9)			
N ⁺	[N II] λ 6548.10	1	$2.556^{+0.023}_{-0.026} \times 10^{-5}$
N ⁺	[N II] λ 6583.50	3	$2.694^{+0.026}_{-0.027} \times 10^{-5}$
O ⁰	[O I] λ 6300.34	3	$1.167^{+0.011}_{-0.010} \times 10^{-5}$
O ⁰	[O I] λ 6363.78	1	$1.234^{+0.017}_{-0.017} \times 10^{-5}$
O ⁺	[O II] λ 3726.03	2	$2.836^{+0.021}_{-0.020} \times 10^{-5}$

O ⁺	[O II] λ 3728.82	1	$3.636^{+0.025}_{-0.025} \times 10^{-5}$
O ²⁺	[O III] λ 4958.91	1	$5.601^{+0.021}_{-0.022} \times 10^{-4}$
O ²⁺	[O III] λ 5006.84	3	$5.603^{+0.020}_{-0.020} \times 10^{-4}$
Ne ²⁺	[Ne III] λ 3868.75	1	$8.258^{+0.047}_{-0.057} \times 10^{-5}$
S ⁺	[S II] λ 6716.44	1	$7.105^{+0.071}_{-0.075} \times 10^{-7}$
S ⁺	[S II] λ 6730.82	2	$7.105^{+0.068}_{-0.069} \times 10^{-7}$
S ²⁺	[S III] λ 6312.10	1	$9.201^{+0.074}_{-0.063} \times 10^{-6}$
Cl ²⁺	[Cl III] λ 5517.66	1	$9.660^{+0.384}_{-0.405} \times 10^{-8}$
Cl ²⁺	[Cl III] λ 5537.60	1	$9.658^{+0.279}_{-0.263} \times 10^{-8}$
Ar ²⁺	[Ar III] λ 7135.80	1	$2.464^{+0.025}_{-0.026} \times 10^{-6}$
Ar ³⁺	[Ar IV] λ 4711.37	1	$6.804^{+0.219}_{-0.222} \times 10^{-7}$
Ar ³⁺	[Ar IV] λ 4740.17	1	$7.636^{+0.090}_{-0.082} \times 10^{-7}$
Ar ⁴⁺	[Ar V] λ 7005.67	1	$1.121^{+0.114}_{-0.127} \times 10^{-8}$
Fe ²⁺	[Fe III] λ 4733.91	1	$6.723^{+2.086}_{-2.182} \times 10^{-7}$
Fe ²⁺	[Fe III] λ 5270.40	8	$1.548^{+0.320}_{-0.318} \times 10^{-7}$

Hb 4 (N-knot) (PNG003.1+02.9)

N ⁺	[N II] λ 6548.10	1	$4.667^{+0.205}_{-0.185} \times 10^{-5}$
N ⁺	[N II] λ 6583.50	3	$5.121^{+0.246}_{-0.183} \times 10^{-5}$
O ⁰	[O I] λ 6300.34	3	$1.427^{+0.157}_{-0.127} \times 10^{-5}$
O ⁰	[O I] λ 6363.78	1	$8.572^{+1.241}_{-1.152} \times 10^{-6}$
O ⁺	[O II] λ 3726.03	38	$1.641^{+0.049}_{-0.051} \times 10^{-4}$
O ⁺	[O II] λ 7319.99	1	$2.427^{+0.130}_{-0.108} \times 10^{-4}$
O ²⁺	[O III] λ 4958.91	1	$3.502^{+0.067}_{-0.062} \times 10^{-4}$
O ²⁺	[O III] λ 5006.84	3	$3.728^{+0.060}_{-0.049} \times 10^{-4}$
Ne ²⁺	[Ne III] λ 3868.75	1	$1.581^{+0.041}_{-0.047} \times 10^{-4}$
S ⁺	[S II] λ 6716.44	1	$1.139^{+0.077}_{-0.067} \times 10^{-6}$
S ⁺	[S II] λ 6730.82	1	$1.138^{+0.072}_{-0.055} \times 10^{-6}$
Ar ²⁺	[Ar III] λ 7135.80	1	$1.754^{+0.091}_{-0.075} \times 10^{-6}$

Hb 4 (S-knot) (PNG003.1+02.9)

N ⁺	[N II] λ 6548.10	1	$4.283^{+0.332}_{-0.230} \times 10^{-5}$
N ⁺	[N II] λ 6583.50	3	$4.988^{+0.362}_{-0.249} \times 10^{-5}$
O ⁰	[O I] λ 6300.34	3	$2.463^{+0.223}_{-0.183} \times 10^{-5}$
O ⁰	[O I] λ 6363.78	1	$2.771^{+0.854}_{-0.723} \times 10^{-5}$
O ⁺	[O II] λ 3726.03	43	$1.901^{+0.076}_{-0.103} \times 10^{-4}$
O ⁺	[O II] λ 7319.99	1	$2.402^{+0.199}_{-0.151} \times 10^{-4}$
O ²⁺	[O III] λ 4958.91	1	$2.633^{+0.041}_{-0.034} \times 10^{-4}$
O ²⁺	[O III] λ 5006.84	3	$2.899^{+0.044}_{-0.037} \times 10^{-4}$
Ne ²⁺	[Ne III] λ 3868.75	1	$9.928^{+0.368}_{-0.484} \times 10^{-5}$
S ⁺	[S II] λ 6716.44	1	$1.023^{+0.090}_{-0.059} \times 10^{-6}$
S ⁺	[S II] λ 6730.82	1	$1.022^{+0.082}_{-0.060} \times 10^{-6}$
Ar ²⁺	[Ar III] λ 7135.80	1	$1.761^{+0.142}_{-0.107} \times 10^{-6}$

IC 1297 (PNG358.3-21.6)

N ⁰	[N I] λ 5199.84	1	$2.613^{+0.689}_{-0.665} \times 10^{-7}$
N ⁺	[N II] λ 6548.10	1	$1.163^{+0.019}_{-0.023} \times 10^{-5}$
N ⁺	[N II] λ 6583.50	3	$1.228^{+0.023}_{-0.027} \times 10^{-5}$
O ⁰	[O I] λ 6300.34	3	$4.082^{+0.078}_{-0.099} \times 10^{-6}$
O ⁰	[O I] λ 6363.78	1	$4.143^{+0.136}_{-0.141} \times 10^{-6}$
O ⁺	[O II] λ 3726.03	1	$6.824^{+0.091}_{-0.079} \times 10^{-5}$
O ²⁺	[O III] λ 4958.91	1	$4.130^{+0.030}_{-0.026} \times 10^{-4}$
O ²⁺	[O III] λ 5006.84	3	$3.989^{+0.015}_{-0.014} \times 10^{-4}$
Ne ²⁺	[Ne III] λ 3868.75	3	$1.142^{+0.014}_{-0.012} \times 10^{-4}$

Physical and chemical properties of WR planetary nebulae

Ne ²⁺	[Ne III] λ 3967.46	1	$1.745^{+0.019}_{-0.018} \times 10^{-4}$
S ⁺	[S II] λ 6716.44	1	$4.506^{+0.072}_{-0.092} \times 10^{-7}$
S ⁺	[S II] λ 6730.82	1	$4.507^{+0.070}_{-0.098} \times 10^{-7}$
S ²⁺	[S III] λ 6312.10	1	$4.876^{+0.094}_{-0.114} \times 10^{-6}$
Cl ²⁺	[Cl III] λ 5517.66	1	$5.315^{+0.216}_{-0.191} \times 10^{-8}$
Cl ²⁺	[Cl III] λ 5537.60	1	$5.315^{+0.245}_{-0.236} \times 10^{-8}$
Ar ²⁺	[Ar III] λ 7135.80	4	$1.222^{+0.023}_{-0.027} \times 10^{-6}$
Ar ²⁺	[Ar III] λ 7751.43	1	$1.039^{+0.023}_{-0.026} \times 10^{-6}$
Ar ³⁺	[Ar IV] λ 4711.37	1	$3.844^{+0.132}_{-0.115} \times 10^{-7}$
Ar ³⁺	[Ar IV] λ 4740.17	1	$3.770^{+0.076}_{-0.076} \times 10^{-7}$
Fe ²⁺	[Fe III] λ 4769.40	1	$1.178^{+0.364}_{-0.338} \times 10^{-7}$
Fe ²⁺	[Fe III] λ 4881.11	1	$2.054^{+0.466}_{-0.419} \times 10^{-7}$
Fe ²⁺	[Fe III] λ 5270.40	1	$9.097^{+2.698}_{-2.374} \times 10^{-8}$

Th 2-A (PNG306.4–00.6)

N ⁺	[N II] λ 6548.10	1	$3.289^{+0.106}_{-0.099} \times 10^{-5}$
N ⁺	[N II] λ 6583.50	3	$3.648^{+0.089}_{-0.100} \times 10^{-5}$
O ⁰	[O I] λ 6300.34	3	$1.419^{+0.067}_{-0.073} \times 10^{-5}$
O ⁰	[O I] λ 6363.78	1	$1.442^{+0.082}_{-0.072} \times 10^{-5}$
O ⁺	[O II] λ 3728.82	1	$2.403^{+0.047}_{-0.045} \times 10^{-4}$
O ²⁺	[O III] λ 4958.91	1	$3.195^{+0.024}_{-0.029} \times 10^{-4}$
O ²⁺	[O III] λ 5006.84	3	$3.164^{+0.025}_{-0.025} \times 10^{-4}$
Ne ²⁺	[Ne III] λ 3868.75	3	$1.163^{+0.020}_{-0.020} \times 10^{-4}$
Ne ²⁺	[Ne III] λ 3967.46	1	$1.589^{+0.026}_{-0.026} \times 10^{-4}$
S ⁺	[S II] λ 6716.44	1	$4.929^{+0.160}_{-0.150} \times 10^{-7}$
S ⁺	[S II] λ 6730.82	1	$4.932^{+0.180}_{-0.188} \times 10^{-7}$
S ²⁺	[S III] λ 6312.10	1	$2.751^{+0.069}_{-0.074} \times 10^{-6}$
S ²⁺	[S III] λ 9068.60	11	$2.695^{+0.129}_{-0.115} \times 10^{-6}$
Cl ²⁺	[Cl III] λ 5517.66	1	$8.717^{+0.305}_{-0.338} \times 10^{-8}$
Ar ²⁺	[Ar III] λ 7135.80	4	$1.529^{+0.046}_{-0.054} \times 10^{-6}$
Ar ²⁺	[Ar III] λ 7751.43	1	$1.248^{+0.047}_{-0.044} \times 10^{-6}$
Ar ³⁺	[Ar IV] λ 4711.37	1	$3.340^{+0.128}_{-0.123} \times 10^{-7}$
Ar ³⁺	[Ar IV] λ 4740.17	1	$2.745^{+0.155}_{-0.171} \times 10^{-7}$
Fe ²⁺	[Fe III] λ 4881.11	1	$1.695^{+0.177}_{-0.159} \times 10^{-6}$
Fe ²⁺	[Fe III] λ 5270.40	1	$8.223^{+1.734}_{-1.764} \times 10^{-7}$

Pe 1-1 (PNG285.4+01.5)

N ⁺	[N II] λ 6548.10	1	$3.303^{+0.034}_{-0.028} \times 10^{-5}$
N ⁺	[N II] λ 6583.50	3	$3.581^{+0.037}_{-0.032} \times 10^{-5}$
O ⁰	[O I] λ 6300.34	3	$2.401^{+0.022}_{-0.017} \times 10^{-5}$
O ⁰	[O I] λ 6363.78	1	$2.251^{+0.042}_{-0.039} \times 10^{-5}$
O ⁺	[O II] λ 3726.03	3	$1.050^{+0.005}_{-0.007} \times 10^{-4}$
O ⁺	[O II] λ 3728.82	1	$1.061^{+0.005}_{-0.006} \times 10^{-4}$
O ²⁺	[O III] λ 4958.91	1	$3.235^{+0.009}_{-0.008} \times 10^{-4}$
O ²⁺	[O III] λ 5006.84	3	$3.272^{+0.013}_{-0.010} \times 10^{-4}$
Ne ²⁺	[Ne III] λ 3868.75	3	$8.599^{+0.036}_{-0.050} \times 10^{-5}$
Ne ²⁺	[Ne III] λ 3967.46	1	$8.005^{+0.033}_{-0.041} \times 10^{-5}$
S ⁺	[S II] λ 6716.44	1	$6.439^{+0.102}_{-0.094} \times 10^{-7}$
S ⁺	[S II] λ 6730.82	2	$6.439^{+0.075}_{-0.055} \times 10^{-7}$
S ²⁺	[S III] λ 6312.10	1	$3.542^{+0.133}_{-0.140} \times 10^{-6}$
S ²⁺	[S III] λ 9068.60	15	$3.604^{+0.057}_{-0.051} \times 10^{-6}$
Cl ²⁺	[Cl III] λ 5537.60	1	$2.259^{+0.568}_{-0.575} \times 10^{-8}$

Ar ²⁺	[Ar III] λ 7135.80	4	$1.647^{+0.017}_{-0.015} \times 10^{-6}$
Ar ²⁺	[Ar III] λ 7751.43	1	$1.574^{+0.021}_{-0.018} \times 10^{-6}$
Ar ³⁺	[Ar IV] λ 4711.37	1	$1.374^{+0.408}_{-0.393} \times 10^{-7}$
Ar ⁴⁺	[Ar V] λ 4625.53	1	$1.844^{+0.309}_{-0.314} \times 10^{-5}$
Fe ²⁺	[Fe III] λ 4733.91	1	$2.150^{+1.517}_{-1.491} \times 10^{-6}$
Fe ²⁺	[Fe III] λ 4769.40	6	$7.033^{+3.215}_{-3.023} \times 10^{-7}$
Fe ²⁺	[Fe III] λ 4881.11	5	$2.392^{+0.438}_{-0.435} \times 10^{-6}$
Fe ²⁺	[Fe III] λ 5270.40	7	$3.621^{+1.281}_{-1.351} \times 10^{-7}$

M 1-32 (PNG011.9+04.2)

N ⁰	[N I] λ 5199.84	1	$5.846^{+0.140}_{-0.120} \times 10^{-6}$
N ⁰	[N I] λ 5200.26	1	$5.313^{+0.181}_{-0.196} \times 10^{-6}$
N ⁺	[N II] λ 6548.10	1	$1.696^{+0.080}_{-0.071} \times 10^{-4}$
N ⁺	[N II] λ 6583.50	3	$1.848^{+0.076}_{-0.063} \times 10^{-4}$
O ⁰	[O I] λ 6300.34	3	$3.284^{+0.104}_{-0.093} \times 10^{-5}$
O ⁰	[O I] λ 6363.78	1	$3.286^{+0.131}_{-0.103} \times 10^{-5}$
O ⁺	[O II] λ 3726.03	2	$1.598^{+0.030}_{-0.036} \times 10^{-4}$
O ⁺	[O II] λ 3728.82	1	$1.511^{+0.030}_{-0.039} \times 10^{-4}$
O ²⁺	[O III] λ 4958.91	1	$2.199^{+0.036}_{-0.032} \times 10^{-4}$
O ²⁺	[O III] λ 5006.84	3	$2.184^{+0.032}_{-0.028} \times 10^{-4}$
Ne ²⁺	[Ne III] λ 3868.75	1	$1.799^{+0.032}_{-0.045} \times 10^{-5}$
S ⁺	[S II] λ 6716.44	1	$2.058^{+0.109}_{-0.092} \times 10^{-6}$
S ⁺	[S II] λ 6730.82	2	$2.059^{+0.101}_{-0.085} \times 10^{-6}$
S ²⁺	[S III] λ 6312.10	1	$1.006^{+0.042}_{-0.038} \times 10^{-5}$
Cl ²⁺	[Cl III] λ 5517.66	1	$1.151^{+0.069}_{-0.065} \times 10^{-7}$
Cl ²⁺	[Cl III] λ 5537.60	2	$1.058^{+0.053}_{-0.051} \times 10^{-7}$
Ar ²⁺	[Ar III] λ 7135.80	1	$3.343^{+0.136}_{-0.116} \times 10^{-6}$
Ar ³⁺	[Ar IV] λ 4711.37	1	$1.209^{+0.132}_{-0.128} \times 10^{-7}$
Fe ²⁺	[Fe III] λ 4701.62	1	$7.711^{+1.072}_{-1.075} \times 10^{-6}$
Fe ²⁺	[Fe III] λ 4881.11	3	$8.316^{+0.311}_{-0.316} \times 10^{-6}$
Fe ²⁺	[Fe III] λ 5270.40	5	$7.931^{+0.144}_{-0.135} \times 10^{-6}$

M 3-15 (PNG006.8+04.1)

N ⁺	[N II] λ 6548.10	1	$2.316^{+0.042}_{-0.039} \times 10^{-5}$
N ⁺	[N II] λ 6583.50	3	$2.412^{+0.036}_{-0.033} \times 10^{-5}$
O ⁰	[O I] λ 6300.34	3	$1.289^{+0.037}_{-0.034} \times 10^{-5}$
O ⁰	[O I] λ 6363.78	1	$1.091^{+0.085}_{-0.091} \times 10^{-5}$
O ⁺	[O II] λ 3726.03	2	$7.390^{+0.063}_{-0.069} \times 10^{-5}$
O ⁺	[O II] λ 3728.82	1	$6.566^{+0.062}_{-0.065} \times 10^{-5}$
O ²⁺	[O III] λ 4958.91	1	$5.865^{+0.028}_{-0.029} \times 10^{-4}$
O ²⁺	[O III] λ 5006.84	3	$6.010^{+0.021}_{-0.022} \times 10^{-4}$
Ne ²⁺	[Ne III] λ 3868.75	1	$7.640^{+0.069}_{-0.066} \times 10^{-5}$
S ⁺	[S II] λ 6716.44	1	$6.586^{+0.138}_{-0.120} \times 10^{-7}$
S ⁺	[S II] λ 6730.82	2	$6.586^{+0.142}_{-0.140} \times 10^{-7}$
S ²⁺	[S III] λ 6312.10	1	$5.790^{+0.324}_{-0.313} \times 10^{-6}$
Ar ³⁺	[Ar IV] λ 4711.37	1	$3.426^{+0.889}_{-0.839} \times 10^{-7}$
Ar ³⁺	[Ar IV] λ 4740.17	1	$3.312^{+0.586}_{-0.599} \times 10^{-7}$
Fe ²⁺	[Fe III] λ 4769.40	1	$4.609^{+5.817}_{-4.609} \times 10^{-7}$

M 1-25 (PNG004.9+04.9)

Physical and chemical properties of WR planetary nebulae

N ⁰	[N I] λ 5199.84	1	$8.036^{+1.326}_{-1.302} \times 10^{-7}$
N ⁺	[N II] λ 6548.10	1	$9.031^{+0.042}_{-0.064} \times 10^{-5}$
N ⁺	[N II] λ 6583.50	3	$9.541^{+0.049}_{-0.071} \times 10^{-5}$
O ⁰	[O I] λ 6300.34	3	$1.011^{+0.031}_{-0.033} \times 10^{-5}$
O ⁰	[O I] λ 6363.78	1	$7.703^{+0.406}_{-0.430} \times 10^{-6}$
O ⁺	[O II] λ 3726.03	1	$2.616^{+0.010}_{-0.010} \times 10^{-4}$
O ²⁺	[O III] λ 4958.91	1	$3.736^{+0.010}_{-0.014} \times 10^{-4}$
O ²⁺	[O III] λ 5006.84	3	$3.783^{+0.009}_{-0.013} \times 10^{-4}$
Ne ²⁺	[Ne III] λ 3868.75	1	$2.137^{+0.008}_{-0.006} \times 10^{-5}$
S ⁺	[S II] λ 6716.44	1	$1.254^{+0.012}_{-0.014} \times 10^{-6}$
S ⁺	[S II] λ 6730.82	2	$1.254^{+0.009}_{-0.012} \times 10^{-6}$
S ²⁺	[S III] λ 6312.10	1	$1.190^{+0.031}_{-0.032} \times 10^{-5}$
Cl ²⁺	[Cl III] λ 5517.66	1	$6.686^{+1.082}_{-1.082} \times 10^{-8}$
Cl ²⁺	[Cl III] λ 5537.60	2	$5.647^{+1.003}_{-1.043} \times 10^{-8}$
Ar ²⁺	[Ar III] λ 5191.82	1	$3.067^{+1.298}_{-1.276} \times 10^{-6}$
Ar ²⁺	[Ar III] λ 7135.80	258	$3.554^{+0.019}_{-0.023} \times 10^{-6}$
Ar ³⁺	[Ar IV] λ 4711.37	1	$2.235^{+0.272}_{-0.278} \times 10^{-7}$
Fe ²⁺	[Fe III] λ 4881.11	1	$1.026^{+0.149}_{-0.153} \times 10^{-6}$
Fe ²⁺	[Fe III] λ 5270.40	2	$1.406^{+0.296}_{-0.300} \times 10^{-6}$
Hen 2-142 (PNG327.1-02.2)			
N ⁺	[N II] λ 6548.10	1	$9.959^{+0.900}_{-0.957} \times 10^{-5}$
N ⁺	[N II] λ 6583.50	3	$1.039^{+0.102}_{-0.103} \times 10^{-4}$
O ⁰	[O I] λ 6300.34	3	$1.116^{+0.096}_{-0.102} \times 10^{-5}$
O ⁰	[O I] λ 6363.78	1	$1.076^{+0.091}_{-0.096} \times 10^{-5}$
O ⁺	[O II] λ 3726.03	1	$4.398^{+0.394}_{-0.340} \times 10^{-4}$
O ²⁺	[O III] λ 4958.91	1	$2.386^{+0.048}_{-0.055} \times 10^{-6}$
O ²⁺	[O III] λ 5006.84	3	$3.011^{+0.048}_{-0.055} \times 10^{-6}$
S ⁺	[S II] λ 6716.44	1	$8.707^{+0.947}_{-0.940} \times 10^{-7}$
S ⁺	[S II] λ 6730.82	2	$8.687^{+0.894}_{-1.017} \times 10^{-7}$
S ²⁺	[S III] λ 6312.10	1	$2.693^{+0.281}_{-0.308} \times 10^{-6}$
Cl ²⁺	[Cl III] λ 5517.66	1	$9.211^{+1.261}_{-1.361} \times 10^{-8}$
Cl ²⁺	[Cl III] λ 5537.60	3	$9.212^{+0.918}_{-1.127} \times 10^{-8}$
Hen 3-1333 (PNG332.9-09.9)			
N ⁺	[N II] λ 6548.10	1	$3.444^{+0.090}_{-0.081} \times 10^{-4}$
O ⁰	[O I] λ 6300.34	3	$3.126^{+0.088}_{-0.076} \times 10^{-4}$
O ⁰	[O I] λ 6363.78	1	$3.478^{+0.178}_{-0.194} \times 10^{-4}$
O ⁺	[O II] λ 3726.03	5	$3.493^{+0.060}_{-0.069} \times 10^{-3}$
O ⁺	[O II] λ 7319.99	2	$2.566^{+0.088}_{-0.076} \times 10^{-3}$
O ⁺	[O II] λ 7330.73	1	$2.465^{+0.079}_{-0.074} \times 10^{-3}$
S ⁺	[S II] λ 6716.44	1	$2.698^{+0.789}_{-0.873} \times 10^{-5}$
S ⁺	[S II] λ 6730.82	2	$5.489^{+0.442}_{-0.443} \times 10^{-5}$
S ²⁺	[S III] λ 9068.60	1	$7.554^{+0.322}_{-0.320} \times 10^{-7}$
Hen 2-113 (PNG321.0+03.9)			
N ⁺	[N II] λ 6548.10	1	$1.094^{+0.033}_{-0.035} \times 10^{-4}$
N ⁺	[N II] λ 6583.50	3	$1.216^{+0.047}_{-0.051} \times 10^{-4}$
O ⁰	[O I] λ 6300.34	3	$2.034^{+0.077}_{-0.087} \times 10^{-5}$
O ⁰	[O I] λ 6363.78	1	$2.616^{+0.134}_{-0.133} \times 10^{-5}$
O ⁺	[O II] λ 3726.03	3	$2.907^{+0.081}_{-0.069} \times 10^{-4}$
O ⁺	[O II] λ 3728.82	1	$8.058^{+0.224}_{-0.191} \times 10^{-4}$

S ⁺	[S II] λ 6716.44	1	$3.826^{+0.551}_{-0.535} \times 10^{-6}$
S ⁺	[S II] λ 6730.82	2	$5.299^{+0.378}_{-0.409} \times 10^{-6}$
S ²⁺	[S III] λ 6312.10	1	$3.486^{+0.266}_{-0.266} \times 10^{-6}$
S ²⁺	[S III] λ 9068.60	20	$2.119^{+0.122}_{-0.123} \times 10^{-6}$

K 2-16 (PNG352.9+11.4)

N ⁺	[N II] λ 6548.10	1	$4.887^{+0.441}_{-0.414} \times 10^{-5}$
N ⁺	[N II] λ 6583.50	3	$7.580^{+0.353}_{-0.338} \times 10^{-5}$
O ⁺	[O II] λ 3726.03	1	$1.450^{+0.052}_{-0.053} \times 10^{-4}$
O ⁺	[O II] λ 3728.82	1	$1.452^{+0.050}_{-0.054} \times 10^{-4}$
O ²⁺	[O III] λ 4958.91	1	$5.289^{+0.213}_{-0.240} \times 10^{-5}$
O ²⁺	[O III] λ 5006.84	3	$5.770^{+0.134}_{-0.145} \times 10^{-5}$
S ⁺	[S II] λ 6716.44	1	$3.137^{+0.167}_{-0.147} \times 10^{-6}$
S ⁺	[S II] λ 6730.82	1	$2.723^{+0.289}_{-0.295} \times 10^{-6}$

NGC 6578 (PNG010.8-01.8)

N ⁺	[N II] λ 6548.10	1	$4.792^{+0.078}_{-0.082} \times 10^{-6}$
N ⁺	[N II] λ 6583.50	3	$5.238^{+0.069}_{-0.078} \times 10^{-6}$
O ⁰	[O I] λ 6300.34	3	$4.042^{+1.373}_{-1.531} \times 10^{-7}$
O ⁰	[O I] λ 6363.78	1	$4.870^{+1.235}_{-1.359} \times 10^{-7}$
O ⁺	[O II] λ 3726.03	1	$4.732^{+0.043}_{-0.045} \times 10^{-5}$
O ²⁺	[O III] λ 4958.91	1	$5.481^{+0.036}_{-0.041} \times 10^{-4}$
O ²⁺	[O III] λ 5006.84	3	$5.495^{+0.046}_{-0.051} \times 10^{-4}$
Ne ²⁺	[Ne III] λ 3868.75	3	$1.799^{+0.016}_{-0.015} \times 10^{-4}$
Ne ²⁺	[Ne III] λ 3967.46	1	$3.446^{+0.026}_{-0.022} \times 10^{-4}$
S ⁺	[S II] λ 4068.60	1	$8.714^{+0.053}_{-0.055} \times 10^{-7}$
S ⁺	[S II] λ 6716.44	3	$1.386^{+0.030}_{-0.030} \times 10^{-7}$
S ⁺	[S II] λ 6730.82	5	$1.386^{+0.032}_{-0.031} \times 10^{-7}$
S ²⁺	[S III] λ 6312.10	1	$5.114^{+0.113}_{-0.127} \times 10^{-6}$
S ²⁺	[S III] λ 9068.60	27	$5.005^{+0.101}_{-0.109} \times 10^{-6}$
Cl ²⁺	[Cl III] λ 5517.66	1	$6.968^{+1.051}_{-1.006} \times 10^{-8}$
Cl ²⁺	[Cl III] λ 5537.60	1	$6.397^{+0.721}_{-0.800} \times 10^{-8}$
Ar ²⁺	[Ar III] λ 7135.80	4	$2.425^{+0.035}_{-0.036} \times 10^{-6}$
Ar ²⁺	[Ar III] λ 7751.43	1	$2.205^{+0.038}_{-0.036} \times 10^{-6}$
Ar ³⁺	[Ar IV] λ 4711.37	1	$5.368^{+0.518}_{-0.544} \times 10^{-7}$
Ar ³⁺	[Ar IV] λ 4740.17	1	$4.918^{+0.325}_{-0.345} \times 10^{-7}$
Fe ²⁺	[Fe III] λ 4701.62	2	$1.220^{+1.022}_{-0.927} \times 10^{-6}$
Fe ²⁺	[Fe III] λ 4733.91	1	$3.346^{+0.964}_{-0.984} \times 10^{-6}$
Fe ²⁺	[Fe III] λ 4881.11	5	$2.019^{+0.470}_{-0.464} \times 10^{-6}$

M 2-42 (PNG008.2-04.8)

N ⁰	[N I] λ 5199.84	1	$1.853^{+0.157}_{-0.172} \times 10^{-7}$
N ⁰	[N I] λ 5200.26	1	$1.862^{+0.215}_{-0.197} \times 10^{-7}$
N ⁺	[N II] λ 6548.10	1	$7.828^{+0.216}_{-0.241} \times 10^{-6}$
N ⁺	[N II] λ 6583.50	3	$8.087^{+0.247}_{-0.272} \times 10^{-6}$
O ⁰	[O I] λ 6300.34	3	$4.231^{+0.138}_{-0.131} \times 10^{-6}$
O ⁰	[O I] λ 6363.78	1	$4.472^{+0.190}_{-0.181} \times 10^{-6}$
O ⁺	[O II] λ 3726.03	1	$2.900^{+0.086}_{-0.084} \times 10^{-5}$
O ²⁺	[O III] λ 4958.91	1	$3.569^{+0.027}_{-0.025} \times 10^{-4}$
O ²⁺	[O III] λ 5006.84	3	$3.609^{+0.071}_{-0.072} \times 10^{-4}$
Ne ²⁺	[Ne III] λ 3868.75	3	$9.420^{+0.244}_{-0.228} \times 10^{-5}$
Ne ²⁺	[Ne III] λ 3967.46	1	$5.847^{+0.142}_{-0.122} \times 10^{-5}$

Physical and chemical properties of WR planetary nebulae

S ⁺	[S II] λ 4068.60	1	$4.655^{+0.108}_{-0.086} \times 10^{-7}$
S ⁺	[S II] λ 6716.44	3	$3.079^{+0.104}_{-0.110} \times 10^{-7}$
S ⁺	[S II] λ 6730.82	4	$3.082^{+0.098}_{-0.105} \times 10^{-7}$
S ²⁺	[S III] λ 6312.10	1	$5.345^{+0.149}_{-0.159} \times 10^{-6}$
Cl ²⁺	[Cl III] λ 5517.66	1	$8.970^{+0.260}_{-0.301} \times 10^{-8}$
Cl ²⁺	[Cl III] λ 5537.60	1	$7.888^{+0.162}_{-0.175} \times 10^{-8}$
Ar ²⁺	[Ar III] λ 5191.82	1	$1.019^{+0.188}_{-0.203} \times 10^{-6}$
Ar ²⁺	[Ar III] λ 7135.80	192	$1.213^{+0.043}_{-0.050} \times 10^{-6}$
Ar ³⁺	[Ar IV] λ 4711.37	1	$3.740^{+0.178}_{-0.173} \times 10^{-7}$
Ar ³⁺	[Ar IV] λ 4740.17	1	$3.739^{+0.097}_{-0.099} \times 10^{-7}$
Fe ²⁺	[Fe III] λ 4701.62	2	$2.511^{+1.526}_{-1.620} \times 10^{-7}$
Fe ²⁺	[Fe III] λ 4733.91	1	$5.220^{+2.328}_{-2.238} \times 10^{-7}$
Fe ²⁺	[Fe III] λ 4769.40	6	$5.807^{+0.491}_{-0.520} \times 10^{-7}$
Fe ²⁺	[Fe III] λ 4881.11	5	$2.892^{+0.334}_{-0.348} \times 10^{-7}$
Fe ²⁺	[Fe III] λ 5270.40	8	$2.555^{+0.194}_{-0.187} \times 10^{-7}$

NGC 6567 (PNG011.7–00.6)

N ⁰	[N I] λ 5199.84	1	$7.959^{+1.202}_{-1.140} \times 10^{-8}$
N ⁰	[N I] λ 5200.26	1	$8.004^{+2.103}_{-2.157} \times 10^{-8}$
N ⁺	[N II] λ 6548.10	1	$2.549^{+0.063}_{-0.075} \times 10^{-6}$
N ⁺	[N II] λ 6583.50	3	$2.606^{+0.050}_{-0.061} \times 10^{-6}$
O ⁰	[O I] λ 6300.34	3	$2.788^{+0.040}_{-0.053} \times 10^{-6}$
O ⁰	[O I] λ 6363.78	1	$3.184^{+0.076}_{-0.087} \times 10^{-6}$
O ⁺	[O II] λ 3726.03	13	$1.831^{+0.013}_{-0.012} \times 10^{-5}$
O ⁺	[O II] λ 7319.99	1	$5.059^{+0.051}_{-0.061} \times 10^{-5}$
O ²⁺	[O III] λ 4958.91	1	$2.074^{+0.011}_{-0.011} \times 10^{-4}$
O ²⁺	[O III] λ 5006.84	3	$2.109^{+0.021}_{-0.024} \times 10^{-4}$
Ne ²⁺	[Ne III] λ 3868.75	3	$4.199^{+0.025}_{-0.021} \times 10^{-5}$
Ne ²⁺	[Ne III] λ 3967.46	1	$5.289^{+0.034}_{-0.028} \times 10^{-5}$
S ⁺	[S II] λ 6716.44	1	$6.567^{+0.155}_{-0.180} \times 10^{-8}$
S ⁺	[S II] λ 6730.82	2	$6.566^{+0.140}_{-0.169} \times 10^{-8}$
S ²⁺	[S III] λ 6312.10	1	$1.110^{+0.017}_{-0.021} \times 10^{-6}$
Cl ²⁺	[Cl III] λ 5517.66	1	$1.798^{+0.127}_{-0.137} \times 10^{-8}$
Cl ²⁺	[Cl III] λ 5537.60	2	$1.798^{+0.065}_{-0.066} \times 10^{-8}$
Ar ²⁺	[Ar III] λ 5191.82	1	$3.407^{+0.929}_{-0.963} \times 10^{-7}$
Ar ²⁺	[Ar III] λ 7135.80	92	$3.757^{+0.034}_{-0.044} \times 10^{-7}$
Ar ²⁺	[Ar III] λ 7751.43	22	$3.431^{+0.040}_{-0.045} \times 10^{-7}$
Ar ³⁺	[Ar IV] λ 4711.37	1	$1.134^{+0.211}_{-0.218} \times 10^{-7}$
Ar ³⁺	[Ar IV] λ 4740.17	1	$8.899^{+0.513}_{-0.511} \times 10^{-8}$
Fe ²⁺	[Fe III] λ 5270.40	1	$9.675^{+3.316}_{-3.271} \times 10^{-8}$

NGC 6629 (PNG009.4–05.0)

N ⁰	[N I] λ 5200.26	1	$7.857^{+4.495}_{-4.416} \times 10^{-8}$
N ⁺	[N II] λ 6548.10	1	$2.718^{+0.041}_{-0.042} \times 10^{-6}$
N ⁺	[N II] λ 6583.50	3	$2.976^{+0.030}_{-0.033} \times 10^{-6}$
O ⁺	[O II] λ 3726.03	1	$7.284^{+0.054}_{-0.054} \times 10^{-5}$
O ²⁺	[O III] λ 4958.91	1	$3.586^{+0.028}_{-0.027} \times 10^{-4}$
O ²⁺	[O III] λ 5006.84	3	$3.576^{+0.026}_{-0.027} \times 10^{-4}$
Ne ²⁺	[Ne III] λ 3868.75	3	$8.131^{+0.049}_{-0.051} \times 10^{-5}$
Ne ²⁺	[Ne III] λ 3967.46	1	$1.858^{+0.012}_{-0.012} \times 10^{-4}$
S ⁺	[S II] λ 6716.44	1	$5.544^{+0.180}_{-0.193} \times 10^{-8}$
S ⁺	[S II] λ 6730.82	2	$5.545^{+0.096}_{-0.101} \times 10^{-8}$

S ²⁺	[S III] λ 6312.10	1	$2.532^{+0.092}_{-0.093} \times 10^{-6}$
S ²⁺	[S III] λ 9068.60	22	$1.876^{+0.032}_{-0.032} \times 10^{-6}$
Cl ²⁺	[Cl III] λ 5517.66	1	$5.393^{+0.304}_{-0.311} \times 10^{-8}$
Cl ²⁺	[Cl III] λ 5537.60	1	$4.879^{+0.592}_{-0.620} \times 10^{-8}$
Ar ²⁺	[Ar III] λ 7135.80	1	$1.492^{+0.017}_{-0.018} \times 10^{-6}$
Ar ³⁺	[Ar IV] λ 4711.37	1	$1.681^{+0.132}_{-0.134} \times 10^{-7}$
Ar ³⁺	[Ar IV] λ 4740.17	1	$1.257^{+0.161}_{-0.160} \times 10^{-7}$
Fe ²⁺	[Fe III] λ 4881.11	1	$6.890^{+1.025}_{-1.042} \times 10^{-7}$
Fe ²⁺	[Fe III] λ 5270.40	2	$3.032^{+0.450}_{-0.437} \times 10^{-7}$

Sa 3-107 (PNG358.0-04.6)

N ⁺	[N II] λ 6548.10	1	$1.771^{+0.038}_{-0.029} \times 10^{-6}$
N ⁺	[N II] λ 6583.50	3	$1.975^{+0.034}_{-0.031} \times 10^{-6}$
O ⁰	[O I] λ 6363.78	1	$6.971^{+0.783}_{-0.740} \times 10^{-7}$
O ²⁺	[O III] λ 4958.91	1	$8.185^{+0.052}_{-0.048} \times 10^{-5}$
O ²⁺	[O III] λ 5006.84	3	$8.240^{+0.070}_{-0.069} \times 10^{-5}$
S ⁺	[S II] λ 6716.44	1	$3.377^{+0.165}_{-0.144} \times 10^{-8}$
S ⁺	[S II] λ 6730.82	1	$3.379^{+0.143}_{-0.111} \times 10^{-8}$
S ²⁺	[S III] λ 6312.10	1	$5.273^{+0.636}_{-0.668} \times 10^{-7}$
Cl ²⁺	[Cl III] λ 5517.66	1	$1.694^{+0.239}_{-0.190} \times 10^{-8}$
Cl ²⁺	[Cl III] λ 5537.60	1	$1.429^{+0.341}_{-0.270} \times 10^{-8}$
Ar ²⁺	[Ar III] λ 5191.82	1	$4.713^{+1.388}_{-1.424} \times 10^{-7}$
Ar ³⁺	[Ar IV] λ 4711.37	1	$5.598^{+1.032}_{-0.982} \times 10^{-8}$
Ar ⁴⁺	[Ar V] λ 7005.67	1	$1.280^{+0.279}_{-0.227} \times 10^{-8}$
Fe ²⁺	[Fe III] λ 4769.40	1	$3.803^{+1.539}_{-1.584} \times 10^{-7}$
Fe ²⁺	[Fe III] λ 5270.40	1	$2.586^{+0.728}_{-0.663} \times 10^{-7}$

Table 12. Ionic abundances derived from ORLs.

Ion	Line	Weight	Abund.
PB 6 (PNG278.8+04.9)			
He ⁺	He I λ 4471.50	1	$4.508^{+0.065}_{-0.078} \times 10^{-2}$
He ⁺	He I λ 5875.66	3	$4.670^{+0.057}_{-0.064} \times 10^{-2}$
He ⁺	He I λ 6678.16	1	$4.338^{+0.096}_{-0.123} \times 10^{-2}$
He ²⁺	He II λ 4685.68	1	$1.028^{+0.003}_{-0.004} \times 10^{-1}$
C ²⁺	C II λ 6461.95	1	$3.546^{+0.221}_{-0.197} \times 10^{-4}$
N ²⁺	N II λ 4613.87	1	$7.217^{+1.653}_{-1.962} \times 10^{-4}$
N ²⁺	N II λ 4788.13	2	$5.221^{+0.242}_{-0.283} \times 10^{-3}$
N ²⁺	N II λ 5676.02	3	$4.043^{+0.094}_{-0.115} \times 10^{-3}$
N ²⁺	N II λ 5931.78	2	$2.171^{+0.094}_{-0.115} \times 10^{-3}$
N ³⁺	N III λ 4640.64	1	$3.310^{+0.192}_{-0.200} \times 10^{-4}$
O ²⁺	O II λ 4491.23	1	$6.238^{+1.245}_{-1.566} \times 10^{-4}$
M 3-30 (PNG017.9-04.8)			
He ⁺	He I λ 4471.50	1	$7.573^{+0.146}_{-0.143} \times 10^{-2}$
He ⁺	He I λ 5875.66	4	$8.722^{+0.056}_{-0.048} \times 10^{-2}$
He ⁺	He I λ 6678.16	1	$8.491^{+0.107}_{-0.080} \times 10^{-2}$
He ²⁺	He II λ 4685.68	1	$6.527^{+0.012}_{-0.014} \times 10^{-2}$
C ²⁺	C II λ 6461.95	1	$1.681^{+0.105}_{-0.110} \times 10^{-3}$
N ²⁺	N II λ 4601.48	1	$3.912^{+0.398}_{-0.347} \times 10^{-3}$
N ²⁺	N II λ 5927.81	1	$1.796^{+0.113}_{-0.114} \times 10^{-3}$
O ²⁺	O II λ 4650.84	2	$5.953^{+0.351}_{-0.399} \times 10^{-3}$
O ²⁺	O II λ 4661.63	2	$2.643^{+0.618}_{-0.531} \times 10^{-3}$
O ²⁺	O II λ 4676.23	1	$2.389^{+0.332}_{-0.398} \times 10^{-3}$
Hb 4 (shell) (PNG003.1+02.9)			
He ⁺	He I λ 4471.50	1	$9.920^{+0.098}_{-0.098} \times 10^{-2}$
He ⁺	He I λ 5875.66	4	$1.095^{+0.004}_{-0.005} \times 10^{-1}$
He ⁺	He I λ 6678.16	1	$8.495^{+0.063}_{-0.077} \times 10^{-2}$
He ²⁺	He II λ 4685.68	1	$1.098^{+0.003}_{-0.003} \times 10^{-2}$
C ²⁺	C II λ 6151.43	1	$5.094^{+0.345}_{-0.453} \times 10^{-4}$
C ²⁺	C II λ 6461.95	3	$3.766^{+0.246}_{-0.251} \times 10^{-4}$
C ³⁺	C III λ 4647.42	1	$3.809^{+0.650}_{-0.761} \times 10^{-4}$
N ²⁺	N II λ 4442.02	8	$6.710^{+1.321}_{-1.435} \times 10^{-3}$
N ²⁺	N II λ 4459.93	1	$4.305^{+0.407}_{-0.512} \times 10^{-2}$
N ²⁺	N II λ 4621.39	17	$2.889^{+1.160}_{-1.020} \times 10^{-4}$
N ²⁺	N II λ 5676.02	30	$4.760^{+0.580}_{-0.568} \times 10^{-4}$
N ²⁺	N II λ 5931.78	23	$1.821^{+0.231}_{-0.288} \times 10^{-4}$
O ²⁺	O II λ 4610.20	4	$5.386^{+0.896}_{-1.060} \times 10^{-3}$
O ²⁺	O II λ 4641.81	77	$7.736^{+0.813}_{-0.698} \times 10^{-3}$
O ²⁺	O II λ 4661.63	40	$8.894^{+1.572}_{-1.922} \times 10^{-4}$
O ²⁺	O II λ 4669.27	1	$1.667^{+0.283}_{-0.300} \times 10^{-2}$
Hb 4 (N-knot) (PNG003.1+02.9)			
He ⁺	He I λ 5875.66	4	$8.536^{+0.218}_{-0.144} \times 10^{-2}$
He ⁺	He I λ 6678.16	1	$7.227^{+1.121}_{-0.921} \times 10^{-2}$
Hb 4 (S-knot) (PNG003.1+02.9)			
He ⁺	He I λ 5875.66	1	$7.043^{+0.367}_{-0.259} \times 10^{-2}$

IC 1297 (PNG358.3–21.6)			
He ⁺	He I λ 4471.50	7	$8.697^{+0.132}_{-0.111} \times 10^{-2}$
He ⁺	He I λ 5875.66	20	$8.910^{+0.064}_{-0.060} \times 10^{-2}$
He ⁺	He I λ 6678.16	6	$5.811^{+0.100}_{-0.102} \times 10^{-2}$
He ⁺	He I λ 7281.35	1	$6.710^{+0.082}_{-0.106} \times 10^{-2}$
He ²⁺	He II λ 4685.68	1	$2.988^{+0.007}_{-0.007} \times 10^{-2}$
C ²⁺	C II λ 6151.43	1	$8.093^{+1.642}_{-1.163} \times 10^{-4}$
C ²⁺	C II λ 6461.95	3	$7.137^{+1.281}_{-1.138} \times 10^{-4}$
C ³⁺	C III λ 4647.42	1	$2.659^{+1.149}_{-1.176} \times 10^{-4}$
N ²⁺	N II λ 4552.53	1	$6.291^{+3.074}_{-2.457} \times 10^{-4}$
N ²⁺	N II λ 4607.16	2	$2.509^{+0.991}_{-0.932} \times 10^{-4}$
N ²⁺	N II λ 4788.13	2	$4.747^{+1.115}_{-1.028} \times 10^{-4}$
N ²⁺	N II λ 4803.29	3	$1.795^{+0.474}_{-0.331} \times 10^{-4}$
N ²⁺	N II λ 5666.63	6	$1.944^{+0.516}_{-0.422} \times 10^{-4}$
N ²⁺	N II λ 5679.56	11	$5.883^{+2.982}_{-2.817} \times 10^{-5}$
N ²⁺	N II λ 5686.21	2	$3.752^{+0.950}_{-0.958} \times 10^{-4}$
N ²⁺	N II λ 5931.78	2	$3.487^{+1.087}_{-1.004} \times 10^{-4}$
N ³⁺	N III λ 4640.64	1	$5.291^{+0.104}_{-0.092} \times 10^{-4}$
O ²⁺	O II λ 4610.20	1	$5.123^{+0.535}_{-0.413} \times 10^{-3}$
O ²⁺	O II λ 4661.63	12	$7.055^{+0.958}_{-0.924} \times 10^{-4}$
O ²⁺	O II λ 4676.23	7	$4.984^{+1.122}_{-1.142} \times 10^{-4}$
Th 2-A (PNG306.4–00.6)			
He ⁺	He I λ 4471.50	1	$5.516^{+0.108}_{-0.147} \times 10^{-2}$
He ⁺	He I λ 5875.66	4	$7.855^{+0.105}_{-0.119} \times 10^{-2}$
He ⁺	He I λ 6678.16	1	$4.776^{+0.144}_{-0.127} \times 10^{-2}$
He ²⁺	He II λ 4685.68	1	$4.227^{+0.025}_{-0.023} \times 10^{-2}$
C ²⁺	C II λ 6151.43	1	$1.012^{+0.083}_{-0.100} \times 10^{-2}$
C ²⁺	C II λ 6461.95	3	$2.221^{+0.262}_{-0.269} \times 10^{-3}$
N ²⁺	N II λ 4432.73	1	$9.957^{+0.967}_{-0.914} \times 10^{-3}$
N ²⁺	N II λ 4788.13	1	$1.777^{+0.399}_{-0.481} \times 10^{-3}$
N ²⁺	N II λ 4803.29	2	$2.140^{+0.430}_{-0.402} \times 10^{-3}$
N ²⁺	N II λ 5676.02	2	$1.629^{+0.429}_{-0.420} \times 10^{-3}$
N ²⁺	N II λ 5679.56	6	$7.939^{+0.642}_{-0.809} \times 10^{-4}$
N ²⁺	N II λ 5710.77	1	$4.463^{+0.589}_{-0.628} \times 10^{-3}$
N ²⁺	N II λ 5931.78	1	$1.829^{+0.360}_{-0.307} \times 10^{-3}$
N ³⁺	N III λ 4640.64	1	$1.031^{+0.130}_{-0.164} \times 10^{-4}$
O ²⁺	O II λ 4924.53	1	$7.781^{+0.937}_{-0.819} \times 10^{-3}$
Pe 1-1 (PNG285.4+01.5)			
He ⁺	He I λ 4471.50	5	$1.164^{+0.047}_{-0.050} \times 10^{-1}$
He ⁺	He I λ 5875.66	16	$1.062^{+0.006}_{-0.005} \times 10^{-1}$
He ⁺	He I λ 6678.16	5	$7.991^{+0.093}_{-0.093} \times 10^{-2}$
He ⁺	He I λ 7281.35	1	$8.956^{+0.050}_{-0.050} \times 10^{-2}$
C ²⁺	C II λ 6151.43	1	$1.718^{+0.039}_{-0.039} \times 10^{-3}$
C ²⁺	C II λ 6461.95	2	$1.755^{+0.134}_{-0.148} \times 10^{-3}$
C ³⁺	C III λ 4647.42	1	$3.731^{+0.919}_{-1.068} \times 10^{-4}$
N ²⁺	N II λ 4432.73	2	$3.326^{+1.104}_{-0.820} \times 10^{-3}$
N ²⁺	N II λ 4788.13	1	$3.571^{+0.844}_{-0.917} \times 10^{-3}$
N ²⁺	N II λ 5931.78	1	$9.284^{+1.080}_{-1.178} \times 10^{-4}$
N ²⁺	N II λ 5941.65	3	$5.922^{+0.955}_{-0.953} \times 10^{-4}$
O ²⁺	O II λ 4661.63	1	$2.053^{+0.304}_{-0.402} \times 10^{-3}$

M 1-32 (PNG011.9+04.2)			
He ⁺	He I λ 4471.50	1	$1.054^{+0.017}_{-0.015} \times 10^{-1}$
He ⁺	He I λ 5875.66	4	$1.353^{+0.022}_{-0.018} \times 10^{-1}$
He ⁺	He I λ 6678.16	1	$1.301^{+0.043}_{-0.035} \times 10^{-1}$
C ²⁺	C II λ 6151.43	1	$1.899^{+0.264}_{-0.228} \times 10^{-3}$
C ²⁺	C II λ 6461.95	3	$1.901^{+0.214}_{-0.188} \times 10^{-3}$
N ²⁺	N II λ 4552.53	1	$4.063^{+0.801}_{-0.763} \times 10^{-3}$
N ²⁺	N II λ 4601.48	2	$2.458^{+0.420}_{-0.390} \times 10^{-3}$
N ²⁺	N II λ 4788.13	1	$2.823^{+0.677}_{-0.597} \times 10^{-3}$
N ²⁺	N II λ 5686.21	1	$6.377^{+1.154}_{-0.863} \times 10^{-4}$
N ²⁺	N II λ 5710.77	2	$1.682^{+0.222}_{-0.199} \times 10^{-3}$
O ²⁺	O II λ 4890.86	1	$6.058^{+1.718}_{-1.625} \times 10^{-3}$
M 3-15 (PNG006.8+04.1)			
He ⁺	He I λ 4471.50	1	$1.201^{+0.149}_{-0.126} \times 10^{-1}$
He ⁺	He I λ 5875.66	4	$1.132^{+0.009}_{-0.009} \times 10^{-1}$
He ⁺	He I λ 6678.16	1	$9.124^{+0.132}_{-0.125} \times 10^{-2}$
C ²⁺	C II λ 6151.43	1	$1.352^{+0.273}_{-0.278} \times 10^{-3}$
C ³⁺	C III λ 4651.47	1	$4.384^{+1.263}_{-1.182} \times 10^{-3}$
N ²⁺	N II λ 4643.09	1	$3.645^{+1.212}_{-1.225} \times 10^{-3}$
N ²⁺	N II λ 4803.29	1	$1.599^{+0.230}_{-0.201} \times 10^{-3}$
N ²⁺	N II λ 5710.77	1	$2.234^{+0.451}_{-0.445} \times 10^{-3}$
M 1-25 (PNG004.9+04.9)			
He ⁺	He I λ 4471.50	7	$1.020^{+0.016}_{-0.015} \times 10^{-1}$
He ⁺	He I λ 5875.66	20	$1.345^{+0.003}_{-0.004} \times 10^{-1}$
He ⁺	He I λ 6678.16	6	$8.605^{+0.097}_{-0.098} \times 10^{-2}$
He ⁺	He I λ 7281.35	1	$9.862^{+0.031}_{-0.045} \times 10^{-2}$
C ²⁺	C II λ 6461.95	1	$8.055^{+0.994}_{-0.891} \times 10^{-4}$
C ³⁺	C III λ 4647.42	1	$4.452^{+1.123}_{-1.186} \times 10^{-4}$
N ²⁺	N II λ 4630.54	3	$2.023^{+0.297}_{-0.305} \times 10^{-3}$
N ²⁺	N II λ 5710.77	1	$2.987^{+0.374}_{-0.380} \times 10^{-3}$
O ²⁺	O II λ 4638.85	1	$4.167^{+0.605}_{-0.546} \times 10^{-3}$
Hen 2-142 (PNG327.1-02.2)			
He ⁺	He I λ 4471.50	1	$2.036^{+0.245}_{-0.249} \times 10^{-2}$
He ⁺	He I λ 6678.16	1	$2.378^{+0.188}_{-0.177} \times 10^{-2}$
NGC 6578 (PNG010.8-01.8)			
He ⁺	He I λ 4471.50	9	$1.129^{+0.020}_{-0.018} \times 10^{-1}$
He ⁺	He I λ 5875.66	25	$1.199^{+0.006}_{-0.006} \times 10^{-1}$
He ⁺	He I λ 6678.16	7	$1.181^{+0.016}_{-0.015} \times 10^{-1}$
He ⁺	He I λ 7281.35	1	$1.196^{+0.010}_{-0.010} \times 10^{-1}$
He ²⁺	He II λ 4685.68	1	$3.831^{+0.179}_{-0.174} \times 10^{-4}$
C ²⁺	C II λ 6151.43	1	$6.921^{+2.002}_{-1.897} \times 10^{-4}$
C ²⁺	C II λ 6461.95	3	$1.041^{+0.060}_{-0.053} \times 10^{-3}$
C ³⁺	C III λ 4647.42	1	$1.177^{+0.093}_{-0.095} \times 10^{-3}$
N ²⁺	N II λ 4432.73	2	$1.342^{+0.477}_{-0.474} \times 10^{-3}$
N ²⁺	N II λ 4788.13	1	$1.124^{+0.364}_{-0.338} \times 10^{-3}$
N ²⁺	N II λ 5676.02	2	$4.903^{+1.136}_{-1.215} \times 10^{-4}$
N ²⁺	N II λ 5686.21	1	$1.216^{+0.203}_{-0.176} \times 10^{-3}$
N ²⁺	N II λ 5927.81	1	$7.227^{+2.254}_{-1.943} \times 10^{-4}$

N ²⁺	N II λ 5941.65	4	$1.785^{+0.236}_{-0.225} \times 10^{-4}$
N ³⁺	N III λ 4640.64	1	$1.277^{+0.198}_{-0.198} \times 10^{-4}$
O ²⁺	O II λ 4477.90	1	$7.676^{+1.534}_{-1.804} \times 10^{-3}$
O ²⁺	O II λ 4491.23	2	$4.011^{+2.156}_{-1.664} \times 10^{-3}$
O ²⁺	O II λ 4602.13	2	$1.811^{+0.979}_{-0.825} \times 10^{-3}$
O ²⁺	O II λ 4661.63	12	$2.798^{+0.231}_{-0.222} \times 10^{-3}$
O ²⁺	O II λ 4890.86	1	$9.227^{+1.546}_{-1.380} \times 10^{-3}$

M 2-42 (PNG008.2-04.8)

He ⁺	He I λ 4471.50	4	$1.118^{+0.011}_{-0.011} \times 10^{-1}$
He ⁺	He I λ 4921.93	1	$1.222^{+0.085}_{-0.080} \times 10^{-2}$
He ⁺	He I λ 5875.66	11	$1.008^{+0.015}_{-0.013} \times 10^{-1}$
He ²⁺	He II λ 4685.68	1	$2.730^{+0.053}_{-0.059} \times 10^{-4}$
C ²⁺	C II λ 6151.43	1	$3.170^{+0.285}_{-0.322} \times 10^{-4}$
C ²⁺	C II λ 6461.95	2	$5.357^{+0.240}_{-0.201} \times 10^{-4}$
C ³⁺	C III λ 4651.47	1	$3.202^{+0.127}_{-0.125} \times 10^{-3}$
N ²⁺	N II λ 4607.16	1	$7.180^{+1.014}_{-1.080} \times 10^{-4}$
N ²⁺	N II λ 4788.13	1	$6.485^{+0.211}_{-0.257} \times 10^{-3}$
N ²⁺	N II λ 5710.77	1	$1.328^{+0.326}_{-0.289} \times 10^{-4}$
N ³⁺	N III λ 4640.64	1	$1.714^{+0.072}_{-0.068} \times 10^{-4}$
O ²⁺	O II λ 4477.90	1	$1.932^{+0.520}_{-0.648} \times 10^{-3}$
O ²⁺	O II λ 4491.23	2	$2.333^{+0.983}_{-1.349} \times 10^{-3}$
O ²⁺	O II λ 4602.13	1	$7.951^{+3.279}_{-3.598} \times 10^{-4}$
O ²⁺	O II λ 4609.44	2	$1.658^{+0.130}_{-0.126} \times 10^{-3}$
O ²⁺	O II λ 4661.63	10	$5.892^{+0.580}_{-0.613} \times 10^{-4}$
O ²⁺	O II λ 4673.73	2	$3.372^{+0.450}_{-0.567} \times 10^{-3}$

NGC 6567 (PNG011.7-00.6)

He ⁺	He I λ 4471.50	21	$9.277^{+0.082}_{-0.082} \times 10^{-2}$
He ⁺	He I λ 5047.74	1	$7.081^{+0.240}_{-0.346} \times 10^{-2}$
He ⁺	He I λ 5875.66	65	$9.926^{+0.031}_{-0.044} \times 10^{-2}$
He ⁺	He I λ 6678.16	18	$6.388^{+0.076}_{-0.073} \times 10^{-2}$
He ²⁺	He II λ 4685.68	1	$5.422^{+0.209}_{-0.194} \times 10^{-4}$
C ²⁺	C II λ 6151.43	1	$7.555^{+0.650}_{-0.714} \times 10^{-4}$
C ²⁺	C II λ 6461.95	2	$1.150^{+0.026}_{-0.034} \times 10^{-3}$
C ³⁺	C III λ 4651.47	1	$1.877^{+0.240}_{-0.202} \times 10^{-3}$
N ²⁺	N II λ 4788.13	1	$1.630^{+0.234}_{-0.215} \times 10^{-3}$
O ²⁺	O II λ 4890.86	1	$5.915^{+0.846}_{-0.875} \times 10^{-3}$

NGC 6629 (PNG009.4-05.0)

He ⁺	He I λ 4471.50	7	$9.505^{+0.130}_{-0.145} \times 10^{-2}$
He ⁺	He I λ 5875.66	20	$9.919^{+0.059}_{-0.058} \times 10^{-2}$
He ⁺	He I λ 6678.16	6	$1.016^{+0.009}_{-0.008} \times 10^{-1}$
He ⁺	He I λ 7281.35	1	$1.080^{+0.006}_{-0.009} \times 10^{-1}$
C ²⁺	C II λ 6151.43	1	$6.978^{+1.000}_{-1.245} \times 10^{-4}$
C ²⁺	C II λ 6461.95	3	$3.091^{+0.442}_{-0.453} \times 10^{-4}$
O ²⁺	O II λ 4638.85	12	$4.667^{+2.831}_{-2.649} \times 10^{-4}$
O ²⁺	O II λ 4650.84	13	$4.344^{+1.875}_{-2.728} \times 10^{-4}$
O ²⁺	O II λ 4661.63	13	$1.066^{+0.089}_{-0.109} \times 10^{-3}$
O ²⁺	O II λ 4696.35	1	$6.530^{+1.822}_{-1.622} \times 10^{-3}$

Sa 3-107 (PNG358.0-04.6)

Physical and chemical properties of WR planetary nebulae

He ⁺	He I λ 4471.50	1	$1.073^{+0.029}_{-0.030} \times 10^{-1}$
He ⁺	He I λ 5875.66	3	$1.227^{+0.009}_{-0.008} \times 10^{-1}$
He ⁺	He I λ 6678.16	1	$1.214^{+0.016}_{-0.017} \times 10^{-1}$
He ²⁺	He II λ 4685.68	1	$1.216^{+0.045}_{-0.046} \times 10^{-3}$
C ²⁺	C II λ 6151.43	1	$8.021^{+1.250}_{-1.232} \times 10^{-4}$
C ²⁺	C II λ 6461.95	3	$8.087^{+0.671}_{-0.654} \times 10^{-4}$
C ³⁺	C III λ 4647.42	1	$5.762^{+0.650}_{-0.714} \times 10^{-4}$
N ²⁺	N II λ 4803.29	2	$6.488^{+1.210}_{-1.135} \times 10^{-4}$
N ²⁺	N II λ 5710.77	1	$1.019^{+0.161}_{-0.174} \times 10^{-3}$
N ²⁺	N II λ 5941.65	2	$8.314^{+1.008}_{-1.060} \times 10^{-4}$
N ³⁺	N III λ 4640.64	1	$1.224^{+0.172}_{-0.178} \times 10^{-4}$

Table 13. Mean ionic and total elemental abundances relative to hydrogen derived from ORLs and CELs.

Ion	Type	Ref.	Abund.
PB 6 (PNG278.8+04.9)			
He ⁺ /H	ORL		$4.571^{+0.051}_{-0.057} \times 10^{-2}$
He ²⁺ /H	ORL		$1.028^{+0.003}_{-0.004} \times 10^{-1}$
He/H	ORL		$1.486^{+0.008}_{-0.008} \times 10^{-1}$
C ²⁺ /H	ORL		$3.546^{+0.221}_{-0.197} \times 10^{-4}$
<i>icf</i> (C)	ORL	WL07	$2.938^{+0.103}_{-0.081}$
C/H	ORL	WL07	$1.042^{+0.103}_{-0.071} \times 10^{-3}$
<i>icf</i> (C)	ORL	DMS14	$3.728^{+1.793}_{-1.978}$
C/H	ORL	DMS14	$1.322^{+0.735}_{-0.899} \times 10^{-3}$
N ²⁺ /H	ORL		$3.455^{+0.098}_{-0.113} \times 10^{-3}$
N ³⁺ /H	ORL		$3.310^{+0.192}_{-0.200} \times 10^{-4}$
<i>icf</i> (N)	ORL	WL07	$1.131^{+0.007}_{-0.007}$
N/H	ORL	WL07	$4.280^{+0.176}_{-0.166} \times 10^{-3}$
O ²⁺ /H	ORL		$6.238^{+1.245}_{-1.566} \times 10^{-4}$
<i>icf</i> (O)	ORL	WL07	$2.938^{+0.051}_{-0.038}$
O/H	ORL	WL07	$1.833^{+0.496}_{-0.503} \times 10^{-3}$
N ⁺ /H	CEL		$4.376^{+0.172}_{-0.162} \times 10^{-5}$
<i>icf</i> (N)	CEL	KB94	$8.661^{+0.408}_{-0.337}$
N/H	CEL	KB94	$3.790^{+0.332}_{-0.215} \times 10^{-4}$
<i>icf</i> (N)	CEL	DMS14	$7.525^{+5.819}_{-4.423}$
N/H	CEL	DMS14	$3.293^{+3.016}_{-2.089} \times 10^{-4}$
O ⁰ /H	CEL		$6.579^{+0.219}_{-0.229} \times 10^{-6}$
O ⁺ /H	CEL		$4.928^{+0.164}_{-0.142} \times 10^{-5}$
O ²⁺ /H	CEL		$1.453^{+0.017}_{-0.018} \times 10^{-4}$
<i>icf</i> (O)	CEL	KB94	$2.194^{+0.023}_{-0.020}$
O/H	CEL	KB94	$4.268^{+0.107}_{-0.085} \times 10^{-4}$
<i>icf</i> (O)	CEL	DMS14	$2.402^{+0.673}_{-0.673}$
O/H	CEL	DMS14	$4.672^{+1.562}_{-1.452} \times 10^{-4}$
Ne ²⁺ /H	CEL		$3.816^{+0.111}_{-0.083} \times 10^{-5}$
Ne ³⁺ /H	CEL		$2.825^{+0.134}_{-0.148} \times 10^{-4}$
<i>icf</i> (Ne)	CEL	KB94	$2.938^{+0.103}_{-0.067}$
Ne/H	CEL	KB94	$1.121^{+0.064}_{-0.041} \times 10^{-4}$
<i>icf</i> (Ne)	CEL	DMS14	$3.457^{+1.789}_{-1.765}$
Ne/H	CEL	DMS14	$1.319^{+0.822}_{-0.804} \times 10^{-4}$
S ⁺ /H	CEL		$3.868^{+0.136}_{-0.134} \times 10^{-7}$
S ²⁺ /H	CEL		$2.229^{+0.072}_{-0.082} \times 10^{-6}$
<i>icf</i> (S)	CEL	KB94	$1.481^{+0.022}_{-0.019}$
S/H	CEL	KB94	$3.873^{+0.182}_{-0.175} \times 10^{-6}$

Physical and chemical properties of WR planetary nebulae

<i>icf</i> (S)	CEL	DMS14	$2.626^{+1.365}_{-1.441}$
S/H	CEL	DMS14	$6.869^{+4.523}_{-4.240} \times 10^{-6}$
Cl^{2+}/H	CEL		$2.935^{+0.083}_{-0.091} \times 10^{-8}$
<i>icf</i> (Cl)	CEL	L00	$1.738^{+0.138}_{-0.104}$
Cl/H	CEL	L00	$5.101^{+0.479}_{-0.413} \times 10^{-8}$
<i>icf</i> (Cl)	CEL	DMS14	$3.931^{+2.162}_{-2.433}$
Cl/H	CEL	DMS14	$1.154^{+0.780}_{-0.840} \times 10^{-7}$
Ar^{2+}/H	CEL		$5.410^{+0.232}_{-0.258} \times 10^{-7}$
Ar^{3+}/H	CEL		$7.511^{+0.050}_{-0.042} \times 10^{-7}$
Ar^{4+}/H	CEL		$3.716^{+0.199}_{-0.201} \times 10^{-7}$
<i>icf</i> (Ar)	CEL	KB94	$1.131^{+0.013}_{-0.016}$
Ar/H	CEL	KB94	$1.881^{+0.060}_{-0.060} \times 10^{-6}$
<i>icf</i> (Ar)	CEL	DMS14	$2.870^{+2.944}_{-2.870}$
Ar/H	CEL	DMS14	$1.552^{+1.966}_{-1.552} \times 10^{-6}$
Fe^{2+}/H	CEL		$1.638^{+0.141}_{-0.138} \times 10^{-7}$
<i>icf</i> (Fe)	CEL	ITL94	$10.826^{+0.566}_{-0.497}$
Fe/H	CEL	ITL94	$1.773^{+0.212}_{-0.182} \times 10^{-6}$
<i>adf</i> (N^{2+})	ORL/CEL		$26.782^{+2.406}_{-2.402}$
<i>adf</i> (N)	ORL/CEL	KB94	$11.292^{+1.123}_{-1.345}$
<i>adf</i> (N)	ORL/CEL	DMS14	$12.997^{+48.697}_{-12.997}$
<i>adf</i> (O^{2+})	ORL/CEL		$4.295^{+1.097}_{-1.245}$
<i>adf</i> (O)	ORL/CEL	KB94	$4.295^{+1.452}_{-1.470}$
<i>adf</i> (O)	ORL/CEL	DMS14	$3.923^{+3.117}_{-2.141}$
M 3-30 (PNG017.9–04.8)			
He^+/H	ORL		$8.492^{+0.061}_{-0.043} \times 10^{-2}$
He^{2+}/H	ORL		$6.527^{+0.012}_{-0.014} \times 10^{-2}$
He/H	ORL		$1.502^{+0.007}_{-0.006} \times 10^{-1}$
C^{2+}/H	ORL		$1.681^{+0.105}_{-0.110} \times 10^{-3}$
<i>icf</i> (C)	ORL	WL07	$1.572^{+0.033}_{-0.034}$
C/H	ORL	WL07	$2.643^{+0.178}_{-0.213} \times 10^{-3}$
<i>icf</i> (C)	ORL	DMS14	$2.403^{+1.283}_{-1.176}$
C/H	ORL	DMS14	$4.040^{+2.327}_{-2.289} \times 10^{-3}$
N^{2+}/H	ORL		$2.854^{+0.241}_{-0.215} \times 10^{-3}$
<i>icf</i> (N)	ORL	WL07	$1.572^{+0.030}_{-0.034}$
N/H	ORL	WL07	$4.486^{+0.423}_{-0.434} \times 10^{-3}$
O^{2+}/H	ORL		$3.916^{+0.357}_{-0.324} \times 10^{-3}$
<i>icf</i> (O)	ORL	WL07	$1.572^{+0.009}_{-0.010}$
O/H	ORL	WL07	$6.156^{+0.661}_{-0.613} \times 10^{-3}$
N^+/H	CEL		$9.520^{+0.156}_{-0.123} \times 10^{-6}$
<i>icf</i> (N)	CEL	KB94	$21.002^{+0.497}_{-0.474}$
N/H	CEL	KB94	$1.999^{+0.058}_{-0.051} \times 10^{-4}$
<i>icf</i> (N)	CEL	DMS14	$16.727^{+13.502}_{-9.988}$
N/H	CEL	DMS14	$1.592^{+1.799}_{-1.163} \times 10^{-4}$
O^+/H	CEL		$1.955^{+0.018}_{-0.019} \times 10^{-5}$

O^{2+}/H	CEL		$2.612^{+0.023}_{-0.020} \times 10^{-4}$
$icf(O)$	CEL	KB94	$1.463^{+0.010}_{-0.011}$
O/H	CEL	KB94	$4.106^{+0.054}_{-0.051} \times 10^{-4}$
$icf(O)$	CEL	DMS14	$1.450^{+0.304}_{-0.304}$
O/H	CEL	DMS14	$4.069^{+1.065}_{-1.018} \times 10^{-4}$
Ne^{2+}/H	CEL		$9.368^{+0.099}_{-0.098} \times 10^{-5}$
$icf(Ne)$	CEL	KB94	$1.572^{+0.034}_{-0.033}$
Ne/H	CEL	KB94	$1.473^{+0.043}_{-0.034} \times 10^{-4}$
$icf(Ne)$	CEL	DMS14	$1.695^{+0.780}_{-0.795}$
Ne/H	CEL	DMS14	$1.588^{+0.953}_{-0.872} \times 10^{-4}$
S^+/H	CEL		$4.120^{+0.061}_{-0.049} \times 10^{-7}$
S^{2+}/H	CEL		$5.059^{+0.136}_{-0.116} \times 10^{-6}$
$icf(S)$	CEL	KB94	$1.944^{+0.013}_{-0.013}$
S/H	CEL	KB94	$1.064^{+0.033}_{-0.029} \times 10^{-5}$
$icf(S)$	CEL	DMS14	$2.461^{+1.137}_{-1.229}$
S/H	CEL	DMS14	$1.347^{+0.742}_{-0.783} \times 10^{-5}$
Cl^{2+}/H	CEL		$6.004^{+0.286}_{-0.271} \times 10^{-8}$
$icf(Cl)$	CEL	L00	$2.102^{+0.102}_{-0.112}$
Cl/H	CEL	L00	$1.262^{+0.089}_{-0.088} \times 10^{-7}$
$icf(Cl)$	CEL	DMS14	$15.381^{+7.568}_{-8.758}$
Cl/H	CEL	DMS14	$9.234^{+5.529}_{-6.151} \times 10^{-7}$
Ar^{2+}/H	CEL		$1.522^{+0.028}_{-0.026} \times 10^{-6}$
Ar^{3+}/H	CEL		$5.488^{+0.119}_{-0.125} \times 10^{-7}$
$icf(Ar)$	CEL	KB94	$1.050^{+0.002}_{-0.002}$
Ar/H	CEL	KB94	$2.174^{+0.042}_{-0.042} \times 10^{-6}$
$icf(Ar)$	CEL	DMS14	$2.198^{+2.011}_{-2.198}$
Ar/H	CEL	DMS14	$3.346^{+3.385}_{-3.346} \times 10^{-6}$
Fe^{2+}/H	CEL		$2.179^{+0.380}_{-0.368} \times 10^{-6}$
$icf(Fe)$	CEL	ITL94	$26.253^{+0.582}_{-0.566}$
Fe/H	CEL	ITL94	$5.720^{+1.205}_{-1.135} \times 10^{-5}$
$adf(N^{2+})$	ORL/CEL		$22.439^{+2.369}_{-2.274}$
$adf(N)$	ORL/CEL	KB94	$22.439^{+2.776}_{-2.842}$
$adf(N)$	ORL/CEL	DMS14	$28.173^{+13975.388}_{-28.173}$
$adf(O^{2+})$	ORL/CEL		$14.995^{+1.617}_{-1.576}$
$adf(O)$	ORL/CEL	KB94	$14.995^{+1.970}_{-1.891}$
$adf(O)$	ORL/CEL	DMS14	$15.129^{+8.191}_{-4.314}$
Hb 4 (shell) (PNG003.1+02.9)			
He^+/H	ORL		$1.037^{+0.005}_{-0.005} \times 10^{-1}$
He^{2+}/H	ORL		$1.098^{+0.003}_{-0.003} \times 10^{-2}$
He/H	ORL		$1.147^{+0.006}_{-0.006} \times 10^{-1}$
C^{2+}/H	ORL		$4.098^{+0.235}_{-0.284} \times 10^{-4}$
C^{3+}/H	ORL		$3.809^{+0.650}_{-0.761} \times 10^{-4}$
$icf(C)$	ORL	WL07	$1.055^{+0.000}_{-0.000}$
C/H	ORL	WL07	$8.345^{+1.246}_{-1.158} \times 10^{-4}$

Physical and chemical properties of WR planetary nebulae

<i>icf</i> (C)	ORL	DMS14	$1.771^{+0.511}_{-0.505}$
C/H	ORL	DMS14	$7.260^{+2.479}_{-2.762} \times 10^{-4}$
N ²⁺ /H	ORL		$1.520^{+0.166}_{-0.197} \times 10^{-3}$
<i>icf</i> (N)	ORL	WL07	$1.129^{+0.011}_{-0.011}$
N/H	ORL	WL07	$1.716^{+0.243}_{-0.276} \times 10^{-3}$
O ²⁺ /H	ORL		$5.487^{+0.613}_{-0.591} \times 10^{-3}$
<i>icf</i> (O)	ORL	WL07	$1.129^{+0.007}_{-0.007}$
O/H	ORL	WL07	$6.193^{+0.913}_{-0.818} \times 10^{-3}$
N ⁺ /H	CEL		$2.660^{+0.023}_{-0.026} \times 10^{-5}$
<i>icf</i> (N)	CEL	KB94	$20.379^{+0.208}_{-0.209}$
N/H	CEL	KB94	$5.421^{+0.089}_{-0.088} \times 10^{-4}$
<i>icf</i> (N)	CEL	DMS14	$20.299^{+11.227}_{-8.064}$
N/H	CEL	DMS14	$5.399^{+3.339}_{-2.353} \times 10^{-4}$
O ⁰ /H	CEL		$1.184^{+0.012}_{-0.010} \times 10^{-5}$
O ⁺ /H	CEL		$3.103^{+0.021}_{-0.019} \times 10^{-5}$
O ²⁺ /H	CEL		$5.602^{+0.019}_{-0.020} \times 10^{-4}$
<i>icf</i> (O)	CEL	KB94	$1.069^{+0.005}_{-0.005}$
O/H	CEL	KB94	$6.323^{+0.046}_{-0.043} \times 10^{-4}$
<i>icf</i> (O)	CEL	DMS14	$1.058^{+0.080}_{-0.080}$
O/H	CEL	DMS14	$6.257^{+0.499}_{-0.543} \times 10^{-4}$
Ne ²⁺ /H	CEL		$8.258^{+0.047}_{-0.057} \times 10^{-5}$
<i>icf</i> (Ne)	CEL	KB94	$1.129^{+0.010}_{-0.009}$
Ne/H	CEL	KB94	$9.320^{+0.132}_{-0.132} \times 10^{-5}$
<i>icf</i> (Ne)	CEL	DMS14	$1.214^{+0.242}_{-0.321}$
Ne/H	CEL	DMS14	$1.002^{+0.210}_{-0.292} \times 10^{-4}$
S ⁺ /H	CEL		$7.105^{+0.062}_{-0.066} \times 10^{-7}$
S ²⁺ /H	CEL		$9.201^{+0.074}_{-0.063} \times 10^{-6}$
<i>icf</i> (S)	CEL	KB94	$1.925^{+0.006}_{-0.007}$
S/H	CEL	KB94	$1.908^{+0.023}_{-0.017} \times 10^{-5}$
<i>icf</i> (S)	CEL	DMS14	$1.943^{+0.387}_{-0.571}$
S/H	CEL	DMS14	$1.926^{+0.470}_{-0.629} \times 10^{-5}$
Cl ²⁺ /H	CEL		$9.659^{+0.307}_{-0.295} \times 10^{-8}$
<i>icf</i> (Cl)	CEL	L00	$2.074^{+0.032}_{-0.028}$
Cl/H	CEL	L00	$2.003^{+0.086}_{-0.083} \times 10^{-7}$
<i>icf</i> (Cl)	CEL	DMS14	$28.943^{+6.637}_{-10.537}$
Cl/H	CEL	DMS14	$2.796^{+0.739}_{-1.180} \times 10^{-6}$
Ar ²⁺ /H	CEL		$2.464^{+0.025}_{-0.026} \times 10^{-6}$
Ar ³⁺ /H	CEL		$7.220^{+0.150}_{-0.138} \times 10^{-7}$
Ar ⁴⁺ /H	CEL		$1.121^{+0.114}_{-0.127} \times 10^{-8}$
<i>icf</i> (Ar)	CEL	KB94	$1.052^{+0.001}_{-0.001}$
Ar/H	CEL	KB94	$3.362^{+0.044}_{-0.042} \times 10^{-6}$
<i>icf</i> (Ar)	CEL	DMS14	$1.660^{+1.152}_{-1.323}$
Ar/H	CEL	DMS14	$4.090^{+3.550}_{-3.934} \times 10^{-6}$
Fe ²⁺ /H	CEL		$2.123^{+0.469}_{-0.461} \times 10^{-7}$

Danehkar

<i>icf</i> (Fe)	CEL	ITL94	$25.474^{+0.266}_{-0.272}$
Fe/H	CEL	ITL94	$5.408^{+1.517}_{-1.215} \times 10^{-6}$
<i>adf</i> (N ²⁺)	ORL/CEL		$3.165^{+0.480}_{-0.488}$
<i>adf</i> (N)	ORL/CEL	KB94	$3.165^{+0.604}_{-0.610}$
<i>adf</i> (N)	ORL/CEL	DMS14	$3.178^{+147.533}_{-3.178}$
<i>adf</i> (O ²⁺)	ORL/CEL		$9.795^{+1.488}_{-1.265}$
<i>adf</i> (O)	ORL/CEL	KB94	$9.795^{+1.912}_{-1.565}$
<i>adf</i> (O)	ORL/CEL	DMS14	$9.899^{+2.248}_{-1.717}$
Hb 4 (N-knot) (PNG003.1+02.9)			
He ⁺ /H	ORL		$8.274^{+0.391}_{-0.285} \times 10^{-2}$
He/H	ORL		$8.274^{+0.391}_{-0.285} \times 10^{-2}$
N ⁺ /H	CEL		$5.007^{+0.250}_{-0.210} \times 10^{-5}$
<i>icf</i> (N)	CEL	KB94	$3.210^{+0.372}_{-0.323}$
N/H	CEL	KB94	$1.607^{+0.261}_{-0.234} \times 10^{-4}$
<i>icf</i> (N)	CEL	DMS14	$8.855^{+3.808}_{-2.691}$
N/H	CEL	DMS14	$4.434^{+2.399}_{-2.012} \times 10^{-4}$
O ⁰ /H	CEL		$1.284^{+0.157}_{-0.120} \times 10^{-5}$
O ⁺ /H	CEL		$1.661^{+0.062}_{-0.059} \times 10^{-4}$
O ²⁺ /H	CEL		$3.672^{+0.064}_{-0.057} \times 10^{-4}$
<i>icf</i> (O)	CEL	KB94	$1.000^{+0.054}_{-0.047}$
O/H	CEL	KB94	$5.333^{+0.427}_{-0.353} \times 10^{-4}$
<i>icf</i> (O)	CEL	DMS14	$1.000^{+0.030}_{-0.030}$
O/H	CEL	DMS14	$5.333^{+0.267}_{-0.264} \times 10^{-4}$
Ne ²⁺ /H	CEL		$1.581^{+0.041}_{-0.047} \times 10^{-4}$
<i>icf</i> (Ne)	CEL	KB94	$1.452^{+0.151}_{-0.143}$
Ne/H	CEL	KB94	$2.296^{+0.321}_{-0.314} \times 10^{-4}$
<i>icf</i> (Ne)	CEL	DMS14	$2.827^{+0.542}_{-0.689}$
Ne/H	CEL	DMS14	$4.470^{+1.160}_{-1.393} \times 10^{-4}$
S ⁺ /H	CEL		$1.138^{+0.071}_{-0.055} \times 10^{-6}$
<i>icf</i> (S)	CEL	KB94	$8.662^{+0.361}_{-0.270}$
S/H	CEL	KB94	$9.861^{+1.048}_{-0.647} \times 10^{-6}$
<i>icf</i> (S)	CEL	DMS14	$1.032^{+0.212}_{-0.293}$
S/H	CEL	DMS14	$1.174^{+0.375}_{-0.420} \times 10^{-6}$
Ar ²⁺ /H	CEL		$1.754^{+0.091}_{-0.075} \times 10^{-6}$
<i>icf</i> (Ar)	CEL	KB94	$1.452^{+0.204}_{-0.109}$
Ar/H	CEL	KB94	$2.547^{+0.521}_{-0.316} \times 10^{-6}$
<i>icf</i> (Ar)	CEL	DMS14	$1.140^{+0.756}_{-0.869}$
Ar/H	CEL	DMS14	$1.998^{+1.737}_{-1.998} \times 10^{-6}$
Hb 4 (S-knot) (PNG003.1+02.9)			
He ⁺ /H	ORL		$7.043^{+0.367}_{-0.259} \times 10^{-2}$
He/H	ORL		$7.043^{+0.367}_{-0.259} \times 10^{-2}$
N ⁺ /H	CEL		$4.812^{+0.291}_{-0.206} \times 10^{-5}$
<i>icf</i> (N)	CEL	KB94	$2.481^{+0.280}_{-0.253}$
N/H	CEL	KB94	$1.194^{+0.176}_{-0.142} \times 10^{-4}$
<i>icf</i> (N)	CEL	DMS14	$5.979^{+2.385}_{-1.643}$
N/H	CEL	DMS14	$2.877^{+1.126}_{-0.974} \times 10^{-4}$
O ⁰ /H	CEL		$2.540^{+0.292}_{-0.247} \times 10^{-5}$
O ⁺ /H	CEL		$1.913^{+0.097}_{-0.127} \times 10^{-4}$

Physical and chemical properties of WR planetary nebulae

O^{2+}/H	CEL		$2.833^{+0.036}_{-0.032} \times 10^{-4}$
$icf(O)$	CEL	KB94	$1.000^{+0.052}_{-0.052}$
O/H	CEL	KB94	$4.746^{+0.268}_{-0.313} \times 10^{-4}$
$icf(O)$	CEL	DMS14	$1.000^{+0.030}_{-0.030}$
O/H	CEL	DMS14	$4.746^{+0.198}_{-0.241} \times 10^{-4}$
Ne^{2+}/H	CEL		$9.928^{+0.368}_{-0.484} \times 10^{-5}$
$icf(Ne)$	CEL	KB94	$1.675^{+0.110}_{-0.131}$
Ne/H	CEL	KB94	$1.663^{+0.131}_{-0.175} \times 10^{-4}$
$icf(Ne)$	CEL	DMS14	$3.456^{+0.579}_{-0.794}$
Ne/H	CEL	DMS14	$3.432^{+0.602}_{-0.928} \times 10^{-4}$
S^+/H	CEL		$1.022^{+0.069}_{-0.044} \times 10^{-6}$
$icf(S)$	CEL	KB94	$7.087^{+0.388}_{-0.257}$
S/H	CEL	KB94	$7.246^{+0.727}_{-0.405} \times 10^{-6}$
$icf(S)$	CEL	DMS14	$0.979^{+0.216}_{-0.278}$
S/H	CEL	DMS14	$1.001^{+0.249}_{-0.336} \times 10^{-6}$
Ar^{2+}/H	CEL		$1.761^{+0.142}_{-0.107} \times 10^{-6}$
$icf(Ar)$	CEL	KB94	$1.675^{+0.260}_{-0.164}$
Ar/H	CEL	KB94	$2.950^{+0.665}_{-0.370} \times 10^{-6}$
$icf(Ar)$	CEL	DMS14	$1.074^{+0.700}_{-0.821}$
Ar/H	CEL	DMS14	$1.891^{+1.349}_{-1.604} \times 10^{-6}$
IC 1297 (PNG358.3–21.6)			
He^+/H	ORL		$8.254^{+0.058}_{-0.057} \times 10^{-2}$
He^{2+}/H	ORL		$2.988^{+0.007}_{-0.007} \times 10^{-2}$
He/H	ORL		$1.124^{+0.008}_{-0.008} \times 10^{-1}$
C^{2+}/H	ORL		$7.376^{+1.232}_{-1.114} \times 10^{-4}$
C^{3+}/H	ORL		$2.659^{+1.149}_{-1.176} \times 10^{-4}$
$icf(C)$	ORL	WL07	$1.170^{+0.003}_{-0.003}$
C/H	ORL	WL07	$1.174^{+0.311}_{-0.290} \times 10^{-3}$
$icf(C)$	ORL	DMS14	$1.927^{+0.669}_{-0.770}$
C/H	ORL	DMS14	$1.421^{+0.800}_{-0.663} \times 10^{-3}$
N^{2+}/H	ORL		$2.028^{+0.365}_{-0.290} \times 10^{-4}$
N^{3+}/H	ORL		$5.291^{+0.104}_{-0.092} \times 10^{-4}$
$icf(N)$	ORL	WL07	$1.134^{+0.003}_{-0.003}$
N/H	ORL	WL07	$8.297^{+0.700}_{-0.509} \times 10^{-4}$
O^{2+}/H	ORL		$8.539^{+0.815}_{-0.782} \times 10^{-4}$
$icf(O)$	ORL	WL07	$1.437^{+0.013}_{-0.012}$
O/H	ORL	WL07	$1.227^{+0.151}_{-0.145} \times 10^{-3}$
N^0/H	CEL		$2.613^{+0.689}_{-0.665} \times 10^{-7}$
N^+/H	CEL		$1.212^{+0.020}_{-0.026} \times 10^{-5}$
$icf(N)$	CEL	KB94	$8.475^{+0.157}_{-0.183}$
N/H	CEL	KB94	$1.027^{+0.036}_{-0.044} \times 10^{-4}$
$icf(N)$	CEL	DMS14	$7.268^{+4.645}_{-3.578}$
N/H	CEL	DMS14	$8.807^{+6.324}_{-4.598} \times 10^{-5}$
O^0/H	CEL		$4.098^{+0.085}_{-0.110} \times 10^{-6}$

O ⁺ /H	CEL		$6.824_{-0.079}^{+0.091} \times 10^{-5}$
O ²⁺ /H	CEL		$4.024_{-0.016}^{+0.016} \times 10^{-4}$
<i>icf</i> (O)	CEL	KB94	$1.229_{-0.009}^{+0.009}$
O/H	CEL	KB94	$5.783_{-0.068}^{+0.063} \times 10^{-4}$
<i>icf</i> (O)	CEL	DMS14	$1.205_{-0.179}^{+0.179}$
O/H	CEL	DMS14	$5.670_{-1.011}^{+1.035} \times 10^{-4}$
Ne ²⁺ /H	CEL		$1.293_{-0.014}^{+0.015} \times 10^{-4}$
<i>icf</i> (Ne)	CEL	KB94	$1.437_{-0.019}^{+0.018}$
Ne/H	CEL	KB94	$1.858_{-0.045}^{+0.039} \times 10^{-4}$
<i>icf</i> (Ne)	CEL	DMS14	$1.532_{-0.582}^{+0.505}$
Ne/H	CEL	DMS14	$1.981_{-0.836}^{+0.773} \times 10^{-4}$
S ⁺ /H	CEL		$4.507_{-0.092}^{+0.057} \times 10^{-7}$
S ²⁺ /H	CEL		$4.876_{-0.114}^{+0.094} \times 10^{-6}$
<i>icf</i> (S)	CEL	KB94	$1.471_{-0.009}^{+0.008}$
S/H	CEL	KB94	$7.838_{-0.260}^{+0.207} \times 10^{-6}$
<i>icf</i> (S)	CEL	DMS14	$1.598_{-0.669}^{+0.530}$
S/H	CEL	DMS14	$8.511_{-3.516}^{+3.039} \times 10^{-6}$
Cl ²⁺ /H	CEL		$5.315_{-0.206}^{+0.201} \times 10^{-8}$
<i>icf</i> (Cl)	CEL	L00	$1.607_{-0.068}^{+0.062}$
Cl/H	CEL	L00	$8.544_{-0.698}^{+0.565} \times 10^{-8}$
<i>icf</i> (Cl)	CEL	DMS14	$8.375_{-4.092}^{+3.028}$
Cl/H	CEL	DMS14	$4.451_{-2.402}^{+1.787} \times 10^{-7}$
Ar ²⁺ /H	CEL		$1.185_{-0.030}^{+0.024} \times 10^{-6}$
Ar ³⁺ /H	CEL		$3.807_{-0.099}^{+0.098} \times 10^{-7}$
<i>icf</i> (Ar)	CEL	KB94	$1.134_{-0.007}^{+0.008}$
Ar/H	CEL	KB94	$1.776_{-0.062}^{+0.049} \times 10^{-6}$
<i>icf</i> (Ar)	CEL	DMS14	$1.620_{-1.482}^{+1.337}$
Ar/H	CEL	DMS14	$1.921_{-1.921}^{+1.843} \times 10^{-6}$
Fe ²⁺ /H	CEL		$1.380_{-0.201}^{+0.235} \times 10^{-7}$
<i>icf</i> (Fe)	CEL	ITL94	$10.593_{-0.224}^{+0.189}$
Fe/H	CEL	ITL94	$1.462_{-0.288}^{+0.294} \times 10^{-6}$
<i>adf</i> (N ²⁺)	ORL/CEL		$2.838_{-0.524}^{+0.691}$
<i>adf</i> (N)	ORL/CEL	KB94	$8.080_{-0.726}^{+0.971}$
<i>adf</i> (N)	ORL/CEL	DMS14	$9.421_{-9.421}^{+21.019}$
<i>adf</i> (O ²⁺)	ORL/CEL		$2.122_{-0.248}^{+0.256}$
<i>adf</i> (O)	ORL/CEL	KB94	$2.122_{-0.324}^{+0.350}$
<i>adf</i> (O)	ORL/CEL	DMS14	$2.164_{-0.510}^{+0.684}$

Th 2-A (PNG306.4–00.6)

He ⁺ /H	ORL		$6.952_{-0.107}^{+0.086} \times 10^{-2}$
He ²⁺ /H	ORL		$4.227_{-0.023}^{+0.025} \times 10^{-2}$
He/H	ORL		$1.118_{-0.013}^{+0.011} \times 10^{-1}$
C ²⁺ /H	ORL		$4.196_{-0.402}^{+0.347} \times 10^{-3}$
<i>icf</i> (C)	ORL	WL07	$2.412_{-0.087}^{+0.074}$
C/H	ORL	WL07	$1.012_{-0.128}^{+0.109} \times 10^{-2}$

Physical and chemical properties of WR planetary nebulae

<i>icf</i> (C)	ORL	DMS14	$2.121^{+0.740}_{-1.037}$
C/H	ORL	DMS14	$8.900^{+4.090}_{-5.676} \times 10^{-3}$
N ²⁺ /H	ORL		$2.166^{+0.175}_{-0.174} \times 10^{-3}$
N ³⁺ /H	ORL		$1.031^{+0.130}_{-0.164} \times 10^{-4}$
<i>icf</i> (N)	ORL	WL07	$1.458^{+0.034}_{-0.024}$
N/H	ORL	WL07	$3.308^{+0.458}_{-0.423} \times 10^{-3}$
O ²⁺ /H	ORL		$7.781^{+0.937}_{-0.819} \times 10^{-3}$
<i>icf</i> (O)	ORL	WL07	$2.412^{+0.053}_{-0.048}$
O/H	ORL	WL07	$1.877^{+0.305}_{-0.246} \times 10^{-2}$
N ⁺ /H	CEL		$3.558^{+0.094}_{-0.099} \times 10^{-5}$
<i>icf</i> (N)	CEL	KB94	$3.184^{+0.121}_{-0.146}$
N/H	CEL	KB94	$1.133^{+0.066}_{-0.070} \times 10^{-4}$
<i>icf</i> (N)	CEL	DMS14	$2.778^{+1.615}_{-1.362}$
N/H	CEL	DMS14	$9.883^{+6.926}_{-6.429} \times 10^{-5}$
O ⁰ /H	CEL		$1.425^{+0.066}_{-0.068} \times 10^{-5}$
O ⁺ /H	CEL		$2.403^{+0.047}_{-0.045} \times 10^{-4}$
O ²⁺ /H	CEL		$3.172^{+0.024}_{-0.026} \times 10^{-4}$
<i>icf</i> (O)	CEL	KB94	$1.373^{+0.022}_{-0.022}$
O/H	CEL	KB94	$7.652^{+0.161}_{-0.180} \times 10^{-4}$
<i>icf</i> (O)	CEL	DMS14	$1.351^{+0.257}_{-0.257}$
O/H	CEL	DMS14	$7.533^{+1.760}_{-1.772} \times 10^{-4}$
Ne ²⁺ /H	CEL		$1.269^{+0.019}_{-0.019} \times 10^{-4}$
<i>icf</i> (Ne)	CEL	KB94	$2.412^{+0.074}_{-0.085}$
Ne/H	CEL	KB94	$3.062^{+0.134}_{-0.135} \times 10^{-4}$
<i>icf</i> (Ne)	CEL	DMS14	$2.423^{+0.998}_{-1.136}$
Ne/H	CEL	DMS14	$3.075^{+1.838}_{-1.946} \times 10^{-4}$
S ⁺ /H	CEL		$4.930^{+0.143}_{-0.150} \times 10^{-7}$
S ²⁺ /H	CEL		$2.700^{+0.147}_{-0.144} \times 10^{-6}$
<i>icf</i> (S)	CEL	KB94	$1.139^{+0.010}_{-0.012}$
S/H	CEL	KB94	$3.636^{+0.256}_{-0.266} \times 10^{-6}$
<i>icf</i> (S)	CEL	DMS14	$1.312^{+0.547}_{-0.667}$
S/H	CEL	DMS14	$4.189^{+2.419}_{-3.033} \times 10^{-6}$
Cl ²⁺ /H	CEL		$8.717^{+0.305}_{-0.338} \times 10^{-8}$
<i>icf</i> (Cl)	CEL	L00	$1.347^{+0.176}_{-0.180}$
Cl/H	CEL	L00	$1.174^{+0.195}_{-0.192} \times 10^{-7}$
<i>icf</i> (Cl)	CEL	DMS14	$2.574^{+1.150}_{-1.489}$
Cl/H	CEL	DMS14	$2.244^{+1.493}_{-1.634} \times 10^{-7}$
Ar ²⁺ /H	CEL		$1.473^{+0.045}_{-0.053} \times 10^{-6}$
Ar ³⁺ /H	CEL		$3.042^{+0.123}_{-0.130} \times 10^{-7}$
<i>icf</i> (Ar)	CEL	KB94	$1.458^{+0.078}_{-0.056}$
Ar/H	CEL	KB94	$2.591^{+0.209}_{-0.160} \times 10^{-6}$
<i>icf</i> (Ar)	CEL	DMS14	$1.429^{+1.294}_{-1.429}$
Ar/H	CEL	DMS14	$2.106^{+2.419}_{-2.106} \times 10^{-6}$
Fe ²⁺ /H	CEL		$1.258^{+0.150}_{-0.148} \times 10^{-6}$

<i>icf</i> (Fe)	CEL	ITL94	$3.980^{+0.166}_{-0.191}$
Fe/H	CEL	ITL94	$5.009^{+0.772}_{-0.713} \times 10^{-6}$
<i>adf</i> (N ²⁺)	ORL/CEL		$46.116^{+7.125}_{-5.566}$
<i>adf</i> (N)	ORL/CEL	KB94	$29.196^{+7.162}_{-5.241}$
<i>adf</i> (N)	ORL/CEL	DMS14	$33.472^{+148.020}_{-33.472}$
<i>adf</i> (O ²⁺)	ORL/CEL		$24.528^{+4.277}_{-3.331}$
<i>adf</i> (O)	ORL/CEL	KB94	$24.528^{+5.868}_{-4.209}$
<i>adf</i> (O)	ORL/CEL	DMS14	$24.913^{+14.877}_{-6.856}$
Pe 1-1 (PNG285.4+01.5)			
He ⁺ /H	ORL		$1.026^{+0.013}_{-0.011} \times 10^{-1}$
He/H	ORL		$1.026^{+0.013}_{-0.011} \times 10^{-1}$
C ²⁺ /H	ORL		$1.743^{+0.119}_{-0.128} \times 10^{-3}$
C ³⁺ /H	ORL		$3.731^{+0.919}_{-1.068} \times 10^{-4}$
<i>icf</i> (C)	ORL	WL07	$1.323^{+0.003}_{-0.003}$
C/H	ORL	WL07	$2.799^{+0.505}_{-0.478} \times 10^{-3}$
<i>icf</i> (C)	ORL	DMS14	$1.554^{+0.212}_{-0.378}$
C/H	ORL	DMS14	$2.709^{+0.697}_{-0.915} \times 10^{-3}$
N ²⁺ /H	ORL		$1.847^{+0.451}_{-0.333} \times 10^{-3}$
<i>icf</i> (N)	ORL	WL07	$1.323^{+0.033}_{-0.031}$
N/H	ORL	WL07	$2.443^{+0.924}_{-0.686} \times 10^{-3}$
O ²⁺ /H	ORL		$2.053^{+0.304}_{-0.402} \times 10^{-3}$
<i>icf</i> (O)	ORL	WL07	$1.323^{+0.018}_{-0.018}$
O/H	ORL	WL07	$2.716^{+0.608}_{-0.761} \times 10^{-3}$
N ⁺ /H	CEL		$3.511^{+0.041}_{-0.033} \times 10^{-5}$
<i>icf</i> (N)	CEL	KB94	$4.099^{+0.100}_{-0.087}$
N/H	CEL	KB94	$1.439^{+0.057}_{-0.041} \times 10^{-4}$
<i>icf</i> (N)	CEL	DMS14	$12.488^{+5.336}_{-3.661}$
N/H	CEL	DMS14	$4.385^{+2.374}_{-1.573} \times 10^{-4}$
O ⁰ /H	CEL		$2.363^{+0.029}_{-0.023} \times 10^{-5}$
O ⁺ /H	CEL		$1.053^{+0.006}_{-0.007} \times 10^{-4}$
O ²⁺ /H	CEL		$3.263^{+0.013}_{-0.010} \times 10^{-4}$
<i>icf</i> (O)	CEL	KB94	$1.000^{+0.014}_{-0.014}$
O/H	CEL	KB94	$4.316^{+0.082}_{-0.073} \times 10^{-4}$
<i>icf</i> (O)	CEL	DMS14	$1.000^{+0.030}_{-0.030}$
O/H	CEL	DMS14	$4.316^{+0.171}_{-0.178} \times 10^{-4}$
Ne ²⁺ /H	CEL		$8.450^{+0.043}_{-0.050} \times 10^{-5}$
<i>icf</i> (Ne)	CEL	KB94	$1.323^{+0.030}_{-0.028}$
Ne/H	CEL	KB94	$1.118^{+0.039}_{-0.033} \times 10^{-4}$
<i>icf</i> (Ne)	CEL	DMS14	$2.430^{+0.412}_{-0.542}$
Ne/H	CEL	DMS14	$2.053^{+0.425}_{-0.480} \times 10^{-4}$
S ⁺ /H	CEL		$6.439^{+0.088}_{-0.065} \times 10^{-7}$
S ²⁺ /H	CEL		$3.600^{+0.072}_{-0.063} \times 10^{-6}$
<i>icf</i> (S)	CEL	KB94	$1.208^{+0.007}_{-0.006}$
S/H	CEL	KB94	$5.125^{+0.173}_{-0.127} \times 10^{-6}$
<i>icf</i> (S)	CEL	DMS14	$1.106^{+0.187}_{-0.278}$
S/H	CEL	DMS14	$4.695^{+1.127}_{-1.436} \times 10^{-6}$
Cl ²⁺ /H	CEL		$2.259^{+0.568}_{-0.575} \times 10^{-8}$
<i>icf</i> (Cl)	CEL	L00	$1.424^{+0.067}_{-0.054}$

Physical and chemical properties of WR planetary nebulae

Cl/H	CEL	L00	$3.215^{+1.290}_{-1.083} \times 10^{-8}$
<i>icf</i> (Cl)	CEL	DMS14	$4.099^{+0.202}_{-0.743}$
Cl/H	CEL	DMS14	$9.257^{+3.631}_{-4.148} \times 10^{-8}$
Ar ²⁺ /H	CEL		$1.632^{+0.022}_{-0.017} \times 10^{-6}$
Ar ³⁺ /H	CEL		$1.374^{+0.408}_{-0.393} \times 10^{-7}$
Ar ⁴⁺ /H	CEL		$1.844^{+0.309}_{-0.314} \times 10^{-5}$
<i>icf</i> (Ar)	CEL	KB94	$1.323^{+0.019}_{-0.021}$
Ar/H	CEL	KB94	$2.674^{+0.814}_{-0.739} \times 10^{-5}$
<i>icf</i> (Ar)	CEL	DMS14	$1.205^{+0.790}_{-0.913}$
Ar/H	CEL	DMS14	$1.967^{+1.823}_{-1.887} \times 10^{-6}$
Fe ²⁺ /H	CEL		$1.098^{+0.260}_{-0.232} \times 10^{-6}$
<i>icf</i> (Fe)	CEL	ITL94	$5.123^{+0.133}_{-0.115}$
Fe/H	CEL	ITL94	$5.626^{+2.037}_{-1.651} \times 10^{-6}$
<i>adf</i> (N ²⁺)	ORL/CEL		$16.976^{+5.356}_{-4.514}$
<i>adf</i> (N)	ORL/CEL	KB94	$16.976^{+8.224}_{-7.107}$
<i>adf</i> (N)	ORL/CEL	DMS14	$5.572^{+38.969}_{-5.572}$
<i>adf</i> (O ²⁺)	ORL/CEL		$6.292^{+1.321}_{-1.678}$
<i>adf</i> (O)	ORL/CEL	KB94	$6.292^{+1.947}_{-2.370}$
<i>adf</i> (O)	ORL/CEL	DMS14	$6.292^{+1.963}_{-2.357}$
M 1-32 (PNG011.9+04.2)			
He ⁺ /H	ORL		$1.294^{+0.022}_{-0.018} \times 10^{-1}$
He/H	ORL		$1.294^{+0.022}_{-0.018} \times 10^{-1}$
C ²⁺ /H	ORL		$1.901^{+0.241}_{-0.197} \times 10^{-3}$
<i>icf</i> (C)	ORL	WL07	$1.717^{+0.087}_{-0.081}$
C/H	ORL	WL07	$3.263^{+0.624}_{-0.507} \times 10^{-3}$
<i>icf</i> (C)	ORL	DMS14	$1.564^{+0.187}_{-0.375}$
C/H	ORL	DMS14	$2.972^{+0.784}_{-0.872} \times 10^{-3}$
N ²⁺ /H	ORL		$2.258^{+0.291}_{-0.251} \times 10^{-3}$
<i>icf</i> (N)	ORL	WL07	$1.717^{+0.084}_{-0.077}$
N/H	ORL	WL07	$3.877^{+0.763}_{-0.558} \times 10^{-3}$
O ²⁺ /H	ORL		$6.058^{+1.718}_{-1.625} \times 10^{-3}$
<i>icf</i> (O)	ORL	WL07	$1.717^{+0.034}_{-0.045}$
O/H	ORL	WL07	$1.040^{+0.401}_{-0.348} \times 10^{-2}$
N ⁰ /H	CEL		$5.579^{+0.160}_{-0.140} \times 10^{-6}$
N ⁺ /H	CEL		$1.810^{+0.082}_{-0.062} \times 10^{-4}$
<i>icf</i> (N)	CEL	KB94	$2.395^{+0.135}_{-0.119}$
N/H	CEL	KB94	$4.333^{+0.444}_{-0.297} \times 10^{-4}$
<i>icf</i> (N)	CEL	DMS14	$5.649^{+2.047}_{-1.336}$
N/H	CEL	DMS14	$1.022^{+0.472}_{-0.294} \times 10^{-3}$
O ⁰ /H	CEL		$3.285^{+0.119}_{-0.095} \times 10^{-5}$

O ⁺ /H	CEL		$1.569^{+0.032}_{-0.035} \times 10^{-4}$
O ²⁺ /H	CEL		$2.188^{+0.035}_{-0.025} \times 10^{-4}$
<i>icf</i> (O)	CEL	KB94	$1.000^{+0.021}_{-0.021}$
O/H	CEL	KB94	$3.757^{+0.126}_{-0.101} \times 10^{-4}$
<i>icf</i> (O)	CEL	DMS14	$1.000^{+0.030}_{-0.030}$
O/H	CEL	DMS14	$3.757^{+0.177}_{-0.113} \times 10^{-4}$
Ne ²⁺ /H	CEL		$1.799^{+0.032}_{-0.045} \times 10^{-5}$
<i>icf</i> (Ne)	CEL	KB94	$1.717^{+0.079}_{-0.079}$
Ne/H	CEL	KB94	$3.089^{+0.205}_{-0.189} \times 10^{-5}$
<i>icf</i> (Ne)	CEL	DMS14	$3.569^{+0.653}_{-0.785}$
Ne/H	CEL	DMS14	$6.420^{+1.310}_{-1.792} \times 10^{-5}$
S ⁺ /H	CEL		$2.059^{+0.107}_{-0.070} \times 10^{-6}$
S ²⁺ /H	CEL		$1.006^{+0.042}_{-0.038} \times 10^{-5}$
<i>icf</i> (S)	CEL	KB94	$1.076^{+0.011}_{-0.009}$
S/H	CEL	KB94	$1.304^{+0.088}_{-0.059} \times 10^{-5}$
<i>icf</i> (S)	CEL	DMS14	$0.975^{+0.186}_{-0.244}$
S/H	CEL	DMS14	$1.181^{+0.346}_{-0.367} \times 10^{-5}$
Cl ²⁺ /H	CEL		$1.089^{+0.058}_{-0.043} \times 10^{-7}$
<i>icf</i> (Cl)	CEL	L00	$1.296^{+0.144}_{-0.118}$
Cl/H	CEL	L00	$1.411^{+0.243}_{-0.169} \times 10^{-7}$
<i>icf</i> (Cl)	CEL	DMS14	$2.395^{+0.171}_{-0.432}$
Cl/H	CEL	DMS14	$2.607^{+0.370}_{-0.561} \times 10^{-7}$
Ar ²⁺ /H	CEL		$3.343^{+0.136}_{-0.116} \times 10^{-6}$
Ar ³⁺ /H	CEL		$1.209^{+0.132}_{-0.128} \times 10^{-7}$
<i>icf</i> (Ar)	CEL	KB94	$1.717^{+0.187}_{-0.155}$
Ar/H	CEL	KB94	$5.949^{+1.003}_{-0.677} \times 10^{-6}$
<i>icf</i> (Ar)	CEL	DMS14	$1.065^{+0.699}_{-0.792}$
Ar/H	CEL	DMS14	$3.562^{+3.089}_{-3.510} \times 10^{-6}$
Fe ²⁺ /H	CEL		$8.035^{+0.204}_{-0.202} \times 10^{-6}$
<i>icf</i> (Fe)	CEL	ITL94	$2.993^{+0.187}_{-0.148}$
Fe/H	CEL	ITL94	$2.405^{+0.231}_{-0.158} \times 10^{-5}$
<i>adf</i> (N ²⁺)	ORL/CEL		$8.947^{+1.703}_{-1.623}$
<i>adf</i> (N)	ORL/CEL	KB94	$8.947^{+2.574}_{-2.170}$
<i>adf</i> (N)	ORL/CEL	DMS14	$3.793^{+4.043}_{-2.744}$
<i>adf</i> (O ²⁺)	ORL/CEL		$27.687^{+10.381}_{-9.691}$
<i>adf</i> (O)	ORL/CEL	KB94	$27.687^{+14.263}_{-12.226}$
<i>adf</i> (O)	ORL/CEL	DMS14	$27.687^{+14.103}_{-12.631}$
M 3-15 (PNG006.8+04.1)			
He ⁺ /H	ORL		$1.107^{+0.031}_{-0.027} \times 10^{-1}$
He/H	ORL		$1.107^{+0.031}_{-0.027} \times 10^{-1}$
C ²⁺ /H	ORL		$1.352^{+0.273}_{-0.278} \times 10^{-3}$
C ³⁺ /H	ORL		$4.384^{+1.263}_{-1.182} \times 10^{-3}$
<i>icf</i> (C)	ORL	WL07	$1.119^{+0.001}_{-0.002}$
C/H	ORL	WL07	$6.418^{+2.131}_{-1.811} \times 10^{-3}$

Physical and chemical properties of WR planetary nebulae

<i>icf</i> (C)	ORL	DMS14	$1.627^{+0.336}_{-0.372}$
C/H	ORL	DMS14	$2.199^{+0.900}_{-0.758} \times 10^{-3}$
N ²⁺ /H	ORL		$2.493^{+0.543}_{-0.534} \times 10^{-3}$
<i>icf</i> (N)	ORL	WL07	$1.119^{+0.049}_{-0.042}$
N/H	ORL	WL07	$2.790^{+0.745}_{-0.693} \times 10^{-3}$
N ⁺ /H	CEL		$2.388^{+0.037}_{-0.032} \times 10^{-5}$
<i>icf</i> (N)	CEL	KB94	$9.396^{+0.412}_{-0.364}$
N/H	CEL	KB94	$2.244^{+0.134}_{-0.101} \times 10^{-4}$
<i>icf</i> (N)	CEL	DMS14	$35.060^{+17.194}_{-11.465}$
N/H	CEL	DMS14	$8.373^{+4.902}_{-3.180} \times 10^{-4}$
O ⁰ /H	CEL		$1.240^{+0.045}_{-0.040} \times 10^{-5}$
O ⁺ /H	CEL		$7.115^{+0.060}_{-0.064} \times 10^{-5}$
O ²⁺ /H	CEL		$5.974^{+0.020}_{-0.022} \times 10^{-4}$
<i>icf</i> (O)	CEL	KB94	$1.000^{+0.032}_{-0.030}$
O/H	CEL	KB94	$6.685^{+0.235}_{-0.216} \times 10^{-4}$
<i>icf</i> (O)	CEL	DMS14	$1.000^{+0.030}_{-0.030}$
O/H	CEL	DMS14	$6.685^{+0.237}_{-0.222} \times 10^{-4}$
Ne ²⁺ /H	CEL		$7.640^{+0.069}_{-0.066} \times 10^{-5}$
<i>icf</i> (Ne)	CEL	KB94	$1.119^{+0.048}_{-0.041}$
Ne/H	CEL	KB94	$8.550^{+0.470}_{-0.336} \times 10^{-5}$
<i>icf</i> (Ne)	CEL	DMS14	$1.737^{+0.282}_{-0.363}$
Ne/H	CEL	DMS14	$1.327^{+0.270}_{-0.321} \times 10^{-4}$
S ⁺ /H	CEL		$6.586^{+0.130}_{-0.122} \times 10^{-7}$
S ²⁺ /H	CEL		$5.790^{+0.324}_{-0.313} \times 10^{-6}$
<i>icf</i> (S)	CEL	KB94	$1.517^{+0.020}_{-0.018}$
S/H	CEL	KB94	$9.781^{+0.741}_{-0.699} \times 10^{-6}$
<i>icf</i> (S)	CEL	DMS14	$1.481^{+0.242}_{-0.357}$
S/H	CEL	DMS14	$9.550^{+2.279}_{-2.465} \times 10^{-6}$
Ar ³⁺ /H	CEL		$3.369^{+0.638}_{-0.652} \times 10^{-7}$
<i>icf</i> (Ar)	CEL	KB94	$1.119^{+0.008}_{-0.009}$
Ar/H	CEL	KB94	$3.770^{+0.769}_{-0.952} \times 10^{-7}$
Fe ²⁺ /H	CEL		$4.609^{+5.817}_{-4.609} \times 10^{-7}$
<i>icf</i> (Fe)	CEL	ITL94	$11.744^{+0.546}_{-0.458}$
Fe/H	CEL	ITL94	$5.414^{+8.205}_{-5.414} \times 10^{-6}$
<i>adf</i> (N ²⁺)	ORL/CEL		$12.433^{+3.357}_{-3.532}$
<i>adf</i> (N)	ORL/CEL	KB94	$12.433^{+4.141}_{-4.346}$
<i>adf</i> (N)	ORL/CEL	DMS14	$3.332^{+5.643}_{-3.332}$
M 1-25 (PNG004.9+04.9)			
He ⁺ /H	ORL		$1.182^{+0.005}_{-0.005} \times 10^{-1}$
He/H	ORL		$1.182^{+0.005}_{-0.005} \times 10^{-1}$
C ²⁺ /H	ORL		$8.055^{+0.994}_{-0.891} \times 10^{-4}$
C ³⁺ /H	ORL		$4.452^{+1.123}_{-1.186} \times 10^{-4}$
<i>icf</i> (C)	ORL	WL07	$1.694^{+0.004}_{-0.003}$
C/H	ORL	WL07	$2.118^{+0.436}_{-0.472} \times 10^{-3}$

<i>icf</i> (C)	ORL	DMS14	$1.561^{+0.155}_{-0.366}$
C/H	ORL	DMS14	$1.257^{+0.221}_{-0.384} \times 10^{-3}$
N ²⁺ /H	ORL		$2.264^{+0.309}_{-0.280} \times 10^{-3}$
<i>icf</i> (N)	ORL	WL07	$1.694^{+0.013}_{-0.013}$
N/H	ORL	WL07	$3.835^{+0.584}_{-0.626} \times 10^{-3}$
O ²⁺ /H	ORL		$4.167^{+0.605}_{-0.546} \times 10^{-3}$
<i>icf</i> (O)	ORL	WL07	$1.694^{+0.010}_{-0.008}$
O/H	ORL	WL07	$7.057^{+1.202}_{-1.155} \times 10^{-3}$
N ⁰ /H	CEL		$8.036^{+1.326}_{-1.302} \times 10^{-7}$
N ⁺ /H	CEL		$9.413^{+0.042}_{-0.063} \times 10^{-5}$
<i>icf</i> (N)	CEL	KB94	$2.441^{+0.020}_{-0.024}$
N/H	CEL	KB94	$2.298^{+0.027}_{-0.032} \times 10^{-4}$
<i>icf</i> (N)	CEL	DMS14	$5.828^{+1.962}_{-1.360}$
N/H	CEL	DMS14	$5.486^{+1.976}_{-1.972} \times 10^{-4}$
O ⁰ /H	CEL		$9.506^{+0.328}_{-0.322} \times 10^{-6}$
O ⁺ /H	CEL		$2.616^{+0.010}_{-0.010} \times 10^{-4}$
O ²⁺ /H	CEL		$3.771^{+0.008}_{-0.012} \times 10^{-4}$
<i>icf</i> (O)	CEL	KB94	$1.000^{+0.005}_{-0.005}$
O/H	CEL	KB94	$6.388^{+0.036}_{-0.042} \times 10^{-4}$
<i>icf</i> (O)	CEL	DMS14	$1.000^{+0.030}_{-0.030}$
O/H	CEL	DMS14	$6.388^{+0.235}_{-0.233} \times 10^{-4}$
Ne ²⁺ /H	CEL		$2.137^{+0.008}_{-0.006} \times 10^{-5}$
<i>icf</i> (Ne)	CEL	KB94	$1.694^{+0.013}_{-0.014}$
Ne/H	CEL	KB94	$3.619^{+0.034}_{-0.038} \times 10^{-5}$
<i>icf</i> (Ne)	CEL	DMS14	$3.506^{+0.571}_{-0.753}$
Ne/H	CEL	DMS14	$7.491^{+1.257}_{-1.960} \times 10^{-5}$
S ⁺ /H	CEL		$1.254^{+0.008}_{-0.010} \times 10^{-6}$
S ²⁺ /H	CEL		$1.190^{+0.031}_{-0.032} \times 10^{-5}$
<i>icf</i> (S)	CEL	KB94	$1.080^{+0.002}_{-0.002}$
S/H	CEL	KB94	$1.420^{+0.050}_{-0.054} \times 10^{-5}$
<i>icf</i> (S)	CEL	DMS14	$0.977^{+0.158}_{-0.239}$
S/H	CEL	DMS14	$1.285^{+0.257}_{-0.392} \times 10^{-5}$
Cl ²⁺ /H	CEL		$5.994^{+0.933}_{-0.866} \times 10^{-8}$
<i>icf</i> (Cl)	CEL	L00	$1.194^{+0.066}_{-0.067}$
Cl/H	CEL	L00	$7.154^{+1.660}_{-1.357} \times 10^{-8}$
<i>icf</i> (Cl)	CEL	DMS14	$2.441^{+0.101}_{-0.426}$
Cl/H	CEL	DMS14	$1.463^{+0.262}_{-0.443} \times 10^{-7}$
Ar ²⁺ /H	CEL		$3.552^{+0.023}_{-0.027} \times 10^{-6}$
Ar ³⁺ /H	CEL		$2.235^{+0.272}_{-0.278} \times 10^{-7}$
<i>icf</i> (Ar)	CEL	KB94	$1.694^{+0.022}_{-0.018}$
Ar/H	CEL	KB94	$6.395^{+0.141}_{-0.146} \times 10^{-6}$
<i>icf</i> (Ar)	CEL	DMS14	$1.070^{+0.693}_{-0.800}$
Ar/H	CEL	DMS14	$3.802^{+2.857}_{-3.434} \times 10^{-6}$
Fe ²⁺ /H	CEL		$1.279^{+0.226}_{-0.244} \times 10^{-6}$

Physical and chemical properties of WR planetary nebulae

<i>icf</i> (Fe)	CEL	ITL94	$3.052^{+0.024}_{-0.029}$
Fe/H	CEL	ITL94	$3.904^{+0.888}_{-0.984} \times 10^{-6}$
<i>adf</i> (N ²⁺)	ORL/CEL		$16.687^{+2.713}_{-2.541}$
<i>adf</i> (N)	ORL/CEL	KB94	$16.687^{+3.022}_{-3.364}$
<i>adf</i> (N)	ORL/CEL	DMS14	$6.990^{+19.050}_{-4.578}$
<i>adf</i> (O ²⁺)	ORL/CEL		$11.048^{+1.909}_{-1.831}$
<i>adf</i> (O)	ORL/CEL	KB94	$11.048^{+2.270}_{-2.276}$
<i>adf</i> (O)	ORL/CEL	DMS14	$11.048^{+2.188}_{-2.322}$
Hen 2-142 (PNG327.1-02.2)			
He ⁺ /H	ORL		$2.207^{+0.199}_{-0.222} \times 10^{-2}$
He/H	ORL		$2.207^{+0.199}_{-0.222} \times 10^{-2}$
N ⁺ /H	CEL		$1.029^{+0.102}_{-0.113} \times 10^{-4}$
<i>icf</i> (N)	CEL	KB94	$1.006^{+0.346}_{-0.282}$
N/H	CEL	KB94	$1.035^{+0.495}_{-0.405} \times 10^{-4}$
<i>icf</i> (N)	CEL	DMS14	$1.016^{+0.262}_{-0.226}$
N/H	CEL	DMS14	$1.045^{+0.439}_{-0.364} \times 10^{-4}$
O ⁰ /H	CEL		$1.106^{+0.102}_{-0.114} \times 10^{-5}$
O ⁺ /H	CEL		$4.398^{+0.394}_{-0.340} \times 10^{-4}$
O ²⁺ /H	CEL		$2.855^{+0.050}_{-0.063} \times 10^{-6}$
<i>icf</i> (O)	CEL	KB94	$1.000^{+0.117}_{-0.096}$
O/H	CEL	KB94	$4.427^{+1.226}_{-0.955} \times 10^{-4}$
<i>icf</i> (O)	CEL	DMS14	$1.000^{+0.030}_{-0.030}$
O/H	CEL	DMS14	$4.427^{+0.826}_{-0.742} \times 10^{-4}$
S ⁺ /H	CEL		$8.694^{+0.938}_{-1.118} \times 10^{-7}$
S ²⁺ /H	CEL		$2.693^{+0.281}_{-0.308} \times 10^{-6}$
<i>icf</i> (S)	CEL	KB94	$1.000^{+0.007}_{-0.024}$
S/H	CEL	KB94	$3.562^{+0.583}_{-0.627} \times 10^{-6}$
<i>icf</i> (S)	CEL	DMS14	$0.942^{+0.353}_{-0.396}$
S/H	CEL	DMS14	$3.355^{+1.936}_{-1.897} \times 10^{-6}$
Cl ²⁺ /H	CEL		$9.211^{+1.049}_{-1.354} \times 10^{-8}$
<i>icf</i> (Cl)	CEL	L00	$1.323^{+0.378}_{-0.316}$
Cl/H	CEL	L00	$1.219^{+0.576}_{-0.467} \times 10^{-7}$
<i>icf</i> (Cl)	CEL	DMS14	$1.006^{+0.256}_{-0.353}$
Cl/H	CEL	DMS14	$9.271^{+3.815}_{-4.156} \times 10^{-8}$
Hen 3-1333 (PNG332.9-09.9)			
N ⁺ /H	CEL		$3.444^{+0.090}_{-0.081} \times 10^{-4}$
<i>icf</i> (N)	CEL	KB94	$1.000^{+0.037}_{-0.036}$
N/H	CEL	KB94	$3.444^{+0.224}_{-0.186} \times 10^{-4}$
<i>icf</i> (N)	CEL	DMS14	$1.000^{+0.067}_{-0.068}$
N/H	CEL	DMS14	$3.444^{+0.353}_{-0.323} \times 10^{-4}$
O ⁰ /H	CEL		$3.214^{+0.104}_{-0.099} \times 10^{-4}$
O ⁺ /H	CEL		$3.133^{+0.064}_{-0.061} \times 10^{-3}$
<i>icf</i> (O)	CEL	KB94	$1.000^{+0.000}_{-0.000}$
O/H	CEL	KB94	$3.133^{+0.064}_{-0.061} \times 10^{-3}$
<i>icf</i> (O)	CEL	DMS14	$1.000^{+0.030}_{-0.030}$
O/H	CEL	DMS14	$3.133^{+0.148}_{-0.148} \times 10^{-3}$
S ⁺ /H	CEL		$4.559^{+0.527}_{-0.554} \times 10^{-5}$
S ²⁺ /H	CEL		$7.554^{+0.322}_{-0.320} \times 10^{-7}$

Danehkar

<i>icf</i> (S)	CEL	KB94	$1.000^{+0.000}_{-0.000}$
S/H	CEL	KB94	$4.634^{+0.819}_{-0.894} \times 10^{-5}$
<i>icf</i> (S)	CEL	DMS14	$0.935^{+0.175}_{-0.251}$
S/H	CEL	DMS14	$4.335^{+1.580}_{-1.580} \times 10^{-5}$
Hen 2-113 (PNG321.0+03.9)			
N ⁺ /H	CEL		$1.186^{+0.045}_{-0.037} \times 10^{-4}$
<i>icf</i> (N)	CEL	KB94	$1.000^{+0.036}_{-0.035}$
N/H	CEL	KB94	$1.186^{+0.065}_{-0.060} \times 10^{-4}$
<i>icf</i> (N)	CEL	DMS14	$1.000^{+0.059}_{-0.055}$
N/H	CEL	DMS14	$1.186^{+0.081}_{-0.087} \times 10^{-4}$
O ⁰ /H	CEL		$2.179^{+0.081}_{-0.073} \times 10^{-5}$
O ⁺ /H	CEL		$4.195^{+0.101}_{-0.067} \times 10^{-4}$
<i>icf</i> (O)	CEL	KB94	$1.000^{+0.000}_{0.000}$
O/H	CEL	KB94	$4.195^{+0.101}_{-0.067} \times 10^{-4}$
<i>icf</i> (O)	CEL	DMS14	$1.000^{+0.030}_{-0.030}$
O/H	CEL	DMS14	$4.195^{+0.187}_{-0.149} \times 10^{-4}$
S ⁺ /H	CEL		$4.808^{+0.382}_{-0.357} \times 10^{-6}$
S ²⁺ /H	CEL		$2.184^{+0.149}_{-0.137} \times 10^{-6}$
<i>icf</i> (S)	CEL	KB94	$1.000^{+0.000}_{-0.000}$
S/H	CEL	KB94	$6.992^{+0.554}_{-0.497} \times 10^{-6}$
<i>icf</i> (S)	CEL	DMS14	$0.935^{+0.168}_{-0.238}$
S/H	CEL	DMS14	$6.541^{+1.787}_{-1.915} \times 10^{-6}$
K 2-16 (PNG352.9+11.4)			
N ⁺ /H	CEL		$6.906^{+0.342}_{-0.349} \times 10^{-5}$
<i>icf</i> (N)	CEL	KB94	$1.389^{+0.082}_{-0.077}$
N/H	CEL	KB94	$9.596^{+0.820}_{-0.938} \times 10^{-5}$
<i>icf</i> (N)	CEL	DMS14	$2.100^{+0.463}_{-0.340}$
N/H	CEL	DMS14	$1.450^{+0.426}_{-0.331} \times 10^{-4}$
O ⁺ /H	CEL		$1.451^{+0.041}_{-0.048} \times 10^{-4}$
O ²⁺ /H	CEL		$5.650^{+0.128}_{-0.159} \times 10^{-5}$
<i>icf</i> (O)	CEL	KB94	$1.000^{+0.000}_{0.000}$
O/H	CEL	KB94	$2.016^{+0.050}_{-0.059} \times 10^{-4}$
<i>icf</i> (O)	CEL	DMS14	$1.000^{+0.030}_{-0.030}$
O/H	CEL	DMS14	$2.016^{+0.093}_{-0.106} \times 10^{-4}$
S ⁺ /H	CEL		$2.930^{+0.196}_{-0.207} \times 10^{-6}$
<i>icf</i> (S)	CEL	KB94	$4.140^{+0.079}_{-0.073}$
S/H	CEL	KB94	$1.213^{+0.091}_{-0.101} \times 10^{-5}$
<i>icf</i> (S)	CEL	DMS14	$0.979^{+0.196}_{-0.267}$
S/H	CEL	DMS14	$2.869^{+0.711}_{-0.957} \times 10^{-6}$
NGC 6578 (PNG010.8-01.8)			

He ⁺ /H	ORL		$1.181^{+0.008}_{-0.007} \times 10^{-1}$
He ²⁺ /H	ORL		$3.831^{+0.179}_{-0.174} \times 10^{-4}$
He/H	ORL		$1.185^{+0.010}_{-0.010} \times 10^{-1}$
C ²⁺ /H	ORL		$9.537^{+0.904}_{-0.833} \times 10^{-4}$
C ³⁺ /H	ORL		$1.177^{+0.093}_{-0.095} \times 10^{-3}$
<i>icf</i> (C)	ORL	WL07	$1.086^{+0.001}_{-0.001}$
C/H	ORL	WL07	$2.314^{+0.262}_{-0.264} \times 10^{-3}$
<i>icf</i> (C)	ORL	DMS14	$1.652^{+0.394}_{-0.419}$
C/H	ORL	DMS14	$1.576^{+0.522}_{-0.589} \times 10^{-3}$
N ²⁺ /H	ORL		$6.765^{+1.335}_{-1.282} \times 10^{-4}$
N ³⁺ /H	ORL		$1.277^{+0.198}_{-0.198} \times 10^{-4}$
<i>icf</i> (N)	ORL	WL07	$1.086^{+0.003}_{-0.002}$
N/H	ORL	WL07	$8.733^{+2.257}_{-2.648} \times 10^{-4}$
O ²⁺ /H	ORL		$3.451^{+0.433}_{-0.405} \times 10^{-3}$
<i>icf</i> (O)	ORL	WL07	$1.089^{+0.009}_{-0.010}$
O/H	ORL	WL07	$3.757^{+0.637}_{-0.582} \times 10^{-3}$
N ⁺ /H	CEL		$5.127^{+0.071}_{-0.078} \times 10^{-6}$
<i>icf</i> (N)	CEL	KB94	$12.632^{+0.328}_{-0.407}$
N/H	CEL	KB94	$6.476^{+0.260}_{-0.320} \times 10^{-5}$
<i>icf</i> (N)	CEL	DMS14	$20.933^{+10.755}_{-7.468}$
N/H	CEL	DMS14	$1.073^{+0.729}_{-0.546} \times 10^{-4}$
O ⁰ /H	CEL		$4.249^{+1.422}_{-1.629} \times 10^{-7}$
O ⁺ /H	CEL		$4.732^{+0.043}_{-0.045} \times 10^{-5}$
O ²⁺ /H	CEL		$5.492^{+0.044}_{-0.051} \times 10^{-4}$
<i>icf</i> (O)	CEL	KB94	$1.002^{+0.009}_{-0.009}$
O/H	CEL	KB94	$5.978^{+0.110}_{-0.142} \times 10^{-4}$
<i>icf</i> (O)	CEL	DMS14	$1.002^{+0.032}_{-0.032}$
O/H	CEL	DMS14	$5.975^{+0.245}_{-0.281} \times 10^{-4}$
Ne ²⁺ /H	CEL		$2.211^{+0.018}_{-0.017} \times 10^{-4}$
<i>icf</i> (Ne)	CEL	KB94	$1.089^{+0.029}_{-0.035}$
Ne/H	CEL	KB94	$2.407^{+0.084}_{-0.108} \times 10^{-4}$
<i>icf</i> (Ne)	CEL	DMS14	$19.202^{+3.321}_{-4.484}$
Ne/H	CEL	DMS14	$4.245^{+1.091}_{-1.428} \times 10^{-3}$
S ⁺ /H	CEL		$2.200^{+0.028}_{-0.030} \times 10^{-7}$
S ²⁺ /H	CEL		$5.009^{+0.124}_{-0.141} \times 10^{-6}$
<i>icf</i> (S)	CEL	KB94	$1.659^{+0.013}_{-0.017}$
S/H	CEL	KB94	$8.672^{+0.426}_{-0.506} \times 10^{-6}$
<i>icf</i> (S)	CEL	DMS14	$1.635^{+0.284}_{-0.429}$
S/H	CEL	DMS14	$8.548^{+2.013}_{-2.857} \times 10^{-6}$
Cl ²⁺ /H	CEL		$6.682^{+0.814}_{-0.885} \times 10^{-8}$

<i>icf</i> (Cl)	CEL	L00	$1.731^{+0.125}_{-0.136}$
Cl/H	CEL	L00	$1.157^{+0.233}_{-0.267} \times 10^{-7}$
<i>icf</i> (Cl)	CEL	DMS14	$12.627^{+0.675}_{-2.426}$
Cl/H	CEL	DMS14	$8.437^{+1.452}_{-2.551} \times 10^{-7}$
Ar ²⁺ /H	CEL		$2.381^{+0.039}_{-0.040} \times 10^{-6}$
Ar ³⁺ /H	CEL		$5.143^{+0.431}_{-0.441} \times 10^{-7}$
<i>icf</i> (Ar)	CEL	KB94	$1.086^{+0.006}_{-0.005}$
Ar/H	CEL	KB94	$3.145^{+0.135}_{-0.147} \times 10^{-6}$
<i>icf</i> (Ar)	CEL	DMS14	$1.492^{+0.980}_{-1.141}$
Ar/H	CEL	DMS14	$3.554^{+3.011}_{-3.358} \times 10^{-6}$
Fe ²⁺ /H	CEL		$1.985^{+0.558}_{-0.542} \times 10^{-6}$
<i>icf</i> (Fe)	CEL	ITL94	$15.790^{+0.415}_{-0.500}$
Fe/H	CEL	ITL94	$3.134^{+1.127}_{-1.164} \times 10^{-5}$
<i>adf</i> (N ²⁺)	ORL/CEL		$11.370^{+2.761}_{-2.764}$
<i>adf</i> (N)	ORL/CEL	KB94	$13.485^{+4.437}_{-5.171}$
<i>adf</i> (N)	ORL/CEL	DMS14	$8.137^{+81.933}_{-8.137}$
<i>adf</i> (O ²⁺)	ORL/CEL		$6.284^{+0.980}_{-0.975}$
<i>adf</i> (O)	ORL/CEL	KB94	$6.284^{+1.354}_{-1.234}$
<i>adf</i> (O)	ORL/CEL	DMS14	$6.287^{+1.400}_{-1.252}$

M 2-42 (PNG008.2-04.8)

He ⁺ /H	ORL		$9.800^{+0.125}_{-0.116} \times 10^{-2}$
He ²⁺ /H	ORL		$2.730^{+0.053}_{-0.059} \times 10^{-4}$
He/H	ORL		$9.827^{+0.152}_{-0.145} \times 10^{-2}$
C ²⁺ /H	ORL		$4.628^{+0.209}_{-0.205} \times 10^{-4}$
C ³⁺ /H	ORL		$3.202^{+0.127}_{-0.125} \times 10^{-3}$
<i>icf</i> (C)	ORL	WL07	$1.081^{+0.003}_{-0.003}$
C/H	ORL	WL07	$3.960^{+0.179}_{-0.164} \times 10^{-3}$
<i>icf</i> (C)	ORL	DMS14	$1.656^{+0.404}_{-0.424}$
C/H	ORL	DMS14	$7.664^{+2.500}_{-2.408} \times 10^{-4}$
N ²⁺ /H	ORL		$2.445^{+0.092}_{-0.108} \times 10^{-3}$
N ³⁺ /H	ORL		$1.714^{+0.072}_{-0.068} \times 10^{-4}$
<i>icf</i> (N)	ORL	WL07	$1.080^{+0.004}_{-0.004}$
N/H	ORL	WL07	$2.827^{+0.139}_{-0.148} \times 10^{-3}$
O ²⁺ /H	ORL		$1.297^{+0.143}_{-0.218} \times 10^{-3}$
<i>icf</i> (O)	ORL	WL07	$1.083^{+0.018}_{-0.016}$
O/H	ORL	WL07	$1.404^{+0.186}_{-0.245} \times 10^{-3}$
N ⁰ /H	CEL		$1.857^{+0.145}_{-0.154} \times 10^{-7}$
N ⁺ /H	CEL		$8.022^{+0.220}_{-0.261} \times 10^{-6}$
<i>icf</i> (N)	CEL	KB94	$13.438^{+0.672}_{-0.746}$
N/H	CEL	KB94	$1.078^{+0.060}_{-0.082} \times 10^{-4}$
<i>icf</i> (N)	CEL	DMS14	$22.835^{+11.947}_{-8.451}$
N/H	CEL	DMS14	$1.832^{+1.057}_{-0.848} \times 10^{-4}$
O ⁰ /H	CEL		$4.291^{+0.135}_{-0.126} \times 10^{-6}$
O ⁺ /H	CEL		$2.900^{+0.086}_{-0.084} \times 10^{-5}$
O ²⁺ /H	CEL		$3.599^{+0.064}_{-0.069} \times 10^{-4}$

Physical and chemical properties of WR planetary nebulae

<i>icf</i> (O)	CEL	KB94	$1.002^{+0.016}_{-0.017}$
O/H	CEL	KB94	$3.896^{+0.097}_{-0.118} \times 10^{-4}$
<i>icf</i> (O)	CEL	DMS14	$1.002^{+0.031}_{-0.031}$
O/H	CEL	DMS14	$3.895^{+0.165}_{-0.202} \times 10^{-4}$
Ne ²⁺ /H	CEL		$8.527^{+0.235}_{-0.211} \times 10^{-5}$
<i>icf</i> (Ne)	CEL	KB94	$1.083^{+0.043}_{-0.049}$
Ne/H	CEL	KB94	$9.231^{+0.466}_{-0.611} \times 10^{-5}$
<i>icf</i> (Ne)	CEL	DMS14	$28.687^{+4.994}_{-6.776}$
Ne/H	CEL	DMS14	$2.446^{+0.581}_{-0.702} \times 10^{-3}$
S ⁺ /H	CEL		$3.278^{+0.078}_{-0.078} \times 10^{-7}$
S ²⁺ /H	CEL		$5.345^{+0.149}_{-0.159} \times 10^{-6}$
<i>icf</i> (S)	CEL	KB94	$1.690^{+0.024}_{-0.028}$
S/H	CEL	KB94	$9.588^{+0.406}_{-0.427} \times 10^{-6}$
<i>icf</i> (S)	CEL	DMS14	$1.666^{+0.301}_{-0.456}$
S/H	CEL	DMS14	$9.451^{+1.946}_{-2.997} \times 10^{-6}$
Cl ²⁺ /H	CEL		$8.429^{+0.172}_{-0.200} \times 10^{-8}$
<i>icf</i> (Cl)	CEL	L00	$1.794^{+0.110}_{-0.114}$
Cl/H	CEL	L00	$1.512^{+0.106}_{-0.129} \times 10^{-7}$
<i>icf</i> (Cl)	CEL	DMS14	$13.433^{+0.812}_{-2.740}$
Cl/H	CEL	DMS14	$1.132^{+0.077}_{-0.261} \times 10^{-6}$
Ar ²⁺ /H	CEL		$1.212^{+0.049}_{-0.063} \times 10^{-6}$
Ar ³⁺ /H	CEL		$3.739^{+0.119}_{-0.126} \times 10^{-7}$
<i>icf</i> (Ar)	CEL	KB94	$1.080^{+0.008}_{-0.006}$
Ar/H	CEL	KB94	$1.713^{+0.083}_{-0.090} \times 10^{-6}$
<i>icf</i> (Ar)	CEL	DMS14	$1.505^{+0.992}_{-1.155}$
Ar/H	CEL	DMS14	$1.823^{+1.228}_{-1.614} \times 10^{-6}$
Fe ²⁺ /H	CEL		$3.636^{+0.294}_{-0.349} \times 10^{-7}$
<i>icf</i> (Fe)	CEL	ITL94	$16.797^{+0.718}_{-0.764}$
Fe/H	CEL	ITL94	$6.107^{+0.658}_{-0.690} \times 10^{-6}$
<i>adf</i> (N ²⁺)	ORL/CEL		$24.556^{+2.012}_{-1.702}$
<i>adf</i> (N)	ORL/CEL	KB94	$26.225^{+2.870}_{-2.038}$
<i>adf</i> (N)	ORL/CEL	DMS14	$15.432^{+169.433}_{-15.432}$
<i>adf</i> (O ²⁺)	ORL/CEL		$3.603^{+0.509}_{-0.722}$
<i>adf</i> (O)	ORL/CEL	KB94	$3.603^{+0.607}_{-0.779}$
<i>adf</i> (O)	ORL/CEL	DMS14	$3.605^{+0.639}_{-0.768}$
NGC 6567 (PNG011.7–00.6)			
He ⁺ /H	ORL		$9.163^{+0.034}_{-0.046} \times 10^{-2}$
He ²⁺ /H	ORL		$5.422^{+0.209}_{-0.194} \times 10^{-4}$
He/H	ORL		$9.217^{+0.046}_{-0.060} \times 10^{-2}$
C ²⁺ /H	ORL		$1.019^{+0.038}_{-0.042} \times 10^{-3}$
C ³⁺ /H	ORL		$1.877^{+0.240}_{-0.202} \times 10^{-3}$
<i>icf</i> (C)	ORL	WL07	$1.098^{+0.002}_{-0.002}$
C/H	ORL	WL07	$3.180^{+0.453}_{-0.425} \times 10^{-3}$
<i>icf</i> (C)	ORL	DMS14	$1.646^{+0.397}_{-0.406}$

C/H	ORL	DMS14	$1.677^{+0.571}_{-0.530} \times 10^{-3}$
N ²⁺ /H	ORL		$1.630^{+0.234}_{-0.215} \times 10^{-3}$
<i>icf</i> (N)	ORL	WL07	$1.102^{+0.030}_{-0.024}$
N/H	ORL	WL07	$1.797^{+0.337}_{-0.322} \times 10^{-3}$
O ²⁺ /H	ORL		$5.915^{+0.846}_{-0.875} \times 10^{-3}$
<i>icf</i> (O)	ORL	WL07	$1.102^{+0.007}_{-0.007}$
O/H	ORL	WL07	$6.521^{+1.245}_{-1.233} \times 10^{-3}$
N ⁰ /H	CEL		$7.982^{+1.668}_{-1.593} \times 10^{-8}$
N ⁺ /H	CEL		$2.591^{+0.057}_{-0.066} \times 10^{-6}$
<i>icf</i> (N)	CEL	KB94	$11.232^{+0.289}_{-0.240}$
N/H	CEL	KB94	$2.911^{+0.145}_{-0.130} \times 10^{-5}$
<i>icf</i> (N)	CEL	DMS14	$16.959^{+8.772}_{-5.878}$
N/H	CEL	DMS14	$4.395^{+2.740}_{-2.061} \times 10^{-5}$
O ⁰ /H	CEL		$2.887^{+0.048}_{-0.063} \times 10^{-6}$
O ⁺ /H	CEL		$2.062^{+0.016}_{-0.016} \times 10^{-5}$
O ²⁺ /H	CEL		$2.100^{+0.022}_{-0.023} \times 10^{-4}$
<i>icf</i> (O)	CEL	KB94	$1.004^{+0.006}_{-0.006}$
O/H	CEL	KB94	$2.315^{+0.042}_{-0.037} \times 10^{-4}$
<i>icf</i> (O)	CEL	DMS14	$1.003^{+0.033}_{-0.033}$
O/H	CEL	DMS14	$2.314^{+0.109}_{-0.103} \times 10^{-4}$
Ne ²⁺ /H	CEL		$4.471^{+0.027}_{-0.023} \times 10^{-5}$
<i>icf</i> (Ne)	CEL	KB94	$1.102^{+0.031}_{-0.025}$
Ne/H	CEL	KB94	$4.929^{+0.199}_{-0.143} \times 10^{-5}$
<i>icf</i> (Ne)	CEL	DMS14	$4.251^{+0.780}_{-0.963}$
Ne/H	CEL	DMS14	$1.901^{+0.400}_{-0.540} \times 10^{-4}$
S ⁺ /H	CEL		$6.566^{+0.143}_{-0.177} \times 10^{-8}$
S ²⁺ /H	CEL		$1.110^{+0.017}_{-0.021} \times 10^{-6}$
<i>icf</i> (S)	CEL	KB94	$1.600^{+0.012}_{-0.010}$
S/H	CEL	KB94	$1.881^{+0.060}_{-0.063} \times 10^{-6}$
<i>icf</i> (S)	CEL	DMS14	$1.576^{+0.287}_{-0.402}$
S/H	CEL	DMS14	$1.852^{+0.444}_{-0.614} \times 10^{-6}$
Cl ²⁺ /H	CEL		$1.798^{+0.083}_{-0.088} \times 10^{-8}$
<i>icf</i> (Cl)	CEL	L00	$1.695^{+0.085}_{-0.073}$
Cl/H	CEL	L00	$3.047^{+0.316}_{-0.266} \times 10^{-8}$
<i>icf</i> (Cl)	CEL	DMS14	$11.223^{+0.695}_{-2.079}$
Cl/H	CEL	DMS14	$2.018^{+0.215}_{-0.436} \times 10^{-7}$
Ar ²⁺ /H	CEL		$3.692^{+0.038}_{-0.048} \times 10^{-7}$
Ar ³⁺ /H	CEL		$1.012^{+0.145}_{-0.154} \times 10^{-7}$
<i>icf</i> (Ar)	CEL	KB94	$1.098^{+0.007}_{-0.007}$
Ar/H	CEL	KB94	$5.163^{+0.314}_{-0.343} \times 10^{-7}$
<i>icf</i> (Ar)	CEL	DMS14	$1.468^{+0.978}_{-1.113}$
Ar/H	CEL	DMS14	$5.420^{+5.377}_{-5.199} \times 10^{-7}$
Fe ²⁺ /H	CEL		$9.675^{+3.316}_{-3.271} \times 10^{-8}$
<i>icf</i> (Fe)	CEL	ITL94	$14.040^{+0.352}_{-0.290}$

Physical and chemical properties of WR planetary nebulae

Fe/H	CEL	ITL94	$1.358^{+0.689}_{-0.620} \times 10^{-6}$
<i>adf</i> (N ²⁺)	ORL/CEL		$61.727^{+11.067}_{-10.925}$
<i>adf</i> (N)	ORL/CEL	KB94	$61.727^{+14.245}_{-15.105}$
<i>adf</i> (N)	ORL/CEL	DMS14	$40.881^{+310.249}_{-40.881}$
<i>adf</i> (O ²⁺)	ORL/CEL		$28.163^{+5.085}_{-5.486}$
<i>adf</i> (O)	ORL/CEL	KB94	$28.163^{+6.629}_{-7.155}$
<i>adf</i> (O)	ORL/CEL	DMS14	$28.184^{+6.628}_{-7.277}$
NGC 6629 (PNG009.4–05.0)			
He ⁺ /H	ORL		$9.902^{+0.057}_{-0.069} \times 10^{-2}$
He/H	ORL		$9.902^{+0.057}_{-0.069} \times 10^{-2}$
C ²⁺ /H	ORL		$4.063^{+0.491}_{-0.646} \times 10^{-4}$
<i>icf</i> (C)	ORL	WL07	$1.204^{+0.025}_{-0.029}$
C/H	ORL	WL07	$4.890^{+0.670}_{-0.907} \times 10^{-4}$
<i>icf</i> (C)	ORL	DMS14	$1.585^{+0.294}_{-0.398}$
C/H	ORL	DMS14	$6.441^{+1.687}_{-2.399} \times 10^{-4}$
O ²⁺ /H	ORL		$8.111^{+1.439}_{-1.904} \times 10^{-4}$
<i>icf</i> (O)	ORL	WL07	$1.204^{+0.010}_{-0.010}$
O/H	ORL	WL07	$9.762^{+2.289}_{-2.688} \times 10^{-4}$
N ⁰ /H	CEL		$7.857^{+4.495}_{-4.416} \times 10^{-8}$
N ⁺ /H	CEL		$2.912^{+0.032}_{-0.036} \times 10^{-6}$
<i>icf</i> (N)	CEL	KB94	$5.913^{+0.119}_{-0.143}$
N/H	CEL	KB94	$1.722^{+0.048}_{-0.066} \times 10^{-5}$
<i>icf</i> (N)	CEL	DMS14	$20.116^{+9.615}_{-6.551}$
N/H	CEL	DMS14	$5.857^{+3.796}_{-2.566} \times 10^{-5}$
O ⁺ /H	CEL		$7.284^{+0.054}_{-0.054} \times 10^{-5}$
O ²⁺ /H	CEL		$3.578^{+0.028}_{-0.029} \times 10^{-4}$
<i>icf</i> (O)	CEL	KB94	$1.000^{+0.008}_{-0.007}$
O/H	CEL	KB94	$4.307^{+0.056}_{-0.080} \times 10^{-4}$
<i>icf</i> (O)	CEL	DMS14	$1.000^{+0.030}_{-0.030}$
O/H	CEL	DMS14	$4.307^{+0.191}_{-0.195} \times 10^{-4}$
Ne ²⁺ /H	CEL		$1.074^{+0.006}_{-0.007} \times 10^{-4}$
<i>icf</i> (Ne)	CEL	KB94	$1.204^{+0.025}_{-0.029}$
Ne/H	CEL	KB94	$1.293^{+0.034}_{-0.042} \times 10^{-4}$
<i>icf</i> (Ne)	CEL	DMS14	$2.037^{+0.372}_{-0.471}$
Ne/H	CEL	DMS14	$2.188^{+0.537}_{-0.613} \times 10^{-4}$
S ⁺ /H	CEL		$5.545^{+0.105}_{-0.130} \times 10^{-8}$
S ²⁺ /H	CEL		$1.905^{+0.042}_{-0.042} \times 10^{-6}$
<i>icf</i> (S)	CEL	KB94	$1.329^{+0.007}_{-0.009}$
S/H	CEL	KB94	$2.604^{+0.082}_{-0.092} \times 10^{-6}$
<i>icf</i> (S)	CEL	DMS14	$1.254^{+0.229}_{-0.326}$
S/H	CEL	DMS14	$2.459^{+0.700}_{-0.784} \times 10^{-6}$
Cl ²⁺ /H	CEL		$5.136^{+0.439}_{-0.491} \times 10^{-8}$
<i>icf</i> (Cl)	CEL	L00	$1.367^{+0.071}_{-0.070}$
Cl/H	CEL	L00	$7.022^{+0.796}_{-1.014} \times 10^{-8}$
<i>icf</i> (Cl)	CEL	DMS14	$5.913^{+0.370}_{-1.122}$
Cl/H	CEL	DMS14	$3.037^{+0.340}_{-0.796} \times 10^{-7}$
Ar ²⁺ /H	CEL		$1.492^{+0.017}_{-0.018} \times 10^{-6}$

Ar ³⁺ /H	CEL		$1.469^{+0.130}_{-0.158} \times 10^{-7}$
<i>icf</i> (Ar)	CEL	KB94	$1.204^{+0.012}_{-0.010}$
Ar/H	CEL	KB94	$1.972^{+0.046}_{-0.053} \times 10^{-6}$
<i>icf</i> (Ar)	CEL	DMS14	$1.304^{+0.858}_{-0.990}$
Ar/H	CEL	DMS14	$1.946^{+1.667}_{-1.813} \times 10^{-6}$
Fe ²⁺ /H	CEL		$4.318^{+0.544}_{-0.655} \times 10^{-7}$
<i>icf</i> (Fe)	CEL	ITL94	$7.391^{+0.151}_{-0.180}$
Fe/H	CEL	ITL94	$3.191^{+0.491}_{-0.552} \times 10^{-6}$
<i>adf</i> (O ²⁺)	ORL/CEL		$2.267^{+0.444}_{-0.598}$
<i>adf</i> (O)	ORL/CEL	KB94	$2.267^{+0.643}_{-0.725}$
<i>adf</i> (O)	ORL/CEL	DMS14	$2.267^{+0.673}_{-0.717}$
Sa 3-107 (PNG358.0-04.6)			
He ⁺ /H	ORL		$1.194^{+0.012}_{-0.010} \times 10^{-1}$
He ²⁺ /H	ORL		$1.216^{+0.045}_{-0.046} \times 10^{-3}$
He/H	ORL		$1.206^{+0.015}_{-0.012} \times 10^{-1}$
C ²⁺ /H	ORL		$8.070^{+0.784}_{-0.750} \times 10^{-4}$
C ³⁺ /H	ORL		$5.762^{+0.650}_{-0.714} \times 10^{-4}$
<i>icf</i> (C)	ORL	WL07	$1.063^{+0.051}_{-0.029}$
C/H	ORL	WL07	$1.470^{+0.225}_{-0.190} \times 10^{-3}$
<i>icf</i> (C)	ORL	DMS14	$1.677^{+0.501}_{-0.451}$
C/H	ORL	DMS14	$1.353^{+0.573}_{-0.486} \times 10^{-3}$
N ²⁺ /H	ORL		$7.959^{+1.015}_{-0.904} \times 10^{-4}$
N ³⁺ /H	ORL		$1.224^{+0.172}_{-0.178} \times 10^{-4}$
<i>icf</i> (N)	ORL	WL07	$1.062^{+0.056}_{-0.029}$
N/H	ORL	WL07	$9.755^{+1.968}_{-1.707} \times 10^{-4}$
N ⁺ /H	CEL		$1.924^{+0.037}_{-0.030} \times 10^{-6}$
<i>icf</i> (N)	CEL	KB94	$17.064^{+24.077}_{-17.064}$
N/H	CEL	KB94	$3.283^{+6.350}_{-3.283} \times 10^{-5}$
<i>icf</i> (N)	CEL	DMS14	$24.074^{+84.685}_{-24.074}$
N/H	CEL	DMS14	$4.631^{+20.551}_{-4.631} \times 10^{-5}$
O ⁰ /H	CEL		$6.971^{+0.783}_{-0.740} \times 10^{-7}$
O ⁺ /H	CEL		$5.158^{+3.465}_{-1.462} \times 10^{-6}$
O ²⁺ /H	CEL		$8.226^{+0.073}_{-0.067} \times 10^{-5}$
<i>icf</i> (O)	CEL	KB94	$1.007^{+0.013}_{-0.012}$
O/H	CEL	KB94	$8.801^{+0.565}_{-0.299} \times 10^{-5}$
<i>icf</i> (O)	CEL	DMS14	$1.006^{+0.035}_{-0.035}$
O/H	CEL	DMS14	$8.790^{+0.646}_{-0.506} \times 10^{-5}$
S ⁺ /H	CEL		$3.378^{+0.145}_{-0.115} \times 10^{-8}$
S ²⁺ /H	CEL		$5.273^{+0.636}_{-0.668} \times 10^{-7}$
<i>icf</i> (S)	CEL	KB94	$1.821^{+0.370}_{-0.322}$
S/H	CEL	KB94	$1.022^{+0.326}_{-0.285} \times 10^{-6}$
<i>icf</i> (S)	CEL	DMS14	$1.790^{+5.669}_{-1.790}$
S/H	CEL	DMS14	$1.004^{+3.727}_{-1.004} \times 10^{-6}$
Cl ²⁺ /H	CEL		$1.562^{+0.280}_{-0.211} \times 10^{-8}$
<i>icf</i> (Cl)	CEL	L00	$1.937^{+0.974}_{-0.765}$

Physical and chemical properties of WR planetary nebulae

Cl/H	CEL	L00	$3.025^{+2.243}_{-1.625} \times 10^{-8}$
<i>icf</i> (Cl)	CEL	DMS14	$17.043^{+51.933}_{-17.043}$
Cl/H	CEL	DMS14	$2.661^{+10.481}_{-2.661} \times 10^{-7}$
Ar ²⁺ /H	CEL		$4.713^{+1.388}_{-1.424} \times 10^{-7}$
Ar ³⁺ /H	CEL		$5.598^{+1.032}_{-0.982} \times 10^{-8}$
Ar ⁴⁺ /H	CEL		$1.280^{+0.279}_{-0.227} \times 10^{-8}$
<i>icf</i> (Ar)	CEL	KB94	$1.062^{+1.106}_{-1.062}$
Ar/H	CEL	KB94	$5.737^{+9.018}_{-5.737} \times 10^{-7}$
<i>icf</i> (Ar)	CEL	DMS14	$1.557^{+1.074}_{-1.227}$
Ar/H	CEL	DMS14	$7.338^{+7.380}_{-7.338} \times 10^{-7}$
Fe ²⁺ /H	CEL		$3.195^{+1.066}_{-1.066} \times 10^{-7}$
<i>icf</i> (Fe)	CEL	ITL94	$21.330^{+164.749}_{-21.330}$
Fe/H	CEL	ITL94	$6.814^{+70.862}_{-6.814} \times 10^{-6}$
<i>adf</i> (N ²⁺)	ORL/CEL		$25.940^{+689.698}_{-25.940}$
<i>adf</i> (N)	ORL/CEL	KB94	$29.715^{+690.154}_{-29.715}$
<i>adf</i> (N)	ORL/CEL	DMS14	$21.063^{+2745.244}_{-21.063}$

Notes: References for *icf* formulas are as follows: Delgado-Inglada et al. (2014); ITL94 – Izotov et al. (1994); KB94 – Kingsburgh & Barlow (1994); L00 – Liu et al. (2000); WL07 – Wang & Liu (2007). For Sa3-107, the CEL O⁺ ionic abundance estimated by using the correlation $S^{2+}/S^+ = 4.892 (O^{2+}/O^+)^{0.419}$ derived in Section 4.1.

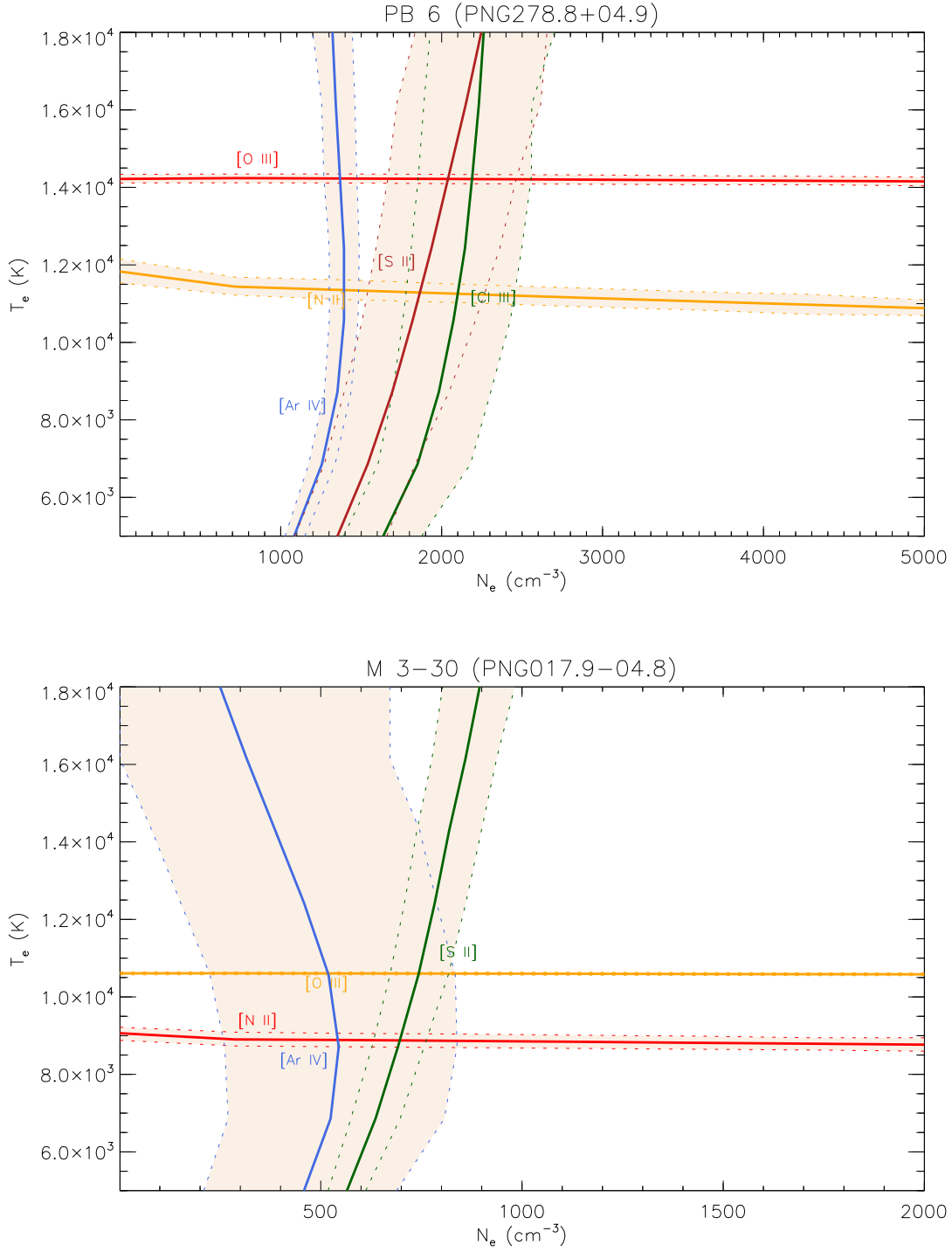


Figure 2. N_e - T_e diagnostic diagrams based on CELs. The upper and lower limits at the 90% confidence level are plotted by the dotted lines.

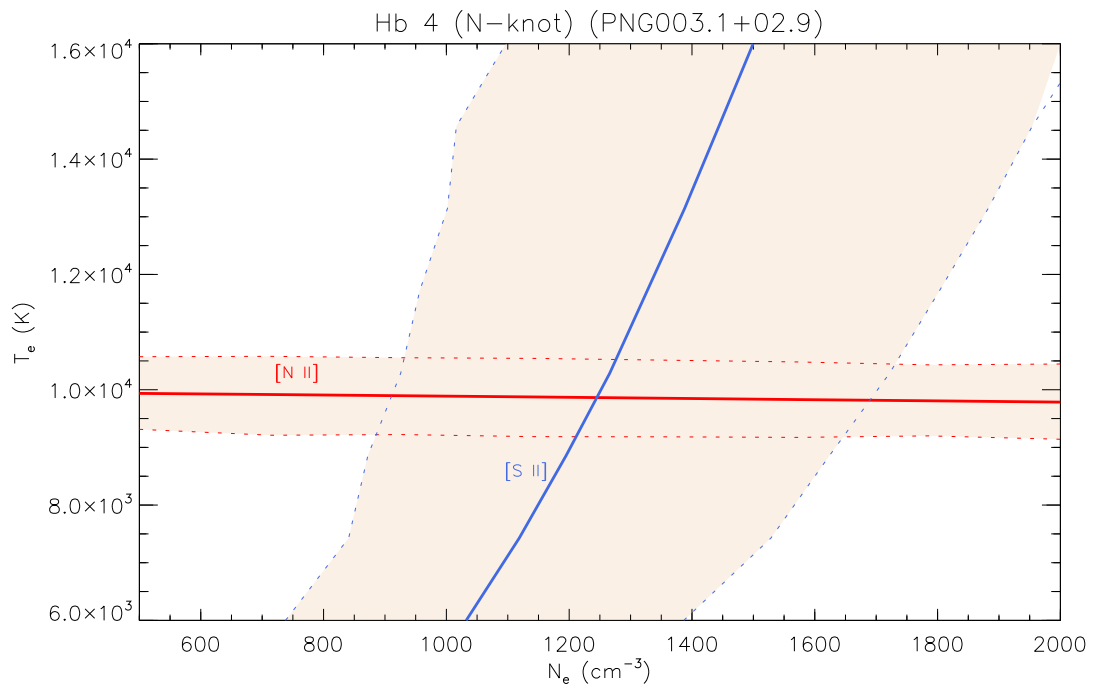
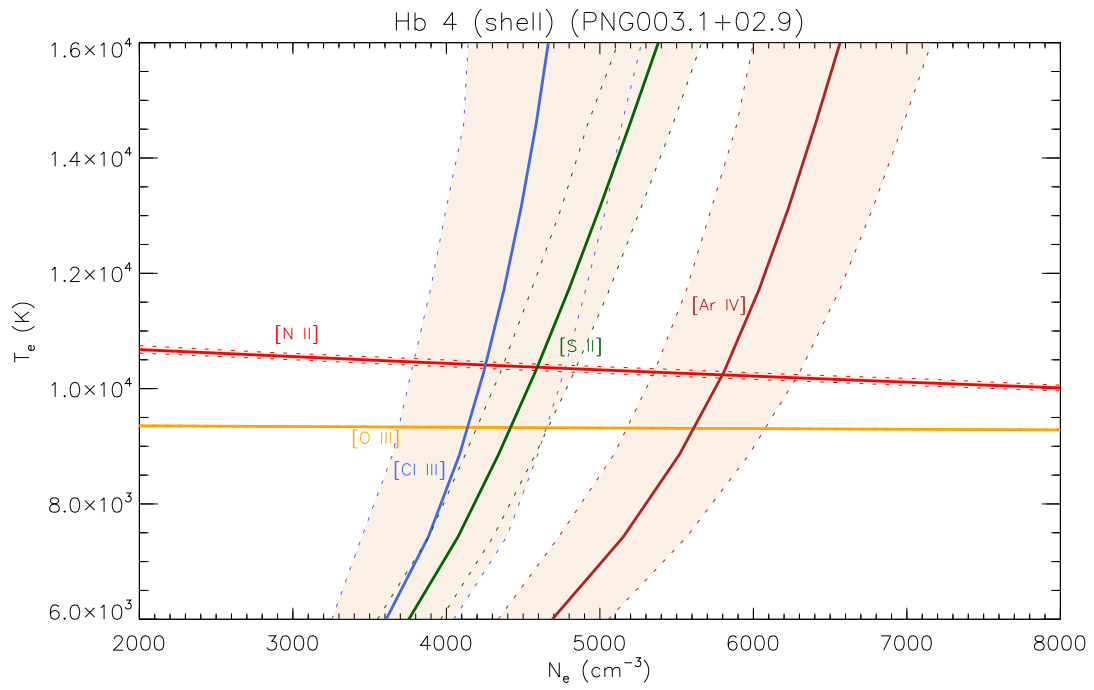


Figure 2. – continued

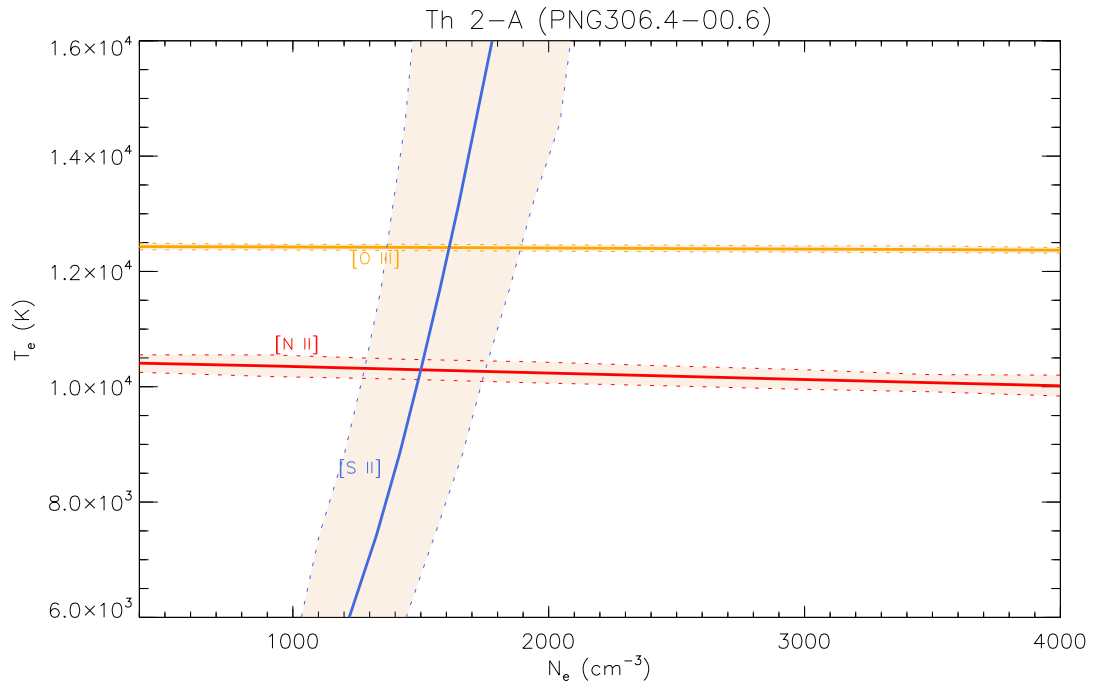
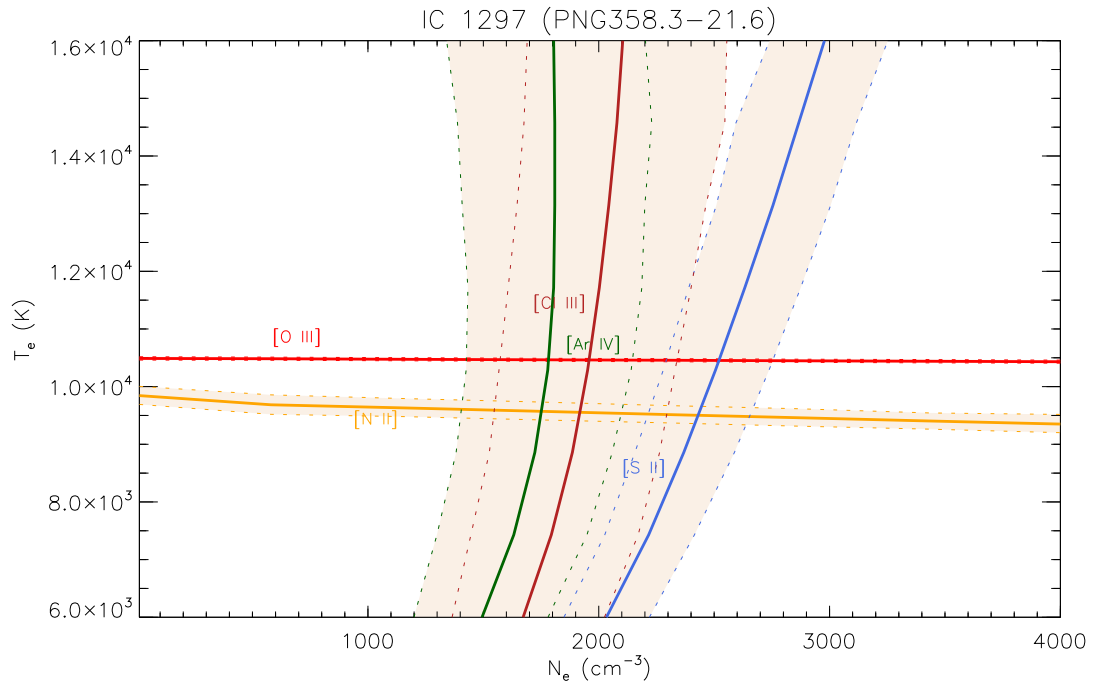


Figure 2. – continued

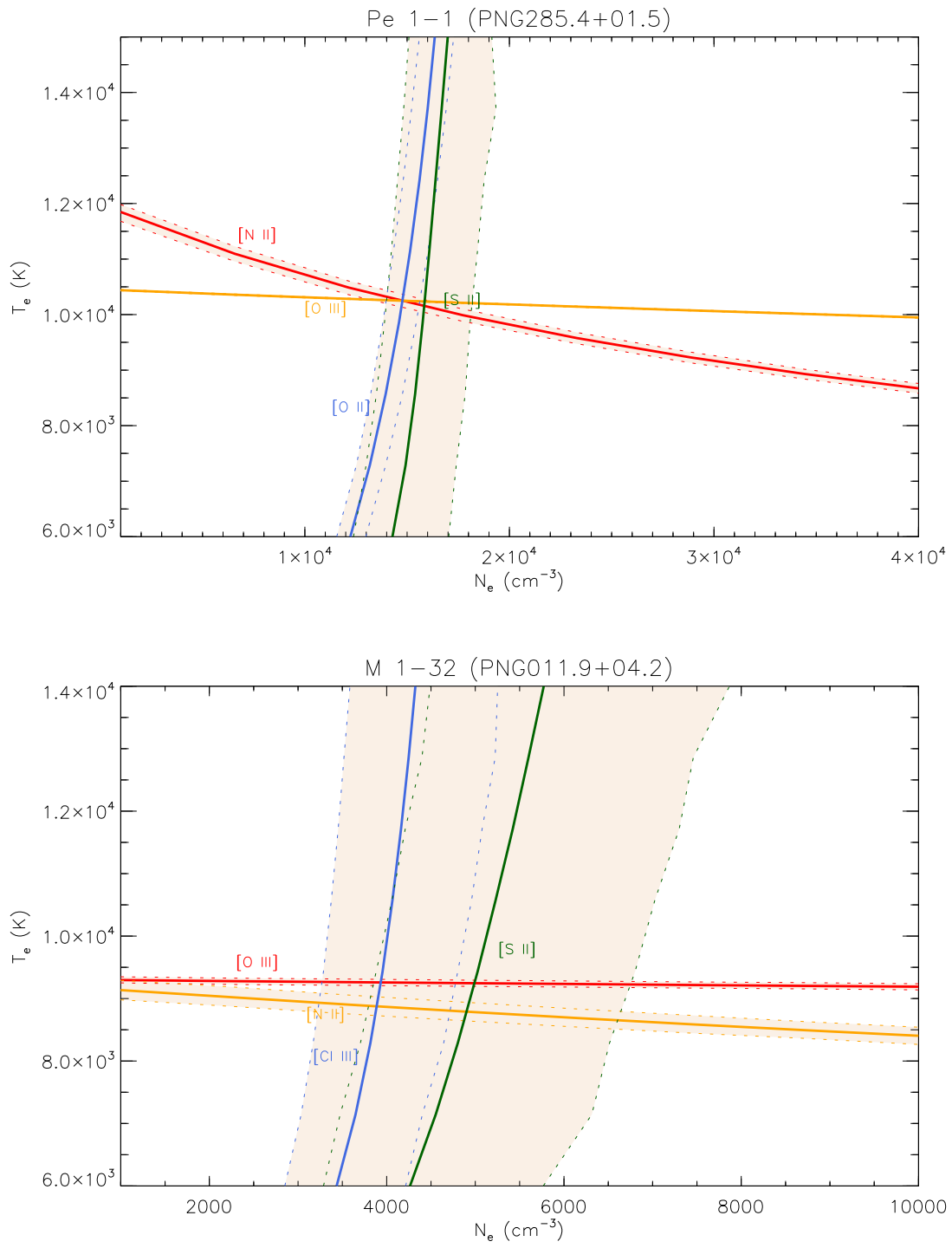


Figure 2. – continued

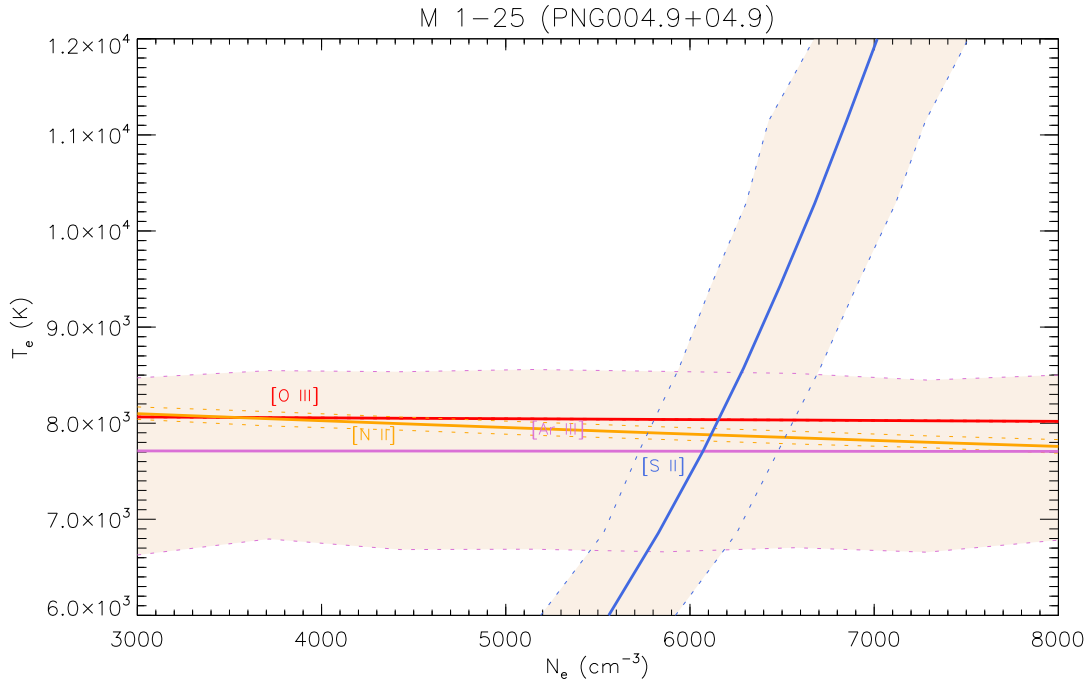
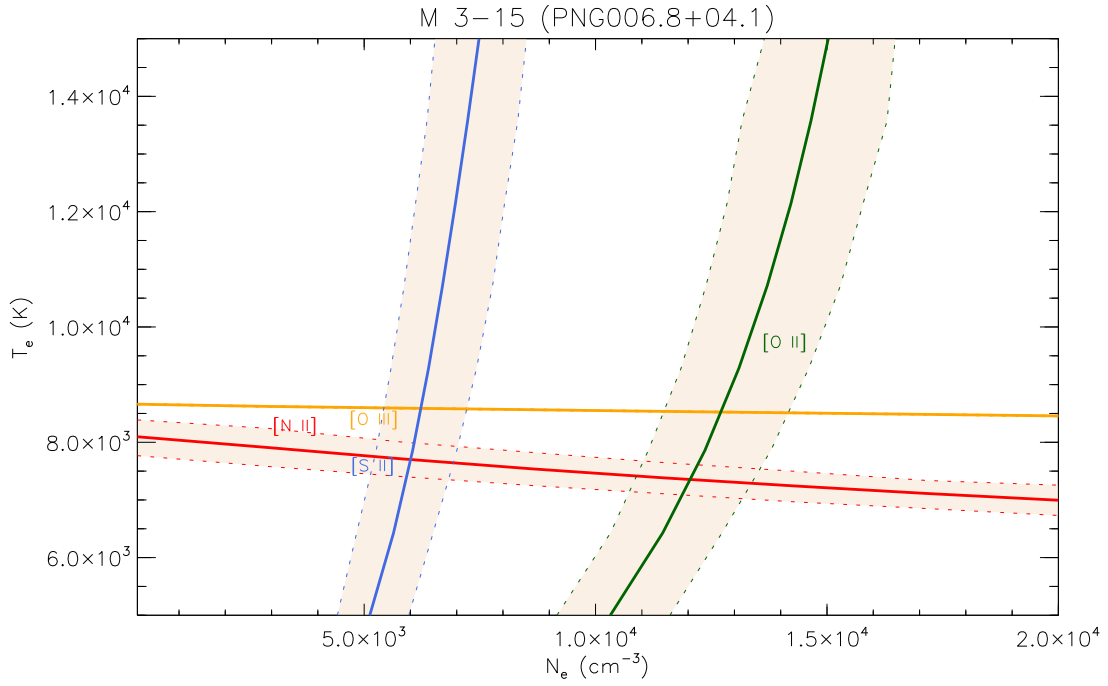


Figure 2. – continued

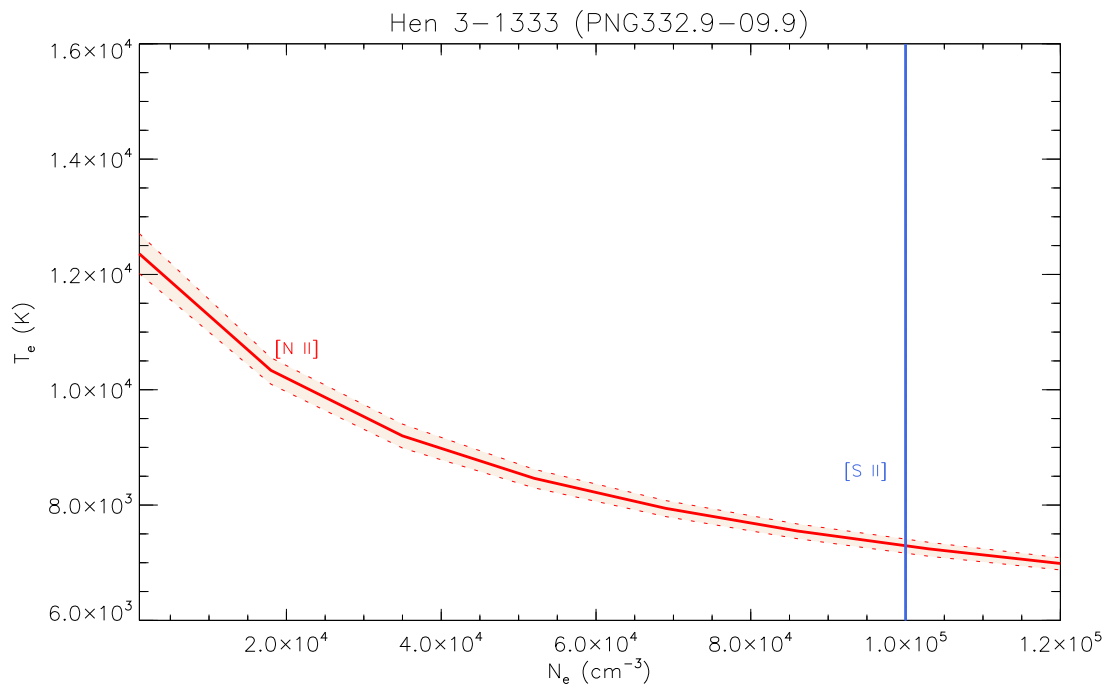
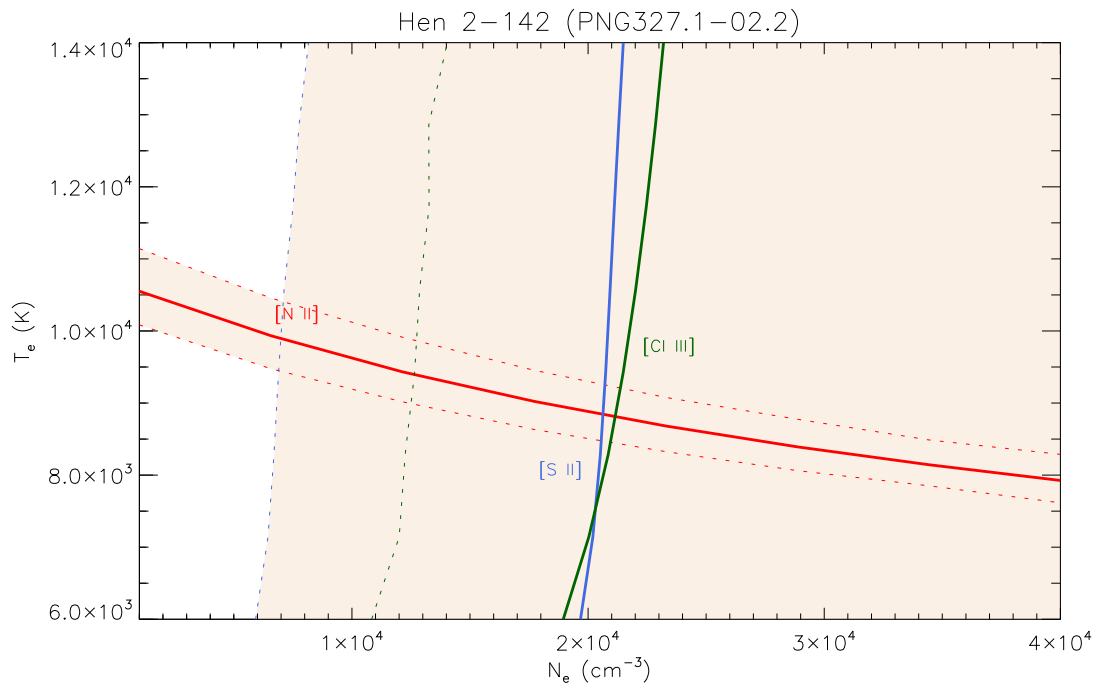


Figure 2. - continued

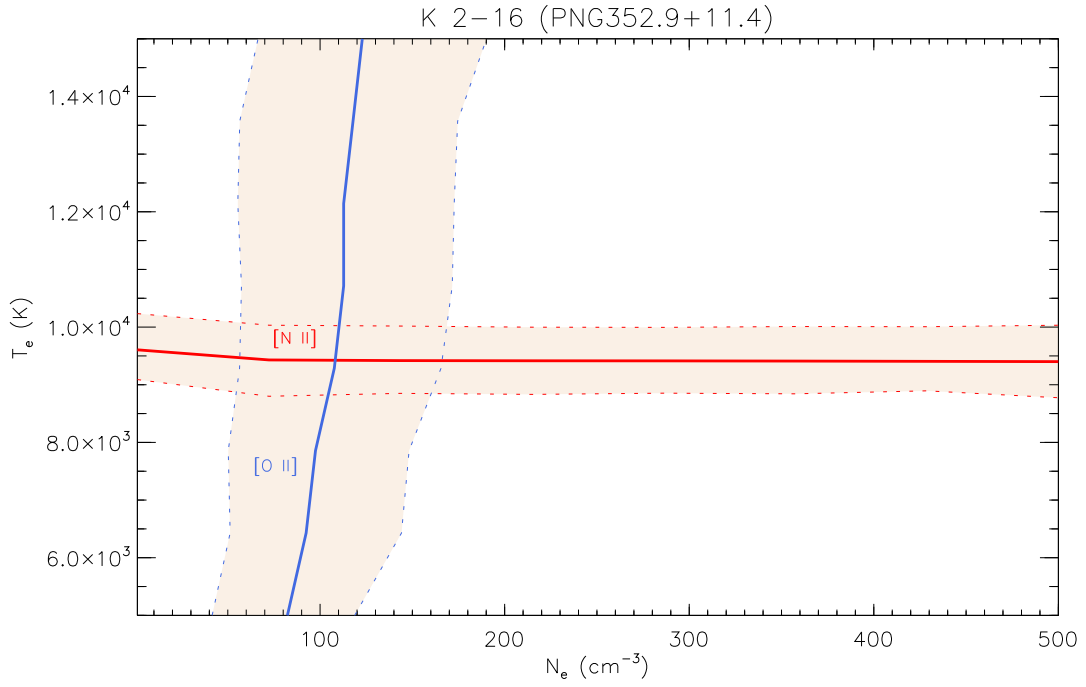
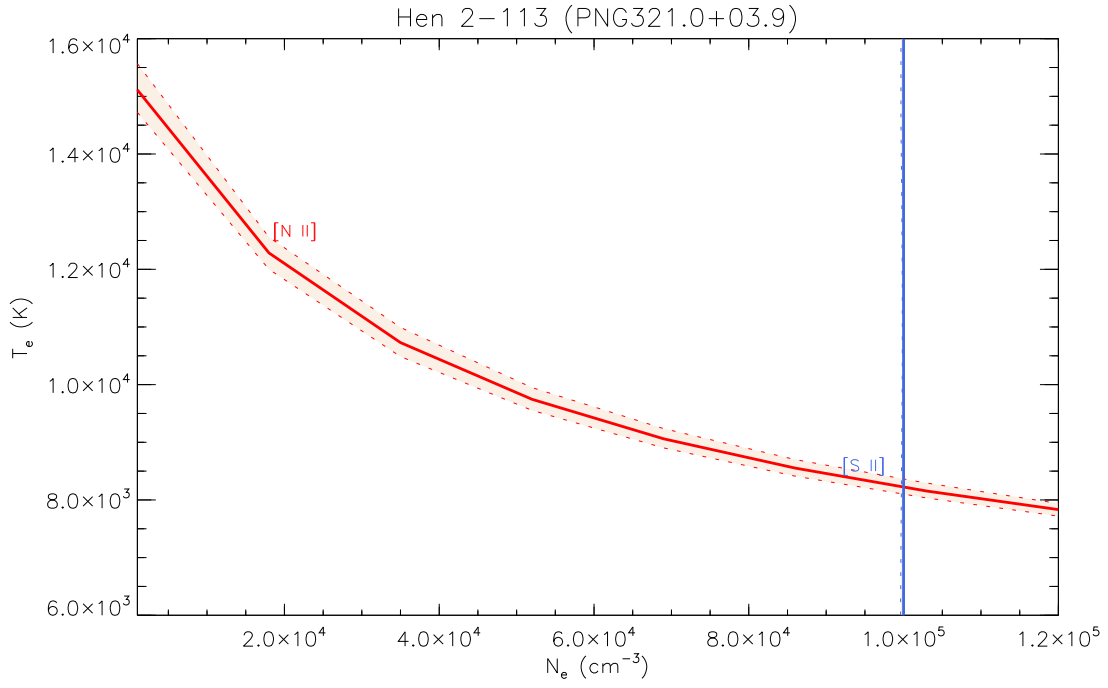


Figure 2. - continued

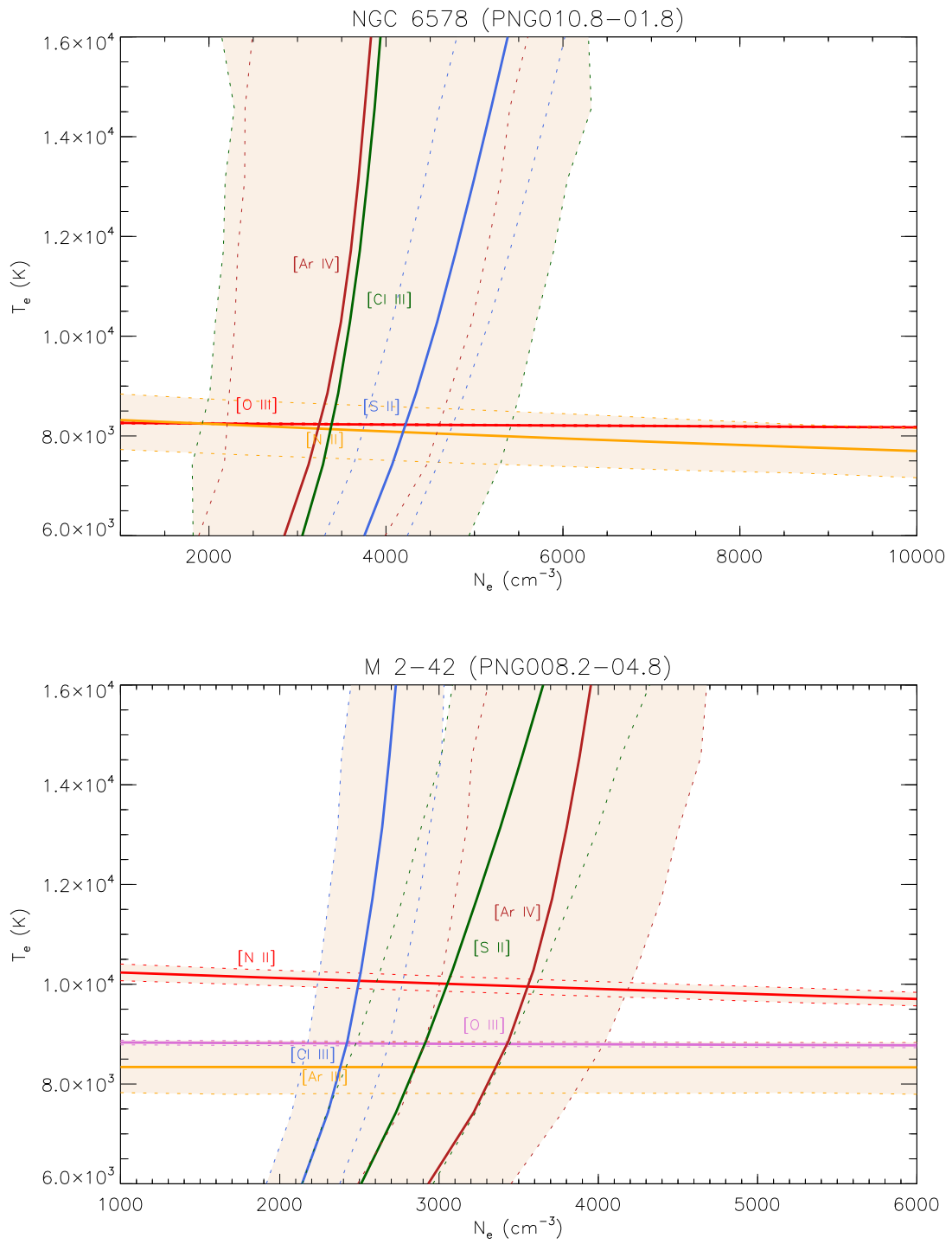


Figure 2. – continued

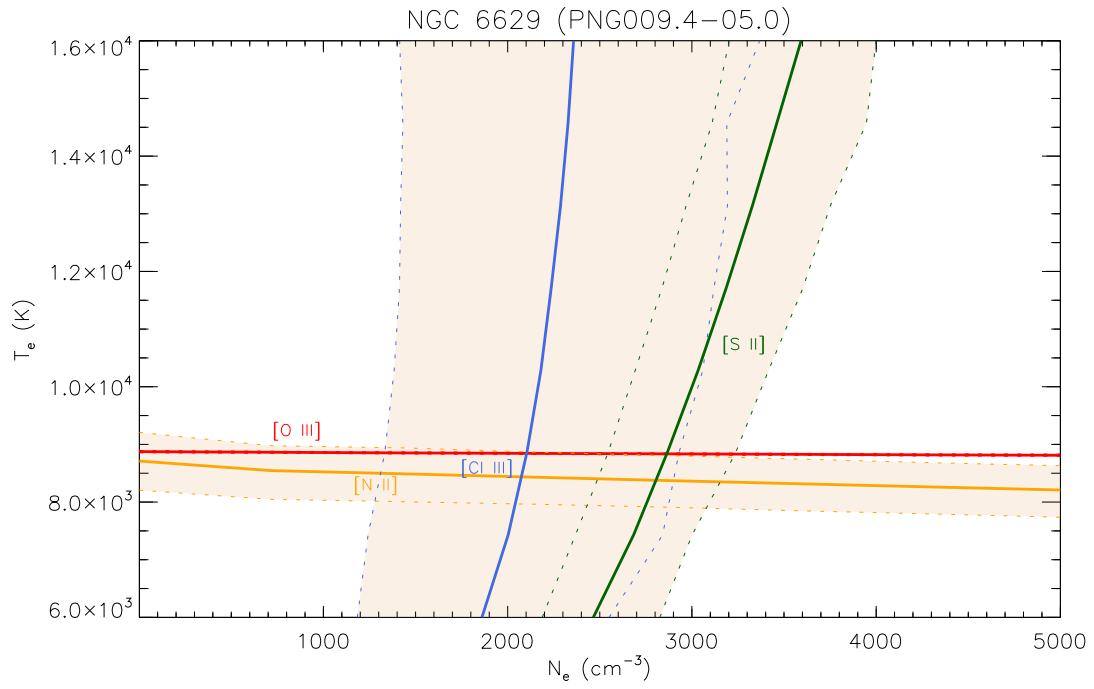
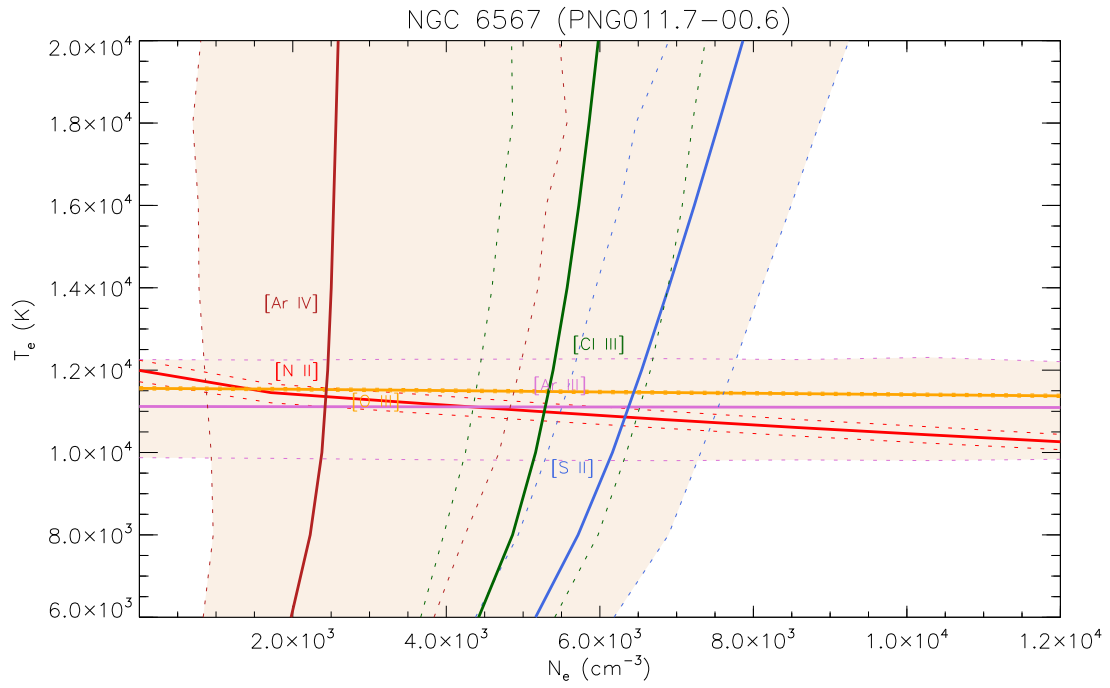


Figure 2. – continued

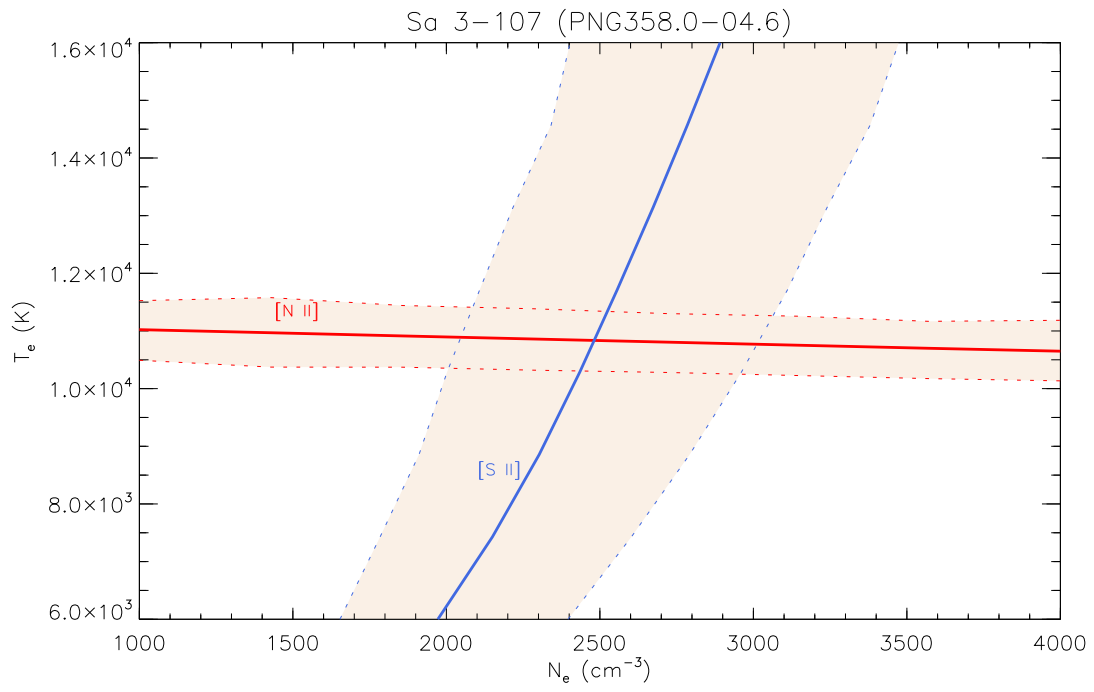


Figure 2. – continued

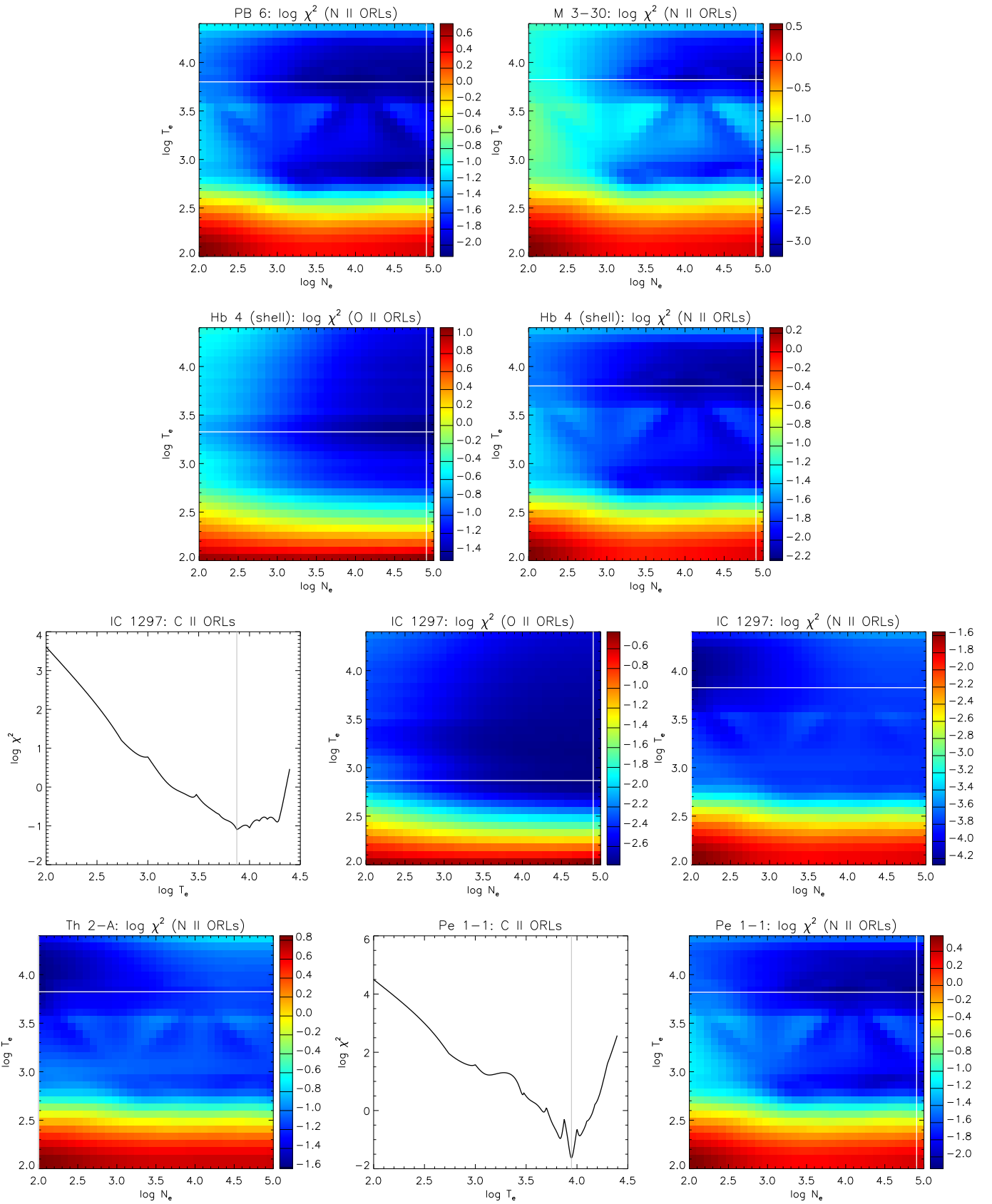


Figure 4. T_e diagnostic diagrams based on C II ORLs, and N_e - T_e diagnostic diagrams based on O II and N II ORLs. The best-fitting physical conditions at χ_{\min}^2 are shown by the solid lines.

Physical and chemical properties of WR planetary nebulae

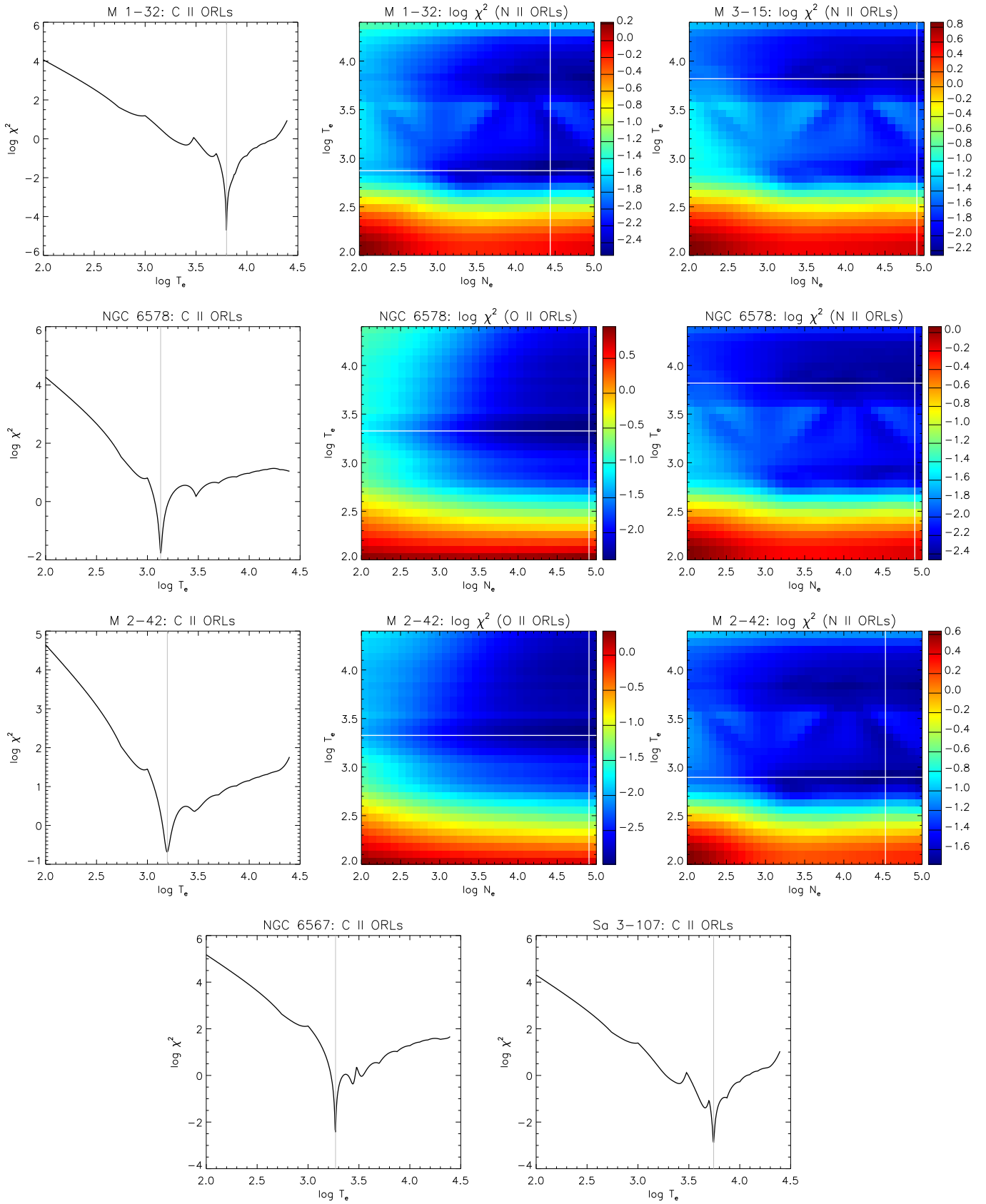


Figure 4. – continued